POLITECNICO DI TORINO
Repository ISTITUZIONALE

Advanced methods for sustainable energy systems in operation and design of district heating networks

(Article begins on next page)

04 August 2020

Doctoral Dissertation

Double-degree Doctoral Program in Energy Engineering at Politecnico di Torino (30th Cycle) and IMT Atlantique

Advanced methods for sustainable energy systems in operation and design of district heating networks

Stefano Coss
* * * * * *

Supervisors

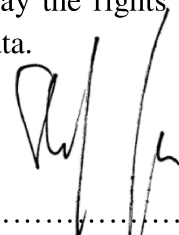Prof. Olivier Le-Corre
Prof. Vittorio Verda
Dr. David Mouquet

Doctoral Examination Committee:
Prof. Enrico Sciubba, University of Rome
Prof. Luis Serra De Renobales, University of Zaragoza
Prof. Diogo Queiros-Conde, University Paris Ouest
Prof. Emanuela Colombo, Politecnico di Milano
Prof. Maurizio Sasso, University of Sannio

Politecnico di Torino
September 14, 2018

I hereby declare that, the contents and organisation of this dissertation constitute my own original work and does not compromise in any way the rights of third parties, including those relating to the security of personal data.

....

Stefano Coss

Turin, September 14, 2018

Acknowledgments

life is a journey, not a destination

This principle, which I try to follow in my personal life, is even truer for the successful completion of a PhD. Many people have contributed and supported me during this academic journey, to which I want to express my special thanks.

At first, I want to thank all the members of my family, especially my parents, my wife Trang, my daughter Amélie-An and my friends who have mentally supported me and gave me motivation and support to achieve my goals.

Furthermore I want to thank the Select+ program coordinators, especially Mrs. Chamindie Senaratne and Prof. Bruno Lacarrière for their everlasting efforts to manage difficulties in the administrative procedures of the program.

My research work could not be possible without the supervision of Prof. Olivier Le-Corre and Prof. Vittorio Verda who have accompanied me in the research process. Through their academic excellence and long-term experience, they guided me through the vast amount of research areas and pinpointed the most promising questions to study.

Furthermore, I want to thank all people involved in the InnoEnergy PhD school, especially Ms. Christine Dominjon and Dr. Isabelle Schuster. InnoEnergy opened up a new world of how academic research can impact society and mankind through innovation and entrepreneurship.

At last, I also want to thank Dr. David Mouquet and Dr. Alexandre Lima for their support during my research year at Veolia VERI. The experience from industrial perspective and the insights on real business needs are an essential element of this thesis.

Table of content

List of figures

List of tables

Abstract

Energy transition, decarbonisation and sustainability are terms often used when referring to solutions which tackle climate change to reduce its negative impacts on human society. Fossil fuel consumption is widely accepted to be one of the major drivers for climate change. It is used in industrial production, mobility, power generation as well as for heating and cooling purposes. As a matter of fact, residential and commercial heating applications contribute a significant amount to the utilization of fossil fuels such as oil or natural gas.

District heating networks are systems used to provide heating service, fueled by the by-products of power generation, but are gaining more and more significance in the energy transition and decarbonisation of the heating sector. In district heating networks, heat can be produced with relatively low specific carbon emission (cogeneration, biomass etc.) and efficiently distributed to a large amount of consumers through dedicated networks. In many aspects those systems are superior to distributed generation from oil- or gas burners installed in individual households. However, drawbacks such as network losses or the lack of demand-response information increase the complexity of efficient operation.

Proposed solutions favor the transition from district heating networks to smart thermal networks, considered as one of the backbones of the future interconnected smart energy system. There, both centralized- and decentralized production and consumption is occurs in interconnected distribution networks, such as the power, gas- or heat grids. This implies many challenges for future district heating operation, such as third-party access, distributed renewable energy- or waste-heat integration and prosumers. This is especially true for large networks, which might function as smart thermal networks in the future.

In comparison to that, small-to medium scaled systems supplying small villages or small parts of a city, might not be applicable to develop towards smart thermal networks, simply because distributed renewables/waste heat is not available or the size of the network is limiting smart network operation. For those systems, the strategy of

using renewable energy as a primary source of centralized production (such as biomass) seems more promising.

Based on this problem setting, this thesis tackles two major research areas:

- Operation of DHN in the context of smart thermal networks
- Design of DHN regarding sustainability guidelines

One of the major challenges is the development of methods for the assessment of DHN in smart thermal network operation. For that, this thesis proposes a new methodology of assessing DHN operation from the perspective of Thermoeconomics. A thermoeconomic model is developed on the basis of a dynamic simulation of pressure and temperature distribution which applies the theory of exergy costing to graph-based network topologies. The aim of this research is to develop a method to assess decentralized energy- and exergy conversion as well as the analysis of individual contributions on inefficiencies and losses through thermoeconomic costing. The analysis is based on the exergetic flows in the district heating network, which allows integrating any type of thermal energy generation into the analysis. One of the main contributions is the formulation of exergetic cost balances to the control volumes of the network, simulated through a finite-volume approach. The methodology provides new formulations of cost generation in transient network operation and boils down to an algebraic matrix equation which can be directly integrated into graph-based network models, given the associated conditions. One major outcome is the ability to benchmark different consumers according to their individual cost generation, as seen in the following figure.
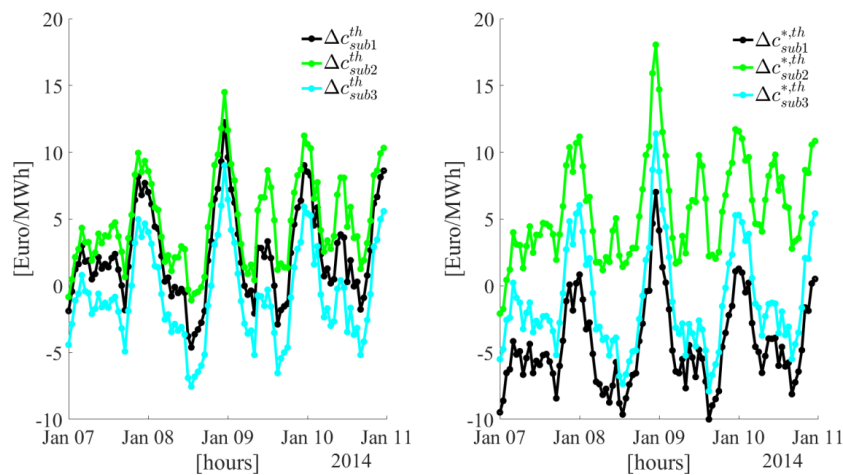
Figure: Benchmark results of substations in a DHN system (see chapter 4 for details)

Furthermore, this thesis investigates how small-to medium scaled systems can be effectively designed according to the principles of sustainability. A special focus is laid upon the usefulness for practitioners in industry, which need to integrated policy targets into design decisions.

Drawbacks through current state of the art design methodology are overcome through the formulation of a design model which considers:

- Supply-focused energy services
- Demand-focused energy services

It offers to possibility to study the effect of demand side measures (DSM) on the sustainability of the system using a design approach for a centralized heating plants to improve sizing of peak-, medium,- and base-load units. Results of multi-criteria analysis show that traditional design approaches using common sizing techniques for the heating units neglect possible improvements towards carbon emission reduction or emergy flow. Findings are based on the analysis of a centralized biomass-fired heating plant vs. a decentralized gas-boiler system.

For evaluating the impact of DSM on possible design improvements a new indicator called *load deviation index (LDI)* is proposed, see following equation.

$$LDI = \frac{P_{ideal}}{P_{mean}} = \frac{2}{P_{max} + P_{min}} \frac{\phi}{T}$$

This indicator is able to quantify yearly heat load demands through a single numerical value which can be used for benchmarking and for the assessment of possible improvements through DSM. A multi-objective optimization of a generic DHN system supports the usefulness of the LDI through providing evidence that a higher LDI (closer to 1) leads to a more sustainable production according to the design decision.

Furthermore it offers a link between the design methodology and the DSM itself which makes it a useful tool for industrial practice.

Résumé étendu

La transition énergétique, la décarbonisation et le développement durable sont les termes les plus importants mentionnés concernant les solutions qui concernent le changement climatique pour en réduire ses impacts négatifs dans la société humaine. La consommation de combustibles fossiles est largement reconnue comme l'un des principaux moteurs du changement climatique. Il est utilisé dans la production industrielle, la mobilité, la production d'énergie ainsi qu'à des fins de chauffage et de climatisation. En fait, les applications de chauffage résidentiel et commercial contribuent de manière significative à l'utilisation de combustibles fossiles tels que le pétrole ou le gaz naturel.

Les réseaux de chauffage urbain sont des systèmes historiquement utilisés pour fournir des services de chauffage, pouvant être alimentés à partir de la production d'électricité, qui prennent de plus en plus d'importance dans les transitions énergétiques et la décarbonisation du secteur du chauffage. Dans les réseaux de chauffage urbain, la chaleur peut être produite avec de faibles émissions de carbone (cogénération, biomasse, etc.) et être distribuée efficacement à un grand nombre de consommateurs par le biais de réseaux. À bien des égards, ces systèmes sont supérieurs à la production distribuée par les brûleurs à mazout ou à gaz dans les ménages individuels. Cependant, les inconvénients tels que les pertes de réseau ou le manque d'informations sur la réponse à la demande augmentent la complexité d'un fonctionnement efficace.

Les solutions proposées favorisent la transition des réseaux de chauffage urbain aux réseaux thermiques intelligents, qui constituent l'un des piliers du futur système d'énergie intelligent interconnecté. Là, la production et la consommation centralisées et décentralisées se produisent dans des réseaux de distribution interconnectés, tels que les réseaux d'électricité, de gaz ou de chaleur. Cela implique de nombreux défis pour les futures opérations de chauffage urbain, telles que l'accès par des tiers, l'énergie distribuée renouvelable ou l'intégration de la chaleur résiduelle et les prosommateurs. Ceci est particulièrement vrai pour les grands réseaux, qui pourraient fonctionner comme des réseaux thermiques intelligents.

En comparaison, les systèmes petits ou moyens fournissant des petites parties d'une ville peuvent ne pas être applicables à des réseaux thermiques intelligents, tout simplement parce que les énergies renouvelables distribuées / la chaleur perdue ne sont pas disponibles ou la taille du réseau limite le fonctionnement du réseau. Pour ces systèmes, la stratégie consistant à utiliser l'énergie renouvelable comme principale source de production centralisée (comme la biomasse) semble plus prometteuse.

Sur la base de ce problème, cette thèse aborde deux domaines de recherche majeurs:

- Exploitation d'un réseau de chaleur urbain (District Heating Network *DHN*) dans le contexte des réseaux thermiques intelligents
- Conception d'un DHN dans le contexte du développement durable

L'un des principaux défis est le développement de méthodes pour l'évaluation des *DHN* dans le fonctionnement du réseau thermique intelligent. Pour cela, cette thèse propose une nouvelle méthodologie d'évaluation du fonctionnement des *DHN* à partir d'une perspective d'analyse thermo-économique. Un modèle thermoéconomique est développé sur la base des coûts exergétiques et appliqué à un modèle de simulation dynamique de la distribution de pression et de température. Le but de cette recherche est de développer une méthode pour évaluer la production décentralisée d'énergie et d'exergie ainsi que l'analyse des contributions individuelles sur les inefficacités et les pertes à travers les coûts thermoéconomiques. L'analyse est basée sur les flux exergétiques dans le DHN qui permet d'intégrer n'importe quel type de génération d'énergie thermique dans l'analyse. L'une des principales contributions est la formulation de bilans de coûts exergétiques pour les volumes de contrôle du réseau simulés par une approche à volume fini. La méthodologie fournit de nouvelles formulations de la génération de coûts dans le fonctionnement du réseau transitoire et se résume à une équation matricielle algébrique qui peut être directement intégrée dans des modèles de réseaux basés sur un graphique, étant donné les conditions associées. L'un des principaux résultats est la possibilité de comparer différents consommateurs en fonction de leur propre génération de coûts, comme le montre la figure suivante.
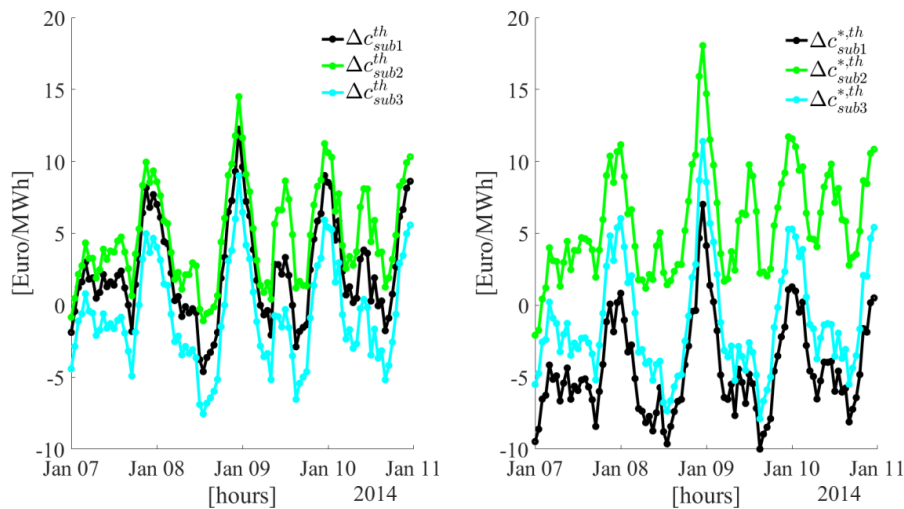
Figure: Benchmark des sous-stations dans un système DHN (voir chapitre 4)

En outre, cette thèse étudie comment les systèmes à petite et moyenne échelle peuvent être conçus efficacement selon des principes de développement durable. Un accent particulier est mis sur le produit « chaleur » au niveau de la conception (design) industriel d'un point de vue commercial. Les inconvénients de la méthodologie de conception actuelle sont surmontés grâce à la formulation de services énergétiques axés sur l'offre et la demande des DHN. Cela inclut le développement d'un modèle de centrale de chauffage à des fins de conception basé sur une approche de conception multi-unités pour un dimensionnement amélioré des unités de charge de pointe, moyenne et de base. De plus, les mesures de la demande (Demand Side Management *DSM*) et leur impact respectif dans les considérations de conception sont analysées et prises en compte. Grâce à une analyse multicritère, les résultats montrent que les approches de conception traditionnelles utilisant des techniques de dimensionnement communes pour les unités de chauffage négligent les améliorations possibles en matière de réduction des émissions de carbone ou de flux d'émulsion. Les constatations reposent sur l'analyse d'une centrale de chauffage à biomasse centralisée par rapport à un système de chaudière à gaz décentralisée.

Pour évaluer l'impact de *DSM* sur les améliorations de conception possibles, un nouvel indicateur appelé indice de déviation de charge (Load Deviation Index *LDI*) est proposé.

$$LDI = \frac{P_{ideal}}{P_{mean}} = \frac{2}{P_{max} + P_{min}} \frac{\phi}{T}$$

Cet indicateur est capable de quantifier les demandes de charge thermique annuelle à l'aide d'une valeur numérique unique qui peut être utilisée pour le benchmarking et pour l'évaluation des améliorations possibles de *DSM*. Une optimisation multi-objectif d'un système de *DHN* générique soutient l'utilité du *LDI*, mettant en exergue qu'un *LDI* plus élevé (plus proche de 1) conduit à une production plus durable selon la décision de conception

En outre, il offre un lien entre la méthodologie de conception et le DSM lui-même, ce qui en fait un outil utile pour la pratique industrielle.

Nomenclature

Latin symbols	Description	Unit (SI)
a	Element of incidence matrix	[-]
A	Incidence matrix	[-]
b	Branch	[-]
c	Unit energy cost	[€/J]
ce	Specific carbon emission	[CO2/kg]
cp	Specific heat capacity	[J/kgK]
C	Heat capacity (in Part A)	[kJ/K]
C	Costs (in Part B)	[Euro]
$\dot{C}$	Energy cost flow	[€/s]
Cap	(Load) capacity	[kg]
d	Distance	[m]
e	Specific energy	[J/unit]
Em	Emergy	[seJ]
f	(Cost) factor	[€/J]
$\dot{F}$	General flow	[-]
k	Unit exergy cost	[€/J]
$\dot{K}$	Exergy cost flow	[€/s]
lf	Load factor	[1]
M	Mass	[kg]
$\dot{m}$	Mass flow	[kg/s]
n, m	Nodes in SN and RN	[-]

p	Pressure	[Pa]
P	Thermal power	[W]
sT	Solar transformity	[seJ/unit]
t	Time (in Part A)	[s]
t	Cumulative hours (in Part B)	[h]
T	Temperature (in Part A)	[K]
T	Operating hours (in Part B)	[h]
UA	Heat transfer coefficient	[J/K]
Y	Yield	[%]
z	Specific thermoeconomic cost	[€/J]
$\dot{Z}$	Thermoeconomic cost flow	[€/s]

Greek symbols	Description	Unit (SI)
$\alpha, \beta \dots \omega$	Design variables	[1]
ε	HX effectiveness	[1]
η	Efficiency	[1]
ρ	Water density	[kg/m3]
ϕ	Energy (in Part A)	[J]
ϕ	Thermal heat (in Part B)	[MWh]
$\dot{\phi}$	Energy flow	[W]
ψ	Exergy	[J]
$\dot{\psi}$	Exergy flow	[W]

Superscripts	Description
av	(Annual) average
$design$	Design condition
it	Iteration
low	Lower bound
me	Mechanical
net	Network
nom	Nominal (load)
opt	Optimum
ref	Reference (scenario)
rel	Relative
s	Scenario
t	Timestep
th	Thermal
tot	Total
up	Upper bound

Subscripts	Description
A	Ash
$base$	Base load increase measure
B	Biomass heating unit
cap	Capital/Investment
$capex$	Capital expenditures
cn	Consumer

CN	All consumers in DHN system
d	Downstream node
D	(Exergy) Destruction
Di	Diesel
en	(Based on) energy
ex	(Based on) exergy
ext	External (inside system)
ext^*	External (outside system)
$extIn$	External inflows
$extIn^*$	External inflows (outside system)
$extOut$	External outflows
$Emp.$	Employees
G	Gas fired heating unit
HL	Heat load
hp	Heating plant
HP	Heating plant
$ideal$	Ideal (load profile)
L	(Energy) Loss
m	Node in the DHRN
max	Maximum capacity (in Part A)
max	Maximum load (in Part B)
$mean$	(Arithmetic) mean
min	Minimum capacity (in Part A)
min	Minimum load (in Part B)
n	Node in the DHSN
$norm$	Normalized

NG	Natural gas
$opex$	Operational expenditures
$peak$	Peak load reduction measure
pl	Plant component
pr	Producer
PR	All producers in DHN system
ref	Reference environment
req	Requested
ret	Returned
$smooth$	Smoothing measure
sub	Substation
sys	System
T	Transport
TI	Thermal insulation (DSM)
u	Upstream node (in Part A)
u	Heating unit (in Part B)
up	Upstream phase
$util$	Utilization phase
wp	Waste heat plant
W	Wood

Abbreviations	Description
BB	Black-box
CHP(s)	Cogeneration power plant(s)
Cr	Criteria

COM	Commercial consumers
CO2	Carbon emission – carbon footprint
CV	Control volume
DHN(s)	District heating network(s)
DSM	Demand side measures
ESI	Emergy sustainability index
ESL	Energetic system layer
EU	European Union
HP(s)	Heating plant(s)
IP(s)	Industrial plant(s)
LCA	Life-Cycle-Analysis
LDI	Load deviation index
LHV	Lower heating value
MILP	Mixed integer linear programming
MOO	Multi objective optimization
NPV	Net present value
NTU	Number of transfer units
PER	Primary energy ratio
RE	Renewable energy
REP(s)	Renewable energy plant(s)
RES	Residential consumers
RER	Renewable energy ratio
RF	Relational factor
RN	Return network
ROI	Return on investment
SN	Supply network

SOO	Single objective optimization
STN(s)	Smart thermal network(s)
STTH	Semi-transient, thermo-hydraulic (model)
THSL	Thermo-hydraulic system layer
TESL	Thermoeconomic system layer
TSM	Thermochemical storage
WB	White-box

List of publications

<u>Contributions to peer-reviewed journals</u>

Coss S., Verda V., Le Corre O. (2018): Characterization and impact assessment of DSM for future DHN systems design using the load deviation index. Journal of Cleaner Production, 182, 338-351

Coss S., Guelpa E., Letournel E., Le Corre O., Verda V. (2017): Formulation of exergy cost analysis to graph-based thermal network models. Journal of Entropy, 19(3), 1-12

Coss S., Rebillard C., Verda V., Le Corre O. (2017): Sustainability assessment of energy services using complex multi-layer system models. Journal of Cleaner Production, 142, 23-38

<u>Conference contributions</u>

Coss S., Verda V., Le Corre O. (2018): Waste-heat integration in smart thermal networks - A dynamic thermoeconomic approach. Proceedings of the 10th International Conference on Applied Energy (ICAE2018), 22-25 August 2018, Hong Kong, China

Coss S., Rebillard C., Verda V., Le Corre O. (2017): Characterization of Heat Demand Using an Emergy-based Indicator for Sustainability Optimization. Emergy Synthesis 9, Proceedings of the 9th. Biennial Emergy Conference, 153-166

Coss S., Guelpa E., Rebillard C., & Verda V., Le Corre O. (2016): Industrial waste heat integration for providing energy service to district heating networks. ECOS conference proceedings

Coss S., Verda V., Rebillard C., Le Corre O. (2015): Multi-criteria analysis of a wood-fired heating plant. IEEES7 Conference Proceedings, Valencienne 2015

Chapter 1: Introduction to the thesis

The first chapter is dedicated to an introduction of the thesis which covers two main parts. First, the background and research motivation is addressed, leading to a clear understanding of the research topics covered in this work. The second part provides an outline of the manuscript covering two research areas: Operation and design of district heating networks (DHNs).

1.1 Background and Motivation

Today's energy system is going through radical changes which affect several energy sectors like power generation, heating and cooling, mobility etc. Those sectors can be broadly categorized into three large groups: industry, transport and buildings. Large efforts are taken to prevent or keep global warming and its effects on climate change under a certain limit. This has been agreed on the Climate Convention 2015 in Paris. One main outcome was the radical reduction of carbon emissions in all sectors of the energy system towards a so-called zero-emission economy.

Key words like *energy transition* and *decarbonization* are strategies to implement climate-related goals. Energy transition refers to the change of the current energy system towards a climate-friendly system with a new way of how energy is converted, distributed and consumed. Decarbonization is a property of this new energy system and refers to the fact that conversion, distribution and consumption of energy are free of carbon emissions. One main strategy of achieving that is the use of renewable energy sources in combination with an intelligent or smart design of the energy system itself.

Energy transition should therefore lead to an energy system often referred to as *smart energy system,* in which today's disconnected systems are merged and build up an interconnected system of several energy sectors. Currently, systems such as electricity production and distribution, distribution of natural gas and oil for decentralized heating or thermal grids like district heating- and cooling networks for centralized heating are implemented in a disconnected way and do therefore not provide the possibility of interchanging energy vectors. This interchangeability of energy vectors,

such as electricity to heat and vice-versa, would be necessary for a vast and broad adoption of renewable energy sources into a smart energy system.

Considering that solar- and wind energy technologies provide fluctuating, unpredictable amounts of power, their integration would results in a smart energy system able to receive, store and distribute energy in a flexible way. This integration can be achieved through interconnecting the electricity grid with the distribution systems of natural gas and thermal networks, which then allows interchanging energy vectors (electricity, heat/cool, natural gas) between those system through energy conversion technologies such as power-to-heat/cool, gas-to-power/heat and others. This furthermore allows surplus energy from solar- or wind generation, to be converted into natural gas or thermal heat/cool. Hence the actual yield of wind- and solar generation could be increased to attain higher share of renewable energy utilization. Thermal networks such as district heating networks might play an important role in those flexible energy systems in the future.

Today, DHNs are mainly used to provide heating service to consumers through a hot-water distribution network. Those networks are operated in different sizes, ranging from large networks covering whole districts or even cities, to small-scale stand-alone systems in small villages or even rural areas.

Large systems are often operated through (multiple) cogeneration plants (CHPs) which produce electricity and thermal heat at the same time. This system set-up is already an interconnection of the electricity grid with the thermal network, because it allows adjusting the amount of electricity and heat produced and therefore provides flexibility to the power generation. In small-scale applications, often only one heat production plant is installed which provides heat according to the consumer's demand without the generation of electricity. Biomass-fueled heating plants are an example of those.

When analyzing those heat networks from the perspective of smart energy systems, thermal networks which operate on district- or city level are most promising for implementing so called *smart thermal networks*. In comparison to small-scale systems, where solar- or wind energy might not be present, large DHN systems are able to integrate large amounts of renewable energy through interconnection to the power- or gas grid.

Those smart thermal networks could integrate renewable energy sources like solar thermal heat, biomass heating plants or industrial waste heat directly into the network, while also allowing renewable energy from the power grid, through different conversion technologies, being converted into thermal energy. This adds flexibility both in terms of spatial- and temporal scale since the heat network itself, apart from being able to distribute energy over spatial scale, also acts as a storage component for the energy system. Hence, smart heat- and cooling networks can act as the backbone of future energy systems.

Based on this background analysis, two research areas can be extracted. First, large networks, which are able to integrate different energy sources while providing heating service to a variety of consumers with different exergetic demands, need advanced methods to understand system behavior during flexible, smart network operation. This area is commonly known as 4th- generation district heating networks. The main objectives are the reduction of network temperature and the integration of the thermal network into the energy system as a whole, as previously explained.

Second, in the case a smart thermal network is not feasible, either because multiple sources of renewable energy are not available or the network is too small to provide flexibility and storage for the energy system as a whole, the aim must be to decarbonize the thermal heat generation. Therefore, the focus must lie on proper design of the production plant according to principles of sustainability and also consider legal regulations such as policy targets like carbon-dioxide (CO_2) emission reduction.

1.2   Outline of the thesis

In this thesis, both research areas for the use of district heating networks are addressed. The thesis is divided into two parts:

- Part A: Contributions to DHN operation – a thermoeconomic approach
- Part B: Contributions to DHN design – a multi-perspective approach

In Part A, issues regarding the transition of DHN into smart thermal networks are addressed. The current state of the art shows that there is a lack of information regarding the generation of losses in large networks with multiple producers and consumers. The identification of the causes of those losses is only addressed on a global basis. In the industrial context, this means that, usually, the loss generation (either

thermal or mechanical) in the network is averaged and accounted for equally for every consumer. Hence, the current assignment of costs does not reflect the individual contribution to that cost, but is only estimated in a black-box system approach. Since every consumer, in terms of total energy demand and temperature level, effects the generation of losses in a different way, a way to assign a cost to the use of heating service from the network is necessary, especially for smart thermal networks.

This is especially valuable when different heating systems at the consumer side are installed. Floor-heating systems use much lower operating temperature compared to radiator heating systems, which theoretically allows a lower return temperature and therefore a lower mass flow rate in the network. Thus the impact of the individual demand of thermal energy and its quality (exergy) on the generation of primary energy (at the plant side) is important to assess the feasibility of third-party-access, network extensions with new consumer etc.

To provide this information, the development of a thermoeconomic approach for the estimation of exergetic costs in graph-based network models is carried out. Thermoeconomics is a way of accounting for exergetic losses in energy conversion systems. The application to DHN systems allows assigning a cost to every flow of energy, or more precisely exergy, to the consumers based on their individual contributions to the network losses. From an industrial viewpoint, this helps to better understand the causes and sources of inefficiencies in DHN operation and can provide the basis for demand side measures (DSM) at the consumer side, the implementation of a dynamic pricing mechanisms and the assessment of feasibility of various decentralized integration measures such as solar thermal heat, storage or industrial waste-heat.

In Part B, the second research area is addressed. This involves the design of small-scale DHN systems which are not considered as being part of smart thermal networks, according to the reasons mentioned before. For such systems, a focus on decarbonization through improved design with respect to sustainability targets is more suitable than the analysis of individual contributions on loss generation. The objective of this part is to provide a holistic design methodology for service-oriented DHN design which considers both the supply- and the demand side of the system.

The focus hereby lies on the design perspective from the viewpoint of the DHN industry. More precisely, the sustainable design of DHN systems is addressed from a

business model innovation perspective. This includes the extension of the traditional focus on heat supply only, through considering demand side measures as a part of the design approach. A design method is proposed with which DSM can be modeled and included on a quantitative basis on system level. Hence, improvements of DHN system design towards the utilization of more renewable energy in combination with reduction of primary energy demand and the possibility for new business models are presented.

The theoretical parts of this thesis, chapter 3 for Part A and chapter 6 for Part B, have been disseminated in various publications. In Part A, the theoretical development of exergetic cost analysis for the use in graph-based simulation models has been published in the Journal of Entropy under the title *Formulation of exergy cost analysis to graph-based thermal network models*, while an application of waste heat integration was presented at the ECOS conference 2016 with the title *Industrial waste heat integration for providing energy service to district heating networks*.

Parts of Part B were disseminated mainly in the Journal of Cleaner Production. The study with the title *Sustainability assessment of energy services using complex multi-layer system models* used multi-criteria analysis for the feasibility analysis of centralized heat supply from biomass compared to decentralized gas boilers, while the study with the title *Characterization and impact assessment of DSM for future DHN systems design using the load deviation index* proposes a design approach for sustainable DHN systems including a model for quantifying demand side measures and their impact on optimum design. Various applications of this research have been presented in the IEEES7 conference 2015 under the title *Multi-criteria analysis of a wood-fired heating plant* and at the Biannual Emergy Conference 2016 with the title *Characterization of Heat Demand Using an Emergy-based Indicator for Sustainability Optimization*. For detailed information on the various publications, their references are given in the List of Publications.

Part A:

Contributions to DHN operation –

a thermoeconomic approach

Chapter 2: State of the art – operational level

In this chapter, the state of the art of current research approaches regarding the transformation of district heating networks into smart thermal networks and the corresponding implications is conducted. The aim of this chapter is first, to provide a broad overview over current scientific research in the field of district heating networks especially under the framework of smart energy systems and second, to identify research gaps which are furthermore tackled through the use of thermoeconomics in Part A of this thesis.

2.1 Current research and trends in DHN systems

This section aims in providing a broad overview over current DHN research. This is useful to understand the context in which the works in part A are based upon.

2.1.1 The paradigm of smart energy systems

In order to promote decarbonization and energy transition in the current energy sector, the development of a new paradigm and a new way of "thinking energy" can be observed. This new paradigm is called *smart energy systems* and goes beyond the concept of "energy generation" and "energy utilization". It aims in combining existing and newly developing technologies to one single system for the purpose of energy transition. Thus, "energy system thinking" is the way of linking the different components of today's fragmented energy conversion- and consumption systems to profit from the individual strengths and benefits of technologies while reducing their weaknesses (Mathiesen et.al. 2015).

This concept involves the interdisciplinary design and operation of energy systems providing multi-vector services to (end)consumers. Thus, not the supply of heating or cooling for households, or the production of biofuels nor the maximization of renewable energy shares are primary goal of such a system, but the mere development of an interoperable system which is able to take advantage of system components in a smart way. This system might be able to integrate renewable energy, like solar- and wind energy, up to 100 %, because the drawbacks of fluctuating supply as well as supply-demand mismatch, both in terms of temporal and spatial differences, can be

counter-balanced by other system components, such as networks (to solve spatial mismatch), storages (temporal mismatch) and technologies for interchange of energy vectors, like heat pumps or absorption chillers, power-to-heat/gas and others (to solve demand-supply mismatch). One way of achieving that, is the smart combination of production, transformation and consumption of energy vectors through those technologies.

Given mainly solar- and wind energy as primary renewable energy sources, authors (Mathiesen et.al. 2015) and (Lund et.al. 2014) show how a smart energy system can look like. Crucial parts of that system are networks for electricity, gas and heating- and cooling networks. Those networks, do not only solve the spatial distribution problem, but are furthermore used as "storages" or "intermediate consumers". They are used to store energy from renewable energy sources in the case a direct demand for that energy from (end)users do not exist. As an example, surplus electricity can be converted into heat and injected into a DHN, which itself balances supply-demand variations through thermal storages. Thus, this system has a two-dimensional flexibility in the sense that the heat network is a sink for unused electricity, while additional thermal storage is used when thermal demand is not available. Assuming the functioning of the system, electricity produced by a fluctuating wind turbine can be used at a later time in the form of heat, which leads to a "green" utilization of that thermal service.

Heat networks which are able to perform these tasks are defined as *smart thermal networks* (STN) which are able, according to (Mathiesen et.al. 2015), to "…connect the electricity and heating and enables thermal storage to be utilized for creating additional flexibility and heat losses in the energy system to be recycled as well as the integration of fluctuating supply".

One of the objectives is to function as a flexibility device for the smart energy system through accepting both direct renewable heat (solar, waste heat etc.) as well as other vectors like surplus electricity to balance out demand volatility in the system. Those DHNs, designed as a STN, are defined the backbone of modern energy systems and allow the interconnection of the heat/cool and electricity markets in order to offer synergy potentials for production, transportation and flexibility. Another advantage of using heat networks for this purpose is that their infrastructure already exists and hence no additional investments into networks are necessary.

2.1.2 Towards smart thermal networks (STNs)

Research for DHN systems and smart thermal grids has increased to almost 300 publications per year in 2015 (Li et.al. 2017).This interest in DHN research is easily explained considering the dimensions of different aspects which must be considered. DHN systems research is a field including a vast amount of possible system configuration and system components to be studied. This involves production technologies, research on demand data, demand forecasting, network modeling and many more. When trying to sum up all those different areas, research on STN shows five major areas shown in Figure 2-1 according to (Lund et.al. 2014).
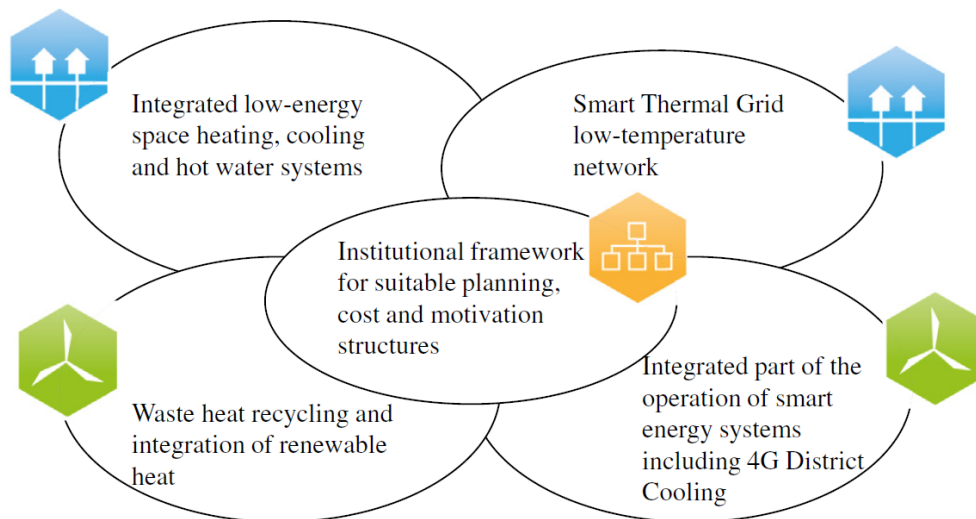
Figure 2-1: Research areas of smart thermal networks

The core research area, an institutional framework for planning and design is proposed. This refers to the fact, that a holistic design and implementation approach must be seeked which includes energy utilities, municipalities and consumers coherently. This is an important issue since the motivations of each stakeholder of a DHN system might vary considerably. While municipalities need to implement policy targets based on (mainly) environmental issues, utilities try to maximize their gains through selling heat to consumers, while consumers suffer from a quasi-monopolistic market with no competition. There are very little incentives for decentralized heat integration from renewable energy or waste heat. Furthermore, demand side measures such as thermal insulation, or behavioral shift is not rewarded based on its real impact on efficiency increase.

A recent paper investigates the pricing regimes in DHN systems under the perspective of incentives towards sustainable developments (Li et.al. 2015). Findings pointed out, that pricing regimes are mainly based on production costs with different assignment regimes, but there is a lack of empowerment of heat consumers. This lack of empowerment is one of the reasons why demand side measures towards reduction of heat demand through e.g. thermal insulation, modern residential heating systems, or behavior shift of consumption patterns are often underdeveloped.

Furthermore, the model in Figure 2-1 proposes both measures at production- and consumption side. On the production side, optimization of production and utilization of renewable energy as well as energy harvesting through the use of excess heat is promoted. On the consumption side, a thermal network must have a broader spectrum of heat demands. This means, that energy services with various temperature ranges should be considered and integrated into the network considering industries, commercial and residential users to be supplied by the network.

The enabling technology for DHN in that context is what is called *4th- generation district heating networks* (Lund et.al. 2014). The main strategy of 4th-gen DHN is a decrease of the network's operating temperature which, is stated, to enable a wider adoption of waste heat utilization, solar thermal integration and a higher efficiency of heat pumping technology.

2.1.3 Research in the context of 4th- generation DHN

Research in the field of DHN is abundant considering the wide range of applications concerned by the different dimensions of smart thermal networks. Nevertheless, it is important to review the current research trends in order to show the drawbacks certain approaches face.

In the case of production optimization, substantial work has been carried out to increase performance of CHP systems both from a technological as well as from a systemic point of view. A recent study about the optimization of urban energy systems (Morvaj et.al. 2016) considers decentralized networks, i.e. networks with multiple producers and consumers and applies multi-objective optimization methods to increase system performance for a multi-vector demand, but admit that the size of the network is limiting the analysis. In this case, optimum design is advancing for "closed"

urban systems with defined demand profiles but cannot be extended to large DHN, because the transient conditions are not taken into account.

Another recent publication optimizes multi-source production from CHPs and boilers using different pressure- and temperature levels of the production units considered. Optimum supply temperatures where found and it was stated that a decrease of thermal loss is not counter-balanced by an increase of pumping power (Vesterlund et.al. 2017). This result clearly fosters the development of low-temperature networks. However, average demand profiles have been used and the network was simulated in steady state condition. However, such approaches might not be applicable for systems with high fluctuation of production, especially when renewable integration or waste heat is concerned.

(Wang et.al. 2015) and (Carpaneto et.al. 2015) have optimized the production from CHP in combination with solar integration and thermal storages. Hourly demand data was used to simulate the amount of renewable energy (RE) to be integrated using a MILP approach. Similarly to (Morvaj et.al. 2016) authors are able to provide a better operation strategy to integrate solar thermal energy into DHN with the help of thermal storage. However, as in the previous case, the analysis is bound by the limitations due to the network size.

Apart from optimization of production from DHN, much effort is taken to utilize waste heat from industrial plants (IPs). Regional studies, as one for Denmark, show that excess heat from IPs is widely available at different temperature levels (Buehler et.al. 2017) and could be of possible use to provide low-temperature heat to DHN consumers. The waste heat integration potential is mainly based on the implementation of heat pumps at the producers' side in order to be utilized within reasonable temperature ranges.

This is definitely true from a technological standpoint, similar to what (Sun et.al. 2014) found out, but might be difficult to achieve in industrial context. Industrial processes aim in reducing temperature levels through e.g. applying Pinch analysis to heat exchanger networks. Investments are recuperated through lowers primary energy consumption. An increase of exhaust temperature, requiring additional investments seems to be unfeasible from a business perspective.

Thus, for the utilization in smart thermal networks, the usefulness of waste heat according to its exergy content is proposed by (Bendig et.al. 2013). They argue that the true feasibility of waste heat integration into DHNs depends on the demand of exergy at a given moment and not necessarily on the network temperature a system designer wants to achieve. Considering a DHN system showing a volatile consumption pattern, low-exergy waste heat might be clearly useful in cases where temperature (and therefore thermal exergy) demand is low.

From a technological viewpoint, one main enabler of achieving higher integration of waste heat and renewable energy is reducing the supply temperature throughout the network stated by 4th- gen DHN. (Wang et.al. 2017) have studied optimal supply temperature in a DHN with renewable integration and storage tanks to improve flexibility. Other case studies focused on the mass flow control of networks with ring topology (Laajalehto et.al. 2014) or at scenarios of reduced supply temperature from the production plants themselves (Kauko et.al. 2017). Those efforts are taken in order to reduce thermal losses, while providing the amount of requested thermal heat by the users. Those measures of decreased supply temperature are the core part of 4th- generation DHN development as stated in (Lund et.al. 2017).

Conceptually, different temperature levels of DHNs are compared from a system perspective and are characterized into high, medium, medium-low, low and ultra-low, each of them categorizing different temperature ranges down to about 30 to 40 °C. It must be noted that such low-temperature networks are not yet fully suitable in many of today's networks simply because of the constraint of a certain minimum temperature at the consumer side. However, in combination with improved heating systems at the building side, ultra-low temperature networks might become applicable. (Baldvinsson & Nakata 2016) also pointed out the gains associated with lower temperature levels from a thermoeconomic viewpoint.

Based on the quoted research, several points can be concluded. In order to achieve a smart thermal network, complex optimization approaches are excluding the network behavior and do not capture future scenarios where a wide range of volatile producers and consumers are connected. In the case of smart networks, there is a need for liberalization of access to the heating infrastructure which enables third-parties like industrial plants to integrate their waste heat. This might also empower consumers in their consumption patterns, so that they can benefit from proper pricing mechanism.

Furthermore, the focus on reducing network temperatures is useful in the case low-temperature is demanded by the consumers. In the case of smart thermal networks, this cannot be guaranteed and a mere focus in temperature reduction would exclude thermal networks to provide heating services to other consumers with higher temperature requests.

In Part A of this thesis, DHN operation is seen as the backbone for future energy systems making no compromise upon its utilization. This means that a future DHN might be a provider of low temperature and high temperature demand depending on its actual purpose. The focus on a particular network temperature misleads from the fact that large DHN do not operate at constant temperature. Moreover, they show a highly fluctuating temperature distribution influenced by daily consumption patterns and storage integration. Considering waste heat integration, this might increase temperature volatility even more, due to industrial production profiles which depend directly on the processes of the industrial plant.

The author proposes a wider view on DHN systems which act as a network of receiving and providing energy services of certain value. Energy services are meant in the sense of providing the possibility of a thermal market similar to the one already existing for power networks. In these markets, third-party access is applied and producers as well as consumers are part of a competition for thermal energy services. The approach of achieving such systems acting as a thermal market, demands for a transparent way of quantification of value of the energy flows and a method of allocating costs of heating service. E.g. an industrial plant, providing a fluctuating amount of waste heat, might be able to provide value to the network, in case temperature demand is low, while at other times, when exergy demand is higher for a certain consumer, the low-exergy waste heat has no value. This situation happens during e.g. changing weather conditions, where temperature supply at the building site is used to control the amount of energy/exergy supplied to the consumer. Hence a flow of low-temperature might supply enough energy at lower supply temperature (assuming the correct flow rate in the network).

Principally, this is true from a thermal perspective, where exergy efficiency is high in the case heat is supplied with a temperature "close" to the temperature requested. Lower temperature difference at the substation's primary side might demand higher mass flow rates in the network in order to supply the given thermal request. This

could lead to an offset of the gains due to a lower temperature difference due to higher friction losses along the pipes. In a comprehensive evaluation of feasibility of low-grade exergy sources, both the thermal- and the mechanical exergy flows must be therefore taken into account.

This work focuses on an approach with which operation of large DHN can be analyzed from an exergetic perspective to provide additional information necessary for a thermal market. If the integration of a certain heat flow is useful at a given moment, the thermal network should be able to accept it as a decentralized inflow. In order to decide whether a given energy stream is useful or not, that energy stream must be valorized during operation.

2.1.4 The need of information upon cost generation

The valorization of energy flows in a large DHN is only possible through a detailed knowledge upon the (dynamic) thermodynamic behavior of the system. In contrast to power networks, where Volts, Amperes and Frequencies are well known, this does not necessarily apply for DHN. DHN operation, according to the experiences of the author, is often opaque in the sense that for some networks, very little is known upon the thermodynamics in the network due to a lack of monitoring equipment and/or control systems. Despite that, in order to provide additional information for operational improvement, commercial software solutions are available.

Termis is a commercial software which uses real-time data of DHN operation for temperature and pressure control strategies. Apart from that, DHN operation is often based on the experience of the operator. This is successful in well-known DHN systems with common consumptions patterns which have been used for decades. This strategy might not be applicable for smart thermal networks, because for those, consumption patterns are unknown and subject to the behavior of the whole energy system. An exception would be real-time monitoring on substation level which could be achieved through IoT equipment.

In the case that detailed information on energy flows is missing, there is no possibility to track efficiency losses such as thermal losses or pressure losses throughout the network. This furthermore hinders the assignment of costs, which are initially assigned to the inflow of energy/exergy into the grid, to energy flows. The need for de-

tailed thermodynamic knowledge of DHN operation is the basis to analyze the loss- and cost generation in DHN systems and is a key issue for STNs.

2.2   Towards smart thermal networks

Based on the findings of the research conducted in the field of smart energy systems and their implications on smart thermal networks, this sections reviews how to achieve valorization of thermal flows in DHN systems.

2.2.1   Exergy as a mean for value accounting

Exergy analysis is the analysis of the availability of work one can extract from a given energy content. It is a way of defining a certain "quality attribute" of energy, in the sense that not every stream of energy has the same usefulness. Despite the fact that every form of energy is equal under the perspective of thermodynamics, they are not equal in their usefulness for certain processes.

Except of e.g. electricity, where energy- and exergy content is equal, this is far from being true for thermal heat or even thermal networks. Considering thermal networks as streams of thermal energy, those streams are streams of energy and exergy. The difference between those two lies in the usefulness of their utilization. Two thermal energy streams with equal energy content but different temperature levels have a different amount of thermal exergy.

The example of a heat pump clearly demonstrates that principle. Given a certain heat request at a temperature level of 60 $^{\circ}$C for heating purpose, the heat pump has to increase the thermal exergy of a given heat source. Assuming the heat source is available at 30 $^{\circ}$C or 50 $^{\circ}$C. The exergy needed to transform the heat source at 30 $^{\circ}$C through increasing its thermal exergy through the heat pump is higher than in the case the heat source is available at 50 $^{\circ}$C. Thus exergy is a measure of how much work is needed to increase the thermal exergy of a given system.

This has led to the development of what is called *exergy cost* (Lozano & Valero 1993). That principle is one of the foundations of valorizing exergy streams through the assignment of a value, more precisely an economic cost, which represents the cost of deploying a certain exergy flow. Due to the fact that the amount of exergy degrades through every transformation, the usefulness for utilization declines (as can

be understood from the previous example). This is reflected by the assignment of a cost, which represents the economic effort necessary to deploy that exergy stream.

In exergy costing so called *fuels* and *products* for components participating in the transformation processes are defined. This definition of fuel and product derives from the theory of exergetic costing, which uses the following approach. Every "effort" taken for a given transformation is considered to be a fuel to the transformation while any "gain" from the transformation is a product of the energy conversion.

This distinction is crucial when applying exergy costing, because it defines first the *origin* of a cost in the system under consideration and second the costing *object*, thus which outflowing stream will be burdened by the cost. It is important to note that every cost flow is either a product- or a fuel flow which is due to the fact that a "loss" of cost is impossible. In order to understand the implications for the field of DHN systems, the next section discusses the relations between energy, exergy and cost from an industrial perspective.

2.2.2 The problem of black-box costing

Costing is a way of keeping track of "value" of certain goods. A certain good usually inherits some sort of value if it is used to supply some costumer's need. The initial value of that good can be defined through assignment of a certain "cost", which the one who deployed the good has to suffer. In economic terms, the value is determined based on the assignment of an economic cost, with the help of a monetary currency.

In the field of energy services in DHN systems, producers also face certain costs of the supplied thermal flows based on the cost of their production. This production cost is assigned to a certain amount of energy from which a specific cost can be determined. This specific cost is called *unit energy cost* and describes the amount of cost inherited by one unit of that energy. Based on the previous explanation, the unit energy cost is therefore a measure of value of a given energy flow.

According to the industrial experience of the author, costing approaches in real-exiting DHN systems are based on black-box (BB) costing due to several practical considerations. This leads to an accounting regime which assigns equal unit costs for each consumer in the system. This approach is easy to apply, since only the total energy supplied to- and from the system must be evaluated. This can be done

through measurements at the production plant and at the substations connected to the DHN. However, this approach does not provide information of the cost generation in the network itself and is therefore not able to capture the value degradation of energy flow in DHN systems. Hence, this approach is not useful when considering smart thermal networks where producers and consumers are spread throughout the network with different exergetic supplies and demands, because their individual contribution to thermal- and mechanical losses and therefore the cost generation might vary considerably from the average black-box costing method.

Different costing approaches for energy services can be imagined in a DHN system. Those approaches can be either based on the energetic- or the exergetic value of the hot water flowing. Apart from energy or exergy considered, the approach can also be differentiated between a black-box approach, where the network behavior is unknown, and a white-box approach where detailed information on the thermodynamics of the network is available. A classification of those approaches is given in Table 2-1.

Table 2-1: Classification of costing approaches in DHN systems

	Energy	Exergy
Black-box (BB) approach	Traditional costing	Black-box exergy costing
White-box (WB) approach	Energy costing	Thermoeconomic costing

Apart from energy losses in DHN systems, the amount of exergy associated with an energy stream also suffers losses, called *exergy destruction*. On one hand side, a DHN can be seen as a black-box where a certain amount of energy enters, and a certain amount of energy exits the system, without information about the system behavior. This approach, in combination with energy as the "value asset", is defined as *traditional costing*. In that approach, only the global entering- and exiting flows from the DHN system are taken into account while losses or transient changes are globally accounted for. Traditional costing refers to the method used by today's industry using uniform pricing for thermal heat utilization. A black-box model using exergy as the value asset (*BB exergy costing*) is imaginable but does not exist in real practice according to author's knowledge. However, once the global exergetic behavior is known, black-box exergy costing can also be carried out.

On the other hand, white-box costing approaches use the real system behavior to account for value loss in the system. Those could be based on energy (*energy costing*) or exergy (*thermoeconomic costing*). In order to understand the specific draw-

backs between BB- and WB costing, the black-box costing approach is analyzed in detail according to Figure 2-2.
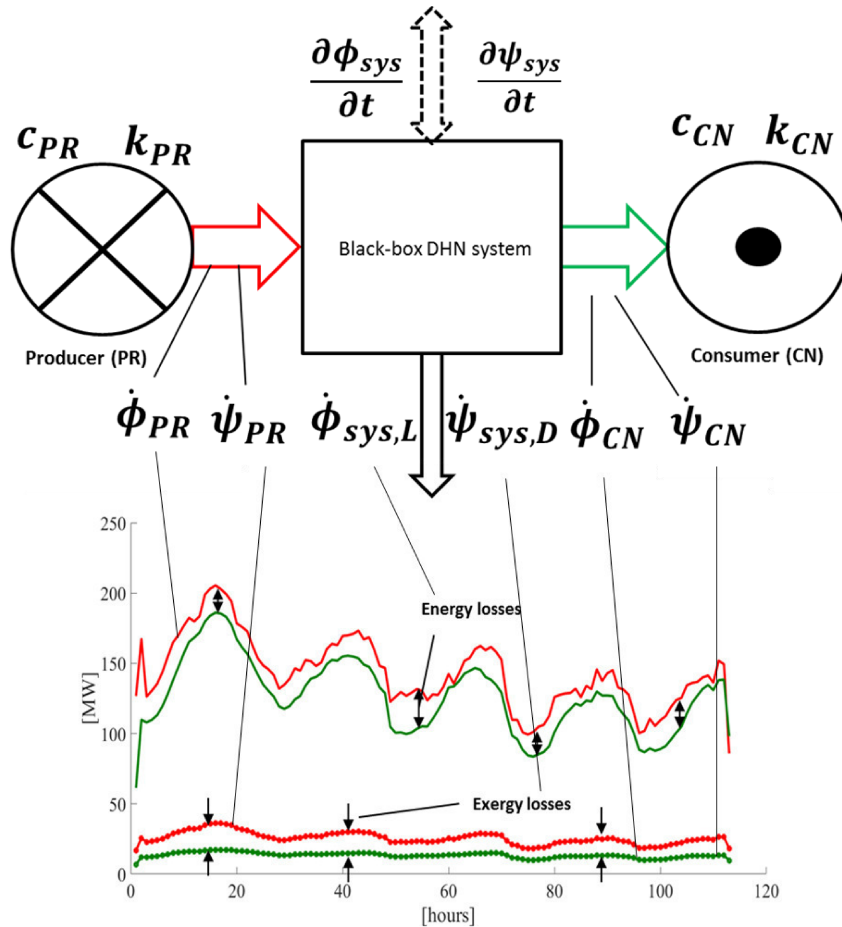
Figure 2-2: Black-box model (up) and global energetic flows (below)

A DHN system as a black-box receives energy service, thus thermal/mechanical energy $(\dot{\phi}_{PR})$ or exergy $(\dot{\psi}_{PR})$, and provides energy service, more precisely heating, expressed as energy $(\dot{\phi}_{CN})$ and exergy $(\dot{\psi}_{CN})$ to consumers. In this thesis, producers (PR) and consumers (CN) are considered as the sum of all producers $\dot{\phi}_{PR} = \sum_i \dot{\phi}_{pr_i}$ and consumers $\dot{\phi}_{CN} = \sum_i \dot{\phi}_{cn_i}$ (similarly for exergy), respectively.

Total amounts of energy and exergy provided by the producers (e.g. heating plants) and received by the consumers (e.g. substations) are displayed over a given timeframe at the downside of Figure 2-2. In the black-box approach, the difference between production and consumption is evaluated as the energy- and exergy losses occurring in the system.

Those losses can be estimated on a system scale and might show variations of magnitude depending on the performance of the system. With knowledge of the flows

shown in Figure 2-2 (below), it is instantly possible to apply black-box costing approach for both energy and exergy leading to equal unit costs for all consumers. This unit cost describes an average cost of utilization of energy from the system where the losses or destruction are accounted based on the global losses and can be used for pricing of the consumers.

This is done through a cost balance for the black-box model leading to (2.1),

$$c_{CN} = \frac{\dot{\phi}_{PR}}{\dot{\phi}_{CN}} c_{PR} \qquad\qquad k_{CN} = \frac{\dot{\psi}_{PR}}{\dot{\psi}_{CN}} k_{PR} \qquad\qquad (2.1)$$

where (c_{CN}) and (k_{CN}) are the unit energy- and exergy costs based on black-box accounting. Those unit costs are average unit costs for every consumer (cn_i) in the system depending on the unit energy- and exergy cost of the producer (c_{CN}, k_{CN}). Remark: Equation (2.1) is only valid with one single producer. Clearly, if there is more than one producer, a weighted unit cost must be calculated if the producers supply energy/exergy at different unit costs.

When average costing is applied in the industrial context, entering and exiting energy/exergy is based on measurements at the supply- and demand side. Based on those measurements, the energy/exergy supplied by all producers and extracted by all consumers are estimated. Based on those flows, black-box costing is applied.

One major drawback of this black-box approach is, that it does not consider for dynamic behavior of the system which unavoidably occur in DHN operation, especially when smart thermal networks are considered. Thus, the dynamic behavior expressed through the change of thermal energy $\left(\frac{\partial \phi_{sys}}{\partial t}\right)$ and exergy $\left(\frac{\partial \psi_{sys}}{\partial t}\right)$ in the system is not taken into consideration. The reason for that is, that only entering and exiting thermal flows are measured for billing purpose, while the thermal behavior of the network (such as warming- and cooling transients) is unknown. This leads to an estimation of losses, as seen in Figure 2-2 below, which solely relies on the difference between inflow and outflow of energy/exergy. Hence the problems related with BB costing approach are twofold:

- Transient behavior of dynamic system operation is neglected
- Only average unit costs, equal for every consumer, are possible to determine

Considering the needs of smart thermal network previously discussed, this BB costing approach does not provide information on individual performance of producers and consumers in the network, because every consumer has the same unit average costs c_{CN}, k_{CN}, regardless of its performance. Due of the fact that a DHN is a dynamic system and shows dynamic behavior of temperature and mass flow, this transient behavior must be considered when evaluating the unit cost of energy/exergy supplied to the consumer. Only then, losses can be correctly determined based on the black-box energy- and exergy balances of the system given in (2.2),

$$\dot{\phi}_{PR} \pm \left|\frac{\partial \phi_{sys}}{\partial t}\right| - \dot{\phi}_{sys,L} - \dot{\phi}_{CN} = 0 \quad \dot{\psi}_{PR} \pm \left|\frac{\partial \psi_{sys}}{\partial t}\right| - \dot{\psi}_{sys,D} - \dot{\psi}_{CN} = 0 \quad (2.2)$$

In (2.2), $\left(\frac{\partial \phi_{sys}}{\partial t}\right)$ is the transient change of energy in the DHN system and $\left(\dot{\phi}_{sys,L}\right)$ is the energy loss (e.g. thermal loss). Similarly $\left(\frac{\partial \psi_{sys}}{\partial t}\right)$ accounts for transient change of exergy, while $\left(\dot{\psi}_{sys,D}\right)$ is the exergy destruction in the system. The transient terms have either positive or negative signs, because the transient term changes its sign depending on if the network heats-up (charges) or cools-down (discharges) at a certain time. Depending on the definition of $\frac{\partial \phi_{sys}}{\partial t}$ and $\frac{\partial \psi_{sys}}{\partial t}$, the term is either negative or positive according to the system balance equations in (2.2).

When considering dynamic system behavior, it can be therefore differentiated between *efficiency* and *yield* of the system. While efficiency accounts only for losses in the system, yield expresses the relation between output to input of a system, see (2.3) - (2.4),

$$\eta_{en,sys} = \frac{\dot{\phi}_{CN}}{\dot{\phi}_{PR} + \frac{\partial \phi_{sys}}{\partial t}} \qquad \qquad \eta_{ex,sys} = \frac{\dot{\psi}_{CN}}{\dot{\psi}_{PR} + \frac{\partial \phi_{sys}}{\partial t}} \qquad (2.3)$$

$$Y_{en,sys} = \frac{\dot{\phi}_{CN}}{\dot{\phi}_{PR}} \qquad \qquad Y_{ex,sys} = \frac{\dot{\psi}_{CN}}{\dot{\psi}_{PR}} \qquad (2.4)$$

where energy $\left(\eta_{en,sys}\right)$ and exergy $\left(\eta_{ex,sys}\right)$ system efficiency are considering the dynamic influence while energy $\left(Y_{en,sys}\right)$ and exergy $\left(Y_{ex,sys}\right)$ yield of the system is neglecting this part. It must be noted, that equations in (2.3) are valid in the case the transient term is positive (which refers to a network charge). When the network is

charged (referring to cooling-down of the network) the transient term must be included in the numerator.

The transient behavior can lead to a situation where the yield is even higher than 100 %, in the case the network is cooling-down so that the inflow of energy is way lower than the outflow. For the efficiency, this is not possible, because the calculation is corrected by the transient term.

In steady-state system operation, efficiency and yield are equal. Considering that black-box costing is applied through (2.1), the following relation can be concluded in (2.5).

$$c_{CN} = \frac{c_{PR}}{Y_{en,sys}} \qquad\qquad k_{CN} = \frac{c_{PR}}{Y_{ex,sys}} \qquad\qquad (2.5)$$

Equation (2.5) is used for traditional energy costing in DHN systems, as described in Table 2-1. It can be concluded that transient system operation is neglected in this approach.

Assuming that transient system operation is known in the black-box approach, a dynamic average unit cost (c_{CN^*}, k_{CN^*}) which is based on the dynamic efficiency of the system can be defined, see (2.6).

$$c_{CN^*} = \frac{c_{PR}}{\eta_{en,sys}} \qquad\qquad k_{CN^*} = \frac{c_{PR}}{\eta_{ex,sys}} \qquad\qquad (2.6)$$

In (2.6) the transient change of energy/exergy is included in the calculation. Even if transient behavior is known, unit energy/exergy costs can still only be determined on average for every consumer in the system. A dynamic, average unit cost cannot be obtained through black-box costing only, because the total losses are averaged for every consumer.

Those are major drawbacks of black-box costing and it is clear, that those approaches are not useful in the context of smart thermal systems with the need of cost transparency. Apart from that, several important differences exist between energy- and exergy costing, which are described in the following section.

2.2.3 1st law- and 2nd law costing

The difference between 1st law- and 2nd law costing is as fundamental as the difference between energy and exergy of an energy stream. As said before, costing is a

way of keeping track of losses. Thus, every such loss of e.g. thermal energy must be accounted for. Considering energy as a 1st- law costing approach, losses of energy like thermal losses due to temperature decrease or heat losses can be accounted for. In the case a certain energy request is met in terms of quantity but not quality of energy, its value is zero given a certain exergy demand. An example would be a DHN consumer which is supplied with an insufficient high temperature even though thermal energy is enough to fulfill the request. In such a case, energy costing does not take into account the real value of that energy stream.

In order to solve this problem, the costing method must be based on a property representing the "real" value of an energy stream. For keeping track of the quality of an energy stream, its exergy value is used. Exergy costing is a 2nd- law costing approach where exergy losses are used as the basis for cost accounting. Those exergy losses, consider all kinds of energy losses, but also consider decrease of temperature as a loss (Comakli et.al. 2004).

Considering DHN systems, every degradation of exergy due to temperature decrease is increasing the unit cost of that stream. Because the cost of that particular stream is constant, a lower exergy value will lead to higher unit exergy costs. This is an important insight which makes costing approaches based on exergy more realistic in terms of capturing the true nature of losses.

Hence, in the following works in Part A of this thesis, a white-box costing approach, which is able to apply energy costing and thermoeconomics to dynamic DHN systems in order to overcome drawbacks related with BB costing, is developed. In order to comply with the principles of thermoeconomic assessment, the next section details current research in the context of DHN systems.

2.2.4 Thermoeconomics for DHN operation

Due to the fact that the value for thermal heat can only be estimated through its exergetic value, the assignment of exergy as the main value of an energetic flow is reasonable. This is important when energy systems are designed with the purpose of providing a certain service to a consumer. This has led to the development of thermoeconomics, which is a way of combining thermodynamic principles and economic mechanism to analyze the value for energy services.

Thermoeconomics has been initially explored for linking the theoretical concept of exergy with economic terms. This idea dates back to the 1920s and was investigated by Lotka, Keenan and others. In the 1960s, thermoeconomics has been established by independent researchers such as Szargut, Baehr, Fratscher, El-Sayed and many more (Sciubba & Wall 2007). Thermoeconomics is a rational approach for understanding the process of cost formation within energy systems. This process is based on the way of using energy resources according to their quality, the latter being expressed through the concept of exergy. Besides economic cost, exergy was also developed for taking into account environmental costs and is therefore linked to sustainability (Wall 1986). Thermoeconomics can be applied to energy systems with different purposes: costing (Tribus & Evans 1962) design improvement (Tsatsaronis & Pisa 1994), optimization (El Sayed 2003), diagnosis (Torres et.al. 2002), control (Verda & Baccino 2012) and others. Since thermoeconomics is a thermodynamic-based method of value tracking, it is highly interesting for the evaluation of district heating networks, because they involve the use of both thermal- and mechanical energy.

Due to the fact that system performance of DHNs is highly related with thermal losses and the temperature levels in the network, thermoeconomics seems to be a reasonable way of accounting for them. A survey of actual literature clearly shows that this approach is used for design of DHN systems (Gładys & Ziebik 2013) calculation of optimum pipe insulation thickness (Keebas et.al. 2011) and performance assessment of renewable energy supply (Kecebas 2011). In (Baldvinsson & Nakata 2014) authors highlight the usefulness of applying exergy analysis and thermoeconomic costing to estimate unit costs of energy services in a DHN. This leads to a better understanding on the economic implications of lower network temperature. Cost accounting based on exergy is particularly useful to evaluate the primary energy savings associated with retrofitting options applied to buildings connected with district heating (Verda & Kona 2012) or to compare the production costs of different producers depending on their position and the quality of their heat produced (Verda et.al. 2016)

Those findings were conducted under the perspective of third-party access such as solar thermal or waste heat integration and show that the thermoeconomic approach provides both technical- as well as economic information of the use of multi-source

integration. These are important aspects in modern district heating systems, where it is crucial to take advantage of heat available from industrial processes, renewable energy or local resources. In addition, this could be a rational basis for regulating third-party access to the heating infrastructure.

It can be concluded that through thermoeconomics, the true nature of losses in a thermal system can be considered and translated into economic terms. Through that, it is possible to keep track of exergetic destructions in a DHN system with the aim of achieving information upon the usefulness of a given thermal flow. Considering the aim of smart thermal networks and 4th generation networks, thermoeconomics is able to provide important information on the actual economical value through translating exergy losses into an increase of costs. Since DHN system are not static but rather very dynamic systems, a dynamic system model is needed if time-depended behavior has to be studied. Hence, a dynamic, thermoeconomic system model must involve a thermodynamic model with which the thermodynamic behavior of the system can be studied.

2.3   The semi-transient thermo-hydraulic (STTH) model

In order to provide information on the thermodynamics of energy flows in a smart thermal network, an appropriate model of the DHN system must be considered. Apart from the abundant models and simulation tools available in the literature, one is selected which has been developed by the author's research group; the semi-transient, thermo-hydraulic (STTH) model developed at Politecnico di Torino, Italy (Guelpa et.al. 2017a).

The model was initially developed for a large DHN in Turin/Italy for the purpose of analyzing large DHN networks from a hydraulic- and thermodynamic perspective. The model consist of two major parts, which are based upon a graph representation: One hydraulic model which solves a pressure-linked mass flow matrix obtained by setting boundary conditions for injecting and extracting flows. The solver considers momentum equation around each branch and mass conservation around every node in the network. It is thus possible to derive the pressure distribution of the network given certain mass flow rates. The second part involves a thermal solver to estimate the transient temperature distribution in the network. This is based upon the application of a transient energy balance to network nodes.

The STTH model has various advantages which include the applicability to large networks with looped structures and a straight forward matrix formulation which can be easily implemented into a numerical code. In order to understand the framework of the STTH model in more detail, a short discussion of the approach is provided.

2.3.1 Graph-based network model

Due to its physical model of interconnected tubes, a DHN can generally be represented as a simple directed graph. A graph is a mathematical structure representing a network through nodes and branches (Wilson 1996). A node is considered as a point in the network while a branch is a connection between two nodes. Directed means, that every flow in every branch has a definite direction. A node is connected to other nodes through several branches, while a branch cannot be connected to more than two nodes.

Given two nodes A and B connected by a branch. If the flow in its branch is directed from A to B, node A is called the *upstream node*, while B is called the *downstream node*. This terminology applies vice-versa for a flow directed from node B to node A. Node A and B are called the *node pair* of the branch. If the nodes of a node pair are equal, its corresponding branch is singular. It must be noted, that such graphs with singularities are not considered in this work, because they do not have any purpose in DHN operation.

The mathematical formulation of the graph includes the incidence matrix (A) ($n \times b$) (Wilson 1996). The incidence matrix uses both node and branch identifiers as dimensions, while a three-value variable (-1, 0, +1) is used for the matrix elements (a_{nb}). If a_{nb} is -1, node (n) is a downstream node of branch (b), while +1 indicates an upstream node of b. If the element is 0, the node is neither upstream nor downstream node of that branch. The incidence matrix is rectangular, except if the sum of both nodes and branches are equal.

2.3.2 Finite-volume method and upwind-scheme

Since the water flow in DHNs is a problem of computational fluid dynamics, a finite-control volume method is considered for the numerical calculation of the network model (Guelpa 2016). The network is divided into control volumes (CV) which can be solved numerically. The resolution of the control volumes depend on the problem to

be solved. In DHN modeling, control volumes are assigned at least to each single node, defined by the network topology. This has two reasons. First, certain variables are assigned to network nodes and must be calculated. Second, a node, which typically represents a connection or junction of some sort, has several different entering and exiting streams. If not, the node might not be useful to consider as a control volume and would unnecessarily increase the problem size.

It is important to notice, that, even if information at a particular point in the network is not needed, it would be useful to increase the numerical resolution and therefore the amount of control volumes for some branches, in cases where a branch is very long or the resolution of the numerical calculation should be increased. Firstly, this is due to effects of "numerical diffusion" through the numerical evaluation of the finite-volumes. Secondly, the resolution of the control volumes has an effect on the accuracy of the temperature and thermal loss calculation, since through CVs are linearizing those effects. The smaller the control volumes are evaluated the smaller the numerical error due to linearization. Hence, for long branches, additional CVs can be useful to increase the accuracy of the numerical scheme.

A node can either be a boundary node or an internal node. A boundary node is a node which is the connection to components of the DHN system like plants, substations or storages. Internal nodes do not interact outside of the DHN and typically represent connections or junctions. The size of the control volume depends on the size of the branches which are connected to its node. The control volume boundaries are set around each node considering half of every branch. For boundary nodes which connect consumers to the network, the size of the control volume considers the total length of the connected branch. For more information consider the initial definition in (Guelpa 2016).

The advantages of this model include the scalability of the problem, the standardized application of graph topology which could possibly include any real existing DHN topology and the stability of the solution of pressure, mass flow and temperature evaluation

The model has been developed for a network located in Turin which is one of the largest networks existing in Italy. Both the thermal- and the hydraulic part of the model have been validated using measured data from the Turin network (Guelpa et.al.

2017a). Based on the validation, several key issues in DHN operation have been addressed including performance improvement through peak-shaving of thermal demand (Guelpa et.al. 2017b) and optimization of pumping strategies using the results of the hydraulic model (Guelpa 2016).

The model is validated and shows useful applications of various parts of DHN research. Furthermore, it can be applied to any looped-network and has advantages especially for large networks due to its formulation of control volumes at network nodes. Due to those advantages, the model has been selected as a basis for the thermoeconomic approach and is used to determine the temperature and pressure distribution of the network under consideration.

2.4   Outlook on the contributions of Part A

The scientific contributions provided in Part A of this thesis are the development of a model for dynamic thermoeconomic simulation of DHN systems. More specifically, the formulation of exergetic costs (among others) is developed for general graph-based network models. The formulation is based upon the theory of exergetic costs and is applied using the STTH model, described in the previous chapter.

In order to achieve that, three system layers are defined, in which thermo-hydraulic, energetic and thermoeconomic variables are determined. This distinction is important to understand the prerequisites needed to calculate thermoeconomic costs. It must be noted, that, even though the formulation of energy balances to the graph-based model is explicitly stated in the coming chapter, it is integrated part of the STTH model. However, it is shown explicitly due to the fact that exergy balances are not part of the STTH model, as it was present in the beginning of this research.

From a research perspective, the information on thermoeconomic costs in the network offers many different applications. One of them being the assessment of individual contributions on costs. It was seen, that in DHN systems, costs are averaged and take only the steady-state losses to determine the costs for the consumers into account. Through thermoeconomics, the impact of consumer demand can be directly converted into a cost of energy/exergy, which offers a benchmark and the possibility to assess a variety of consumer demand properties such as energy demand, temperature request etc. Another application is the study of demand side measures such

as reduction of temperature request through e.g. better indoor heating systems, or the analysis of distributed injection of energy at different levels of temperatures, such as waste heat integration or renewable energy integration. In general, the model provides an additional piece of information for the development of smart thermal networks.

From an industrial perspective, several applications of the model can be imagined. Since this work has been carried out in close relation with industrial practice, the possible applications are highlighted. At first, the possibility to know the individual contribution of costs in a DHN system is of vital importance for the improvement of the system as a whole. It offers the possibility to determine the cause of inefficiencies and can be tackled accordingly. New consumers added to the network can be pre-assessed in their impact on the generation of costs using common energy demand patterns. Furthermore, a dynamic or quasi-dynamic pricing of thermal energy is possible. While dynamic pricing might be difficult to achieve due to non-acceptance by the consumers, quasi-dynamic could be a way to improve overall system performance. There, the pre-agreed pricing for a standard pattern, which can be pre-assessed as stated before, can be taken as a basis, while the price is adjusted if the consumer's demand deviates from it. This allows the thermal request to be better known in advance and can help reducing off-design operations such as high peak-loads.

Chapter 3: Thermoeconomic model for dynamic DHN system simulation

In this chapter, the theoretical development of a model for dynamic thermoeconomic simulation of DHN systems is developed. The aim of this chapter is to provide a comprehensive methodology for applying thermoeconomic analysis to DHN system operation which can be used in the context of smart thermal networks.

The model includes a service-oriented definition of DHN systems including energetic and economic system layers for a time-dependent simulation of operation. Hence, section 3.1 introduces the DHN system including generic components for deployment, distribution and utilization of energy services. Sections 3.2 - 3.3 develop the necessary system layers for every component followed by section 3.4 which provides an integrated matrix formulation for the application of the model to graph-based topology models. In section 3.5, the simulation procedure is summarized, covering two approaches for system simulation.

3.1 Introduction to the DHN system

In this section, the DHN system is introduced. The aim is to provide a generic model which can be used for any kind of DHN system under the assumptions made. At first, 3.1.1 defines the system and its components. Section 3.1.2 introduces the models of the component and its corresponding assumptions based on a service-oriented perspective. At last, section 3.1.3 discusses the general approach for the numerical model of the DHN.

3.1.1 Definition of the DHN system

The architecture of the DHN system focuses to connect producers and consumers through a thermal network. The focus hereby lies on production plants and consumers (final users). The DHN system is composed of the main distribution network (DHN) and the following system components:

- Production plant(s)
- Substation(s)

Even though components like prosumers or storages are not included in this work, the described methodology does not necessarily exclude them.

The purpose of the DHN system is to provide an energy service, more precisely a heating service, to external consumers through the utilization of an external energy service from the producers as shown in Figure 2-2. Based on that, the DHN system is defined in Figure 3-1.
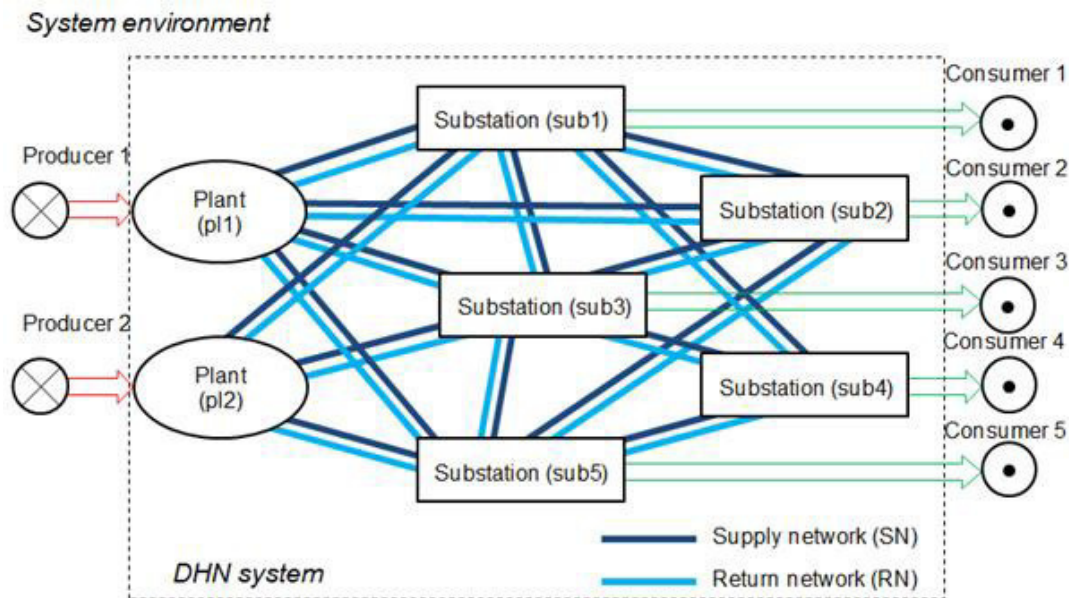
Figure 3-1: Representation of the DHN system

The plant component (pl) is a component to integrate generic producers. It receives an energy service in the form of thermal- and mechanical energy/exergy from the producer. The purpose of the plant component is to function as an auxiliary component connected to the DHN. There it extracts energetic flow from the return network (RN) and increases its energetic level according to the request of the supply network (SN). The DHN in Figure 3-1 is the main distribution network without considering subnetworks. DHN is used to abbreviate main distribution network, while SN and RN are used to refer to the supply network and return network, respectively.

The substation component (sub) is used to integrate generic consumers into the system. The purpose of the component is to integrate the thermodynamic behavior of the consumer request into the system through the exchange of thermal energy/exergy. Plants and substations are called components of the system, while the supply and return network are referred to as the network of the DHN system.

Remark: The definition of the system model complies with the attributes of smart thermal networks as discussed in the state of the art. Even though prosumers and storages are not explicitly shown, a prosumer can be modelled as a plant or substation component depending on its current operation while a storage model can be included at any point of the network.

In order to apply thermoeconomic analysis to the dynamic simulation of the DHN system, the thermo-hydraulic and energetic behavior of the system must be known. Thus, the methodology applied to develop a thermoeconomic model includes three layers of perspective:

1. Thermo-hydraulic system layer (THSL)
2. Energetic system layer (ESL)
3. Thermoeconomic system layer (TESL)

Those layers are hierarchically organized. In the THSL, thermodynamic- and hydraulic models are applied to simulate the pressure and temperature distribution in the system. This is done through the use of the STTH model described in the state of the art, see section 2.3. In using the results of the THSL, the ESL is able to derive energetic flows corresponding with the water flow in the system. Those energetic flows include mechanical energy/exergy corresponding to pumping power and thermal energy- and exergy flows considering the thermal power in the system. Energetic flows in this context refer to energy- and exergy flows alike. Once the energetic flows of the system are known, the thermoeconomic analysis is applied in the TESL. It must be noted, that the energy balances required for the ESL have been previously used in the STTH model developed by (Guelpa 2016), while the required exergy balances (including destructions) are intrinsic part of this work.

The results of the THSL, which are the pressure and temperature distribution in the DHN, are treated as given. For ESL and TESL, the methodology includes the development of models for the DHN system and its respective system components. Those models are applied to consider both pumping power and thermal power through the use of thermal- and mechanical balance equations.

3.1.2 Definition of system components

In this section, the definition of the system components including plants and substations is given. Section 3.1.2.1 deploys a black-box model for the plant, followed by section 3.1.2.2 which provides a thermodynamic model for the substations.

3.1.2.1 Black-box model for plants

The purpose of the plant model is to inject energy/exergy into the SN while reusing the water flow returning from the RN. The plant receives mechanical- and thermal flows to establish the pressure and temperature in the network. More precisely, such a plant extracts a flow of water from the RN, increases its energetic level through the increase of temperature and pressure, and injects it back into the SN.

Examples of such plants are cogeneration plants (CHP(s)), heating plants (HPs), boilers, waste-heat incineration plants, industrial plants (IPs) and renewable energy plants (REPs) like solar thermal- or geothermal plants. It is important to highlight that plants only inject energy/exergy to the SN and extract energy/exergy from the RN.

The objective of the plant component is to function as an auxiliary component for the dynamic simulation of the DHN system. To be precise, the purpose of the component is not to provide exact thermodynamic behavior of the producer but rather to deliberately exclude its behavior in order to focus on the impact of the network and the substations only. This can be explained through the network simulation, where supply- and return are simulated independently and the amount of energy/exergy provided to the system is estimated as the energy/exergy differences between supply- and return flow. Given those assumptions, the generic plant model is defined in Figure 3-2.
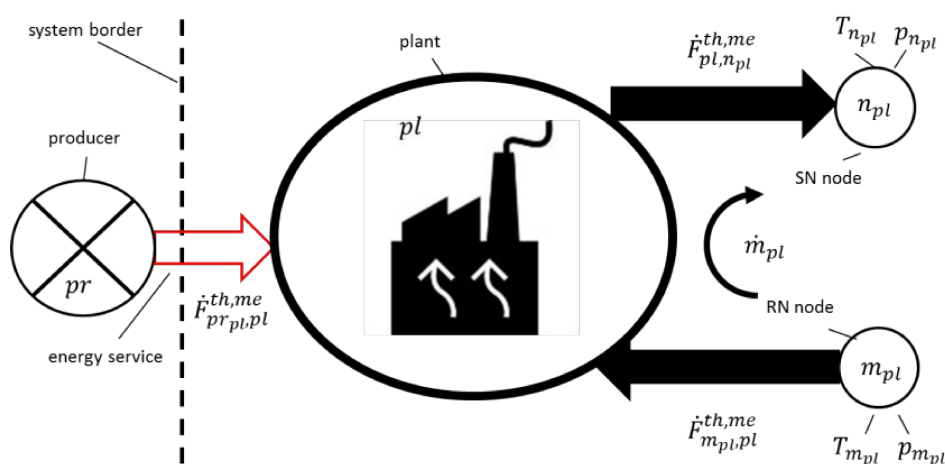
Figure 3-2: Definition of the plant component

The plant model considers thermal- and mechanical flows $\left(\dot{F}^{th,me}\right)$, which can represent a flow of cost or a flow of energy/exergy depending on the system layer under consideration. Those flows $\dot{F}^{th,me}$ are associated with flows either entering from the RN $\left(\dot{F}^{th,me}_{m_{pl},pl}\right)$ at the connection node to the RN $\left(m_{pl}\right)$, entering from the external producer $\left(\dot{F}^{th,me}_{pr_{pl},pl}\right)$ or exiting to the SN $\left(\dot{F}^{th,me}_{pl,n_{pl}}\right)$ at the connection node to the SN $\left(n_{pl}\right)$. A plant is generally connected to the SN through n_{pl} and to the RN through m_{pl}.

Furthermore, the temperature and pressure at the SN node $T_{n_{pl}}, p_{n_{pl}}$ and the RN node $T_{m_{pl}}, p_{m_{pl}}$ represent the temperature and pressure at the connection nodes to the DHN. While the temperature and pressure, set at the SN, are boundary conditions for the SN network, the values at the RN node are a result of the DHN simulation.

It must be noted, that no losses/destructions are included in the plant model, hence the losses associated with the generation of secondary energy (heat) from primary energy (gas, biomass etc.) is not taken into account. Thus, the energy/exergy needed to increase temperature and pressure of the return flow is equal to the energy/exergy requested by the producer. This enables to be independent from the thermodynamic behavior of the producer (e.g. a certain existing production plant) and allows studying the dynamics of the network without the influence of a certain production technology. Hence, the conversion of primary to secondary energy in the plant is not taken into account. Even though thermodynamic behavior of the component is not taken into account, the mass flow rate in the plant component $\dot{m}_{pl}$ is explicitly drawn, because of its use in a later case study.

3.1.2.2 Thermodynamic model for substations

The main objective of a substation is to provide energy service (heating) to an external consumer. This consumer can represent a connected subnetwork or the connection to the internal heating loop of a single building or a dwelling. The impact of the heating request by that consumer depends on various factors such as temperature level, magnitude of energy requested at certain time periods etc. In this work, the consumer is characterized as a subnetwork while the substation, which connects the DHN to the subnetwork, is the component with which the thermodynamic behavior of the subnetwork is integrated. Thus, a substation is modeled on a thermodynamic ba-

sis in order to take operations of a subnetwork and its respective temperature levels and demand profiles into account. According to industrial practice, the substation is modeled as a counter-current heat exchanger (HX), see Figure 3-3.
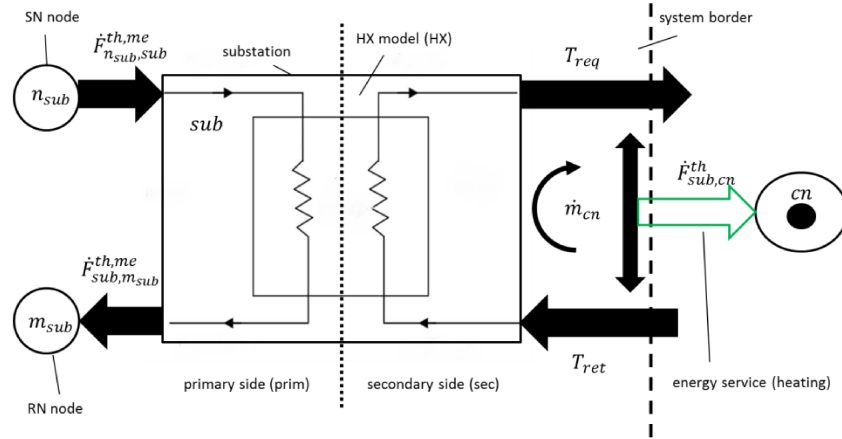
Figure 3-3: Thermodynamic model for substations

It is important to note, that the objective of the substation is to provide a thermal energy service only; thus there is no mechanical energy or exergy provided to the consumer. This thermal energy service is represented by a general flow $\left(\dot{F}_{sub,cn}^{th}\right)$ at the secondary side of the HX model and is exiting the DHN system to the consumer. This flow can be either a cost- or an energetic flow, while the latter represents the thermal energy/exergy demand of the consumer.

On the primary side, one flow $\left(\dot{F}_{n_{sub},sub}^{th,me}\right)$ is entering the substation from the SN at (n_{sub}) while another flow $\left(\dot{F}_{sub,m_{sub}}^{th,me}\right)$ is exiting to the RN at node (m_{sub}). The heating service (green arrow in Figure 3-3) is represented by the energy/exergy difference of the secondary side of the HX model.

To simulate the thermodynamic behavior of the consumer, a mass flow rate $(\dot{m}_{cn})$, representing the mass flow in the subnetwork, is introduced. Additionally, temperature levels of that flow at the inlet (T_{ret}) and outlet (T_{req}) of the secondary side of the HX are introduced to integrate a requested and returning temperature from the consumer. Thus, T_{req} represents the temperature requested by the consumer (e.g. the supply temperature of a subnetwork), while T_{ret} is the temperature of the return line of that subnetwork. This allows integrating both energetic- and exergetic behavior of the heat request where the thermal inertia of the end user is included through the temperature and mass flow rates at the secondary side of the HX.

3.1.3 Numerical DHN model

In this section, a numerical approach for the abstraction of the DHN is provided, which is in accordance to the STTH model. As previously described, the district heating network is composed of two networks, namely supply- and return network. Those have different purposes. The purpose of the SN is to transport energy/exergy from the plants to the substations. Since the DHN is a closed system, the purpose of the RN is to transport the cooled-down water back to the plants. Even though they are interconnected through the system components, their physical topology can be represented with one single model and applied subsequently. The model of the DHN is based on graph theory, which represents the physical topology of the network and can be used for both SN and RN.

Large DHN might cover districts or even whole cities with possibly many plants like CHPs and boilers as well as a vast amount of substations distributed throughout the network. Given that a DHN is mainly composed of tubes and interconnections between those, such large networks are far from being streamlined but rather show many interconnections. Furthermore, due to the operation schedule of the plants in the network, the water flow can vary both in throughput and in direction. Thus, a numerical model for large DHN must represent this described behavior in a mathematical way. For that, the network topology according to graph theory has been chosen.

In order to develop a numerical model for thermoeconomic analysis, the underlying network model must be compatible of the STTH model. Thus, the assumptions of the STTH model are taken into account for the formulation of the numerical thermoeconomic model. For that, a generic control volume is defined which is first in accordance with the STTH model and second able to integrate the principles of different costing techniques as presented in this work.

The objective of a control volume is to divide the network into subsequent sections to which the balance equations can be applied numerically. Since the calculation of energy, exergy or cost related variables are based on different physical behavior, various different control volumes are needed. Those can be generated through adaptation of the generic control volume definition in Figure 3-4, which introduces the nomenclature used for the balance equations.
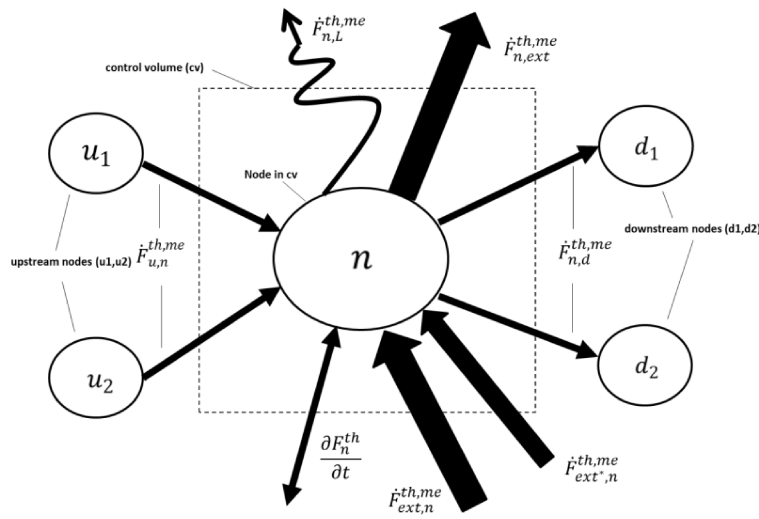
Figure 3-4: Generic control volume (CV) definition

First of all, it must be noted that the control volume definition is developed based on an arbitrary node (n). This node might either be a node in the SN n or a node in the RN (m). For reasons of better readability, this distinction is not explicitly shown in Figure 3-4. In the generic model, the control volume of a node n including two upstream (u_1, u_2) and two downstream (d_1, d_2) nodes are given. Furthermore, this control volume (cv) could be located anywhere in the network graph, either as a simple connection/junction or a connection to another system component as a boundary node.

The generic control volume includes several generic flows $\left(\dot{F}^{th,me}\right)$ which could represent cost flows and energetic flows. Flows associated with branches of the graph, are either upstream $\left(\dot{F}_{u,n}^{th,me}\right)$ or downstream $\left(\dot{F}_{n,d}^{th,me}\right)$ flows. Furthermore, external flows entering $\left(\dot{F}_{ext,n}^{th,me}, \dot{F}_{ext^*,n}^{th,me}\right)$ and exiting $\left(\dot{F}_{n,ext}^{th,me}\right)$ are considered. A flow $\dot{F}_{ext,n}^{th,me}$ is an external flow entering from a system component, while a flow $\dot{F}_{ext^*,n}^{th,me}$ is entering from the system environment. This distinction is important, when e.g. cost flows of investment and maintenance are considered. In order to take dynamic change of thermal flows into account, a term $\left(\frac{\partial F_n^{th}}{\partial t}\right)$ is introduced. This term considers change in thermal energy/exergy/cost in the control volume. The flow $\left(\dot{F}_{n,L}^{th,me}\right)$ is associated with losses (or destruction) in the control volume.

The generic CV is used for a better understanding of the numerical concept in this work. According to the system layer under consideration, adoptions to this CV model

are detailed in the corresponding sections. As for the branch flows, several external in- and outflows could appear for a certain control volume. Here, those are represented only by one combined flow.

The control volume balances involve the calculation of flow variables at branches and other properties assigned to network nodes. Therefore, the finite-volume method must include a mathematical relation between node and branch variables. For that, the upwind scheme is used (Patankar 1980). When applying the upwind scheme to the control volumes, the branch variables are calculated on the basis of their upstream nodes. This means, that e.g. the flow of energy cost in the branch is calculated based on the unit cost of its corresponding upstream node. This cost flow is assigned to the branch and enters with the calculated value at the control volume boarder of its downstream node. This is equally applied to every variable associated with a branch in the network.

3.2 Energetic system layer (ESL)

Given the temperature and pressure distribution obtained through applying the STTH model, the calculation of energetic flows must be carried out. This is done through the energetic system layer (ESL).

3.2.1 Definition of energetic flows and properties

First of all, a classification of the used energetic flows and properties is presented in Table 3-1.

Table 3-1: Classification of variables in the ESL

		Energy	Exergy
Thermal	Flow	Thermal energy $\left(\dot{\phi}^{th}\right)$	Thermal exergy $\left(\dot{\psi}^{th}\right)$
	Prop.	Thermal loss $\left(\dot{\phi}_L^{th}\right)$	Thermal exergy destruction $\left(\dot{\psi}_D^{th}\right)$
		Transient energy $\left(\frac{\delta\phi^{th}}{\delta t}\right)$	Transient exergy $\left(\frac{\delta\psi^{th}}{\delta t}\right)$
Mechanical	Flow	Mechanical energy $\left(\dot{\phi}^{me}\right)$	Mechanical exergy cost $\left(\dot{\psi}^{me}\right)$
	Prop.	Mechanical loss $\left(\dot{\phi}_L^{me}\right)$	Mechanical exergy destruction $\left(\dot{\psi}_D^{me}\right)$

Flows and properties are calculated for both energy and exergy, based upon either pressure or temperature. Thermal energy $\left(\dot{\phi}^{th}\right)$ and exergy $\left(\dot{\psi}^{th}\right)$ flows are consequences of the temperature (T) level of the water in the network and are assigned to network branches. Thermal losses $\left(\dot{\phi}_L^{th}\right)$ and thermal destruction $\left(\dot{\psi}_D^{th}\right)$ arise in the control volumes and are therefore assigned to network nodes. Equally this is done for transient energy $\left(\frac{\delta\phi^{th}}{\delta t}\right)$ and transient exergy $\left(\frac{\delta\psi^{th}}{\delta t}\right)$.

Based on the pressure (p) levels in the network, the same is true for mechanical energy $\left(\dot{\phi}^{me}\right)$ and exergy $\left(\dot{\psi}^{me}\right)$ flows as well as for the mechanical losses $\left(\dot{\phi}_L^{me}\right)$ and destructions $\left(\dot{\psi}_D^{me}\right)$, with the difference, that no transient mechanical flow exist. Since the water is considered incompressible, the pressure propagation travels with the speed of sound and is therefore independent of time when evaluation steps of hours or even minutes are considered. This assumption is used in this work and therefore allows neglecting a dynamic change in pressure in the network. However there could be cases where mechanical transients might be present and therefore need to be considered, but this is not true for DHN system. Given the time resolution of the evaluation, usually in hours or minutes and the propagation of pressure change with the speed of sound (>300 m/s), a transient pressure change does not occur due to the instantaneous change of pressure for e.g. an hourly timestep.

Although mechanical energy and exergy are explicitly mentioned for the sake of completeness, it must be noted that they are practically equal, which directly follows from the definition of physical exergy (Kotas 1995).

It was mentioned, that only the definition of thermal and- mechanical exergy is intrinsic part of this work. Therefore, only the control volume for exergy is developed in the next section. For the sake of completeness, the control volumes for energy analysis are given in the Appendix; see Figure A-1 and the corresponding equations (A.1) – (A.5).

3.2.2 ESL for the DHN model

In this section the ESL for the DHN is developed in order to provide the necessary information on exergy flows and exergy properties in the network. It is divided into two parts, considering both thermal- and mechanical streams. For every costing ap-

proach, the generic control volume in Figure 3-4 is used as a basis and adapted accordingly.

3.2.2.1 Calculation of thermal exergy

The thermal exergy flows and properties for the control volumes of the DHN model are derived. This involves the calculation of each single flow and property based on the given balance equations and the respective thermodynamic equations. Figure 3-5 shows the control volume for a general node n for thermal exergy.
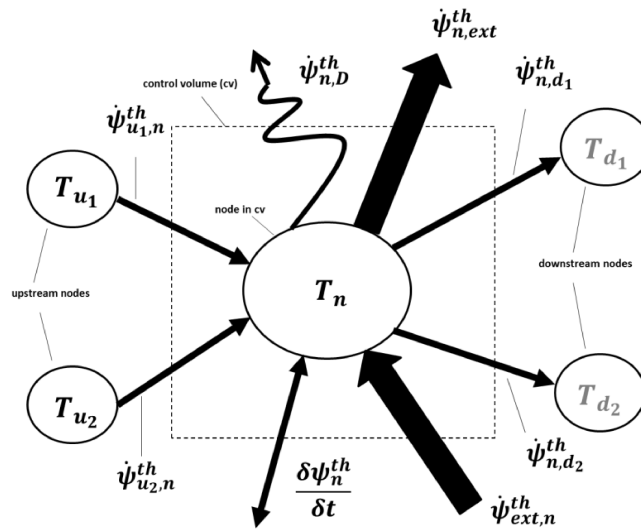
Figure 3-5: Control volume for thermal exergy

Here, the temperatures (T_n) are given at each CV node. The thermal flows are depended on the temperature at the upstream node. Every entering- and exiting branch is associated with a thermal exergy flow, while external exergy flows entering and existing are also considered. The reason for the shaded representation of the downstream nodes is, because they are not part of the control volume balance.

Two thermal exergy flows from upstream nodes are entering the cv $\left(\dot{\psi}_{u_1,n}^{th}, \dot{\psi}_{u_2,n}^{th}\right)$, while two others $\left(\dot{\psi}_{n,d_1}^{th}, \dot{\psi}_{n,d_2}^{th}\right)$ are exiting the CV to the downstream nodes. Furthermore, external flows are considered. Those are flows entering $\left(\dot{\psi}_{ext,n}^{th}\right)$ or exiting $\left(\dot{\psi}_{n,ext}^{th}\right)$ to other system components. Dynamic change of exergy in the CV $\left(\frac{\delta\psi_n^{th}}{\delta t}\right)$ must be considered in order to account for the dynamic behavior of the network. In order to account for exergetic losses, thermal destruction $\left(\dot{\psi}_{n,D}^{th}\right)$ is defined in the CV, because every (irreversible) energetic transformation is accompanied by an increase of entropy (Baehr & Kabelac 2009).

According to the definition of the CV, the following control volume balance for thermal exergy can be written down in (3.1).

$$\sum_i \dot{\psi}_{u_i,n}^{th} + \dot{\psi}_{ext,n}^{th} - \sum_j \dot{\psi}_{n,d_j}^{th} - \dot{\psi}_{n,ext}^{th} - \frac{\delta \psi_n^{th}}{\delta t} - \dot{\psi}_{n,D}^{th} = 0 \qquad (3.1)$$

Entering external exergy flows $\dot{\psi}_{ext,n}^{th}$ between the network and system components are boundary conditions to the control volume. Given that the temperature at each network node is known, thermal exergy flows in the branches $\left(\dot{\psi}_{u_i,n}^{th}, \dot{\psi}_{n,d_j}^{th} \right)$ as well as exergy flows exiting to system components $\left(\dot{\psi}_{n,ext}^{th} \right)$ can generally be calculated through (3.2),

$$\dot{\psi}_{u,n}^{th} = \dot{m}_{u,n} \cdot cp \left[T_u - T_{ref} - T_{ref} \, ln \left(\frac{T_u}{T_{ref}} \right) \right] \qquad (3.2)$$

where $\left(\dot{m}_{u,n} \right)$ is the mass flow rate from the upstream to the downstream node, or the mass flow rate exiting to the system component, T_u is the temperature at the upstream node, T_{ref} is the reference temperature of the system environment which is generally set at 10 °C and (cp) is the heat capacity which is used constant with a value of 4.186 kJ/kgK (equal to cv for water under the present assumptions). It must be noted that (3.2) can be used to determine both exergy flows of branches entering $\dot{\psi}_{u_i,n}^{th}$ and exiting $\dot{\psi}_{n,d_j}^{th}$ in the CV.

Transient thermal exergy $\frac{\delta \psi_n^{th}}{\delta t}$ accounts for the dynamic behavior of exergy stored and released in the control volume, caused by a change of temperature (T_n) at the control volume node in time. For evaluation of $\frac{\delta \psi_n^{th}}{\delta t}$, the change of exergy in the control volume with respect to time is calculated using (3.3),

$$\frac{\delta \psi_n^{th}}{\delta t} = \frac{\delta}{\delta t} \left\{ M_n \cdot cp \left[T_n - T_{ref} - T_{ref} \, ln \left(\frac{T_n}{T_{ref}} \right) \right] \right\} \qquad (3.3)$$

where (M_n) is the mass in the control volume. Differentiated with respect to time, this numerically leads to (3.4),

$$\frac{\Delta \psi_n^{th}}{\Delta t} = M_n \cdot cp \left\{ \left[\frac{T_n^t - T_n^{t-1}}{\Delta t} \right] - \left[\frac{T_{ref}}{T_n^t} \left(\frac{T_n^t - T_n^{t-1}}{\Delta t} \right) \right] \right\} \qquad (3.4)$$

where (T_n^t) is the temperature of node n at timestep Δt and (T_n^{t-1}) is the temperature of that node at the previous timestep. It must be noted that all variables necessary for the calculation of those exergy flows are provided by the STTH model.

An example explains the behavior in more detail. During steady state, downstream nodes must show lower temperatures than their upstream nodes, due to the thermal losses along the branch. In case the direction of the flow reverses, the temperature of the upstream node is now lower than its downstream node. This will lead to a temperature decrease in that control volume depending on the velocity in the branches. During the following cooling phase, the control volume without transient term would show a violated exergy balance, due to the fact that more exergy is exiting then entering (because those flows depend on the upstream temperatures). Therefore, there must be the term $\frac{\delta \psi_n^{th}}{\delta t}$ added to the balance, which accounts for the exergy stored or released during unsteady heating- or cooling phases of the control volume. The thermal exergy destruction $(\dot{\psi}_{n,D}^{th})$ can finally be derived through the exergy balance in (3.1).

3.2.2.2 Calculation of mechanical exergy

The mechanical exergy flows are a consequence of the pressure distribution in the network, see Figure 3-6.
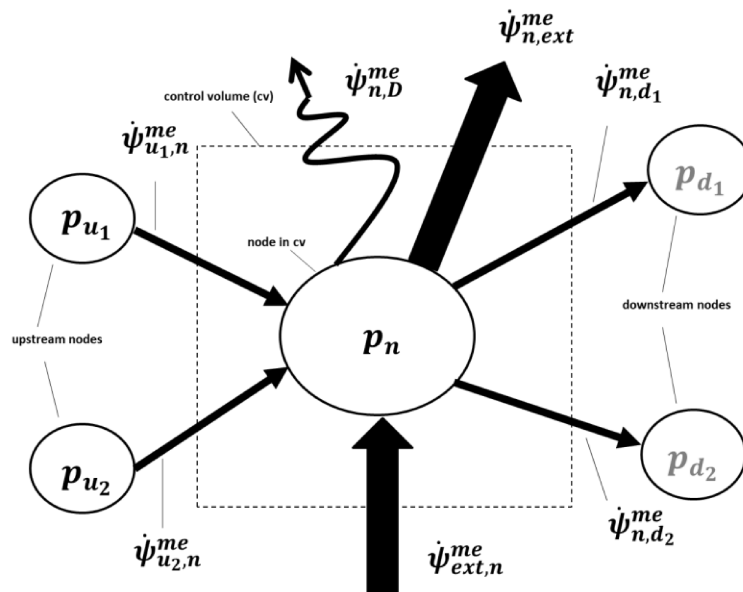
Figure 3-6: Control volume for mechanical exergy

Mechanical exergy flows are associated with branches, while pressure values are associated with nodes. Similarly to the thermal part, mechanical exergy flows are calculated based on mass flow rates in the branch and the pressure of the upstream node. There are inflows of mechanical exergy $\left(\dot\psi_{u_1,n}^{me}, \dot\psi_{u_2,n}^{me}\right)$ from upstream nodes and exiting mechanical exergy flows $\left(\dot\psi_{u,d_1}^{me}, \dot\psi_{n,d_2}^{me}\right)$ to downstream nodes. Furthermore external mechanical exergy inflowing $\left(\dot\psi_{ext,n}^{me}\right)$ and outflowing $\left(\dot\psi_{n,ext}^{me}\right)$ represent flows to other system components. Mechanical exergy destruction $\left(\dot\psi_{n,D}^{me}\right)$ also occurs in the cv.

The main difference to the thermal model is the lack of a transient term for the change in mechanical exergy in the control volume. The reason has been already discussed and lies in the assumption of the STTH model (Guelpa 2016).

The balance equation for the control volume for mechanical exergy is written in (3.5).

$$\sum_i \dot\psi_{u_i,n}^{me} + \dot\psi_{ext,n}^{me} - \sum_j \dot\psi_{n,d_j}^{me} - \dot\psi_{n,ext}^{me} - \dot\psi_{n,D}^{me} = 0 \qquad (3.5)$$

External inflows $\left(\dot\psi_{ext,n}^{me}\right)$ are boundary conditions to the control volume. Exergy flows in the branches $\left(\dot\psi_{u_i,n}^{me}, \dot\psi_{n,d_j}^{me}\right)$ and to external system components $\left(\dot\psi_{n,ext}^{me}\right)$ can be derived through (3.6) after (Kotas 1995),

$$\dot\psi_{u,n}^{me} = \dot m_{u,n} \left[\frac{p_u - p_{ref}}{\rho}\right] \qquad (3.6)$$

where (p_u) is the pressure of the upstream node, (p_{ref}) is the reference pressure of the system environment (set at 1 bar) and (ρ) is the density of the water which is considered to be constant and evaluated at 100 °C. Finally, mechanical destruction $\dot\psi_{n,D}^{me}$ can be calculated solving the mechanical exergy balance in (3.5).

3.2.3 ESL for system components

In this section, the calculation of thermal energy and exergy is given for the system components. This includes the necessary equations for the plant and substation components.

3.2.3.1 ESL for the plant

The ESL model for plant components consists of two inflowing- and one outflowing energy/exergy flow, see Figure 3-7.

The two inflowing streams are associated with energy/exergy returning from the RN $\left(\dot{\phi}_{m_{pl},pl}^{th,me}, \dot{\psi}_{m_{pl},pl}^{th,me}\right)$ and energy/exergy extracted from the producer $\left(\dot{\phi}_{pr_{pl},pl}^{th,me}, \psi_{pr_{pl},pl}^{th,me}\right)$. The third stream represents energy/exergy supplied to the SN $\left(\dot{\phi}_{pl,n_{pl}}^{th,me}, \dot{\psi}_{pl,n_{pl}}^{th,me}\right)$, which is, in fact, the amount of energy/exergy requested by the SN.
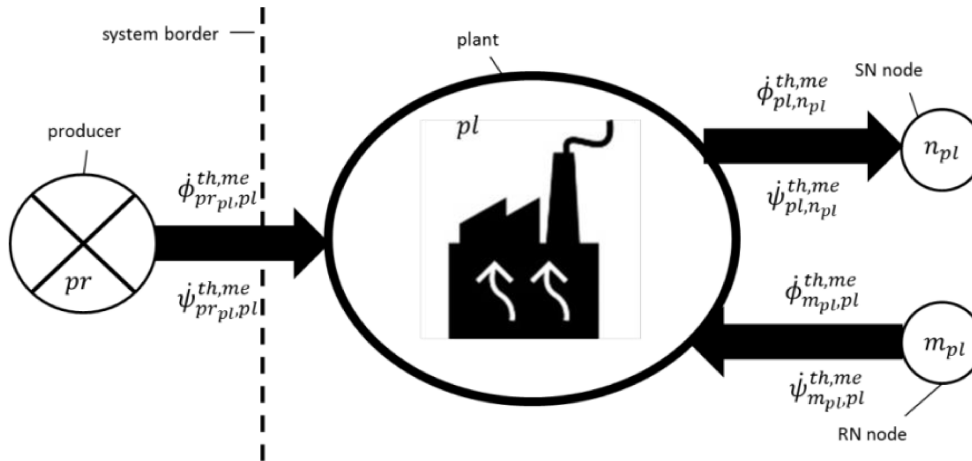
Figure 3-7: ESL model for the plant component

The energy and exergy extracted from the producer, which represents the energy and exergy requested by an existing production plant, is defined as the difference between the returning energy/exergy by the RN and the requested energy/exergy by the SN.

Considering those assumptions, thermal- and mechanical energy flows are calculated through the following balance equation in (3.7),

$$\dot{\phi}_{pr_{pl},pl}^{th,me} - \dot{\phi}_{m_{pl},pl}^{th,me} - \dot{\phi}_{pl,n_{pl}}^{th,me} = 0 \tag{3.7}$$

where $\dot{\phi}_{m_{pl},pl}^{th,me}$ is equal to the energy extracted $\dot{\phi}_{m_{pl},ext}^{th,me}$ from node m_{pl} and $\dot{\phi}_{pl,n_{pl}}^{th,me}$ is a boundary condition to the component which depends on the amount of energy requested at node n_{pl}. Given both this energy request and the energy extracted from the RN, the amount of energy requested from the producer $\dot{\phi}_{pr_{pl},pl}^{th,me}$ can be determined through (3.7). This flow $\dot{\phi}_{pr_{pl},pl}^{th,me}$ is the amount of mechanical- or thermal energy provided by the producer and therefore the energy service which has to be provided to the DHN system as a whole.

Similarly as for energy, the exergy balance for the plant component is written in (3.8),

$$\dot{\psi}_{pr_{pl},pl}^{th,me} - \dot{\psi}_{m_{pl},pl}^{th,me} - \dot{\psi}_{pl,n_{pl}}^{th,me} = 0 \tag{3.8}$$

where $\dot{\psi}_{m_{pl},pl}^{th,me}$ is equal to exergy extracted $\dot{\psi}_{m_{pl},ext}^{th,me}$ from node m_{pl} and $\dot{\psi}_{pl,n_{pl}}^{th,me}$ is a boundary condition to the component which depends on the amount of exergy requested at node n_{pl}. Given both this exergy request and the exergy extracted from the RN, the amount of exergy requested from the producer $\dot{\psi}_{pr_{pl},pl}^{th,me}$ can be determined through (3.8). This flow $\dot{\psi}_{pr_{pl},pl}^{th,me}$ is the amount of mechanical or thermal exergy provided by the producer.

3.2.3.2 ESL for the substation

The ESL of the substation component is used to represent thermodynamic behavior of the consumers. Figure 3-8 shows the ESL model for a general substation.
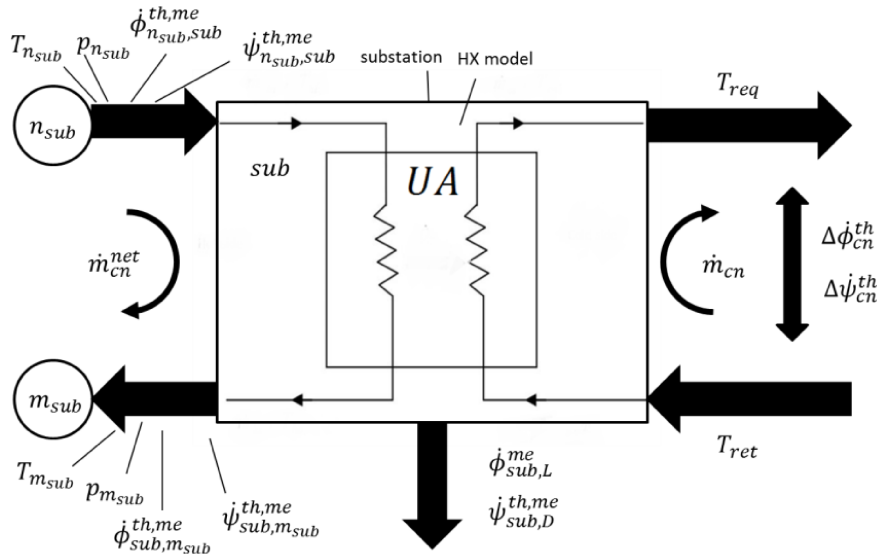
Figure 3-8: ESL model for substation component

Since the SN and RN are connected at the primary side of the HX model, energetic streams are associated with energy/exergy entering $\left(\dot{\phi}_{n_{sub},sub}^{th,me}, \dot{\psi}_{n_{sub},sub}^{th,me}\right)$ and exiting $\left(\dot{\phi}_{sub,m_{sub}}^{th,me}, \dot{\psi}_{sub,m_{sub}}^{th,me}\right)$ the HX model.

Entering flows $\dot{\phi}_{n_{sub},sub}^{th,me}, \dot{\psi}_{n_{sub},sub}^{th,me}$ are calculated from the energy- and exergy control volume balances of node n_{sub}. In Figure 3-8, the temperature and pressure of the upstream node are assigned to those flows. For exiting flows $\dot{\phi}_{sub,m_{sub}}^{th,me}, \dot{\psi}_{sub,m_{sub}}^{th,me}$ the

energetic flows are calculated from the substation model and resulting temperatures and pressures are set as boundary conditions to the RN in the THSL.

The secondary side is the connection of the substation to its consumer, or more precisely to a connected subnetwork. The energy $\Delta\dot{\phi}_{cn}^{th}$ and exergy $\Delta\dot{\psi}_{cn}^{th}$ differences on the secondary side of the HX model are representing the amount of energy and exergy needed to provide the heating service to the consumer. Thus, this approach considers the effort of increasing the energy/exergy level on the secondary side of the HX model as the thermal energy service. It is important to note, that there is no mechanical energy/exergy difference defined at the consumer side, because the HX only exchanges thermal energy/exergy. Furthermore it must be remarked that this definition includes the exergetic losses on the secondary side in a general way. Depending on the heating system installed in the final consumer, the requested and returning temperature might considerably be different between e.g. a radiator heating or floor heating system. Since a floor heating system operates at much lower requested temperatures, the exergy extracted by the consumer is lower than for a radiator heating system. In any case, the consumer behavior is modeled through a time-constant mass flow rate at the secondary side, which leads to distinct levels of temperature. This is further detailed in the case study at a later stage in this work.

For integrating thermodynamic behavior of the consumer, the substation model includes a mass flow $(\dot{m}_{cn})$, an inflow temperature (T_{ret}) to consider the return temperature of the secondary loop and an outflow temperature (T_{req}) to consider the requested temperature by the consumer. Furthermore a term to consider exergy destruction $(\dot{\psi}_{sub,D}^{th,me})$ is integrated, while energy losses only occur for the mechanical part $(\dot{\phi}_{sub,L}^{me})$. The HX is defined as an ideal heat exchanger without thermal losses.

According to industrial practice, energy/exergy demand of the consumer is mainly based on T_{req} while $\dot{m}_{cn}$ is kept constant. This ensures a temperature control of the consumer. However, due to that and the fact that the STTH model, once executed for the SN, only provides information upon the inflow at the primary side of the HX model, energy- and exergy balance equations or an LMTD approach are not sufficient to solve the HX model.

Hence the NTU-method (Bejan & Kraus 2003) is used and adapted to simulate the HX in the given condition. At first, the topology of the HX must be known. Main pa-

rameter is the (UA) value which must be derived from appropriate data. Second, the mass flow rate entering at the primary $(\dot{m}_{cn}^{net})$ and secondary side $(\dot{m}_{cn})$ must be known. Mass flow rate from the SN is known after execution of the STTH model, while $\dot{m}_{cn}$ can be calibrated based on available data. Furthermore, the temperature $T_{n_{sub}}$ and pressure $p_{n_{sub}}$ from the SN at node n_{sub} are a result of the STTH model.

The NTU method provides the following relation for a counter-current HX, see (3.9),

$$\Delta\dot{\phi}_{cn}^{th} = \varepsilon C_{min}\left(T_{n_{sub}} - T_{ret}\right) \tag{3.9}$$

where (ε) is the effectiveness of the HX and (C_{min}) is the smaller total heat capacity of the exchanging streams. The effectiveness is a function of the number of transfer units (NTU), see (3.10),

$$\varepsilon = \frac{1-e^{-NTU(1-C_r)}}{1-C_r e^{-NTU(1-C_r)}} \tag{3.10}$$

where NTU can be derived through (3.11).

$$NTU = \frac{UA}{C_{min}} \tag{3.11}$$

This relation is valid for a counter-flow HX with a heat capacity relation (C_r) smaller than 1, given through (3.12),

$$C_r = \frac{C_{min}}{C_{max}} = \frac{min(C_{net}, C_{cn})}{max(C_{net}, C_{cn})} \tag{3.12}$$

where the total heat capacities are derived through (3.13)

$$C_{net} = cp \cdot \dot{m}_{cn}^{net} \ , \ C_{cn} = cp \cdot \dot{m}_{cn} \tag{3.13}$$

The energy balance equations (without energy losses) on both sides of the HX are written in (3.14).

$$\Delta\dot{\phi}_{cn}^{th} = \dot{m}_{cn}^{net} cp\left(T_{n_{sub}} - T_{m_{sub}}\right) = \dot{m}_{cn} cp\left(T_{req} - T_{ret}\right) \tag{3.14}$$

In those equations, ε can be determined and further used in (3.9) which can then be substituted into the energy balance on the right side of (3.14) to derive T_{ret}. Once both temperatures on one side are known, the energy balances can be executed to derive $\Delta\dot{\phi}_{cn}^{th}$ and all other remaining variables.

This approach enables a dynamic simulation of the HX based on the temperature $T_{n_{sub}}$ entering from the SN. Furthermore it assures that the temperature at the RN node depends on the thermodynamic behavior of the consumer side.

Given all thermal energy flows in the component, the remaining thermal exergy flows $\left(\dot{\psi}_{n_{sub},sub}^{th,me}, \dot{\psi}_{sub,m_{sub}}^{th,me}, \Delta\dot{\psi}_{cn}^{th}\right)$ can be calculated from the general equation for a thermal exergy flow (Kotas 1995). Finally, the thermal exergy balances can be written down in (3.15),

$$\Delta\dot{\psi}_{cn}^{th} + \dot{\psi}_{sub,D}^{th} - \dot{\psi}_{n_{sub},sub}^{th,me} + \dot{\psi}_{sub,m_{sub}}^{th,me} = 0 \tag{3.15}$$

from which the amount of thermal exergy destruction $\left(\dot{\psi}_{sub,D}^{th}\right)$ can be calculated. Differently to the energy balance in (3.14) the exergy balance considers a loss term which accounts for the exergy destroyed in the substation component. Therefore, even if the substation is an ideal exchanger of thermal energy, exergy losses occur due to the individual temperature requests of the consumer.

Apart from the thermal part of the model, the mechanical energy and exergy flows must be considered at the primary side of the HX. The pressure at the inlet of the HX $p_{n_{sub}}$ is determined by the SN, while the value at the outlet $p_{m_{sub}}$ is determined by the RN. Thus a certain pressure difference at the primary side (Δp_{sub}) will occur, see (3.16).

$$\Delta p_{sub} = p_{n_{sub}} - p_{m_{sub}} \tag{3.16}$$

This pressure difference is the results of the different pressure levels depending on the position of the substation in the network.

The corresponding mechanical energy/exergy flows at the primary side can be derived through the general equation for a mechanical exergy streams (Kotas 1995). The balance for the mechanical part of the HX can finally be written as in (3.17) - (3.18).

$$\dot{\phi}_{n_{sub},sub}^{me} - \dot{\phi}_{sub,m_{sub}}^{me} - \dot{\phi}_{sub,L}^{me} = 0 \tag{3.17}$$

$$\dot{\psi}_{n_{sub},sub}^{me} - \dot{\psi}_{sub,m_{sub}}^{me} - \dot{\psi}_{sub,D}^{me} = 0 \tag{3.18}$$

3.3 Thermoeconomic system layer (TESL)

Based on the results of the ESL, the development of the thermoeconomic system layer (TESL) can be carried out. The TESL considers the thermoeconomic model of the DHN system. The objective is to calculate cost flows associated with the energy service provided to the consumers (heating) using different costing approaches.

At first, the variables used in the TESL are defined and categorized in section 3.3.1, each of them serving a different purpose. Second, the TESL is developed for both the DHN in section 3.3.2 and the system components in section 3.3.3.

3.3.1 Definition of thermoeconomic flows and properties

The TESL consists of thermoeconomic flows and thermoeconomic properties, which are defined and categorized in Table 3-2.

Table 3-2: Classification of variables in the TESL

		Energy costing ($\phi - based$)	Thermoeconomic costing ($\psi - based$)	
Thermal	Flow	Thermal energy cost $\left(\dot{C}^{th}\right)$	Thermal exergy cost $\left(\dot{K}^{th}\right)$	Thermal thermoeconomic cost $\left(\dot{Z}^{th}\right)$
	Prop.	Unit thermal energy cost $\left(c^{th}\right)$	Unit thermal exergy cost $\left(k^{th}\right)$	Unit thermal thermoeconomic cost $\left(z^{th}\right)$
Mechanical	Flow	Mechanical energy cost $\left(\dot{C}^{me}\right)$	Mechanical exergy cost $\left(\dot{K}^{me}\right)$	Mechanical thermoeconomic cost $\left(\dot{Z}^{me}\right)$
	Prop.	Unit mechanical energy cost $\left(c^{me}\right)$	Unit mechanical exergy cost $\left(k^{me}\right)$	Unit mechanical thermoeconomic cost $\left(z^{me}\right)$

Table 3-2 shows the flows and properties in two dimensions; first according to the costing approach and second according to thermal- and mechanical flows. The costing techniques include the white-box approaches of Table 2-1. Thermal energy cost $\left(\dot{C}^{th}\right)$ and unit thermal energy cost $\left(c^{th}\right)$ are used for thermal energy costing, while $\left(\dot{C}^{me}\right)$ and $\left(c^{me}\right)$ are used for mechanical energy costing.

Similarly, thermal exergy/thermoeconomic cost $\left(\dot{K}^{th}, \dot{Z}^{th}\right)$ and unit thermal exergy/thermoeconomic cost $\left(k^{th}, z^{th}\right)$ are used for the thermal part, while mechanical

exergy/thermoeconomic cost $\left(\dot{K}^{me}, \dot{Z}^{me}\right)$ and unit mechanical exergy/thermoeconomic cost (k^{me}, z^{me}) are used for the mechanical part.

Both exergy- and thermoeconomic costing use exergy as the value stream, with the difference that thermoeconomic costs, unlike exergy costs, take also flow-independent costs like investment- or maintenance costs of the DHN system into account. Those could be e.g. investment costs for pumping equipment or costs for thermal energy/exergy production. On the contrary, energy costs use energy as the value stream (energy costing), as well as in the case where investments- or maintenance costs are included to determine the so called techno-economic solution.

Cost flows are associated to value flows. In energy costing, those cost flows are based on energy as a value flow, while in exergy- and thermoeconomic costing exergy is used for that purpose. Thus $\dot{C}^{th}$ and $\dot{C}^{me}$ are costs of thermal- and mechanical energy flows, while $\dot{K}^{th}, \dot{Z}^{th}$ and $\dot{K}^{me}, \dot{Z}^{me}$ are costs of thermal- and mechanical exergy flows, respectively. All of those cost flows are assigned to branches in the DHN model and to flows considered in the component models.

Cost properties are used to provide information about the cost of extraction of a given energetic flow. Unit energy/exergy/thermoeconomic costs are used to evaluate the cost of extraction of energy or exergy. Thus, c^{th} and c^{me} are used to describe the cost of thermal- and mechanical energy extraction at any given point in the DHN. Consequently, the same is true for k^{th}, z^{th} and k^{me}, z^{me} with which the cost of extraction of thermal- and mechanical exergy is evaluated. All given cost properties are assigned to nodes in the TESL; thus at network nodes in the DHN model.

3.3.2 TESL for the DHN model

In this section, the TESL is developed for the DHN model. It can be consequently applied to both SN and RN equally. The overall aim of the DHN model is to calculate costs of energetic flow extracted from the network, called *product cost flows*. This is achieved through the calculation of the cost properties at every point in the network from which the cost of a certain flow exiting the network can be derived.

Principally, for every unit cost variable in Table 3-2, a certain control volume must be defined. For an improved readability, only the thermoeconomic approach is shown in detail in the coming sections. This has two reasons. First the thermoeconomic model

is the most complex one, while the others can easily be derived through simplification and second the main goal of Part A is the development of a thermoeconomic model for DHN systems.

3.3.2.1 Calculation of thermoeconomic costs (thermal)

This section describes the definition and calculation of cost properties and cost flows associates with thermal exergy flows. For that, a control volume and its associated variables must be defined, according to the principles of the respective costing technique. The aim of the cv is to calculate the cost property (in this example z_n^{th}), which then offers the possibility to derive the product cost flows. Exemplarily, Figure 3-9 shows the cv for thermoeconomic costing considering only thermal exergy flows.
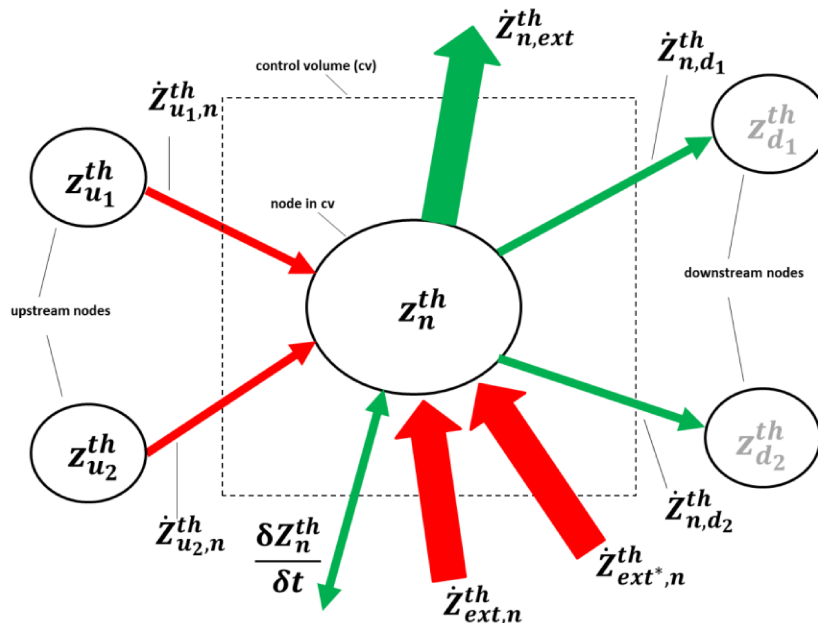
Figure 3-9: Control volume for thermoeconomic costing (thermal)

Based on the generic cv in Figure 3-4, unit thermoeconomic costs (z_n^{th}) are assigned to node n of the cv as well as to its corresponding up- $\left(z_{u_1}^{th}, z_{u_2}^{th}\right)$ and downstream $\left(z_{d_1}^{th}, z_{d_2}^{th}\right)$ nodes. There is a flow of thermoeconomic cost associated with each flow of thermal exergy in the network. This is e.g. a flow entering from an upstream node u_1 to node n, marked as $\dot{Z}_{u_1,n}^{th}$ or a flow from node n to a downstream node d_2, marked as $\dot{Z}_{n,d_2}^{th}$, indicating the node pair as a subscript of a given branch. Furthermore, there can be a flow of cost entering or exiting the control volume from the external surroundings. Those flows are not associated with branches in the graph network but rather represent connections to other system components.

An external cost flow entering can either arise from another system component $\left(\dot{Z}_{ext,n}^{th}\right)$ or consider investment/maintenance costs $\left(\dot{Z}_{ext^*,n}^{th}\right)$ from the system environment. Considering e.g $\dot{Z}_{ext,n}^{th}$, it is used to describe an inflow of thermoeconomic costs either from a plant pl to its associated node n in the SN $\left(\dot{Z}_{pl,n}^{th}\right)$ or from a substation sub to its associated node m in the RN $\left(\dot{Z}_{sub,m}^{th}\right)$. An external flow exiting the CV considers a product flow to another component $\left(\dot{Z}_{n,ext}^{th}\right)$. E.g. $\dot{Z}_{n,ext}^{th}$ is used to describe a thermoeconomic product flow either to a producer pl from its associated node m in the RN $\left(\dot{Z}_{m,pl}^{th}\right)$ or to a substation sub from its associated node n in the SN $\left(\dot{Z}_{n,sub}^{th}\right)$. It must be noted that both, $\dot{Z}_{ext,n}^{th}$ and $\dot{Z}_{n,ext}^{th}$ are external flows in the sense as they are part of the TESL, while in contrast to that, $\dot{Z}_{ext^*,n}^{th}$ is not a flow from a system component, but rather an inflow from the DHN system environment.

In the CV, flows are highlighted with either red or green. A red color indicates a fuel to the CV while a green color stands for a product. The definition of fuel and product has been thoroughly described in the state of the art and is intrinsic part of the theory of exergy costing. Therefore, cost streams from upstream nodes must be defined as fuel streams, while flows to the downstream nodes must be considered as products. This derives from the fact that the objective of a node is to receive a flow from an upstream node and distribute it towards its downstream nodes.

Furthermore, external inflows from other system components must be also considered as fuels to the CV, while external outflows are product flows. This is actually the most important product flow of the CV, if e.g. an outflow of the SN to a substation is considered. This product flow $\dot{Z}_{n,sub}^{th}$ is providing information on the thermoeconomic cost of an exergy stream exiting to the substation. The estimation of this product flow is the overall objective of the TESL for the DHN. The external inflows $\dot{Z}_{ext^*,n}^{th}$ are not fuels in the exergy costing terminology but are treated equally as such.

Additionally, a transient term $\left(\frac{\delta Z_n^{th}}{\delta t}\right)$ must be considered as a product flow. This term represents the dynamic change of costs of thermal exergy in the control volume. The reason for that lies in the underlying dynamic calculation of thermal exergy, which is described in the ESL. The dynamic term considers costs of exergy stored in the control volume during transient conditions. This dynamic change cannot be considered as a loss, since it stores and releases exergy at different timesteps; hence it must be

considered as either product or fuel. It must be highlighted that $\frac{\delta Z_n^{th}}{\delta t}$ is always considered as product flow (green) even if it is entering the CV (as a negative product flow). Remark: This assumption neglects the fact that the real unit cost of a transient flow entering the CV actually depends on the unit cost at which it was stored. Thus a more detailed approach could be to consider the average unit cost during the time when the transient flow is exiting the CV. This average cost can be calculated through the calculation of a storage term and the assessment of the amount of exergy and exergy cost exiting the CV at a certain unit cost. Therefore, an average unit cost during charging is evaluated which can be used as a unit cost for an entering exergy flow during discharging.

With the information on fuel- and product flows, the corresponding CV balance can be written down in (3.19),

$$\sum_i \dot{Z}_{u_i,n}^{th} + \dot{Z}_{ext,n}^{th} + \dot{Z}_{ext^*,n}^{th} - \sum_j \dot{Z}_{n,d_j}^{th} - \dot{Z}_{n,ext}^{th} - \frac{\delta Z_n^{th}}{\delta t} = 0 \qquad (3.19)$$

which states that the sum of product cost flows minus the sum of fuel cost flows is equal to zero. This integrates the fact that costs are preserved for every control volume.

According to the upwind scheme applied in this numerical model, the cost flows of (3.19) are derived through (3.20) – (3.23),

$$\dot{Z}_{u_i,n}^{th} = \dot{\psi}_{u_i,n}^{th} \cdot z_{u_i}^{th} \qquad (3.20)$$

$$\dot{Z}_{n,d_j}^{th} = \dot{\psi}_{n,d_j}^{th} \cdot z_n^{th} \qquad (3.21)$$

$$\dot{Z}_{n,ext}^{th} = \dot{\psi}_{n,ext}^{th} \cdot z_n^{th} \qquad (3.22)$$

$$\frac{\delta Z_n^{th}}{\delta t} = \frac{\delta \psi_n^{th}}{\delta t} \cdot z_n^{th} \qquad (3.23)$$

where $\left(\dot{\psi}_{u_i,n}^{th}\right)$, $\left(\dot{\psi}_{n,d_j}^{th}\right)$ and $\left(\dot{\psi}_{n,ext}^{th}\right)$ are the underlying thermal exergy flows entering from upstream nodes u_i, exiting to the downstream nodes d_j and exiting to an external component, respectively. The term $\left(\frac{\delta \psi_n^{th}}{\delta t}\right)$ refers to the dynamic change of thermal exergy in the CV.

Given that $\dot{Z}_{ext,n}^{th}$ and $\dot{Z}_{ext^*,n}^{th}$ are entering from the surroundings and are therefore boundary conditions to the cv, the cost balance can be rewritten through combining the above equations into (3.24),

$$\sum_i \dot{\psi}_{u_i,n}^{th} \cdot z_{u_i}^{th} + \dot{Z}_{ext,n}^{th} + \dot{Z}_{ext^*,n}^{th} - z_n^{th} \left(\sum_j \dot{\psi}_{n,d_j}^{th} + \dot{\psi}_{n,ext}^{th} + \frac{\delta\psi_n^{th}}{\delta t} \right) = 0 \text{ (3.24)}$$

from which z_n^{th} can be estimated, once the external cost inflows, the thermal exergy flows, the dynamic change of exergy in the CV and the unit costs at the upstream nodes are known. Mentioned before, (3.24) shows that the specific costs at downstream nodes do not take part in the estimation of z_n^{th}.

It is important to assure, that the proposed thermoeconomic model complies with the principles of exergy costing. At first, every flow which is defined to bear costs, is either defined as a fuel or a product flow. Second, exiting product flows have equal unit costs, which directly follows from the upwind-scheme applied. Unavoidably, the control volume suffers a certain amount of exergy destruction, which is not defined as fuel or product. This guarantees that in the case a certain node has only one upstream node, that certain node will always show higher unit costs than its upstream node. In the case several upstream nodes are connected, the node of the CV has a unit cost between the range of their upstream costs depending on the magnitude of exergy flow in the branches.

Hence it can be concluded that through this formulation of the control volume, the principles of thermoeconomic costing are well integrated.

3.3.2.2 Calculation of thermoeconomic costs (mechanical)

Similarly to thermal cost flows, mechanical cost flows must be assigned to mechanical flows of exergy. This section considers those costs associated with mechanical flows of exergy. The aim of the model is, again, to derive the cost properties and the cost flows in the network in order to evaluate the cost of extraction of mechanical exergy at a given point in the network. For that, mechanical thermoeconomic costs are assigned to branches, while unit mechanical thermoeconomic costs are assigned to the nodes of the network, see Figure 3-10.
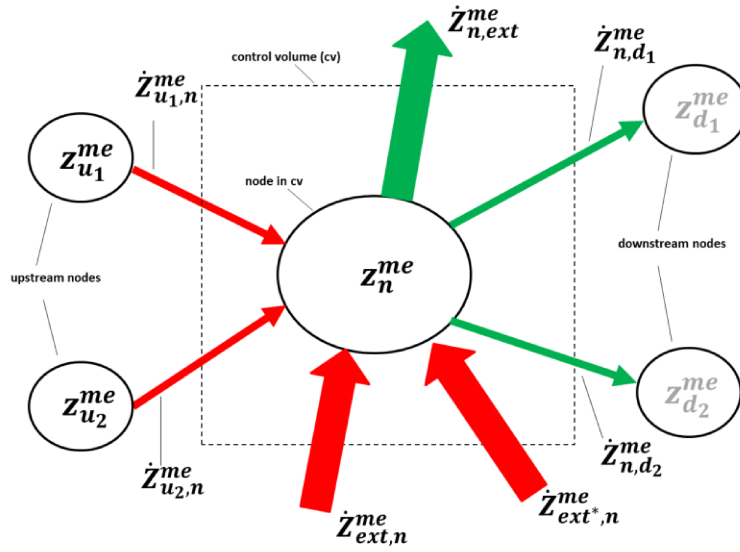
Figure 3-10: Control volume for thermoeconomic costing (mechanical)

Both the definition of the variables to the network topology as well as the definition of product and fuel and their respective calculation is equal to those used for thermal exergy; with one exception. There is no transient term of mechanical exergy considered, because dynamic change of mechanical exergy does not occur in the CV.

The notation is equal to before, thus the mechanical cost balance for thermoeconomic costing can be written as in (3.25),

$$\sum_i \dot{Z}_{u_i,n}^{me} + \dot{Z}_{ext,n}^{me} + \dot{Z}_{ext^*,n}^{me} - \sum_j \dot{Z}_{n,d_j}^{me} - \dot{Z}_{n,ext}^{me} = 0 \tag{3.25}$$

where (3.26) – (3.28) show how the mechanical cost flows are calculated.

$$\dot{Z}_{u_i,n}^{me} = \dot{\psi}_{u_i,n}^{me} \cdot z_{u_i}^{me} \tag{3.26}$$

$$\dot{Z}_{n,d_j}^{me} = \dot{\psi}_{n,d_j}^{me} \cdot z_n^{me} \tag{3.27}$$

$$\dot{Z}_{n,ext}^{me} = \dot{\psi}_{n,ext}^{me} \cdot z_n^{me} \tag{3.28}$$

Given that $\dot{Z}_{ext,n}^{me}$ and $\dot{Z}_{ext^*,n}^{me}$ are boundary conditions, the cost balance can be reformulated through (3.29),

$$\sum_i \dot{\psi}_{u_i,n}^{me} \cdot z_{u_i}^{me} + \dot{Z}_{ext,n}^{me} + \dot{Z}_{ext^*,n}^{me} - z_n^{me} \left(\sum_j \dot{\psi}_{n,d_j}^{me} + \dot{\psi}_{n,ext}^{me} \right) = 0 \tag{3.29}$$

where $\left(\dot{Z}_{u_i,n}^{me} \right)$ is the thermoeconomic cost of a mechanical exergy flow $\left(\dot{\psi}_{u_i,n}^{me} \right)$ entering from an upstream node u_i at a certain cost $\left(z_{u_i}^{me} \right)$, $\left(\dot{Z}_{n,d_j}^{me} \right)$ is the cost for an exergy

flow $\left(\dot{\psi}_{n,d_j}^{me}\right)$ exiting to a downstream node d_j at cost (z_n^{me}) and similarly to that $\left(\dot{Z}_{n,ext}^{me}\right)$ which is the cost associated with mechanical exergy exiting to another system component $(\dot{\psi}_{n,ext}^{me})$. The flows $\left(\dot{Z}_{ext,n}^{me}\right)$ and $\left(\dot{Z}_{ext^*,n}^{me}\right)$, are external cost inflows of the CV. Similarly to z_n^{th}, z_n^{me} can be estimated once the mechanical exergy flows in the network as well as the boundary conditions are available.

In this section, only thermal- and mechanical thermoeconomic costs are described in detail. The remaining definition for energy- and exergy costs and their respective equations are given in the Appendix, see Figure A-2 and Figure A-3 as well as equations (A.6) – (A.9).

Through the definition of the given control volumes, every cost flow as well as every cost property of the TESL defined in Table 3-2 can be determined for the DHN. The TESL for the DHN can be executed once the energy- and exergy flows in the DHN including the costs associated with external cost flows are known.

3.3.3 TESL for system components

In this section, the thermoeconomic model for the system components is developed. This includes the production plants and the substations.

3.3.3.1 TESL of the plant

Plants are system components which are connected to both SN and RN as well as to an external producer from which they receive energy service. In order to consider the costs associated with the operation of such plants, a thermoeconomic model must be established. In the following description, focus is laid upon the thermoeconomic costing of thermal- and mechanical exergy in the component, due to similar reasons as for the DHN. However, models for energy- and exergy costing can be similarly derived. Figure 3-11 shows the thermoeconomic costing model for plants in its general form.

The SN node n_{pl} of a plant is the injection point to the SN, while the node m_{pl} is the extraction point from the RN. The producer corresponds e.g. to an external input of energy/exergy.
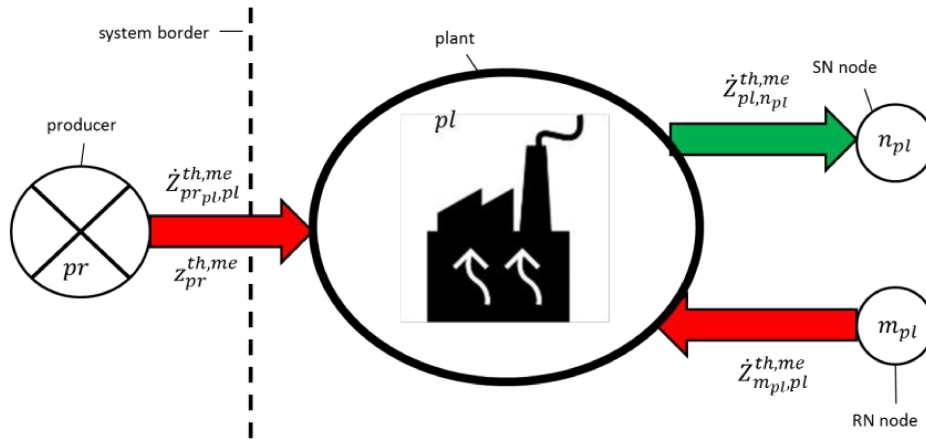
Figure 3-11: TESL of the plant component

Unlike as in the DHN model, arrows do not represent branches but are only used to represent thermoeconomic cost flows, even though their calculation is based on the unit costs of their origin. Thus no upwind scheme is applied to this component.

The thermoeconomic costs from the producer $\left(\dot{Z}^{th,me}_{pr_{pl},pl}\right)$ are the costs associated with its exergy flow $\left(\dot{\psi}^{th,me}_{pr_{pl},pl}\right)$ at a given unit cost $\left(z^{th,me}_{pr}\right)$. The cost of this flow is e.g. based on the price of thermal- or mechanical power in the producer. There is another cost flow associated with the exergy flow returning from the RN $\left(\dot{Z}^{th,me}_{m_{pl},pl}\right)$. This cost flow is equal to the external product flow $\dot{Z}^{th,me}_{m_{pl},ext}$ of node m_{pl} and is therefore determined by the cv balance equation of node m_{pl}.

At last, there is a cost flow associated with the injection of exergy into the SN. This cost flow $\left(\dot{Z}^{th,me}_{pl,n_{pl}}\right)$ is associated with exergy $\left(\dot{\psi}^{th,me}_{pl,n_{pl}}\right)$ supplied to node n_{pl} and is therefore equal to the external fuel $\dot{Z}^{th,me}_{ext,n_{pl}}$ of node n_{pl}.

It can be seen that a plant component consists of two fuel flows (red) and one product flow (green). One fuel flow is associated with the cost received by the producer, while the second one is the cost flow entering from the RN. The definition of fuel flow from the RN is crucial for the TESL of the whole DHN system, since it allows to apply the costing approach to both supply and return network. In combination with the substation model discussed in the next section, this offers the possibility to consider the impact on cost generation of a certain substation on both SN and RN leading to a dynamic simulation of cost generation.

The aim of the plant component is to provide exergy to the SN. Thus the associated cost flow is the product of that component. For a general plant (pl), the thermoeconomic cost balance can therefore be written through (3.30),

$$\dot{Z}_{pl,n_{pl}}^{th,me} - \dot{Z}_{m_{pl},pl}^{th,me} - \dot{Z}_{pr_{pl},pl}^{th,me} = 0 \tag{3.30}$$

which states that the product flow is equal to the fuel flow from producer and return network.

Considering that the cost flow from the RN, calculated from the DHN model, and the unit cost of exergy at the producer are known, the cost flow $\dot{Z}_{pl,n_{pl}}^{th,me}$ entering the SN can be derived through (3.31).

$$\dot{Z}_{pl,n_{pl}}^{th,me} = \dot{\psi}_{pr_{pl},pl}^{th,me} \cdot z_{pr_{pl}}^{th,me} + \dot{Z}_{m_{pl},pl}^{th,me} \tag{3.31}$$

3.3.3.2 TESL of the substation

Similarly to plants, substations are also connected to both supply- and return network. Although, their connection to the DHN is similar, their purpose differs. While the aim of a plant is to provide energy/exergy to the SN, the aim of the substation is to provide an energy service to the consumer. This energy service is represented by the energy $\Delta\dot{\phi}_{cn}^{th}$ or exergy $\Delta\dot{\psi}_{cn}^{th}$ difference at the secondary side of the corresponding HX-model. The TESL model developed for a general substation is given in Figure 3-12.
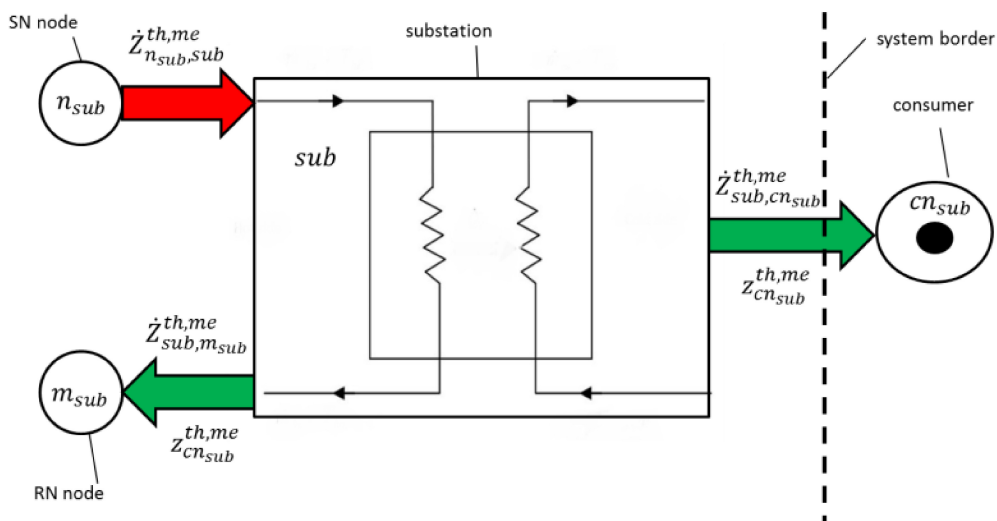
Figure 3-12: TESL of the substation component

In the TESL of the substation, there is one flow associated with a fuel (red) and two flows associated with products (green). The fuel flow $\left(\dot{Z}^{th,me}_{n_{sub},sub}\right)$ is the cost associated with the extraction of exergy $\left(\dot{\psi}^{th,me}_{n_{sub},sub}\right)$ from the SN at the corresponding node n_{sub}. The product flow to the consumer $\left(\dot{Z}^{th,me}_{sub,cn_{sub}}\right)$ represents the thermal exergy flow provided to the consumer (heating service) as well as a cost for the use of mechanical exergy of the substation. Therefore, the calculation of $\dot{Z}^{th}_{sub,cn_{sub}}$ is the overall objective of the TESL while $\dot{Z}^{me}_{sub,cn_{sub}}$ provides additional information upon the impact on pumping costs of the consumer.

The second product flow $\left(\dot{Z}^{th,me}_{sub,m_{sub}}\right)$ is associated with exergy $\dot{\psi}^{th,me}_{sub,m_{sub}}$ injected into the RN at m_{sub}. Even though this flow of cost is not intrinsic purpose of the substation component, it must be considered as either a product or a fuel flow. This is because the flow of exergy back to the plants through the RN is (subtracting losses on the way) reused by the plants and thus not a loss of the substation component. Since this flow of cost is exiting the component, it must be defined as a product flow. In order to better understand the implications of that definition, an example is given, where the purpose of the RN is analyzed from a thermal perspective.

Since a DHN is a closed hydraulic system, the purpose of the RN is to transport the water flow, after the usage by the consumer, back to the producer. In an ideal case, this water flow has as low energy/exergy content as possible to insure the most efficient use of energy/exergy by the DHN system. This also implies that a lower temperature distribution in the RN will lead to low thermal losses/destruction.

Due to the fact that the plant component reuses water from the RN, a certain cost must be assigned to this flow. A flow of exergy returning to the plant through the RN has been distributed through the SN and was left unused by a substation component. Hence, there are two factors influencing the cost of this return flow:

- Cost generation at the substation component
- Cost generation throughout the RN

In the substation component, the unit cost of the returning flow is determined by the utilization of exergy by the consumer. A low exergy extraction on the secondary side of the HX leads to a high exergy destruction in the substation and increases the unit costs of both the exergy supplied to the consumer $\Delta\dot{\psi}^{th}_{cn}$ and returning exergy

$\dot{\psi}_{sub,m_{sub}}^{th,me}$. This is assured through the principles of exergy costing, where product flows must have equal unit costs. Hence, the less exergy is utilized by the consumer, the higher the unit cost of the return flow. The second factor of cost generation corresponds to the exergy destruction in the RN which unavoidably occurs. The higher the exergy content of the return flow, the higher the thermal exergy destruction leading to another increase of unit costs throughout the RN. It can be therefore concluded, that through defining $\dot{Z}_{sub,m_{sub}}^{th}$ as a product flow of the substation, the cost generation throughout the RN between the substations and the plants is taken into account.

It must be noted that this approach includes the cost generation of a certain substation in the evaluation of unit costs entering the RN. Another approach might to be define the unit cost of the return flow equal to the one entering the SN, thus setting both unit costs equal. This might increase the unit of exergy supplied to the consumers and lower the unit cost entering the RN. Both approaches are valid regarding the theory of exergetic cost and further analysis must be done to compare the accuracy of both costing techniques regarding the true impact of individual substations.

Regarding the mechanical part, the assignment of mechanical exergy cost to consumers is more complex. Since in this work, the consumer is modelled through a HX without further analysis of pressure distribution on the secondary side, a direct flow of mechanical exergy as a "service" cannot be formulated. The reason for that, is that all closed circuits have equal pressure drops in the DHN network. The pressure drops at the primary side of the substations can therefore not be used for the evaluation of the individual contribution of the substations to the total pressure losses. Two solutions could be considered to overcome this problem. First, the contributions of pressure losses along SN and RN could be added up and considered as the individual contribution of a certain substation. Second, only the pressure drop on the SN could be taken into account for the individual contribution of mechanical exergy cost and the pressure difference on the primary side of the substation is neglected. The contributions of the RN regarding mechanical costs are then considered at the plant component, which increases the mechanical costs of exergy returning from the RN. In this work, the latter solution is preferred for which the necessary equations are provided. The unit thermoeconomic cost at the RN node must be set equal to the SN node, see (3.32).

$$z_{m_{sub}}^{me} = z_{n_{sub}}^{me} \tag{3.32}$$

This allows associating the cost of mechanical exergy entering from the SN to the individual contribution of the substation after (3.33).

$$\dot{Z}_{sub,cn_{sub}}^{me} = \dot{Z}_{n_{sub},sub}^{me} \tag{3.33}$$

Through this approach, the contribution of mechanical exergy losses of the RN are integrated into the costs associated with the flows in the SN.

It can be concluded, that through the use of the presented system models for both ESL and TESL, the calculation of $z_{cn}^{th,me}$ is possible. This offers the possibility of accounting the individual impacts of cost generation of each single consumer according to the principles of thermoeconomics.

3.4 Matrix formulation for graph-based network topology

In this section the matrix formulation is developed and shown in detail for thermal- and mechanical thermoeconomic costs. The remaining matrix equations for energy and exergy cost are provided in the Appendix, see equations (A.10) – (A.23). The aim is to provide an analytical matrix formulation to solve the control volume balances of every node. This offers a compact integration of the thermoeconomic analysis into the numerical architecture of graph-based network models. The matrix formulation must be able to integrate the thermoeconomic principles considering different costing approaches, like energy or exergy costing.

To represent the network topology, the incidence matrix $\mathbf{A}$ $(n \times b)$ is used. Every branch is associated with a flow of cost, energy or exergy. It is worth mentioning that to apply the upwind scheme integrated into the matrix, the real verses of the flow directions must be considered. This means that the matrix element $a_{n,b}$ of a flow $\dot{\psi}_{u,n}^{th}$ is indicated as in (3.34).

$$a_{n,b} = -\left|\dot{\psi}_{u,n}^{th}\right| \text{ and } a_{u,b} = +\left|\dot{\psi}_{u,n}^{th}\right| \tag{3.34}$$

Practically, A must be updated at each time step of the analysis once the direction of the flow is known by changing the signs in each column of A corresponding with negative mass flow rates.

At first all necessary variables must be written in matrix form, see (3.35) – (3.40).

$$\dot{\psi}^{th,me} = \begin{bmatrix} \left|\dot{\psi}_{b_1}^{th,me}\right| \\ \left|\dot{\psi}_{b_2}^{th,me}\right| \\ ... \\ \left|\dot{\psi}_{b}^{th,me}\right| \end{bmatrix} \quad (3.35)$$

$$\frac{\delta\psi^{th}}{\delta t} = \frac{\delta}{\delta t} \begin{bmatrix} \left|\psi_{n_1}^{th}\right| \\ \left|\psi_{n_2}^{th}\right| \\ ... \\ \left|\psi_{n}^{th}\right| \end{bmatrix} \quad (3.36)$$

$$\dot{\psi}_{extOut}^{th,me} = \begin{bmatrix} \left|\dot{\psi}_{n_1,ext}^{th,me}\right| \\ \left|\dot{\psi}_{n_2,ext}^{th,me}\right| \\ ... \\ \left|\dot{\psi}_{n,ext}^{th,me}\right| \end{bmatrix} \quad (3.37)$$

$$\dot{Z}_{extIn}^{th,me} = \begin{bmatrix} \left|\dot{Z}_{ext,n_1}^{th,me}\right| \\ \left|\dot{Z}_{ext,n_2}^{th,me}\right| \\ ... \\ \left|\dot{Z}_{ext,n}^{th,me}\right| \end{bmatrix} \quad (3.38)$$

$$\dot{Z}_{extIn^*}^{th,me} = \begin{bmatrix} \left|\dot{Z}_{ext^*,n_1}^{th,me}\right| \\ \left|\dot{Z}_{ext^*,n_2}^{th,me}\right| \\ ... \\ \left|\dot{Z}_{ext^*,n}^{th,me}\right| \end{bmatrix} \quad (3.39)$$

$$z^{th,me} = \begin{bmatrix} \left|z_{n_1}^{th,me}\right| \\ \left|z_{n_2}^{th,me}\right| \\ ... \\ \left|z_{n}^{th,me}\right| \end{bmatrix} \quad (3.40)$$

The exergy flow vector $\left(\dot{\psi}^{th,me}\right)$ contains the exergy flows of all branches in the network. The vector of transient flow of exergy $\left(\frac{\delta\psi^{th}}{\delta t}\right)$ contains all transient flows of the network nodes. The vector of external outflows $\left(\dot{\psi}_{extOut}^{th,me}\right)$ contains all external outflows of the nodes and exit the control volumes at the given specific cost $\left(z^{th,me}\right)$, while external inflows $\left(\dot{Z}_{extIn}^{th,me}\right)$ and $\left(\dot{Z}_{extIn^*}^{th,me}\right)$ are considered as boundary conditions. Now the matrix formulation can be set up using the equations (3.35) – (3.40), which leads to the matrix formation for thermal (3.41) and mechanical thermoeconomic costs (3.42),

$$\left\{\left[A \times I\dot{\psi}^{th} \times [A^+]^T\right] + I\left[\dot{\psi}_{extOut}^{th} - \frac{\delta\psi^{th}}{\delta t}\right]\right\} z^{th} = \dot{Z}_{extIn}^{th} + \dot{Z}_{extIn^*}^{th} \quad (3.41)$$

$$\left\{\left[A \times I\dot{\psi}^{me} \times [A^+]^T\right] + I\dot{\psi}_{extOut}^{me}\right\} z^{me} = \dot{Z}_{extIn}^{me} + \dot{Z}_{extIn^*}^{me} \quad (3.42)$$

from which z^{th} and z^{me} can be directly evaluated once matrix A^+ is known. A^+ is used to apply the exergy balance for every network branch in the cv and can be derived through applying (3.43) to every matrix element in A.

$$a_{n,b}^+ = max(a_{n,b}, 0) \quad (3.43)$$

This formulation can be used for any type of DHN topology, where every branch is connected to two nodes. The result is the calculation of unit costs at nodes which

was described as the objective of the thermoeconomic model for the DHN. Based on (3.41) and (3.42), z^{th} and z^{me} are calculated for every sampling time. When analyzing the time-dependent behavior of the DHN, those matrix equations must be applied to each single timestep. In that case, each term must be evaluated based on current flows and the actual directions in the branches. Through these graph-based matrices any number of network nodes and branches can be simulated in the network.

3.5 DHN system simulation

In this section, the DHN system simulation is described in detail. Besides the model development, the DHN simulation can be applied for two different objectives:

- Design and control
- Evaluation

The design and control part of the simulation is implemented to study a control strategy through mass flow rates given different design conditions of the system. This is relevant in cases where a temperature reduction in the network or the integration of a low-temperature source (e.g. waste heat from IPs) into the network is studied. Due to that, the mass flow rate must be adjusted to meet the requirements of the thermal request at lower network temperatures. The evaluation part is used for a full integration of the thermoeconomic model into DHN operation. This means, current operational profiles can be studied from a thermoeconomic viewpoint. This is relevant in case consumer impact on cost generation, thermoeconomic inefficiencies etc. are under investigation Figure 3-13 shows the complete simulation procedure which integrates both simulation parts. The relevant elements of the simulation procedure are discussed in the coming sections.
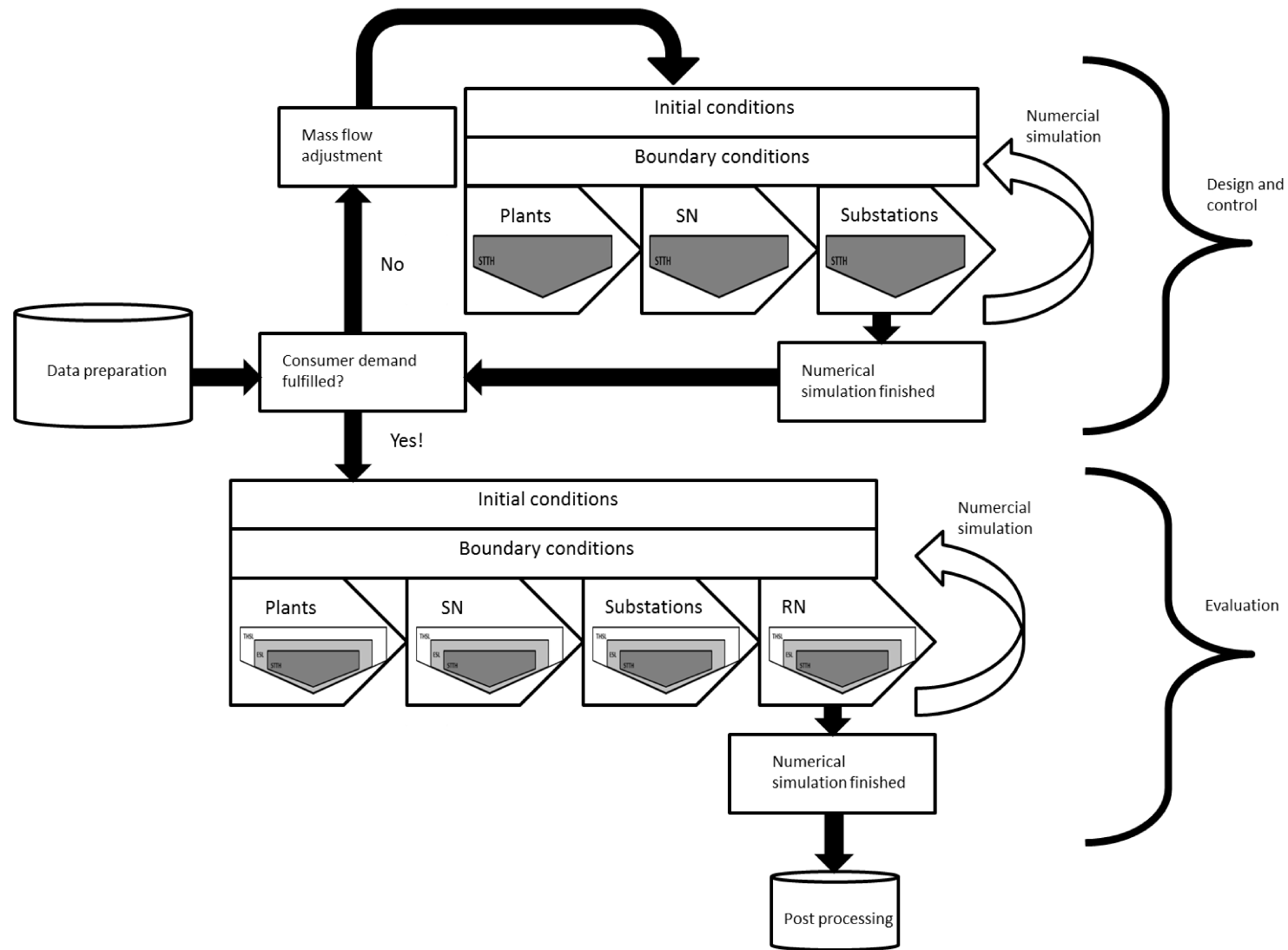
Figure 3-13: Thermoeconomic system simulation procedure

3.5.1 Data preparation

Reference temperature and pressure must be defined for the DHN system. For the DHN, the topology data must be acquired. Since the simulation integrates the STTH model, the necessary data is only roughly mentioned. For more information about the data needed in the STTH model, refer to [(Guelpa 2016)](). For setting up the network topology, position (3-dim coordinates) of nodes, lengths, inner and outer diameters, roughness factors, single loss coefficients and heat transfer coefficients of the tube material is needed.

Furthermore, boundary conditions of the consumers and their position in the network are necessary to calibrate the HX model accordingly. This includes, heat transfer coefficient of the substation, mass flow rate at the secondary side as well as temperature request by the consumer and its corresponding energy demand must be known. Regarding the consumers, thermal energy demand over a given timeframe and its corresponding temperature level can be acquired by an appropriate subnetwork or a building simulation model.

Considering the plant components, their position and boundary conditions must be set. The latter are composed of temperatures levels and at least one pressure value (in the case multiple producers are connected) e.g. at the main pump are necessary.

Given this thermodynamic data, economic data must be gathered to execute the thermoeconomic model. This data includes specific costs of thermal- and mechanical energy provided by the producer(s) and investment- and maintenance costs of the DHN. The unit costs are also boundary conditions which are set at the necessary network nodes of SN and RN.

3.5.2 Design and control procedure

In the design and control procedure, the control of mass flow rate is investigated according to design conditions of the consumers. Due to the fact, that the "correct" mass flow rate is unknown for a given design condition of the substations, it must be acquired through a certain method. In this work, a mass flow adjustment algorithm is developed for that purpose.

The STTH model defines pressure values and temperature as boundary conditions. This results in a certain mass flow rate in the case only one plant is operating. In the

case multiple plants are operating in the network, the mass flow rates must be set as boundary conditions at the plant and substation nodes. After executing of the STTH model, a certain mass flow rate $\dot{m}_{cn}^{net}$ at a certain temperature level T_n results for all nodes connected to substation components. After that, the HX model in Figure 3-8 can be used to determine the energy transferred to the consumer $\Delta\dot{\phi}_{cn}^{th}$. In the case, the consumer design request $\Delta\dot{\phi}_{cn}^{th,design}$ differs from $\Delta\dot{\phi}_{cn}^{th}$ due to e.g. a too low heat transfer, the mass flow rate at the plant components must be adjusted accordingly.

For that the following iterative adjustment procedure is developed. The difference between current energy transferred $\Delta\dot{\phi}_{cn}^{th,it}$ to the energy design request $\Delta\dot{\phi}_{cn}^{th,design}$ is estimated, see (3.44),

$$\Delta\dot{\phi}^{th} = \Delta\dot{\phi}_{cn}^{th,design} - \Delta\dot{\phi}_{cn}^{th,it} \tag{3.44}$$

where $\left(\Delta\dot{\phi}^{th}\right)$ refers to the amount of energy difference between current energy transferred $\left(\Delta\dot{\phi}_{cn}^{th,it}\right)$ at iteration (it) and the design request $\left(\Delta\dot{\phi}_{cn}^{th,design}\right)$. In the case $\Delta\dot{\phi}^{th}$ is negative, not enough energy was provided and the mass flow rate for the next iteration $\dot{m}_{net,it+1}$ (assuming only one plant component) must be increased. The problem associated with a change of mass flow rate is that the temperature resulting at the substation also differs from the previous one, because the flow regime in the network changes. This cannot be avoided due to the methodology used in the STTH model.

Nevertheless, it can be assumed that the temperature will remain close the to one in the previous iteration. In using this assumption the difference in mass flow rate $(\Delta\dot{m})$ can be calculated through (3.45).

$$\Delta\dot{m}_{cn} = \frac{\Delta\dot{\phi}^{th}}{cp\left(T_{n_{sub}} - T_{m_{sub}}\right)} \tag{3.45}$$

Finally, the new mass flow rate at the plant component $\dot{m}_{pl}^{it+1}$ can be derived through adding the sum of all mass flow difference at the primary side of the consumers according to (3.46).

$$\dot{m}_{pl}^{it+1} = \sum_{cn} \dot{m}_{cn}^{net} + \Delta\dot{m}_{cn} \tag{3.46}$$

Once the new mass flow rates at the secondary side of the consumers are known, mass flow rates at the plant component must be updated. In the case, only one producer is operating, the total mass flow rate can be set at the boundary node of the plant according to (3.46). In the case multiples producers are operating, a decision must be made on how to distribute the new mass flow rate among them. Practically, one plant can be used as the "adjusting" plant, changing its mass flow rate during the adjustment procedure. It must be noted that this adjustment procedure is not proofed to converge for every given network or design condition, simply because of the dynamic calculation of temperature within the STTH model. One could also imagine including an iterative update of the temperature. However this has not been performed in this work, because the algorithm converged for the system under investigation, where only one plant was needed to adjust for changes in mass flow rate. In complex networks, with several productions plants, a more detailed algorithm must be developed which might also optimize the mass flow rate according to some criteria, like for example the unit cost at the substations.

It can be seen that in the design and control procedure, only the SN is simulated. The RN is not simulated. The reason for that is that the mass flow rate of the plant is only necessary for simulating the SN, while the RN is simulated with the results of the HX model. Furthermore, the TESL is not executed in this step, because it does not provide any information upon the iterational procedure. However, this is not completely true, if the selection of how mass flow rate is added to the plants is considered in more detail. One could imagine distributing the mass flow rate among the producers according to some decision variable gained from the TESL. Through that, an iterational improvement algorithm could be constructed; but this was not carried out in this work.

3.5.3 Evaluation procedure

Given that either design and control has been executed, or the objective is only to assess a certain DHN operation, the evaluation part of the simulation is carried out. There, all system layers including the thermoeconomic model are applied to the DHN operation. The initial conditions and boundary conditions regarding the STTH model are not changed. However, boundary conditions and initial conditions are assigned for the TESL.

The procedure starts with the assignment of temperature, pressure and mass flow rate at the boundary nodes of the SN of the plant components. Based on that, the ESL and TESL can be applied to the plant in order to calculate the energetic flows and cost flows extracted from the producer. This implies an initial condition at the connection to the RN in order to calculate the cost flow associated with an energetic flow returning from the RN.

The results of the plant model can be used to set the remaining boundary conditions for the SN, which includes the energy, exergy flows and the corresponding unit costs at the SN node. Then, the SN can be simulated for the first timestep, applying first the STTH model to calculate mass flow, temperature and pressure distribution. Based on that energetic- and exergetic analysis is carried out using the models of the ESL. At last, the TESL determines the cost flow distribution among the network in order to derive the product flows exiting to the substation. After the cost flows are known, the substation model can be executed as described. This leads to the calculation of energy/exergy provided to the consumer and supplied back to the RN as well as to the assessment of the unit costs associated with those streams.

The results of the substation model are used for the boundary conditions of the RN. Similarly to the SN, thermodynamic, energetic and economic variables are imposed at the RN nodes connected to the substation. This is followed by the application of all three system layers to the RN which results in energy/exergy and cost distribution among the RN. Finally, the product cost flows of the RN are calculated and are used to calculate the plant components. The procedure is carried out for a given sampling time which must be specified in advance. The modeling procedure is numerically executed for every timestep considered in the simulation. Once the timeframe is simulated, the result of the simulation is then further post-processed which can include the calculation of several key performance indicators depending on the objective of the analysis.

The theoretical developments of the thermoeconomic model are finished. In the next chapter, the framework is applied to a case study of a real-existing DHN system.

Chapter 4: Dynamic thermoeconomic simulation – a case study

In this chapter the thermoeconomic model is applied to a case study in order to show the benefits and information which can be extracted for DHN operation. The aim of the case study is first to investigate the benefits of thermoeconomic analysis in comparison to black-box costing and second to provide insights into the implications waste-heat integration has in the context of dynamic network simulation.

The chapter is divided into two parts. The first part considers a reference scenario which represents the DHN system as in current operation. The reference scenario is used to study the thermoeconomic model in detail as well as its benefits towards costing from an industrial perspective. In the second part, waste-heat integration is studied using scenarios to analyses the impacts of various different waste plant configurations.

4.1 Introduction to the case study

The case study is a DHN system located in Rumania and supplies 138 substations which are connected to various different end-users; from residential buildings to commercial buildings, hospitals etc. Most of the substations are connection to sub-networks which supply those consumers, while some substations are direct users. The latter are directly connected to a building. However, a differentiation is not made upon them from a modeling perspective and the substation model is equally applied to each of them.

An overview of the network topology based on the underlying QGIS data is given in Figure 4-1. The network is operated by one heating plant (hp) located to the south of the network indicated with a red circle. The network spans over the major part of the inner city, while the production plant is situated outside and is connected through a long pipe to the core part of the network.

The various points in the figure represent either internal nodes, such as connections/junctions in the network, or substations (sub_i). Three substations have been highlighted which are located close (substation 3) and far (substation 1+2) away from the plant.

71
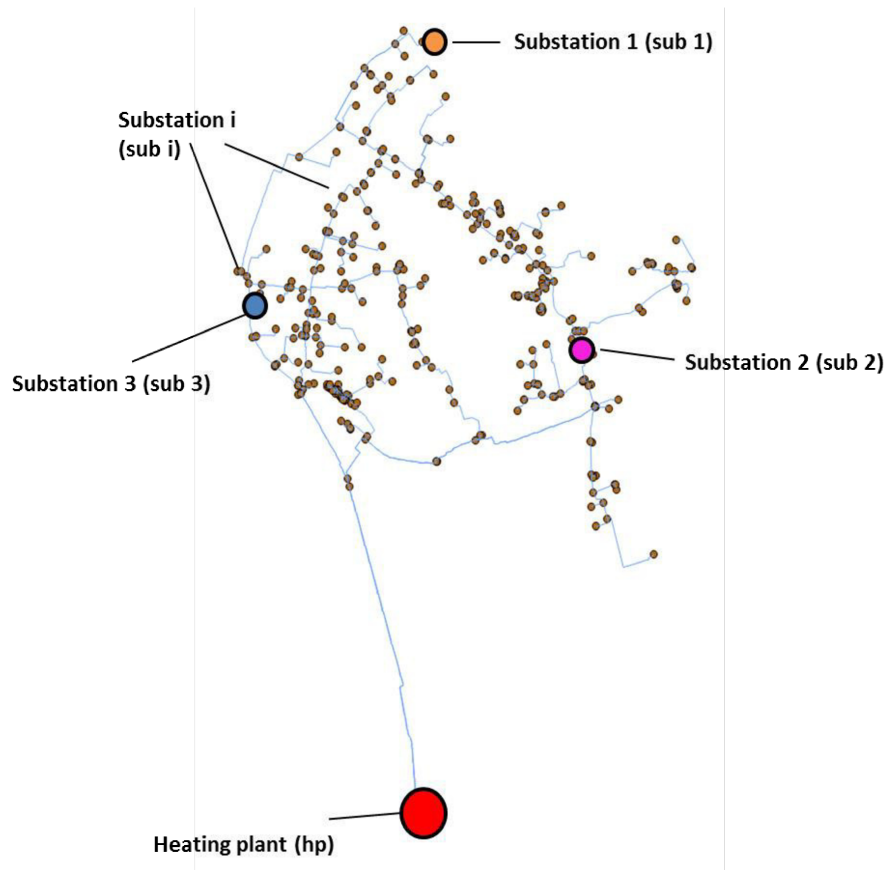
Figure 4-1: Case study network (taken from QGIS)

Those have been selected to investigate the individual impact of their operation on the cost generation of the system and are used to study the results of the thermoeconomic simulation on substation level.

The data on the network is mainly based on a QGIS dataset, which contains information on the network topology. This includes three-dimensional coordinates of nodes, representing positions of substations and the production plant, as well as pipe lengths and diameters including calibrated roughness factors and heat loss coefficients. This data is needed for the STTH-model.

The calibration of the roughness factor has been previously carried out with the help of the software tool Termis. Through Termis, pressure drops in the network can be calibrated using a well-known design pressure and flow distribution. The Termis software is mainly used for monitoring and control of the network during operation. This data can be accessed during offline mode, from which demand profiles were extracted. This is done for the remaining data necessary to run the system layers described in this work. The data includes the necessary information for the substations from

which thermal energy request, supply temperature, mass flow rates and the UA-value have been extracted.

Furthermore, a further calibration and validation of the model was carried out using the Termis data. This was done for the roughness factors of each branch and the specific thermal losses of the tubes. Even though the thermodynamic model was already validated, a re-calibration is useful for a more precise estimation of the loss and exergy destruction terms.

The substation model integrates the consumer demand through a temperature control of the secondary side of the HX model. This thermal demand of the consumer is therefore controlled through T_{req}, because it is assumed that $\dot{m}_{cn}$ is time-constant according to industrial practice. The reason for that assumption is that $\dot{m}_{cn}$ is generally unknown in industrial practice and can therefore be calibrated according to the substation data. This allows representing energy request through a variation in supply temperature of the secondary side of the substation. This assumption is made upon practical reasons of typical substation operation according to the author's knowledge.

Control of energy request of the consumers is typically done through adjustment of T_{req} e.g. in buildings or subnetworks. Thus, during cold periods where outdoor temperature is low, T_{req} is increased to comply with the higher request due to higher heat losses in the connected building. Another advantage of that approach is that thermal exergy request can be studied explicitly at equal thermal energy request. This enables the assessment of the impacts of different temperature levels in the DHN system behavior. While energy request and requested temperature are based on measurements, the remaining data for the substation was calibrated to the return temperature of the DHN. The return temperature is available from measurements.

The case study involves a distinct timeframe of investigation which was available from the data. A four-day timeframe in January 2014 from 07.01.2014 00:00 to 11.01.2014 24:00 is used with an hourly resolution of the given data.

The case study is divided into two parts:

- Reference scenario
- Waste heat integration scenario

In the reference scenario, the DHN system is simulated according to its current configuration, as shown in Figure 4-1. In the reference scenario, only one plant is operating in the network. The reference scenario investigates the results of the thermoeconomic model and points out its usefulness to overcome the drawbacks related with black-box costing.

4.2 Reference scenario: Thermoeconomic analysis

In this part of the case study the reference scenario is used to study two main points:

- Black-box vs. White-box costing
- Individual contribution on cost generation

The first point compares the results obtained by black-box costing of the system with the results obtained by the thermoeconomic model. The second point investigates in detail the costing results of selected substations and provides insights into individual contribution of cost generation.

4.2.1 System analysis

In this section, the results obtained from the application of the THSL and the ESL are presented. This is an important step for analyzing the general behavior of the DHN system from an energetic viewpoint, which provides a good basis for understanding the thermoeconomic modelling results.

4.2.1.1 Thermodynamic analysis – THSL results

Given the data of the reference scenario, the THSL is executed using the STTH model to determine the temperature and pressure distribution in the network for both SN and RN as well as for the system components. The final result of the thermo-hydraulic simulation is the temperature and pressure distribution at every node in the DHN, which furthermore allows calculating the necessary thermodynamic variables for the system components.

In the reference scenario, only one heating plant is operating. Considering that the simulation procedure calculates the values obtained at the return node of the heating plant as a final result of every timestep, the pressure and temperature distribution allows to study the global system behaviour from a thermodynamic viewpoint, see Figure 4-2.
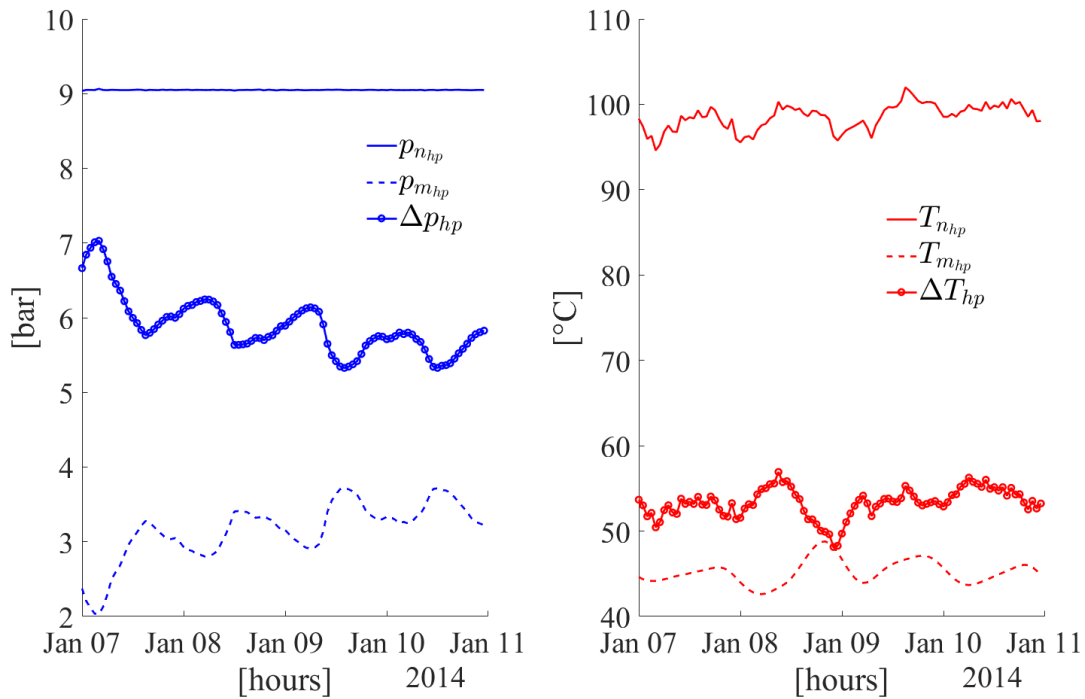
Figure 4-2: Pressure (left) and temperature profiles at the heating plant (hp)

Boundary condition for pressure of about 9 bar are set at the SN node $\left(n_{hp}\right)$ of the heating plant. This is therefore the pressure $\left(p_{n_{hp}}\right)$ at which water is injected into the SN. The pressure at the RN node $\left(p_{m_{hp}}\right)$ is the pressure of the water returning from the RN, while $\left(\Delta p_{hp}\right)$ is the pressure difference at the heating plant.

This pressure difference determines the total pressure resistance of the DHN and is proportional to the mass flow rate at the heating plant $\left(\dot{m}_{hp}\right)$, because the whole pressure level is maintained only by one plant. The higher $\dot{m}_{hp}$ requested by the consumers, the higher Δp_{hp}. This is due to the hydraulic model used in the STTH model.

The temperature set at the boundary node of the plant $\left(T_{n_{hp}}\right)$ is the temperature of the water entering the SN. Here, this value varies between 95 and 102 °C, depending on the timeframe considered. Those values are original data from measurements and correspond to the real supply temperatures during the operation of the system. The temperature returning to the plant from the RN $\left(T_{m_{hp}}\right)$ is the temperature of the water after usage and return from the substations. The temperature difference $\left(\Delta T_{hp}\right)$ is the difference at the plant site and provides insight on the driving force of thermal ener-

gy/exergy request. Here, $T_{m_{hp}}$ varies between 43 – 48 °C, which results to a ΔT_{hp} between 48 and 58 °C. Hence, the average temperature drop of the network is around 50 °C, while distinct peaks and valleys can be furthermore discovered. Those are mainly a result of the substation model (apart from the temperature loss in the RN) and its characteristic behavior. Based on those thermo-hydraulic results, the system analysis can be carried out.

4.2.1.2 Energetic analysis – ESL Results

Both Δp_{hp} and ΔT_{hp} are the main drivers for mechanical and thermal energy/exergy provided by the system. In Figure 4-3, the global results of the ESL are presented for energy analysis including mechanical and thermal energy flows.
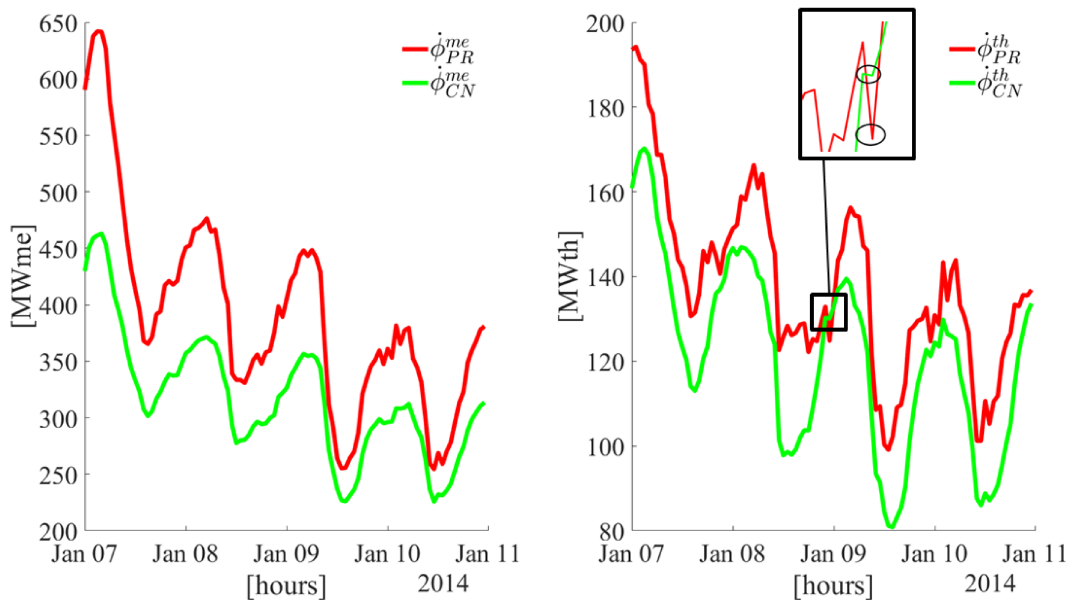
Figure 4-3: Mechanical (left) and thermal (right) energy of the DHN system

Generally, the control strategy used is to decrease mass flow rate during the morning hours, while increasing it from about 06:00 in the morning. Due to Δp_{hp}, the heating plant provides mechanical energy to the system through increasing the pressure level of the return flow. Since the heating plant is the only producer in the system, the total inflow of mechanical energy from producers is equal to the one from the heating plant $\dot{\phi}_{hp}^{me} = \dot{\phi}_{PR}^{me}$. This mechanical energy $\dot{\phi}_{PR}^{me}$ is provided by the plant and depends on the dynamic resistance and the total mass flow rate in the network. In the reference scenario, peak demand is almost 650 MWme in the night of the 07.01 while during the morning hours, mass flow rate is reduced causing a drop in mechanical energy

provided. It can be seen that mechanical energy correlates with the pressure drop in Figure 4-2.

The sum of all pressure drops on substation level leads to an amount of mechanical energy associated with the corresponding pressure drops at the substations. The total amount of mechanical energy at substation level is therefore $\dot{\phi}_{CN}^{me} = \sum_i \dot{\phi}_{sub_i}^{me}$. It must be noted that $\dot{\phi}_{CN}^{me}$ is not a physical outflow of mechanical energy to the consumer but only the mechanical energy on the primary side of the HX model. The difference between $\dot{\phi}_{PR}^{me}$ and $\dot{\phi}_{CN}^{me}$ is the mechanical energy loss of the system.

Since the heating plant must provide a given ΔT_{hp}, thermal energy must be provided while the total thermal energy of the producers is equal to the one supplied by the heating plant $\left(\dot{\phi}_{hp}^{th} = \dot{\phi}_{PR}^{th} \right)$. Peak supply of $\dot{\phi}_{PR}^{th}$ is about 190 MWth and falls with decreasing temperature difference, see Figure 4-3. The total thermal energy provided to the consumers is the sum of all contributions from the substations $\dot{\phi}_{CN}^{th} = \sum_i \Delta \dot{\phi}_{cn_i}^{th}$ and is generally lower then $\dot{\phi}_{PR}^{th}$ with one exception (see detail in Figure 4-3 right) which demands for a more detailed explanation.

According to Figure 2-2, the total inflows and outflows of the DHN system, as presented in Figure 4-3 are the flows which are derived from black-box analysis. It must be remarked that the influence of transient behavior cannot be neglected when the total losses, or the dynamic efficiency of the system is estimated. This means that the difference $\dot{\phi}_{PR}^{th} - \dot{\phi}_{CN}^{th}$ does not represent the thermal losses of the system. This can be seen in Figure 4-3, where a high fluctuation of $\dot{\phi}_{PR}^{th} - \dot{\phi}_{CN}^{th}$ can be observed.

Moreover, at one timestep (indicated as detail) the total outflow is larger than the total inflow of thermal energy $\dot{\phi}_{CN}^{th} > \dot{\phi}_{PR}^{th}$. This can only be caused by the transient behavior of the system where, at this timestep, more thermal energy is exiting to the consumers then entering from the plant due to the time delay of the water flow. This is an important issue to consider when drawing conclusions from total in- and outflow of thermal energy in Figure 4-3.

Hence it is necessary to analyze the transient behavior of the system in more detail, which further allows calculate the losses associated with thermal energy. Since in the mechanical sub model, no transient conditions are included, total mechanical losses can directly be deduced from Figure 4-4.
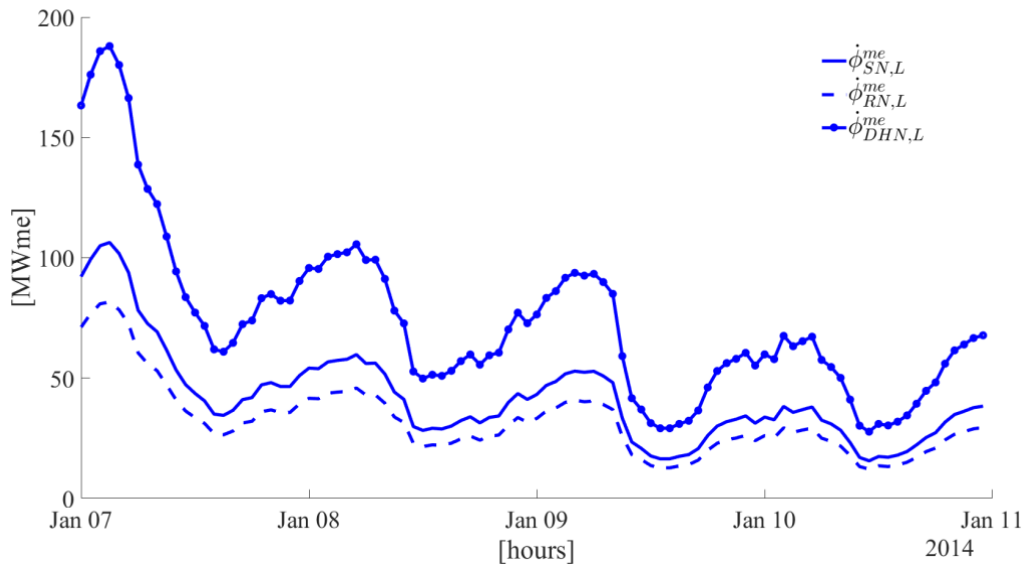
Figure 4-4: Mechanical losses in the network

To provide more detailed insights, the results for both supply- and return network are given separately. In order to analyze both SN and RN a certain notation is introduced. The subscripts (SN) and (RN) stand for the contribution of supply network and return network, respectively, while (DHN) is the sum of both networks showing the contribution of the whole DHN.

Since transient mechanical energy does not occur, the mechanical losses for the whole DHN $\left(\dot{\phi}_{DHN,L}^{me}\right)$ correspond directly to $\dot{\phi}_{PR}^{me} - \dot{\phi}_{CN}^{me}$.

Due to a lack of transient condition, mechanical losses are proportional to the mass flow rate in the networks. Furthermore, the individual losses of the SN $\left(\dot{\phi}_{SN,L}^{me}\right)$ and RN $\left(\dot{\phi}_{RN,L}^{me}\right)$ are shown separately, which allows to investigate the contributions of both networks to mechanical energy loss. It can be observed that the contribution of the SN is higher for the whole timeframe compared to the RN. This can be explained by the higher pressure distribution existing in the SN. Since the pressure losses are a function of the mass flow rate, losses increase at higher pressure levels. In Figure 4-5 the situation for thermal energy is presented.

When analyzing the situation for thermal energy, a more complex picture must be analyzed. First of all, transient thermal energy exists in both SN $\left(\frac{\delta\phi_{SN}^{th}}{\delta t}\right)$ and RN $\left(\frac{\delta\phi_{RN}^{th}}{\delta t}\right)$.
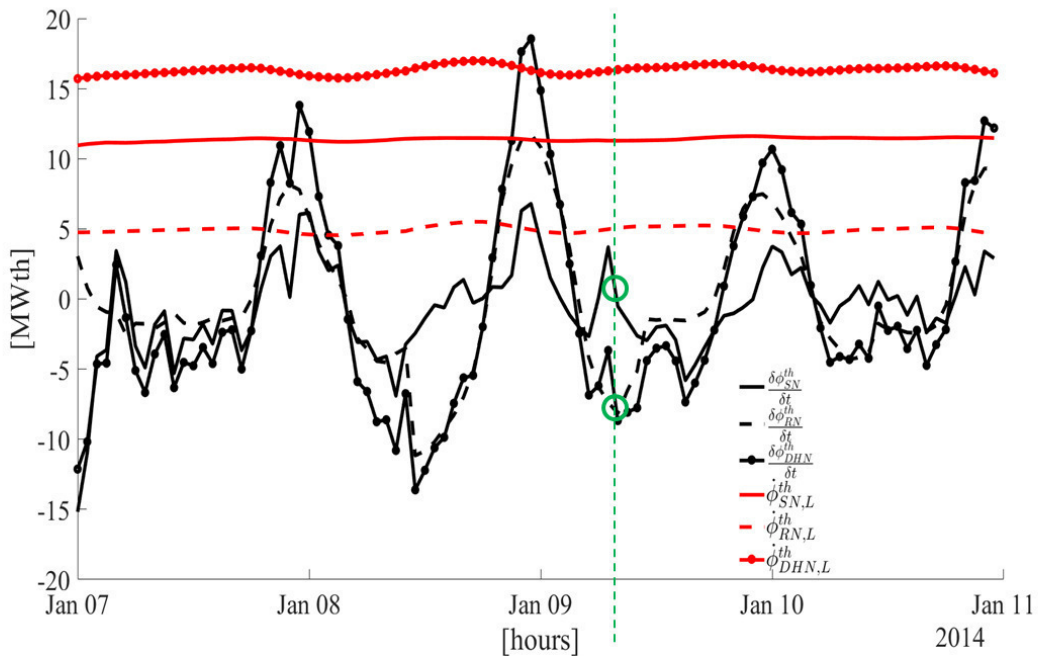
Figure 4-5: Transient energy and thermal energy losses in the DHN

The reasons are cooling-down or heating-up effects of the network depending on the current operation. For most of the periods, transient energy is aligned for both SN and RN, but with a few exceptions, during which one network cools down, while the other heats up.

This can be observed e.g. in the morning period of the 09.01, indicated in the green circles. There, transient energy is positive for the SN, while negative for the RN. Thus, the SN is heating up, while the RN is cooling down during this phase. The sum of both contributions result in the total change of energy of the DHN $\left(\frac{\delta\phi_{DHN}^{th}}{\delta t}\right)$.

With the knowledge of the change in energy in the networks, thermal energy losses can be estimated. It must be reminded, that without the information on transient behavior, the estimation of loss is inaccurate. Given that the total thermal losses of the DHN $\left(\dot{\phi}_{DHN,L}^{th}\right)$ vary around 16 MWth, the contribution of the SN $\left(\dot{\phi}_{SN,L}^{th}\right)$ is with 11 MWth about 2/3 of the total amount of losses. The RN $\left(\dot{\phi}_{RN,L}^{th}\right)$ contributes 1/3 with about 5 MWth. The difference can be explained through the lower temperature distribution in the RN. Since the thermal losses are a function of the temperature at each node, thermal losses are lower for lower network temperatures.

The energetic system layer allows correctly estimating the total thermal losses in the system, which is not possible through measurement of total inflow and outflow of the system only.

4.2.1.3 Exergetic analysis – ESL results

A similar analysis as in section 4.2.1.2 is carried out focusing on the exergetic behavior of the system. Similarly to what was shown for energy in Figure 4-3, Figure 4-6 provides an overview of thermal exergetic flows in the system. The mechanical flows of exergy are equal to the mechanical energy flows in Figure 4-4 and are therefore not repeated.
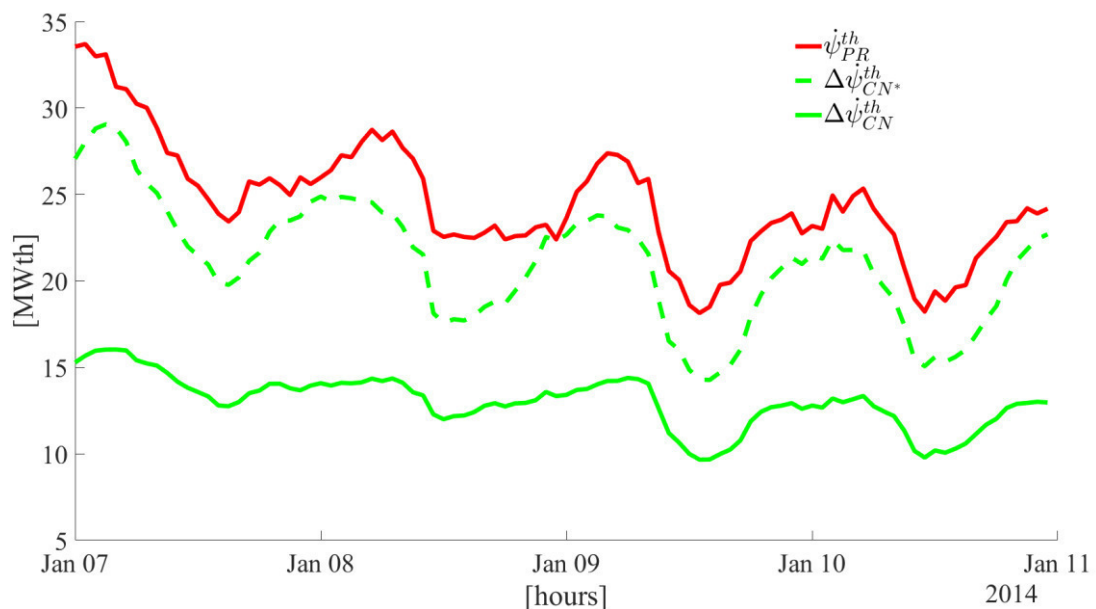
Figure 4-6: Thermal exergy of the DHN system

Regarding the thermal part, exergetic flows are considerably different in magnitude compared to the ones based on energy. Thermal energy is estimated at 195 MWth supplied to the system at the peak on the 07.01, while the exergy content is only about 34 MWth. The profile of thermal exergy flow provided by the producer $\left(\dot{\psi}_{PR}^{th}\right)$ shows a similar behavior as its corresponding thermal energy profile. This is due to the relatively low variation in temperature in the networks. The thermal exergy provided to the consumers $\left(\dot{\psi}_{CN}^{th}\right)$ is much lower than $\dot{\psi}_{PR}^{th}$ which points out a much higher exergy loss compared to energy loss in the system.

The green doted curve is used to show the thermal exergy extracted from the substations at the primary side $\dot{\psi}_{CN^*}^{th}$. This is not shown for thermal energy analysis because

80

the energy difference at both side of the HX model is equal. Thus it can be seen that the profiles of $\dot{\psi}_{CN^*}^{th}$ and $\dot{\psi}_{PR}^{th}$ have very similar shape and are different only due to the loss generation in the SN. Therefore, the very low exergy supplied to the consumer $\dot{\psi}_{CN}^{th}$ must be caused by exergy destruction in the substations. Hence, considering that transient behavior only affects $\dot{\psi}_{CN^*}^{th}$, the difference $\dot{\psi}_{CN^*}^{th} - \dot{\phi}_{CN}^{th}$ correspond purely to exergetic losses in the substations.

At the first timestep, 15 MWth are exiting to the consumers, while 34 MWth are extracted from the producers; with a thermal exergy supplied to the primary side of 27 MWth. The DHN therefore contributes about 1/3 to the difference between entering and exiting thermal exergy stream of the system, while the substation contribution is 2/3. Differently, on the 09.01, the difference in thermal exergy between $\dot{\psi}_{PR}^{th}$ and $\dot{\psi}_{CN^*}^{th}$ is very small or even negative for the same cause as previously explained in Figure 4-3.

In order to further investigate the exergetic behavior of the system, Figure 4-7 is drawn, omitting mechanical exergy, because it is equal to mechanical energy drawn in Figure 4-4.
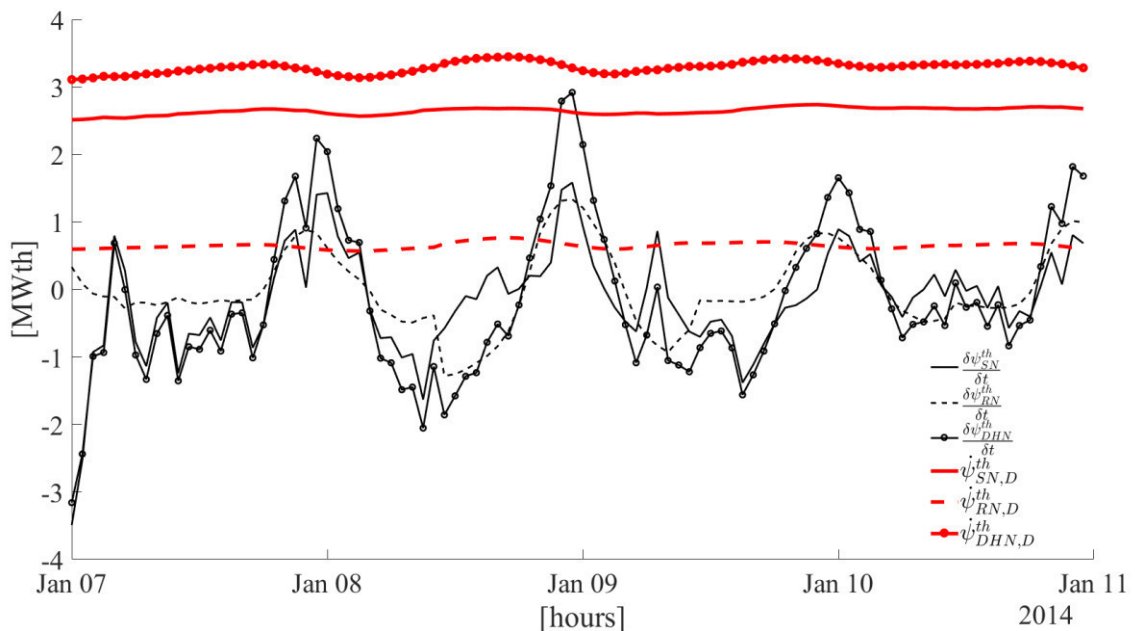
Figure 4-7: Thermal transient exergy and losses in the DHN

Comparing the transient behavior of energy and exergy, similar profiles can be seen; even though the amplitudes of exergy are considerably lower. At the peak around the

09.01, transient change in thermal energy accounts for about 13 MWth, while change in exergy is only 2.8 MWth. This is due to the generally lower exergetic flows in the system.

In the case the transient term is positive, the network is discharging, and thus the temperature in the network decreases. When the transient term is negative, the network's temperature increase. This can be clearly seen comparing Figure 4-7 with the temperature evolution in Figure 4-2. Especially during the 09.01, the high discharge, represented by a high positive exergy transient can be detected due to a decrease in temperature throughout both SN and RN.

An interesting fact can also be seen comparing the individual losses of SN and RN. While for energy, the SN contributed to about 2/3 of the total losses, this value is with 80 % substantially higher for exergy. Thus exergetic losses are relatively higher in the SN compared to its energetic losses. The RN contributes only a small amount to the total exergy losses, which in average is about 0.6 MWth. This can be explained through the higher exergy flows in the SN, operating at higher temperatures. Thus it can be concluded that energy analysis underestimates the contribution of temperature decrease in the SN leading to lower relative losses compared to the RN.

With the knowledge of the energetic flows including transient behavior, the system is analyzed on system level using the equations given in section 2.2.2.

4.2.1.4 Energetic system performance

Based on the energetic and exergetic behavior of the system, the system performance can be investigated on a global basis. At first, the system is analyzed from an energy perspective leading to the results shown in Figure 4-8.

The results are obtained through equations (2.3) – (2.4). The mechanical energy efficiency of the system $\left(\eta_{en,sys}^{me}\right)$ varies between about 70 to 90 % depending on current operation. The average mechanical losses are therefore about 20 % given the whole timeframe. Furthermore it can be seen that $\eta_{en,sys}^{me}$ is invers-proportional to the pressure difference in the network, see Figure 4-2. Thus the higher the pressure difference in the system, the more mechanical loss occurs. This has been previously explained in detail.
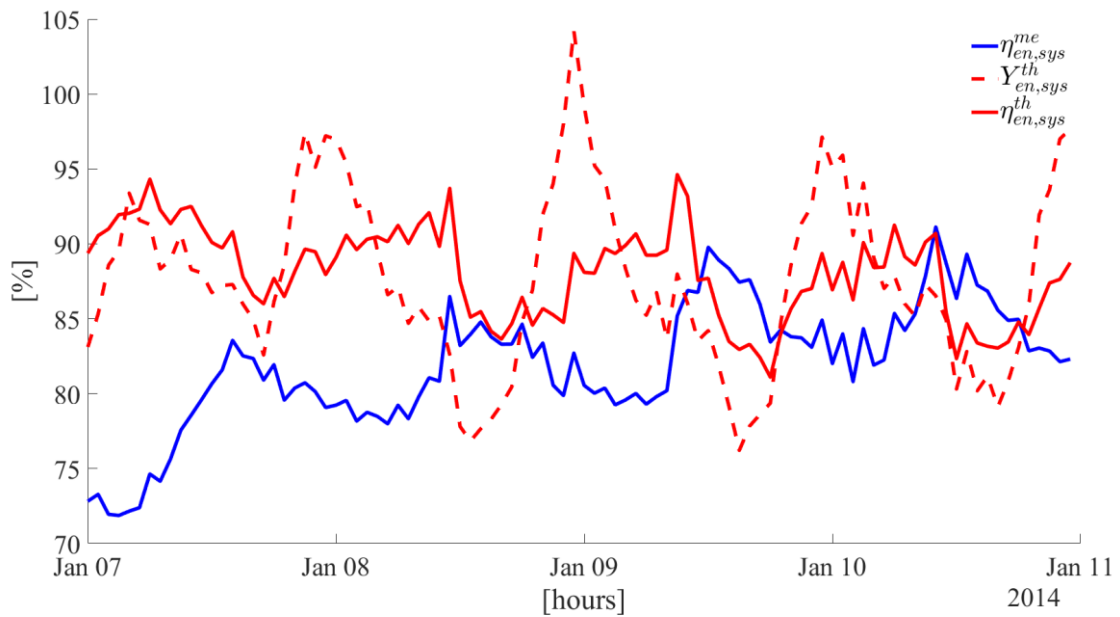
Figure 4-8: Performance analysis of the DHN system – energy perspective

Considering thermal energy, it must be differentiated between the yield $\left(Y_{en,sys}^{th}\right)$ and the efficiency $\left(\eta_{en,sys}^{th}\right)$ of system. The yield is the total output divided by the input, while efficiency takes also the transient change of energy of the system into account. In a steady-state system, yield and efficiency are equal.

Thus, $Y_{en,sys}^{th}$ varies in a much higher way and is effected by the transient behaviour in the DHN. This is due the fact, that while e.g. energy is stored in the DHN, due to the temperature of the network increases, the thermal energy outflow to the consumers is reduced by that amount. Thus considering only inflow and outflow treats this amount of energy stored as a loss. In the opposite way, more energy could be extracted then injected, which leads to a yield greater than one.

Therefore, if efficiency wants to express the performance in the sense of accounting for losses, transient energy must be added to the balance calculation. It can be seen that $\eta_{en,sys}^{th}$ is always below one and varies between 85 and 95 %. Thus thermal losses can be directly deduced from $\eta_{en,sys}^{th}$. Similarly as for mechanical energy, $\eta_{en,sys}^{th}$ is invers-proportional to the temperature difference in the system, see Figure 4-2. It must be noted, that black-box system analysis, which is not able to determine transient system behavior, is not able to calculate energy efficiency correctly. Thus a steady-state approach would only be able to calculate $Y_{en,sys}^{th}$, which has been shown

not to consider the generation of thermal losses correctly. In Figure 4-9 the same analysis is carried out for thermal exergy.
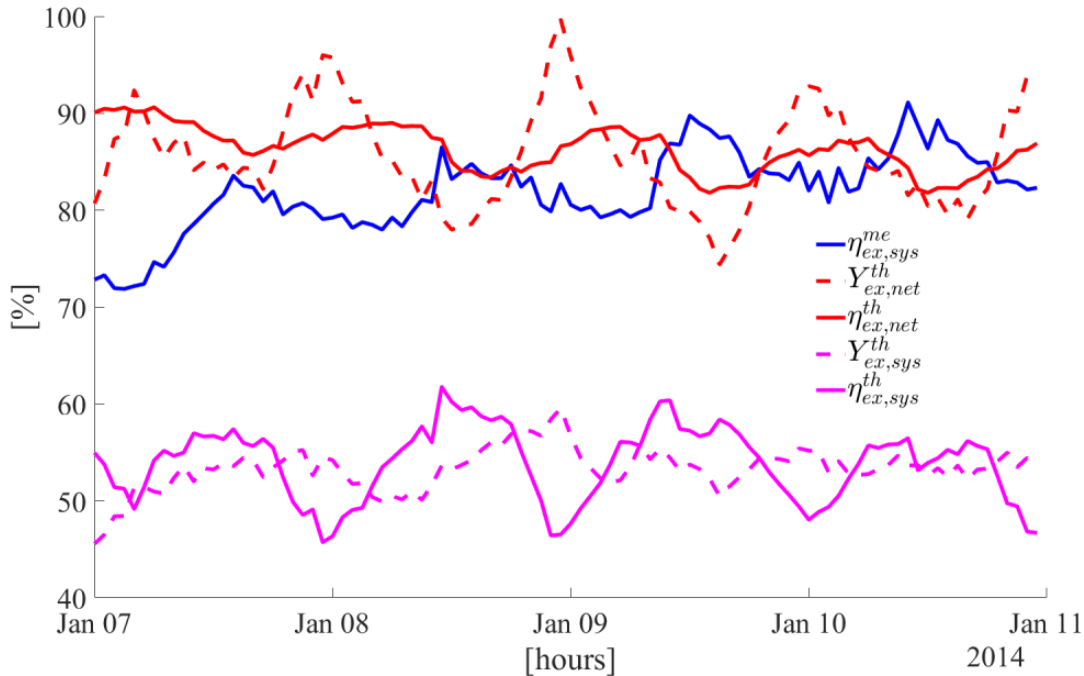
Figure 4-9: Performance analysis of the DHN system – exergy perspective

As before, the results are obtained through equations (2.3) – (2.4), while the results obtained when only the DHN is considered is marked through subscript (net). First of all, mechanical exergy efficiency $\left(\eta_{ex,sys}^{me}\right)$ is equal to $\eta_{en,sys}^{me}$. Furthermore, it must be differentiated between network and system efficiency. Network efficiency only considers the thermal destruction in the DHN while system efficiency also includes thermal destruction in the substation. Exergy efficiency of the network $\left(\eta_{ex,net}^{th}\right)$ varies between 85 and 90 % and is always lower then energy efficiency $\eta_{ex,net}^{th}$, because it takes also exergy destruction due to temperature loss into account. However, the magnitude of difference is not very large in average, but varies considerably for certain timeframes. The detailed comparison of energy- and exergy efficiency shows that during intervals of low temperature difference in the system, energy efficiency tends to overestimate the performance, leading e.g. on the 07.01 to a value of 94 % in comparison to only 90 % for exergy efficiency. During periods of higher temperature difference, the difference between those two values is lower.

These effects only consider the network performance. When including the substation performance, the system yield $Y_{ex,sys}^{th}$ and efficiency $\eta_{ex,sys}^{th}$ can be estimated. Figure

4-9 shows that system efficiency and yield are considerably lower than if only the network is considered. The high impact of exergy destruction in the substation, described in Figure 4-6, is clearly visible. Thermal exergy efficiency varies between 45 and 60 % depending on the timeframe considered. Hence, the substation behavior has a major impact on the exergetic performance of the whole system.

The results of the system analysis show the global behavior the DHN system for mechanical and thermal energy/exergy. In applying the ESL, transient behavior can be correctly estimated and used to determine global yields and efficiencies of the system. Those can be directly used for applying black-box costing to the system.

4.2.2 Analysis of costing approaches

In this section, the different costing techniques according to black-box costing and thermoeconomic costing are assessed. This is done through the results of the TESL on component level to identify the differences in the results of the different approaches. The aim is to compare the results provided by the black-box costing approaches vs. the results obtained from the thermoeconomic costing approach using the TESL. As shown in Table 2-1, the black-box costing results are compared with the white-box approach using energy costing and exergy costing.

Thus three costing techniques are selected:

- Black-box costing (energy + exergy)
- Energy costing
- Exergy costing

The selection of the techniques is done with respect to practical consideration. First of all, black-box costing is the most common way of assigning cost to the substations in a DHN system, even though it is not useful in dynamic environment and with substations of different characteristics. Instead of thermoeconomic costs, energy and exergy costs are used in order to show the differences in both techniques without the influence of external factors such as investment- or maintenance costs. Since those factors only influence the cost generation independently of the dynamic network behavior, the exergy cost analysis is sufficient for the comparison with black-box costing. In order to provide a compact analysis and show the specific drawbacks of the costing techniques, the comparison focuses on thermal energy/exergy only.

4.2.2.1 Black-box costing results

Based on the energy- and exergy flows in the DHN system, the results of the ESL can be used to investigate the global behavior of cost flows of the DHN system. In order to show the usefulness of the approach for dynamic system analysis, external costs such as investment- and maintained costs are omitted with a focus on energy and exergy costing only.

The thermal and mechanical flows of energy and exergy extracted from the producers, see Figure 4-3, are carrying a certain unit cost which must be allocated to the energy service provided to the consumers. These costs must be a-priori determined by the thermoeconomic analysis of the production unit itself. Since the production units are not in the scope of this thesis, the unit costs of inflowing energy/exergy are considered as opportunity costs of electrical energy generation. For that, a standard spot-price for electricity was taken. Through black-box costing, where the actual thermodynamic and energetic behavior is unknown, the only way to account for the losses is the estimation of total inflow and outflow of the system and to increase the unit cost accordingly. This unit cost is furthermore called black-box unit cost. With the result of the energetic system analysis, those black-box unit energy/exergy costs can be obtained through equations (2.5) – (2.6). In Figure 4-10 the result of the black-box costing approach is shown for thermal energy.
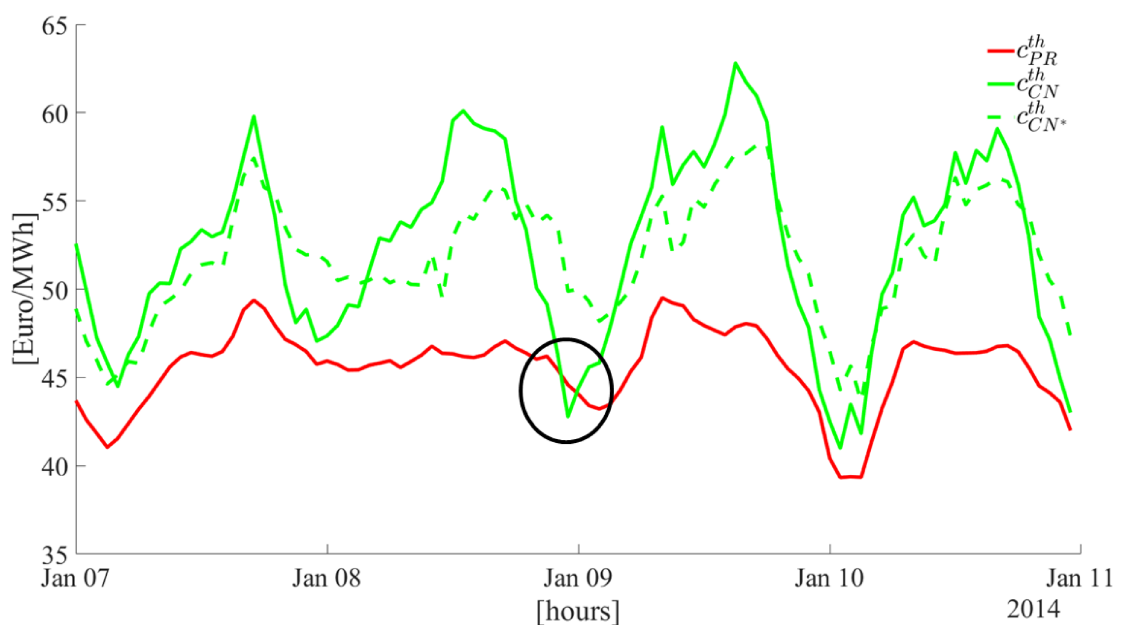
Figure 4-10: Black-box costing approach for thermal energy

The unit costs of thermal energy provided by the producer c_{PR}^{th} is marked with the red curve. It is based on an arbitrary opportunity cost which could be based on the price of electricity or another more complex model which must be calculated in advance. It must be noted that c_{PR}^{th} is a boundary condition for the thermoeconomic model. Thus the cost for one unit of thermal energy used in this work varies between about 38 to 50 Euro/MWh.

Based on the black-box approach, unit thermal costs for the consumers c_{CN}^{th} are increased due to the difference between inflow and outflow. This property is called average unit energy cost. It can be seen, that c_{CN}^{th} shows a high fluctuating profile. Considering the principles of cost accounting, c_{CN}^{th} must be always greater than c_{PR}^{th} because thermal losses unavoidably occur in a real system. Remarkably, this is violated at a certain timeframe indicated in the black circle. This moment corresponds to the same timestep when the total outflow of energy is higher than the total inflow, see Figure 4-3, which was initially caused by transient behavior. Due to the fact that traditional black-box costing cannot account for that, unit energy costs are calculated as if transient change would be a part of the thermal losses. Hence a c_{CN}^{th} larger then c_{PR}^{th} is impossible and therefore provides very misleading results which do not really capture the loss generation in the system.

The transient behavior in the system is calculated form the ESL. It can therefore be used to calculate a corrected value, the dynamic average unit cost after (2.6) which leads to $c_{CN^*}^{th}$. Here, the transient part is taken into account, while the resulting unit costs are based on the average thermal losses in the system. Thus in using $c_{CN^*}^{th}$ for a specific consumer, the total losses are average and accounted for.

The same black-box costing approach can be applied to thermal exergy which is shown in Figure 4-11.

The unit exergy costs of the producer $\left(k_{PR}^{th}\right)$ are almost a factor of ten higher than the corresponding unit energy cost. This is due to the low exergetic value of the energy streams, while the unit exergy cost of the producer has been calculated form its total energy costs. The average unit exergy cost k_{CN}^{th} for the consumers are remarkably higher then k_{PR}^{th} compared relative to energy.
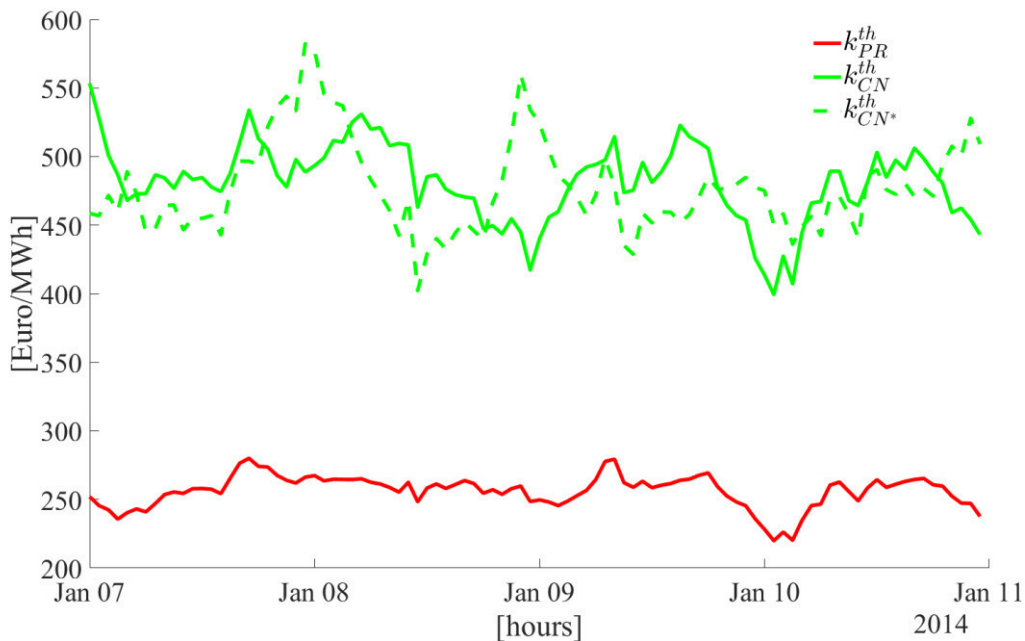
Figure 4-11: Black-box costing approach for thermal exergy

This is mainly due to the high exergetic losses in the substations. Furthermore, this can be seen comparing k_{CN}^{th} with the dynamic average unit cost k_{CN*}^{th}. The relative difference between them is lower than for energy which indicates that the loss generation is not caused by highly transient behavior. Due to the fact that the main cause for the increase of unit costs is the exergy destruction in the substation, the average costing results provide meaningful result, because they are not highly affected by transient behavior. In any case, the unit costs are averaged for all the substations and do not provide information on individual contributions.

4.2.2.2 Thermoeconomic costing results – TESL results

The TESL is applied to the DHN system in order to estimate the distribution of unit energy and exergy costs in the system. At first, the generation of cost throughout the system is analyzed, which provides a deep understanding of the cost generation in the system. This is done using the results of thermal energy and exergy costing for consumer 3, indicated in Figure 4-1. For that, characteristic points are defined, which include the heating plant and the substation of consumer 3 (see Figure 4-1) as well as the network nodes of the plant and the substation connected to the DHN. This allows for the investigation of cost generation throughout the system. The results for energy costing in the TESL are shown in Figure 4-12.
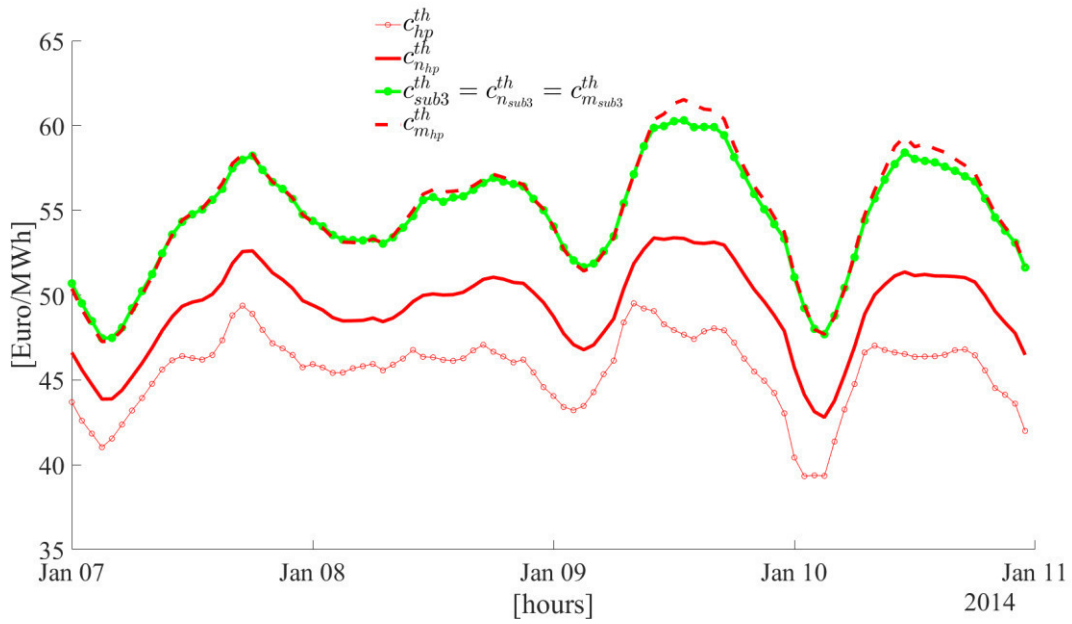
Figure 4-12: System behavior in energy costing

The unit energy cost of energy provided by the heating plant c_{hp}^{th} has already been shown in Figure 4-10. Due to the dynamic calculation, the unit costs of energy supplied to the SN $c_{n_{hp}}^{th}$ by the heating plant is slightly higher due to the use of energy from the RN at higher unit cost relative to $c_{n_{hp}}^{th}$. Throughout the network, energy supplied to substation 3 suffers cumulated losses which are represented by an increase of unit cost, indicated by c_{sub3}^{th}. This unit cost is the cost for extracting one unit of energy from substation 3. Thus it can be seen, that the values are considerably higher than the cost at which energy has entered the SN. At the peak, unit costs are at about 61 Euro/MWh for substation 3, while unit cost of energy supplied to the SN is only 52 Euro/MWh. This means, that it is 9 Euro/MWh more expensive to extract energy from substation 3 then to extract energy at the supply node of the heating plant for the given timestep. It must be noted, that due to the thermoeconomic model of the substation, unit energy cost at the connection nodes $c_{n_{sub3}}^{th}, c_{m_{sub3}}^{th}$ of the substation 3 are equal to c_{sub3}^{th}. Finally, energy is supplied back to the RN at unit cost $c_{m_{sub3}}^{th}$ while at the heating plant, a unit cost of $c_{m_{hp}}^{th}$ arrives. It can be seen that the difference between $c_{m_{hp}}^{th}$ and $c_{m_{sub3}}^{th}$ is very small for most of the time, except between 09.01 and 10.01. Since $c_{m_{hp}}^{th}$ is a measure of average increase of costs throughout the RN, it can be concluded that the use of one unit of energy by the heating plant from the RN

is almost equal to the use of energy by substation 3. This means that the increase of unit cost throughout the RN is very small.

The same analysis can be carried out using exergy costing, which leads to the result obtained in Figure 4-13.
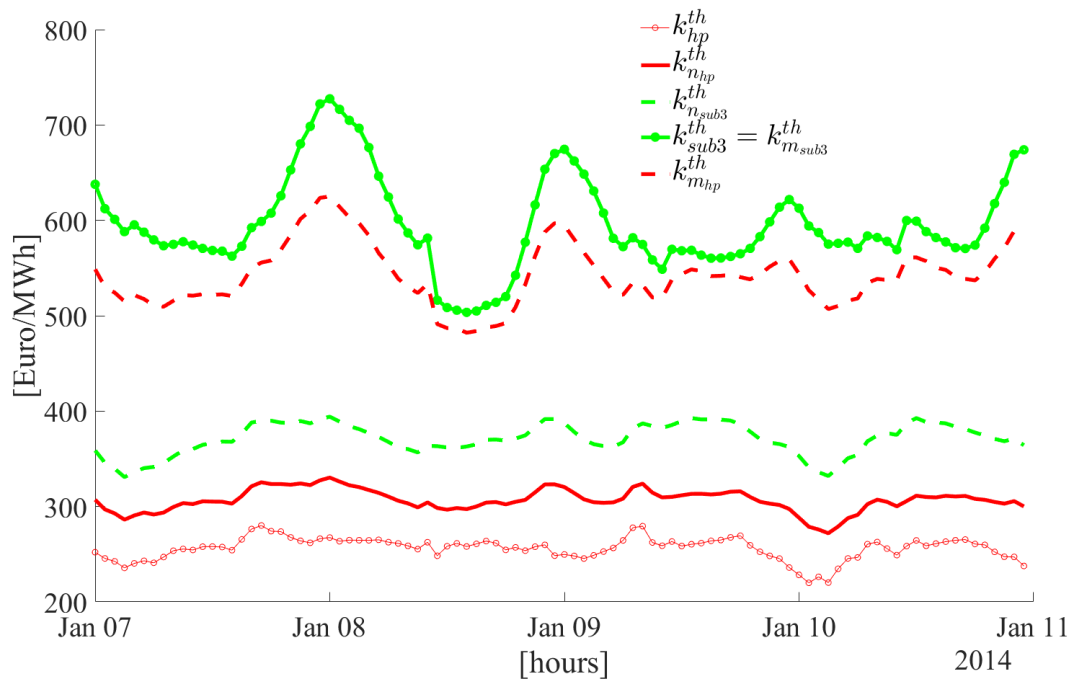
Figure 4-13: System behavior in exergy costing

Similar behavior but different amplitude can be seen for the increase of unit exergy cost k_{hp}^{th} supplied to the SN by the plant. Considering exergy costing, the unit cost of exergy extracted by the substation k_{sub3}^{th} is not equal to the unit cost of exergy entering $k_{n_{sub3}}^{th}$ from the SN. Contrary to energy costing, exergy costing accounts for the high exergetic destruction occurring in the substation, which leads to a much higher value of k_{sub3}^{th} relative to the one obtained by c_{sub3}^{th}. Thus the exergetic behavior of the substation is integrated into k_{sub3}^{th} while this is not possible when calculating c_{sub3}^{th}. This fact also leads to another interesting issue which derives from analysing the unit exergy cost returning at the plant $k_{m_{hp}}^{th}$. It can be seen that, contrary to $c_{m_{hp}}^{th}$, $k_{m_{hp}}^{th}$ is higher then k_{sub3}^{th} which suggests that, considering exergy costing, the use of exergy is more costly for the plant compared to substation 3. Thus while in energy costing, those unit costs were almost always equal, they are definitely not in exergy costing. This means that the impact on the RN is considerably different and depends on the costing technique.

It can be concluded that both costing techniques provide insight into individual behavior, however, energy costing has the drawback of not integrating the thermodynamic behavior of the consumer. Exergy costing on the contrary is able to account for both the individual impact on the cost generation through the DHN and the substation component.

4.2.2.3 Comparison of costing approaches

In Figure 4-10 and Figure 4-11 the resulting unit energy- and exergy cost based on black-box costing are presented. It was already discussed, that those results are equal for every substation in the network because they are based on global calculation. Hence, those unit costs would also be used to assign a unit cost for energy/exergy extracted from substation 3.

It is therefore now possible to compare the results obtained by the black-box costing to the thermoeconomic results of the TESL. The comparison of energy costing and black-box energy costing is given in Figure 4-14, exemplarily for substation 3.
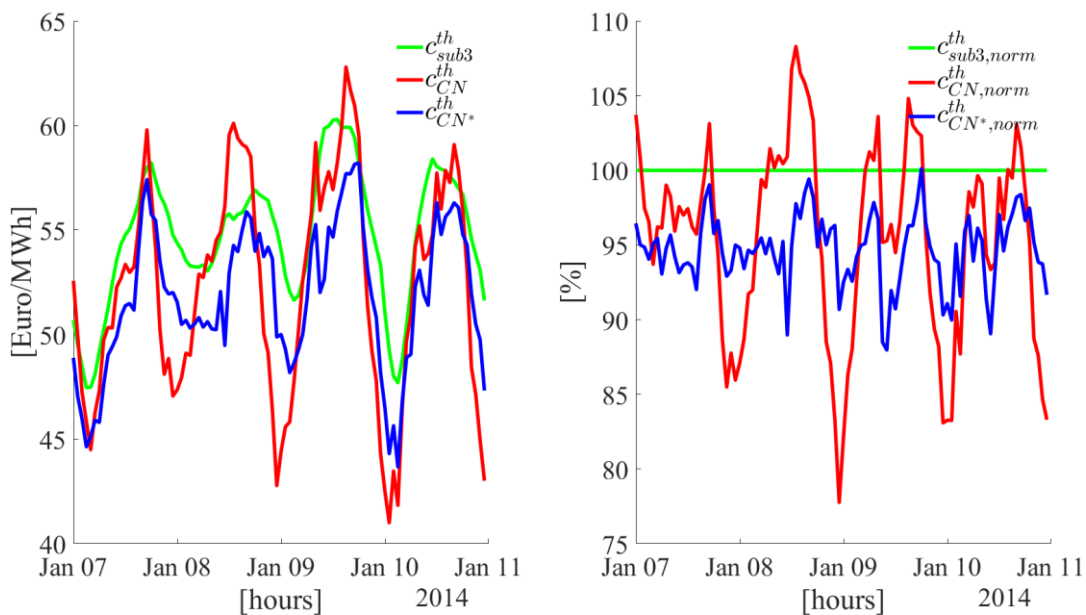
Figure 4-14: Comparison of costing approaches – energy

On the left side of the figure, the unit costs of black-box costing and energy costing are compared. The unit energy cost obtained through energy costing c_{sub3}^{th} shows a less fluctuating profile compared to the black-box results, where especially the peaks are less pronounced. In order to better compare the result, the black-box results are normalized to c_{sub3}^{th} to show the percentage of deviation. The normalized unit cost

$c_{CN^*,norm}^{th}$, shows the relation between average dynamic unit costs to the unit energy cost of substation 3.

It can be seen, that $c_{CN^*,norm}^{th}$ is almost lower then c_{sub3}^{th}. The point is that $c_{CN^*,norm}^{th}$ is in average about 5 to 10 % lower than c_{sub3}^{th} during the whole timeframe, which indicates that the black-box costing method fairly underestimates the true unit energy cost of the substations. Since $c_{CN^*}^{th}$ is averaging the thermal losses throughout the network, a lower relative value of $c_{CN^*,norm}^{th}$ indicates that the individual costs are higher than average. This means, $c_{CN^*}^{th}$ is underestimating the loss generation of substation 3.

Furthermore, $c_{CN^*}^{th}$ is much less fluctuating then c_{CN}^{th} because, c_{CN}^{th} also averages the transient behavior of the network, leading to a unit cost highly inaccurate. This leads to a relative difference of $c_{CN,norm}^{th}$ which is, first much more pronounced in terms of its peaks and second results also in an overestimation of the substation, during timesteps where $c_{CN,norm}^{th}$ is greater than 100 %. In those cases, average unit cost result in higher unit cost compared to c_{sub3}^{th} and thus wrongly contributes more loss generation to substation 3.

The errors obtained through black-box coting are significant and cannot be neglected. In the case, black-box energy costing is done; costing is mainly influenced by transient condition resulting in misleading result for substation 3. Even if transient behavior is corrected through dynamic average costs, overall losses are averaged and underestimate the loss generation of substation 3.

The results obtained by the comparison of energy costing do not reflect the thermodynamic behavior of the substation. In order to compare the costing approaches including the thermodynamic behavior of the substation, exergy costing is compared with the black-box approaches, see Figure 4-15.

Figure 4-15 shows that unit exergy costs of substation 3 k_{sub3}^{th} are much higher then calculated based on average -and dynamic average unit costs. The differences can be investigated in the normalized plot, which shows that $k_{CN^*,norm}^{th}$ and $k_{CN,norm}^{th}$ are below 100 %. This means, that the black-box approach is highly underestimating the generation of exergy destruction of substation 3.
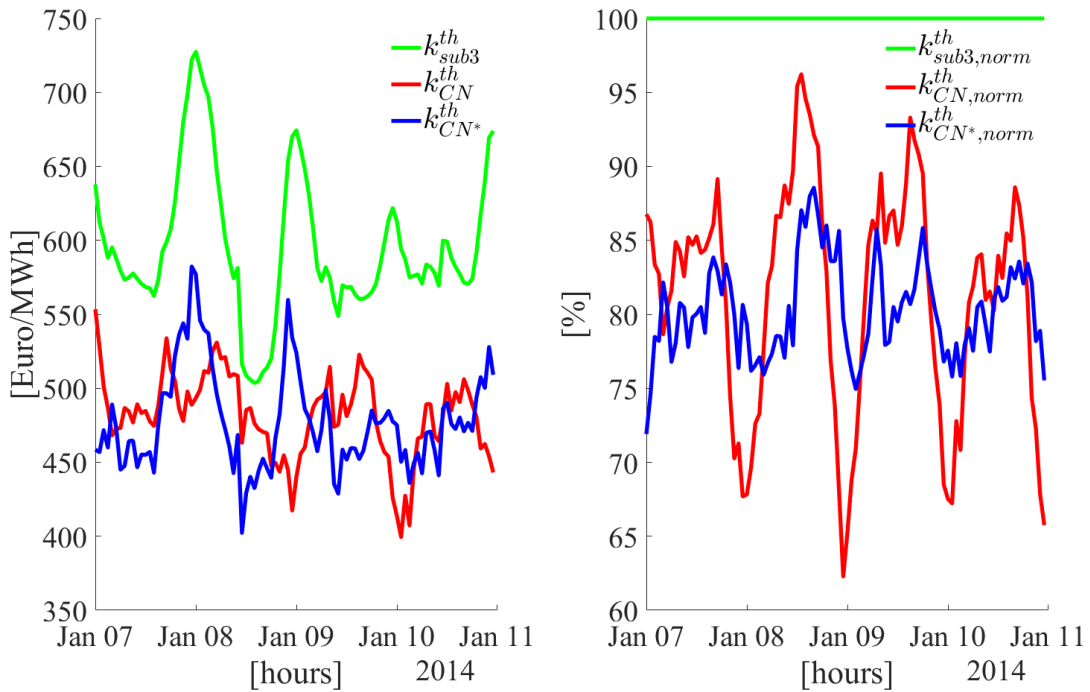
Figure 4-15: Comparison of costing approaches – exergy

Comparing $k_{CN^*,norm}^{th}$ and $k_{CN,norm}^{th}$ the same conclusion as for energy costing are true, with the difference that $k_{CN,norm}^{th}$ is never above 100 %. This is due to the high exergy destruction in the substation, which causes k_{sub3}^{th} to be always higher compared to the value obtained by energy costing.

It can be concluded, that the difference between black-box approach and exergy costing is even higher than for energy costing. The deviation is greater with $k_{CN^*,norm}^{th}$ of about 80 % in average which is much larger than the deviation of $c_{CN^*,norm}^{th}$ of about 5 % in average. This means, that for exergy costing, the error between black-box and thermoeconomic result is with 20 % far more substantial than for energy costing.

4.2.3 Thermoeconomic benchmark of consumers

In this section, the three substations of Figure 4-1 are analyzed in comparison with their black-box results in order to show the deviations of individual substations. Due to a lack of insights into DHN operation for real-exiting networks, it is assumed that in traditional approaches, only average unit costs for energy c_{CN}^{th} and exergy k_{CN}^{th} could be estimated. It is therefore interesting to study the difference between this black-box approach and the thermoeconomic results obtained by the TESL for different substa-

tions. In order to compare energy- and exergy costing, the results of exergy costing, thus k_{sub}^{th} for any substation, must be converted into unit cost of energy. This is done through (4.1),

$$c_{sub}^{*,th} = k_{sub}^{th} \frac{\Delta \dot{\psi}_{sub}^{th}}{\Delta \dot{\phi}_{sub}^{th}} \tag{4.1}$$

where $\left(c_{sub}^{*,th}\right)$ is the unit cost of the substation based on exergy costing. Thus the costing principles are based on exergy, while a direct comparison with c_{sub}^{th} is possible. For simplification, $c_{sub}^{*,th}$ is also referred as unit exergy cost even though it is in fact a unit energy cost based on exergy costing. Figure 4-16 shows the result obtained from the TESL for the three substations.
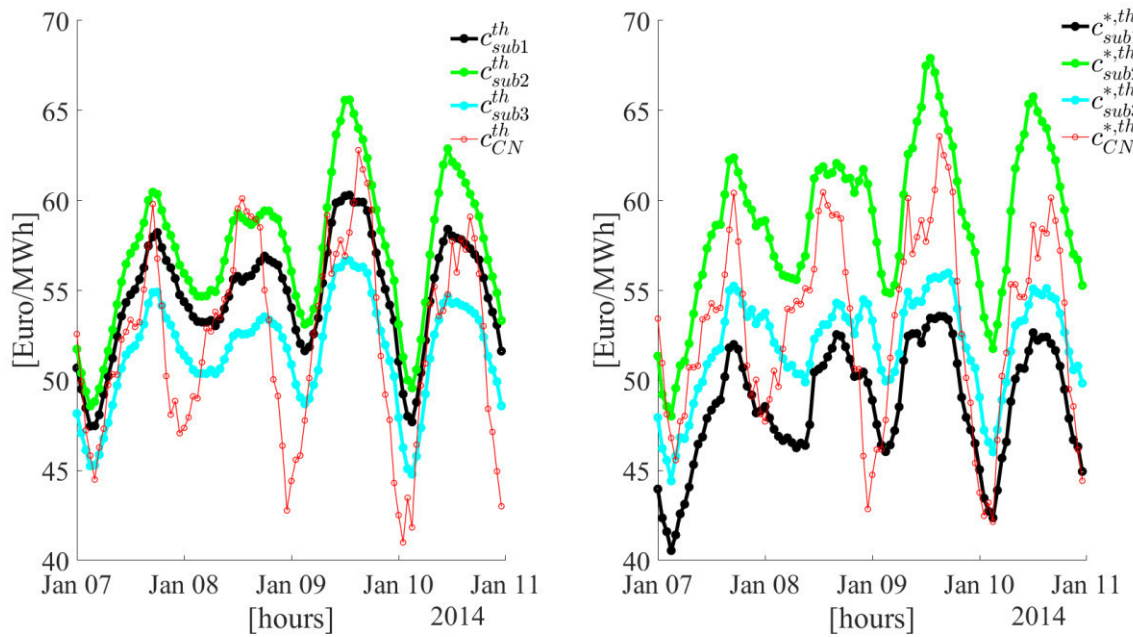
Figure 4-16: Comparison of energy- and exergy costing results for substations

The red line shows the black-box result c_{CN}^{th} and $c_{CN}^{*,th}$ for unit energy and exergy cost. Substation 2 has the highest unit energy cost c_{sub2}^{th} while substation 3 shows the lowest unit energy costs c_{sub3}^{th}. For a given timeframe, the black-box result either underestimates or overestimates the losses. This is equally true regarding exergy costing, with the difference that unit exergy costs of substation 1 and 3 are always lower compared to the average, while substation 2 shows higher peaks in exergy then energy costing. Substation 3 is closest to the plant compared to the others which is reflected by the relatively low unit energy. Interestingly, substation 1, which is located at

the far north side of the network, shows lower unit exergy costs than substation 3, while for energy costs, the opposite is true. Through the conversion of unit exergy into unit energy cost, the amount of exergy compared to the amount of energy has significant influence on the cost estimation. This is the reason for the lower unit costs based in exergy compared to energy.

Thus, benchmarking of consumers highly depend on the costing technique applied, while the influence of the substation cannot be neglected and can even lead to a different benchmark between two substations (as seen for substation 1 and 3). This can be clearly seen, when relative differences are plotted, see Figure 4-17
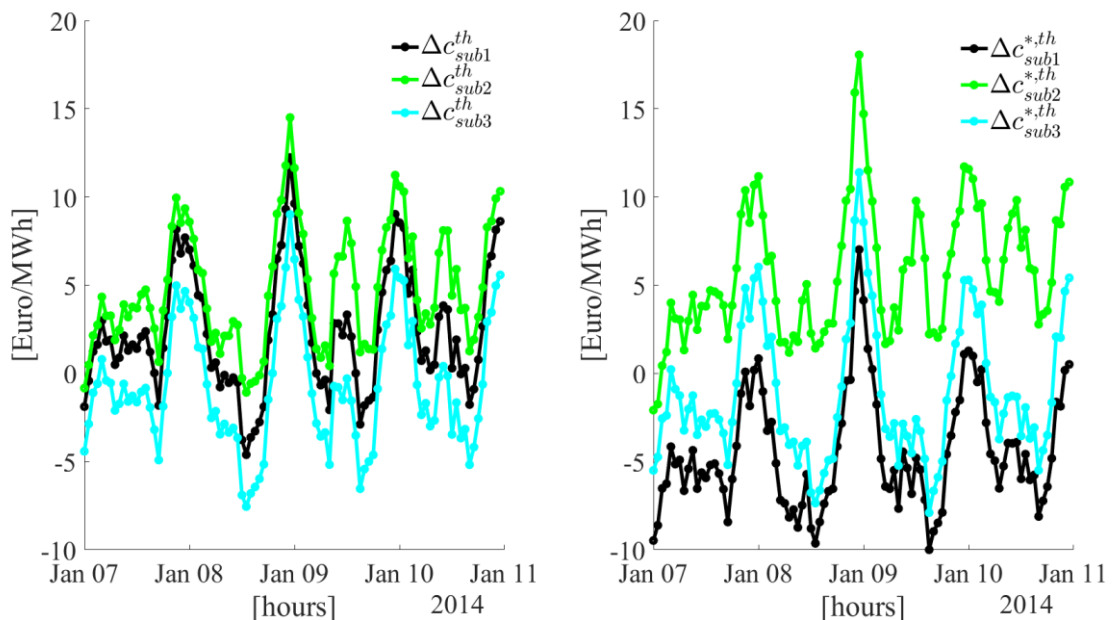
Figure 4-17: Benchmark of substations for energy (left) and exergy (right) costing

The benchmark uses the relative difference, such as $\Delta c_{sub_i}^{th} = c_{sub_i}^{th} - c_{CN}^{th}$ for the results of unit energy and exergy cost. The benchmark shows the difference of unit costs applied from average costs compared to thermoeconomic results. Substation 2 is the most underestimated substation, with a peak difference of about 15 Euro/MWh. This means, the utilization of one unit for energy on the 09.01 is 15 Euro/MWh more expensive, than estimated from a black-box analysis applied in industrial practice. Similarly for exergy, substation 2 is the most expensive with a peak difference of about 18 Euro/MWh. It can be seen that the peak is even more pronounced. Thus this result shows that thermoeconomics offers full transparency on the individual con-

tribution of losses in the system, which, depending on the costing approach, vary considerably to the results which are obtained in traditional costing.

4.3 Impact of waste heat integration

In this section, the impact of waste heat integration on the generation of exergetic costs at the substations is studied. For that, only thermal exergy is analyzed for defined scenarios of waste heat integration. For that, a generic industrial plant is defined, which is integrated similar to the production plant according to Figure 4-18.
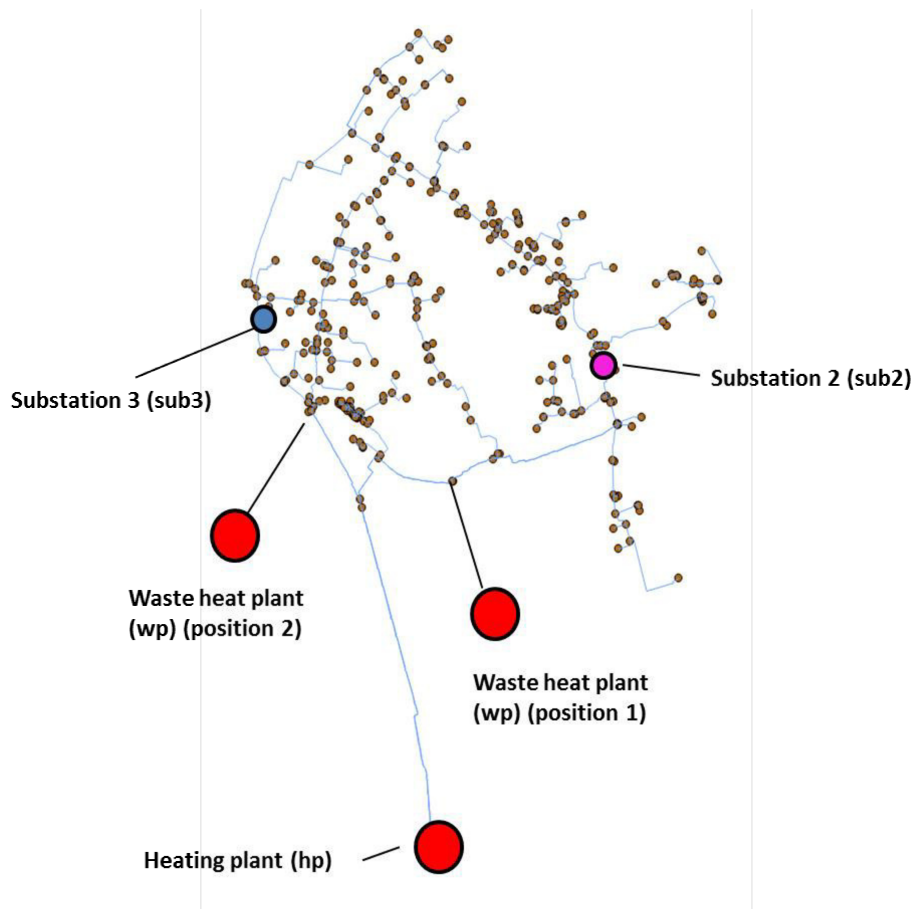
Figure 4-18: DHN system for the waste heat integration study

It must be noted that waste heat plant refers to any industrial plant which has excess heat available for integration. It should not be confused with waste incineration plants, which main purpose is to burn waste. Generally, the waste heat plant is assumed to provide energy in a batch-like process. This considers that waste heat occurs during specific timeframes according to the batch-processes of operation. Furthermore, it offers the possibility to study the dynamic behavior associated with a batch-like integration.

The waste heat plant is integrated at two different positions in order to study the effect of the position of integration on the cost generation in the selected substations. Furthermore two temperature levels at which waste heat is available are taken into consideration. In general the case study of waste heat integration includes two sub studies with a total of 3 scenarios:

- Sub study 1: Effect of position:
  - Scenario 1: Integration at position 1 (s1)
  - Scenario 2: Integration at position 2 (s2)
- Sub study 2: Effect of temperature:
  - Scenario 1: Waste heat temperature: 80 °C (s1)
  - Scenario 3: Waste heat temperature: 60 °C (s3)

The waste heat plant supplies 150 kg/s in a batch profile which has been adjusted according to the timeframe of this work. It was assumed that during phases of high demand, the plant is able to provide a constant of 150 kg/s at a certain temperature, while during the periods of low demand, waste heat integration is stopped. In order not to violate the boundary conditions of the model, a mass flow rate of 0.01 kg/s has been used during the latter phase.

In sub study 1, the waste heat plant is operated at 80 °C for both scenario 1 and scenario 2, while for sub study 2, the temperature is reduced to 60 °C in scenario 3.

4.3.1 Sub study 1: Effect of position

The effect of the position of the waste heat integration is crucial for the analysis of feasible solutions. One influence of the position is the resulting mass flow which depends on the amount of excess mass flow rate due to a lower network temperature. It was already shown, that the mass flow rate of the production plant must be adjusted in order to provide the necessary thermal demand when a low-temperature waste heat source is integrated. This excess mass flow rate is calculated through the adjustment approach shown in section 3.5.2.

Another influence is that the substations are not uniformly affected by the waste heat integration, but the resulting distribution of mass flow might be considerably different at different points in the network. In order to account for that, two positions of possible integration have been chosen in Figure 4-18. Those correspond to positions

slightly after the mass flow supplied by the heating plant divides into two branches, supplying two different areas of the network. Through that positioning it is possible to study the effect on the selected substations. The results of the mass flow adjustment and the corresponding temperatures are given in Figure 4-19.
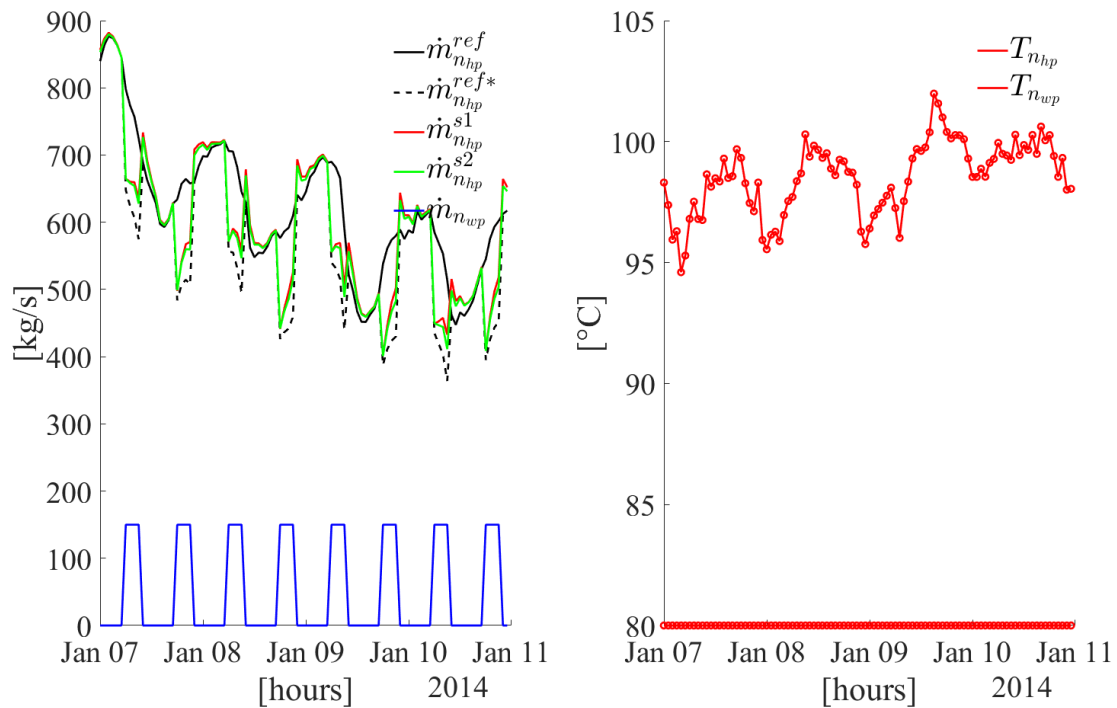
Figure 4-19: Mass flow rates (left) and temperature (right) of scenario 1 and 2

In the left part of the figure, the mass flow rates of the heating- and waste heat plant are shown. The waste heat plant supplies a given mass flow rate $\dot{m}_{n_{wp}}$ at the associated node in the SN, while for the heating plant, the mass flow rates of both reference and waste heat scenarios are given. The temperature of the production plant is unchanged to the reference case, while the temperature of the waste plant is set constant to 80 °C.

It can be seen that the mass flow rates of both waste heat integration scenarios $\dot{m}_{n_{hp}}^{s1}$ and $\dot{m}_{n_{hp}}^{s2}$ show a deviating profile to the reference mass flow rate $\dot{m}_{n_{hp}}^{ref}$. This deviation is caused by the adjustment algorithm, necessary to adjust the mass flow rate according to the reduced temperature in the network. This can be seen comparing $\dot{m}_{n_{hp}}^{ref}$ and $\dot{m}_{n_{hp}}^{ref*}$. The latter is the mass flow rate of the heating plant without adjustment, thus the difference between the mass flow rate of the plant in the reference scenario subtracted by the mass flow rate of the waste plant $\dot{m}_{n_{wp}}$.

Consequently, the mass flow rate of the heating plant is higher for both scenarios compared to the non-adjusted value of $\dot{m}_{n_{hp}}^{ref*}$, while a large difference between the mass flow of the two waste scenarios cannot be detected. Apart from that, the dynamic behavior can be seen in detail. When no flow is integrated during the batch process, the resulting mass flow rate is higher compared to the reference scenario, meaning that even though the integration of low-temperature flow has stopped, higher mass flow rate is still needed to compensate the still existing lower network temperature. During the non-operating phase of the waste plant $\left(\dot{m}_{n_{wp}} = 0.01\right)$, the mass flow rate is relatively higher but tends towards the reference value and meets the initial reference flow when the network temperature is back at the reference temperature.

This is a very important finding and shows the dynamic behavior of mass flow rate and temperature distribution in the network, especially when low-temperature sources are considered. The change in mass flow rate and network temperature effects the generation of cost at the substations in a certain way. This is furthermore studied through the comparison of the selected substations represented in Figure 4-18. In order to understand the outcomes of the exergy cost behavior, the network temperatures at the inlets of substations are provided explicitly, see Figure 4-20.
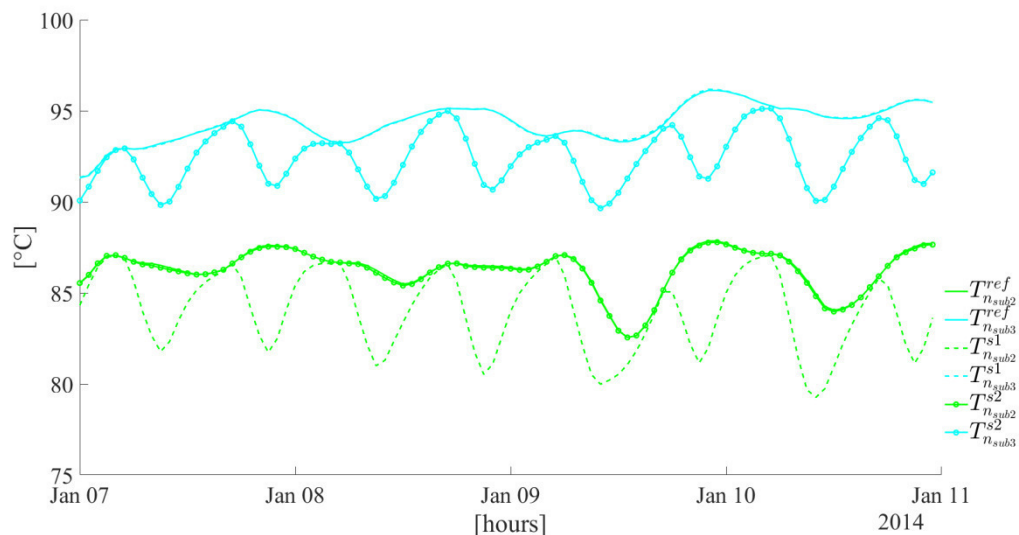
Figure 4-20: Network temperature at SN node of the substations

The two substations and their respective temperatures at the node connected to the SN are shown for the reference and the integration scenarios. In scenario 1, the

waste heat plant is integrated at position 1. In this case, the temperature at substations 2 decreases substantially during the integration phase, while substation 3 is almost not affected. At substation 3 no temperature change can be recorded.

Differently to scenario 1, in scenario 2 the opposite behavior can be concluded, where the low-temperature integration has very little impact on substation 2, but on substation 3.

Thus the resulting temperature at the substations is far from being similar, but depends substantially on the position of the low-temperature source. This is a very interesting finding and clearly shows the changes in temperature distribution of the network according to a low-temperature integration and their effects on the substations at different locations. Furthermore, that has very important implications on the exegetic behavior at each substation which can be analyzed through the results obtained through the exergetic cost analysis. This is exemplarity shown for substation 2 in Figure 4-21.
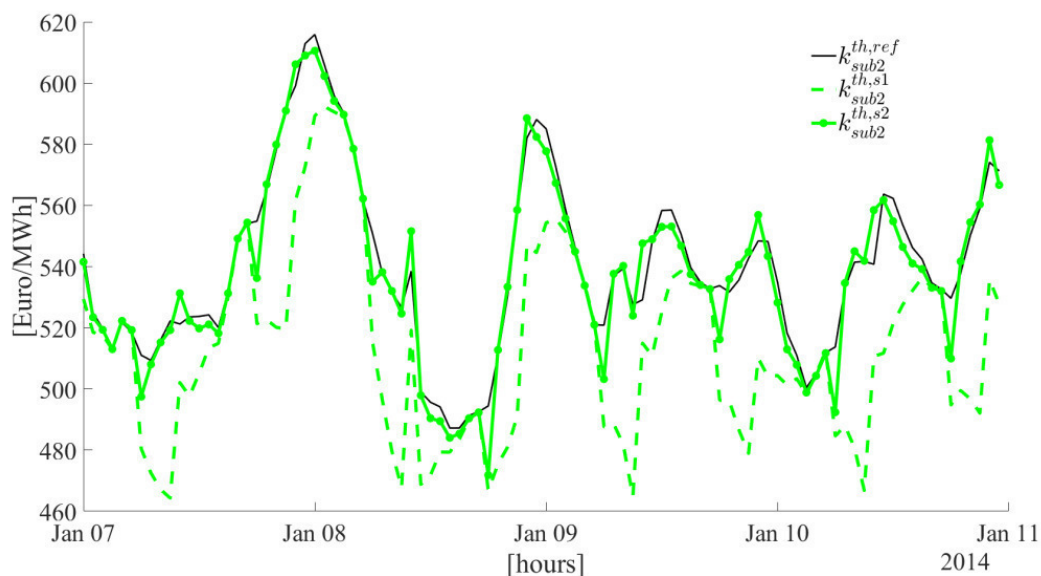
Figure 4-21: Comparison of unit exergetic costs at substation 2

The behavior of unit exergy costs for substation 2 is presented. The value for the reference scenario $k_{sb2}^{th,ref}$ is highlighted to compare the results of the two scenarios. In scenario 1, position 1 is selected which showed substantial impact of the temperature at substation 2, see Figure 4-20. This leads to a deviation in the profile of the unit exergy cost over time for that substation. Detailed analysis shows, that especially during the phases where low-temperature waste is integrated into the network, unit

exergy costs decrease while during the non-operating hours of the waste plant, unit exergy costs increase towards the reference value; but never actually exceeds it. The reason for a reduction in thermal unit exergy cost is the lower temperature at the inlet of substation 2 which is sufficient to provide the thermal demand of the consumer. In comparison to that, in scenario 2, the unit exergy costs are very similar to the reference values with slight increases in costs at several points. This is due to the position in the network. Temperature at the inlet is almost not affected by the integration of the waste heat stream, see Figure 4-20. This means, the variation of unit cost is not directly caused by the low-temperature flow of the waste plant but due to the operation of the whole network.

It can be therefore concluded, that the position of waste heat integration has high implications on the individual contributions of cost generation of the substations. This effect is a very complex mechanism which is caused by different influences such as temperature demand of the substation, adjusted mass flow rate etc. In order to provide another important influence of the cost generation, the effect of different supply temperatures is investigated in the next section.

4.3.2 Sub study 2: Effect of supply temperature

The effect of the temperature of the waste heat stream is an important issue to consider. This is due to the fact that waste heat streams are available at different temperature ranges in industrial practice and are usually classified according to their temperature level. Since this work considers smart thermal networks in its general form, it is interesting to study the effect of the temperature without the need of an additional increase which might a strong barrier in industrial practice.

The analysis is carried out through introducing a new scenario 3, which is equal to scenario 1 with the difference that the temperature of the waste heat stream is assumed at 60 °C instead of 80 °C. The adjustment algorithm must be applied to compensate the lower network temperature and the results are provided in Figure 4-22.

Two temperatures are used for the waste plant, which can be seen on the right side of the figure. The temperature of the heating plant and the mass flow rate of the waste plant remain unchanged. It is interesting to highlight, that with a lower waste heat temperature of 60 °C, the mass flow rate necessary from the heating plant is higher compared to scenario 1.
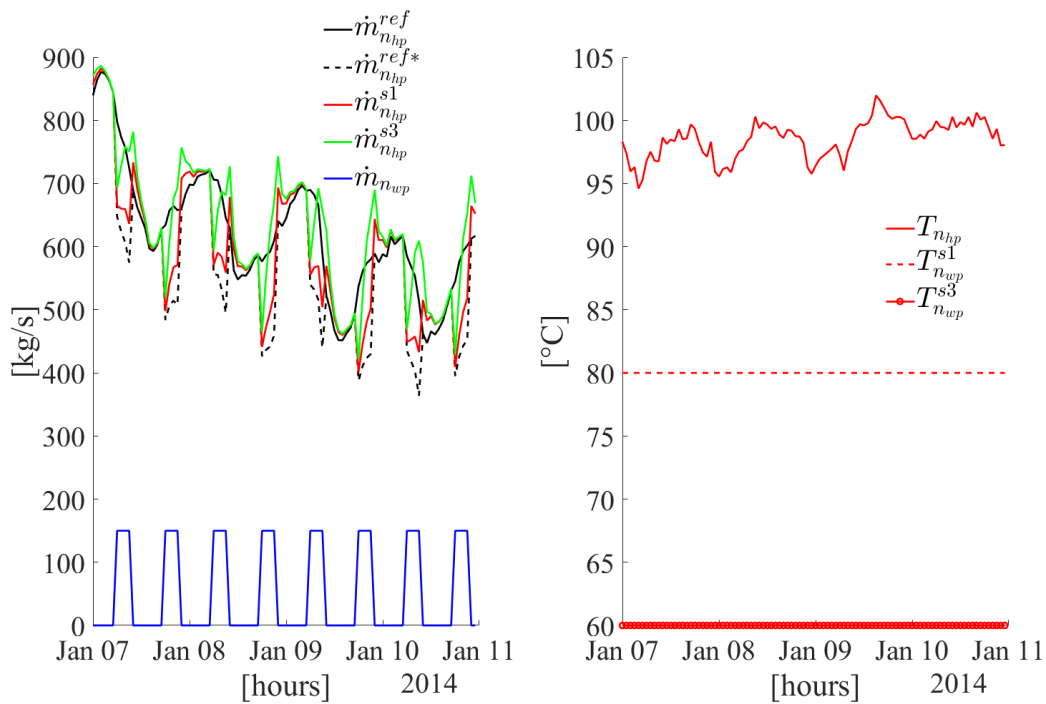
Figure 4-22: Mass flow rates (left) and temperature (right) of scenario 1 and 3

This can be seen at the left side of Figure 4-22, which shows an increase of mass flow rate compared to both the reference scenario and the scenario 1. This is caused by the lower temperature, which increases the necessary mass flow rate in order to supply enough thermal energy to the consumers. This increase in mass flow is very well established as can be seen for substation 2 in Figure 4-23.
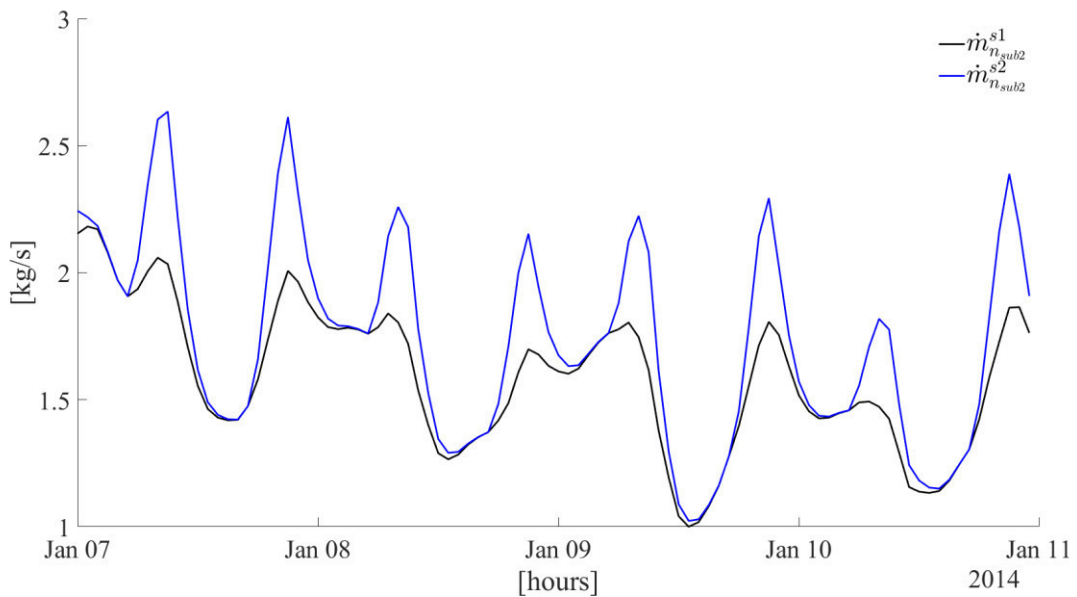
Figure 4-23: Comparison of mass flow rates at substation 2

The mass flow rate in scenario 3 shows substantial higher peaks during the time, when the waste plant is operating and injecting 150 kg/s at 60 °C. Depending on the resulting mass flow rate, a certain temperature at the inlet and the outlet of the primary side of the substation occurs. Those temperatures determine the amount of thermal exergy extracted by the substation and are therefore a major factor to the unit cost generation. The results of the temperatures at substation 2 are represented in Figure 4-24.
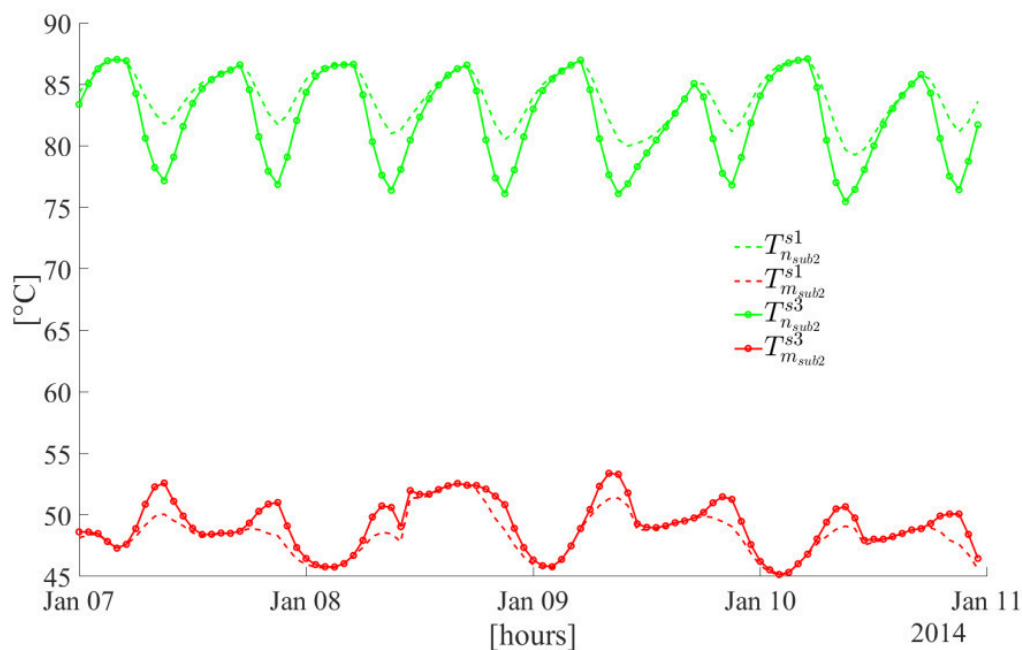
Figure 4-24: Temperatures at the primary side of substation 2

The reoccurring drop in temperature at the SN node of the substation is very well noticeable for both scenarios. While for a waste heat temperature of 80 °C, the temperature drop is about 3 °C in average, this value is substantially higher with a lower temperature of the waste stream. The temperature at the inlet of the substation drops almost to 75 °C during the time of waste heat operation. Furthermore, the resulting outlet temperatures at the node connected to the RN are given. Here it can be seen that the temperature is higher for scenario 3 then for scenario 1 during the time of operation. This is caused by a compensation of higher mass flow rate and decrease of inlet temperature and depends on the thermodynamic modeling results of the HX model of the substation. The fact that the return temperature is higher in scenario 3 leads to a lower temperature drop and therefore to a lower extraction of exergy through the substation. This might counterbalance the gains obtained through a low-

er temperature loss throughout the network. In order to study the effects in detail, Figure 4-25 shows the unit exergy costs at substation 2 for the given scenarios.
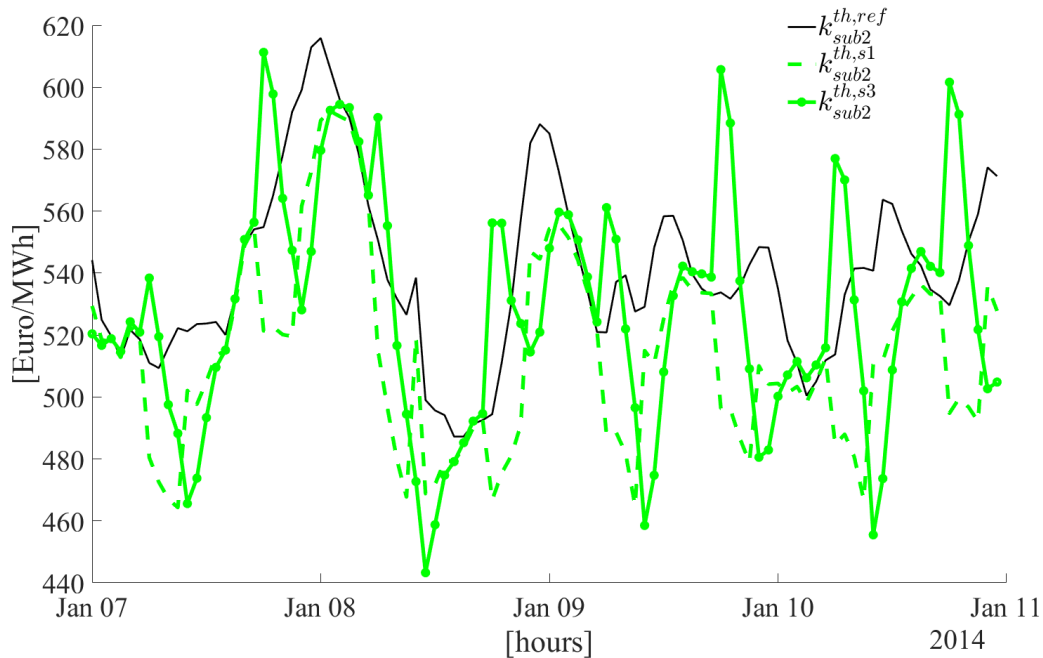
Figure 4-25: Comparison of unit exergy costs for substation 2 in scenario 1+3

The results of the reference curve and of scenario 1 are equal to the one obtained by Figure 4-21. It can be seen that the unit exergy costs for scenario 3 shows a different profile including unit costs both higher and lower compared to the other scenarios. This is a very interesting result, because it could be expected that a lower temperature will automatically decrease the unit cost obtained because of two reasons.

First, the exergetic destructions are generally lower throughout the network. Second, the temperature difference between network temperature and demand temperature is lower which leads to a higher usage of thermal exergy through the heat exchanger process. However in this simulation, the effect of increased mass flow rate shows that this is not automatically true but the gains are counterbalanced by a decreasing temperature difference at the secondary side. This is an important insight and leads to the conclusion that lower network temperatures are not instantly providing lower exergetic costs at certain substations.

The application of the dynamic thermoeconomic model provides deep insights into cost generation from various perspectives and clearly highlights the dynamic influences on cost generation associated with large DHN system.

4.4 Closing remarks

The formulation of thermoeconomics for graph-based network models can be applied to any DHN topology independently of the size of the network or the amounts of producers or consumers connected. The theoretical formulation provides a compact formulation for graph-based networks and is therefore especially suitable for large networks. External factors, such as boundary conditions of unit costs of external fuels or investment- and maintained costs can be comfortably integrated through the given matrix approach.

Furthermore, this approach is in accordance with the theory of exergetic costing. It assigns costs according to the loss of energy or exergy and is therefore able to capture the individual contribution of cost generation in DHN systems. The introduction of auxiliary equations is unnecessary, which avoids extra computational costs which would arise from traditional formulation. The formulation of thermoeconomic costs is an important piece of information for smart thermal network operation, because it enables the assessment of various measures such as waste heat and renewable energy integration or demand side measures such as temperature reduction of the consumers.

The case studies on the comparison of black-box costing vs. thermoeconomic costing revealed the drawbacks of black-box costing in the industrial context. The impacts of dynamic network behavior and individual contribution of the consumer are neglected which leads to wrong allocation of costs. Thermoeconomic provides a more transparent way of assigning the cost, namely individually at the place where inefficiency or thermal/mechanical losses occur. It was seen, that thermoeconomic provides a much clearer picture of the cost generating in network operation and offers the possibility for benchmarking between the consumers. Through that, the impact of consumer demand can be assessed and, if necessary, adapted through several measures such as dynamic pricing for demands with high costs etc.

In using the case study for waste heat integration, important points of the effect of position and temperature as well as the impact of batch-like profiles were discussed. This enables a better understanding of the effects on cost generation waste heat integration has and helps to assess the feasibility of waste heat integration or the integration of renewable energy sources such as solar thermal power.

However some drawbacks of the approach should also be mentioned which need further research. The formulation of transient exergy cost in the control volume is based on the definition of a negative product. This means that the unit cost assigned to transient exergy entering the control volume is equal to the unit cost of the control volume. This does not entirely reflect the physical behavior, because the exergy entering has been previously stored in the control volume at a certain cost. Therefore, a more precise evaluation would consider the integral of the unit cost over time as the unit cost entering. In cases where the unit cost of the transient exergy is close to the unit cost of the node in the control volume, this difference can be neglected.

The definition of the product cost flow as the energy or exergy difference at the secondary side of the HX model might neglect inefficiencies happening in the consumer loop. Thus different heating systems might have different losses associated with their supply temperature. In this work, the secondary side of the HX model has been calibrated trough the secondary mass flow rate. Hence no influence of the consumer side on energy- or exergy efficiency has been considered.

Another issue of thermoeconomic costing arises with the assignment of the individual contribution of mechanical exergy cost at the substation. As mentioned before, mechanical energy cannot be assigned directly to the consumer at the secondary side of the HX model. This is because of the equal pressure drops in closed circuits. In this work, this has been solved through neglecting the pressure difference at the primary side and using only the individual contributions of both supply- and return network. However, more research must be carried out to determine better solutions of assigning mechanical costs to substations.

Part B:

Contributions to DHN design –

a multi-perspective approach

Chapter 5: State of the art – design level

In this chapter, the current state of the art in the field of DHN system design is provided. The focus herby lies on the sustainable design of small-to medium scale DHN systems. This involves the sustainable design using selected environmental methods and improved integration of policy targets.

Section 5.1 describes the policy strategies towards energy transition, decarbonisation and the implications on the increase of renewable energy, especially under the perspective of biomass utilization. Implications on DHN system design and their challenges are described in detail, while in section 5.2 the need for DHN design according to a system for energy service is discussed.

Improved design towards more sustainable DHN systems must include a design according to the principles of sustainability. Section 5.3 therefore provides a systematic overview of commonly used assessment methods for all dimensions of sustainability and discusses its differences and individual benefits and drawbacks. One focus in this work is laid upon the environmental methods *carbon footprint analysis* and *emergy analysis*. Those are further detailed and compared. Section 5.4 and 5.5 provide an overview of the use of multi-criteria analysis and multi-objective optimization in current research of DHN systems, since those methods are a way of integrating different conflicting objectives.

Section 5.6 finally describes the individual contributions of part B of this thesis to sustainable design of DHN systems.

5.1 Policy strategy towards renewable energy

The efforts towards tackling climate change and its corresponding negative effects on society increased considerably during the last decades. Global awareness started in the 1990's, first at the Earth Summit 1992 in Brazil, defining the common "Nations Framework Convention on Climate Change" which paved the way to the first international agreement on common climate-related policy targets, better known as the Kyoto-Protocol (United Nations 1998). Carbon dioxide emissions (CO_2) were found to be a major driver for climate change and specific national targets were set in order to

reduce them. One major strategy is the use of energy sources which do not emit carbon emissions: renewable energy.

Renewable energy is promoted for substitution of conventional fossil fuels on a worldwide basis (EIA 2013). In accordance with the worldwide trends, the European Union (EU) promotes renewable energies and aims to be a worldwide leader through implementing ambitious targets like the Horizon 20-20-20 targets (Horizon 2020) or the directive on energy efficiency (European Parliament 2012). Those strategies emphasize the role of reducing both energy consumption and carbon dioxide emissions by 20% (basis 1990) while energy efficiency and the share of renewable energy should be increased up to 20% (or even higher) until 2020. These legal regulations are replacing the expired Kyoto-Protocol, while during the last United Nations Climate Change Conference in Paris (COP21), the majority of the world's countries agreed on tackling climate change through keeping world's temperature rise (way) below 2 °C (United Nations 2015).

Focusing on the European Union only, 48% of final energy consumption accounts for heating services, 43% of that amount corresponds to the private sector demanding low-temperature heat (< 250 °C) for space heating and domestic hot water. This results in 15% of final energy consumption in the EU (RHC 2011). This high demand of heating service can either be met by decentralized installations like individual boilers, heat pumps or by centralized heating systems such as district heating networks in any scale, ranging from kW to GW of installed thermal power. As previously described in part A of this thesis, district heating networks are considered a major player in smart energy systems, where they act as a backbone of storage and distribution of low-temperature energy.

However, considering that DHN range from a broad scale of sizes, the requirements of those systems may vary from case to case. District heating networks are centralized solutions of heat supply, connecting several heat consumers to one (or more) heat producers through a thermal grid of water. According to works done by Lund, Mathiesen and others (Mathiesen et.al. 2015; Lund et.al. 2010), such thermal networks are considered as a backbone of future energy systems, with high demands on flexibility due to renewable energy integration. Thermal networks overcome both spatial and temporal mismatch through the ability of transporting energy over large distances and the storage behavior of the thermal grid itself. Current developments fo-

cus on 4th. generation networks (Lund et.al. 2014), able to lower network temperature, integrate renewable energy or integration waste heat from e.g. industrial plants.

While for large-scale systems, the intelligent operation of multi sources and consumers is in the focus of investigation, small-scale systems covering heating service for a single district might not be interconnected to the electricity- or gas network. In those cases, the DHN is operating as a stand-alone system. For such systems, the aim is not to function as a smart thermal grid but rather to supply the given heat demand in the most sustainable way. For smart thermal grids, sustainability may be highly variable due to the fluctuating in- and outflow of different energy vectors. This is not the case for small-scale systems connecting a set of consumers with e.g. one single CHP or heating plant. There, the focus is rather on proper design in order to comply with targets based on policy- and sustainability concerns as well as profitability of the heating service.

It can be concluded that for small-scale systems, the policy targets like reduction of primary energy consumption or reduced carbon emissions directly affect the system design and must therefore be taken into account.

5.1.1 Implications for small-scale DHN systems

The previously described policy targets aim to define certain conditions under which a DHN system is operating. One major term to describe the strategy for those systems is decarbonisation. Decarbonisation is the strategy of reducing the utilization of fossil fuels through a substitution through renewable energy.

Decarbonisation of small-to-medium scale DHNs is possible through a variety of measures like utilization of renewable energy sources (RES) such as biomass-based heat generation, biofuels, integration of solar energy or heat pumps and advanced geothermal technology (RHC 2011). The aim for decarbonisation does not necessarily exclude the utilization of fuels with carbon emissions such as biomass or bioenergy fuels under certain conditions.

As a reaction of environmental concerns and legal pressure, biomass is promoted and implemented as a renewable energy source, both for domestic as well as for industrial applications. In the latter case, it is mainly used for heating purposes substituting fossil fuels like oil, natural gas and coal, through e.g. co-firing technology (Sai-

dur et.al. 2011). Due to that, energy production from biofuels and especially from traditional biomass has reached a high level of production of about 57 EJ in 2013 (REN21 2014) and is still promoted to gain higher shares due to an increase in worldwide energy demand (Edrisi and Abhilash 2015). Despite the fact that utilization of solid biomass accounts to the vast majority in both heat (77%) and electricity generation (71%) from bioenergy sources worldwide and the utilization of about 13 Mio. T in the EU in 2014, its global generation potential is still rising in all parts of the world (REN21 2016). Therefore, heat supply from biomass is a reasonable way of increasing the share of renewable energy in small scale DHN.

The advantage of the use of biomass is, that its combustion is carbon neutral if the harvesting and replacement is of equal amount. This is represented through the "carbon payback period" (REN21 2014) and if certain conditions are fulfilled, biomass utilization can be accounted as renewable energy source. Though the conditions, under which biomass utilization is considered to be renewable, are controversial, the EU Parliament clearly confirms it to be in one of their recent directives (European Parliament 2009).

The implementation of biomass technology depends to a good part on fuel market prices and is also (positively) influenced by policies regarding funding and compensations (Saidur et.al. 2011). Besides that, the resource usage itself is influenced by different forces of antagonistic objectives; as can be seen within the example of biomass for co-generation firing vs. synthetic biofuel production (Al-Mansour & Zuwala, 2010) and (Leduc et.al. 2012). Nevertheless, biomass is widely accessible and easily available in most parts of Europe, but neither inexhaustible nor unlimited. One reason is, that excessive use of biomass for energy production leads to societal problems like expulsion of land for agriculture and to a competition between the food and the energy resource market (Brown 2003). Another reason is, that biomass faces general environmental constraints like limited phosphor resources (Valero 2015). Even if combustion of biomass is carbon-neutral in its utilization, side effects like transportation or other carbon emissions related with its usage must be considered (Cowie & Gardner 2007).

5.1.2 Challenges in small-scale DHN system design

Apart from that, modern society needs different sorts of energy services like heating, cooling or electricity, which are provided mainly by industrial sites (Gerber et.al. 2013). Companies and their decision makers dealing with energy services have a crucial interest in developing profitable business models and solutions, which are able to provide energy services in a most sustainable way (Hoyt 2003). The objective of design engineers is to optimize certain economic criteria, like overall investments, return on investment (ROI) or net present value (NPV), while fulfilling legal as well as environmental constraints concerning waste, water, CO_2 emissions and other environmental impacts.

In the field of DHN design, this also includes the integration of legal constraints and policy strategies, which are an important part of urban planning (Gabillet 2015). This applies to eco-districts as well as to DHN located in rural areas, in which proper design decisions upon the size of the heating plant must be made. Since the size affects the way heat is generated, the design of DHN suffers from antagonist objectives. This was pointed out by (Hendricks et.al. 2016), which examined a cost-effective, biomass-fired design of a DHN located in a rural area. There, inefficiencies due to an over-sized biomass plant size where reducing the potential of increased biomass utilization from a cost-perspective.

Another design solution for small-scale DHN using biomass as a main fuel was proposed by (Jamali-Zghal et.al. 2013). There, the feasibility of a DHN in comparison to a decentralized gas boiler system was assessed for a DHN system located in France using carbon footprint and emergy analysis. The distance of the biomass resources to the plant and the corresponding efforts for transportation was proposed as main design decision. Those results suggested maximal supply distances, but neglected the fact, that those are hardly influenced by the system designer. (Andric et.al. 2014) used a similar methodology to assess co-firing of biomass in a coal-based heating plant and concluded similar results.

From an industrial designer's perspective, the use of maximum supply distance seems unpractical, since it can hardly be affected when the DHN system is designed at a specific location. In the case where the supply distance of biomass resources is to large, (Jamali-Zghal et.al. 2013) propose a decentralized gas boiler system to be

more environmental friendly. This is an unsatisfying result from a sustainability view-point. However, a detailed heating plant model or a study on possible heat demand reductions through demand side measures has not been carried out. Focusing on industrial designers, one way to improve design capability is to define the size of the centralized DHN system as the major design variable. This offers not only a focus on the real need of system designers, but furthermore allows studying the impact of DSM measures.

A multi-unit design is an approach of sizing the heating plant in a way so that the base load unit could be e.g. a biomass unit, while medium and peak loads could be covered by gas-fired units. This is in accordance to small-to medium sized heating plants in practice (Danestig 2009). Base load nominal power in heating plant design is often set based on practical values (e.g. 60-65%), because they occur in real applications (Sartor et.al. 2014).

The performance of heat production, usually measured in thermal efficiency, depends on current operation and load conditions. Even though nominal efficiencies are equal to about 65% for biomass boilers and 90% for gas-fired boilers, those values decrease in partial-load operation due to inflexibility (RHC 2012) and thermal losses of different kinds (Torchio et.al. 2009). This assumption is also used in production optimization, as found in various publications (Noussan et.al. 2014; Lundstroem & Wallin 2016), because those authors focus on optimization of real-existing DHN, where nominal powers are a-priori fixed.

The problem related with design according to nominal power is, that the heat load of DHN systems is not constant, but highly dependent on the season and other factors such as the building structure connected or the habits of the consumers. This leads to characteristic load curves which are far from being constant, as studies on German heat loads in DHN show (BMU 2012). When optimum sizing is considered, this leads to an optimization problem of the size of the heating units under the assumptions that partial-load operation during times of lower heating demand highly affects the performance outcome of the system.

5.2 From energy generation to energy service

Implementing policy targets while complying with current strategies of decarbonisation demands a whole new way of assessing improved design. One major problem arises from the current business model applied in DHN operation. Heating service is mainly sold based on the amount of energy which is supplied to the consumer, even if the true cost of generation of a certain thermal energy might differ from that; as seen in Part A of this thesis. Optimum design of a DHN will therefore maximize the throughput of heat which in turn incentivizes a DHN design with maximum heat production. In any case, decarbonisation, green economy and sustainable development are concepts which need to be implemented by businesses, while their stimulation is the task of energy policies (Lund 2009).

This is in sharp contrast to policy targets and environmental concerns, which aim is to minimize heat production. Future DHN systems with increased environmental performance must involve holistic system design including feasible business solutions. A mere focus on heat sales, as promoted by classical business models, is not useful to increase environmental performance since measures like thermal insulation are counter-effective to the increase of heat sales and decision makers in this field are still skeptical towards innovative business models (Apajalahti et.al. 2015). This must be overcome, if future systems should be designed "sustainably".

One solution is to consider DHN system operation as a service to the consumer. This means, that not only sales on heat, but moreover other service measures such as demand side measures (DSM) are integrated, which allow for a service-oriented design. Demand side measures is a term summarizing efforts taken to manipulate the consumer load profiles through e.g. thermal insulation, load management or the adaption of the load profiles in general. DSM are implemented in various parts of heating systems like radiators, ventilation and air heating systems as well as in domestic- or commercial hot water generation (Kaerkkainen et.al. 2004); each of them showing a specific impact onto the load curve. Peak-load, e.g., is reduced through system integration of the building thermal mass (Li & Wang 2015), controlled heat load reduction (Johansson et.al. 2010) or thermal insulation (Lund et.al. 2010). Another approach is the increase of base-load through e.g. integrating increased commercial/industrial heat loads, the use of absorption cooling technologies (Danestig 2009) or the integration of heat storage solutions as proposed by (Verda & Colella

2011). Also combinations of those measures are imaginable which manipulate the heat load in a specific way.

Cross-cutting solutions to decarbonize the heating sector involve both demand- and supply-based measures and are needed to overcome drawbacks from supply-demand mismatch (RHC 2011). This includes optimum design of DHN systems and the integration of DSMs, which either help to reduce heat demand, e.g. through thermal insulation or shift heat demand e.g. through peak-load reduction. The shift from throughput to service-based design and operation has been proposed by (Steinberger et.al. 2009) and can consequently be applied to DHN design to solve the problem of conflicting objectives. This allows improving DHN system design and also helps establishing new business models for DHN operators.

It can be concluded, that future system design for DHN must integrate policy targets while providing performance-based business solutions. Both environmental and business-related objectives must be included in the design and conflicting objectives must be overcome through the application of performance-based business models. For DHN, that involves both optimum design from the perspective of industrial system designers and intelligent implementation of demand side measures. Those service definitions are in accordance with the measures proposed by the Heat Roadmap Europe (Stratego 2015), which promote the use of biomass in district heating networks in combination with DSM such as thermal insulation as a cross-cutting technology emphasizing more research on the sustainability of such solutions.

5.3 Sustainability as a mean for DHN design

Industrial ecology and green process design are concepts to further develop energy service systems towards a more sustainable future (Diwekar 2005); in terms of both legal/environmental and business issues. On the one hand, macroeconomic indicators are used to evaluate policy-related sustainability (Iddrisu & Bhattacharyya 2015; Shen et.al. 2010). On the other hand, a variety of different indicators exist using mixtures of macroeconomic (Diwekar 2005; Kharrazi et.al. 2014), strictly thermodynamic/exergy-based (Koroneos et.al. 2012) or hierarchical-based indicators as in (Yi et.al. 2004; Frangopoulos & Keramioti 2010); all trying to breakdown high-level indicators for the evaluation of industrial processes and systems. Thus, the improvement of sustainability of energy services related with DHN design is a problem which involves

all dimensions of sustainability (Gallopin et.al. 2014; Robert et.al. 2002) while a variety of different actors and stakeholder are involved.

Those requirements demand for an evaluation metric which includes different targets simultaneously. Literature review shows, that design optimization often use one, or two aspects like only technological (Di Somma et.al. 2015) techno-economical (Esen et.al. 2007) or eco-environmental (Capon-Garcia et.al. 2014) objectives, but do not include evaluations targeting the holistic view of sustainable design of thermal systems as proposed by (Lazzaretto & Toffolo 2004).

In order to overcome the drawbacks related with the mere focus on one single objective only, a holistic performance metric must be defined which is able to cover the different objectives DHN designers face. Those include policy targets of reduced carbon emissions, energy efficiency increase and reduction of primary energy needs. (Mallikarjun & Lewis 2014) propose a technology-policy framework for assessing feasibility of distributed energy resources based on a multi-criteria analysis. This concept offers the possibility to include antagonist objectives like system costs and emission reduction and can also be applied to DHN system design.

5.3.1 Classification of assessment methods for sustainability analysis

In part B of this thesis, the aim is to increase the sustainability of DHN system through optimum design. This implies a short analysis on how sustainability is measured and which evaluation methods are applied. The design and optimization of energy service models is a multi-dimensional problem in the sense of sustainability and therefore involves technological, socio-economic and environmental layers (Schwarz et.al. 2002). The different layers have to be addressed through applying assessment methods using certain indicators, which are arranged with the help of a hierarchical sustainability metric. Applications of such metrics were applied to industrial applications (Yi et.al. 2004; Graedel & Allenby 2002).

Therefore, models for energy service design and optimization are multi-layer, multi-criteria models which include a variety of different objectives/targets, design criteria and boundary conditions. Since energy service models are the basis of the business model, any business solution has to be validated in terms of sustainability. A variety of different assessment methods, analysis techniques and indicator definitions can be found in the literature. Those methods determine certain indicators, which are then

taken for system evaluation. (Wang et.al. 2009) carried out an extensive literature review about possible assessment criteria which are used in sustainability evaluation. The review shows that criteria like energy efficiency, carbon footprint or investment- and operational costs are vastly used for evaluating energy systems, while methods based on exergy, like cumulative exergy are not as popular.

The most commonly used criteria are taken and extended through exergy-based methods as well as emergy analysis and classified, in order to prepare a more comprehensive summary for criteria selection. This was carried out using the literature cited by (Wang et.al. 2009) extended by a search in common science databases. Table 5-1 summarizes and classifies them in terms of applicability to the sustainability layer and to its range of application, represented by the spatial scale. For the selection, each method was analyzed according to its "driving unit", sustainability focus and spatial scale. The unit driving the assessment can be either mass, energy, exergy or cost. This differentiation is a way to identify on which basis a certain approach is conducted. While energy can be either used for technological and environmental sustainability analysis, mass flow was seen to be limited to environmental analysis only.

The applicability to sustainability layers are different for each method and should be taken into account when defining sustainability criteria for different evaluation purposes. Another important part is the spatial scale. It refers to the fact that a certain method studies whole eco-economic areas, while others focus on the lifetime of a given product or process. This is crucial when comparing different results of sustainability criteria. In using this criteria to select and classify the various methods, Table 5-1 was developed which is used to (a) give a characterization of assessment methods in sustainability analysis and (b) for the appropriate selection of them in this work.

The indicators ICEC and ECEC in Table 5-1 refer to "industrial cumulative exergy consumption" and "ecological cumulative exergy consumption", respectively. It furthermore shows methods and their corresponding indicators which are used for either analysis of technological- (Tech.), economical- (Eco.) or environmental- (Env.) sustainability analysis. Applications range from whole ecological- or economic systems, like countries or regions, to a life-cycle or to a process/system view only. It can be seen that e.g. energy and exergy are methods mainly used for process analysis,

while EExA, ICEC or emergy are methods applied to broader spatial scales. Table 5-1 gives an overview of the most common existing evaluation techniques but is not complete in its presentation. It provides the reader with an extension of several important methods not covered by (Wang et.al. 2009).

An example of a method not covered by this analysis is Life-Cycle Analysis (LCA). The reason is that this analysis is based on methods which can be implemented into numerical optimization methods without the need of external software. In the case of LCA, information upon the impacts of deployment as well as the impact from upstream- and downstream processes of DHN design is needed. This is outside of the scope of this thesis and the term "sustainability" is used in the limited scope of the methods presented here.

5.3.1 Carbon footprint vs. emergy analysis

In this section, a short review of the carbon footprint method in comparison to the emergy method is provided. Since both of them are used as environmental performance indicators in the theoretical development in Part B, it is worth describing their approach in more detail.

The carbon footprint assessment determines the CO_2 emissions of the energy service system and uses that indicator to evaluate its environmental performance. CO_2 emissions are directly related with the use and consumption of fossil fuels. The theory of carbon-footprint analysis was extracted from the literature based on (Wackernagel & Rees 1996), (Jiang et.al. 2015) and (Weidema et.al. 2008) who provided extensive research on the theoretical development as well as on the practical application of the methods. Based on the popularity and the easiness of use, carbon footprint is one of the most important environmental assessment methods and is also subject to policy targets.

The difference between carbon footprint and CO_2 emissions is basically the system boundary of evaluation. While CO_2 emission are directly related with the use of fossil fuel, which emit CO_2 through their utilization, carbon footprint widens the system border and also takes CO_2 emissions of upstream processes into account. This means, that in the case, even though two fuels have equal amount of CO_2 emissions during utilization, they might have a different carbon footprint due to their history of

deployment. The carbon footprint is therefore a way of accounting of total carbon emissions of a certain energy source.

Another approach for accounting of the environmental burden of a certain product, process or system is the *emergy method*. Emergy analysis allows analyzing the environmental burden of processes that are related with energy carriers but furthermore includes all indirect flows of resources, flows of information or monetary capital (Brown & Ulgiati 2004).

Table 5-1: Classification for assessment methods in sustainable design

	Assessment method		Sustainability layer application		Spatial scale			Reference
	Name	Type	Indicator	Layer	Eco-economy	Life-cycle	Process	
Energy	Energy analysis (EA)	1_{st}	Energy efficiency, Primary energy consumption, Energy intensity	Tech.	√	√	√	(Afgan & Carvalho 2002), (Begic & Afgan 2007), (Bithas & Kalimeris 2013), (Beccali et.al. 2003)
	Embodied energy analysis (EEA)	1_{st}	Embodied energy	Env.	√	√		(Cui et.al. 2015), (Qier et.al. 2014)
Exergy	Exergy analysis (ExA)	2_{nd}	Exergy efficiency, Useful work Indicator	Tech.			√	(Sciubba & Wall 2007), (Dinca et.al. 2007), (Ayres & Warr 2009)
	Extended exergy accounting (EExA)	2_{nd}	Exergy efficiency	Tech.	√	√		(Sciubba 2001)
	Industrial cumulative exergy consumption (ICEC)	2_{nd}	ICEC	Tech.		√		(Szargut et.al. 1988)
	Ecological cumulative exergy consumption (ECEC)	2_{nd}	ECEC	Env.	√			(Hau & Bakshi 2004)
	Thermoeconomics (TE)	2_{nd}	Exergy cost	Eco.	√		√	(Tsatsaronis & Pisa 1994), (Rosen & Dincer 2003)
-	Emergy analysis (EmA)	2_{nd}	Emergy indicators	Env.	√	√		(Odum & Peterson 1996), (Brown & Ulgiati 1997)
Mass	Ecological footprint (EF)	1_{st}	Ecological footprint	Env.	√	√		(Wackernagel et.al. 1999)
	Carbon footprint (CF)	1_{st}	Carbon-dioxide emissons	Env.	√	√	√	(Wackernagel & Rees 1996), (Jiang et.al. 2015)
	Water footprint (WF)	1_{st}	Water footprint	Env.	√			(Chapagain & Hoekstra 2004)
Cost	Investment cost analysis (ICA)	1_{st}	Investment costs	Eco.	√	√		(Loken et.al. 2009)
	Net Present Value analysis (NPV)	1_{st}	NPV, Payback time	Eco.		√		(Papadopoulos & Karagiannidis 2008)

This should not be confused with the concept of *embodied energy analysis*. Emergy in contrast to embodied energy analysis follows the "maximum emergy principle", which is a concept for including the quality of energy from a biological or ecological viewpoint (Herendeen 2004); similar to exergy analysis. Thus emergy is not just accounting for energy used for a particular product, process or system but is furthermore assigning a quality to energy streams. A comprehensive view of the accounting method is given in (Sciubba & Ulgiati 2005), which is followed in this thesis.

The basic concept for analyzing industrial systems is to define the emergy system diagram, exemplarily shown for an energy system which uses natural gas, wood and diesel as fuels in Figure 5-1.
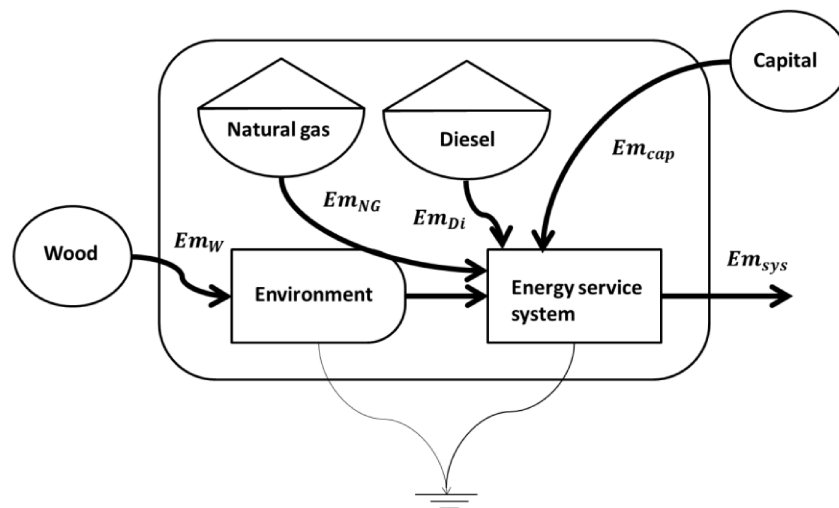
Figure 5-1: Emergy system diagram of a general energy service system

In emergy analysis, the indicated flows are classified according to their nature. For example, wood as a fuel is considered as a renewable energy source and is therefore provided by the environment. The environment is a system concept, which allows accounting biomass as a renewable energy source. In comparison to that, natural gas and diesel are non-renewable sources, while inflow of capital is also related with an emergy flow. The analysis provides a theoretical framework of accounting emergy to capital flows, which makes it possible to take into account e.g. investment costs of infrastructure for industrial systems. Similar to the carbon footprint analysis, emergy analysis uses the energy balance of a system to calculate its emergy flow. This is done through so called "transformities", which transform the energy of a certain flow into emergy into the common unit of solar emJoules. This is actually one major drawback of the method itself. The calculation of transformities depends first

on the reference state called the emergy baseline, thus the total emergy available on earth and second on the assumptions made regarding the calculation of the transformities in processes used during the evaluation. Considering a certain system, the application of the emergy method inherits the assumption made by other authors.

In any case, emergy analysis does not only account for the energy carriers but also includes the emergy flow due to capital investments or labor and goes beyond the framework of what is proposed by carbon footprint analyses. Hence, it is possible to account also for large investments into infrastructure which aim to reduce carbon footprint and might therefore allow assessing the usefulness of those measures.

5.4 Multi-criteria analysis for DHN system design

In this section, an introduction to multi-criteria analysis is given on the basis of the works carried out by (Jamali-Zghal et al. 2013). In that work, the substitution feasibility of a decentralized gas boiler system through a centralized heating plant was assessed through the evaluation of two environmental methods: carbon footprint and emergy analysis.

The design criteria for evaluating the feasibility of this substitution was chosen to be the supply distance of biomass from the centralized plant, which included a transport model to account for the additional energy needed. Furthermore, authors proposed a unification approach for carbon emissions and emergy, using a functional relation between CO_2 and emergy for the given design variable. In using this functional dependence, more insight on when a certain system design is more sustainable than its reference system can be extracted. This offers the possibility to instantly decide whether a change in system design does contribute to a higher sustainability or not.

The unification approach considered emergy and CO_2 only, making it impossible to apply the same approach to different evaluation methods. Therefore, a general methodology for analyzing the impacts of different evaluation methods using practical design criteria was not presented. More effort must be undertaken to generalize the proposed approach for the application to any assessment method and design variable in order to provide a method which can be used for other systems and evaluation techniques as well.

Based on those findings, multi-criteria analysis helps to analyze the connection and dependency between two different assessment methods. Multi-criteria analysis can be used to identify proper system design and performance assessment of DHN, as has been shown for conflicting objectives of energy efficiency and system profitability (Noussan et.al. 2014). This method does not optimize the given objective functions, but does only evaluate their value based in different choices of the design variables. This can be applied when the decision is based on the design variable rather than the objective function.

Hence, the objective is to characterize the influence of one criterion to another one. In other words, the aim is to deduce the result of one criterion, directly from the result of the other one, similar to what is available from Pareto analysis. The approach is described as follows:

Assuming any system consisting of e.g. three design variables α, β, γ applying two dimensional criteria analysis Cr_1, Cr_2, then the relations can be formulated through (5.1).

$$Cr_1 = f(\alpha, \beta, \gamma) \qquad\qquad Cr_2 = f(\alpha, \gamma) \qquad\qquad (5.1)$$

It can be seen, that if Cr_1 changes due to a change in β, no impact on Cr_2 is expected since Cr_2 is independent of β. This is e.g. the case when energy efficiency and emergy flow are analyzed. While emergy flow depends on economic variables like capital expenditures, energy efficiency does not. This means that for a change in capital expenditures, energy efficiency, unlike emergy, will be unaffected. This leads to the fact that for this design criterion, a MOO cannot be applied.

In contrast to that, if Cr_1 changes due to a change of α, Cr_2 will be also affected because it is dependent on that variable. Thus, two criteria can be either:

- depended
- independent

to each other due to a certain design variable. When two criteria are dependent, the impact of one criterion can be directly deduced from the other criterion through evaluating the following functional relation given through (5.2) exemplarily shown for α.

$$Cr_2 = f(Cr_1)_\alpha \qquad\qquad (5.2)$$

This functional relation derives Cr_2 directly from Cr_1, where both criteria are dependent on the design variable α while all other variables are set to be constant. Analytically, this is carried out by inserting the equation of $Cr_1(\alpha)$ into $Cr_1(\alpha)$. This allows to construct a Pareto curve for multi-criteria analysis without the need of setting up a MOO.

A quantification of the relation between two criteria can be generally made by formulating (5.3),

$$RF = \frac{Cr_1}{Cr_2} \tag{5.3}$$

where RF is called the "relational factor" and can be used to deduce Cr_1 from Cr_2 or vice versa. The relational factor can be determined for every possible design variable even if the two criteria are independent. If the change of a certain design variable does affect both criteria to the same magnitude, the relational factor stays constant and shows that this variable has no influence on the relation between the two criteria. Thus, the analysis of this factor provides information about the behavior of evaluation criteria to each other and can be used evaluate certain dependencies in multi-criteria analysis.

5.5   A multi-objective approach for DHN system design

Policy strategies which focus only on one single criterion, like environmental- or economic targets only, do not seem useful for a sustainable energy system design, because the multi-dimensional nature of sustainability is not taken into account. This can be overcome through a multi-objective performance metric which includes both policy and business targets. Multi-objective performance assessment is important, firstly for integrating policy strategies and secondly for increasing the system performance from a business point of view. Highlighted also in previous works (Mallikarjun and Lewis 2014), multi-objective approaches are not only applicable for the selection of appropriate energy technologies but moreover for the design of energy service systems including several targets and design conditions.

Multi-objective refers to the fact that system design must integrate objectives which might not be optimized subsequently due to their antagonist nature. Costs and CO2 reduction are just two popular example from industrial practice, while (Sameti &

Haghighat 2017) provided an overview over the most popular conflicting objects in DHN systems. Furthermore authors provide an extensive overview over applications of optimization of different DHN types. Those can be categorized in mainly two categories:

- Single-objective optimization (SOO)
- Multi-objective optimization (MOO)

While in SOO, one single objective function is optimized, multi-objective optimization aims in providing a set of optimum solutions based on multiple objective functions. This set of solutions is the *Pareto frontier*, which represent the solution, at which the set of objective functions is optimum. Furthermore, there exists the possibility of introducing weighting factors with which a multi objective optimization (MOO) problem can be converted into as SOO. However this method has drawbacks as to the a-priori decision on which objective function is favorable given a certain problem.

5.6   Outlook on the contributions of part B

The contributions of Part B to sustainable design of DHN systems use a multi-perspective approach which is initially based on the works carried out at a small-scale DHN system in Nantes/France (Jamali-Zghal et al. 2013). The DHN system under consideration is used as basis for the development of the following concepts.

First of all, as concluded in part A of this thesis, DHN systems must be treated as energy service systems providing heating service to (end)consumers. Due to the fact, that those system should comply with a variety of policy target regarding technological and environmental advancements, a holistic design approach which goes beyond the view of energy supply only, must be applied. Furthermore, industrial companies have constraints regarding the cost-or profitability of DHN system which might limit appropriate measures to be taken. When DHN systems are considered as energy service systems, measures on the demand side of the DHN system can be included in design which also support to establish new business models. This allows overcoming the mere focus on heat supply by industrial sites.

Second, DHN system design from an industrial viewpoint must include design criteria which can actually be influenced by the system designer. The case study carried out by (Jamali-Zghal et al. 2013) provided unsatisfying solutions for the use of centralized

biomass solutions compared to decentralized gas-boiler systems for several cases. This is mainly caused by the fact, that system design was not oriented according to the designer's selection and did ignore the behavior of the heating plant in terms of partial-load behavior. As seen in part A, energy demand is highly fluctuating and shows characteristic load profiles. When taken into account, this might lead to different design results as proposed by (Jamali-Zghal et al. 2013).

Third, according to the DHC platform, demand side measures (DSM) are considered to be one major cutting-edge technology for increased sustainability in DHN systems. Even though, thermal insulation and load shifting techniques have been identified to improve system operation, no research was found which integrates DSM into DHN system design. This is especially needed if DHN systems are considered as energy service systems, where industries can benefit from new approaches serving the consumer demand of heat.

Those issues are addressed in a multi-perspective approach. Chapter 6 of this thesis is divided into two parts. The first part aims in developing a framework for DHN system design tackling the drawbacks identified. This is done through the development of a DHN system design approach which is suitable for industrial designers. The suitability is based upon the fact that, a balanced view on system detail has been selected.

The DHN system is divided into two parts: The supply part, considering the sustainable supply of heat to the DHN, and the demand part, considering the load profiles of the DHN. The DHN operation is not further detailed in order to provide a compact methodology. However, the results which can be obtained from DHN simulation, as in part A of this thesis, can be integrated to consider dynamic variations of losses.

The heating plant is modelled as a multi-unit plant, which is composed of a set of base-load, medium-load and peak-load units. The design criteria in the industrial context are chosen to be nominal power of the heating units. The performance of heat production from those units is subject to actual heat load of the DHN and included through a partial-load model which can be adjusted according to the designer's needs.

In the demand part, the characteristics of heat demand from DHN systems are discussed based on several key parameters and are modelled as an exponential load

curve. To include DSM into the system design, the behavior of DSM on the load curve is studied which provides a quantitative way of integrating the behavior of various different DSM techniques.

In the second part, a new indicator called *load deviation index (LDI)* is proposed to link DSM and sustainable DHN design. This indicator allows quantifying load curves through one numerical value and can be used to deduce possible design improvements when DSM is applied.

The framework is applied to two case studies. In the first, a first attempt of integrating DSM through thermal insulation is carried out for a multi-criteria analysis of the DHN system used in this work. The design method prosed in the framework is applied and allows to provide a more thorough approach for industrial system designers. In the second case study, DSM measures are analyzed in their general behavior on sustainable system design. Especially the load deviation index is studied in detail using a multi-objective approach to consider all dimensions of sustainability.

Chapter 6: Framework for sustainable DHN system design

In this part of the thesis, a framework for sustainable DHN system design is developed. This includes two parts. In the first part, a system model is described which can be used to design DHN system according to supply- and demand focused energy services. The focus hereby lies on the utilization in industrial practice from a designer/s perspective. This also includes the analysis of demand side measures and their characteristics, especially with respect to the effects on load demand. In the second part, the load deviation index is proposed in developed in order to link possible improvements of DSM on sustainable DHN design.

6.1 Service-oriented model for DHN design

In part A of this thesis, the DHN system was described on operational level, while the need for cost transparency was tackled through a thermoeconomic approach applied to a numerical simulation. This approach was seen to be very useful to consider individual contribution on cost generation in smart thermal networks.

Not every DHN is or will be part of a smart thermal network, due to practical consideration. Very often networks are stand-alone systems which purpose is to provide heating service to a small-to-medium sized town with a definite amount of well-known consumers. Thus in such cases, the challenge of DHN design is to increase the sustainability or performance of the system on a yearly basis. This design cannot be done through analyzing operational data, but must focus on the demand characteristics of the consumers, simply because the operational behavior is not available during design.

Another issue regarding DHN systems is the strong focus on the production of thermal heat without considering the demand characteristics of the consumers. On operation level, the effect of consumer characteristics was studied. Those impact the efficiency and cost generation of associated with heating service.

The state of the art well described the need to move from throughout-based service of selling thermal heat to a service-oriented design of DHN system. This demands for a system model which is able to integrate a methodology used for optimum energy

service design. Taking that into consideration, a service-oriented DHN system is defined as shown in Figure 6-1.
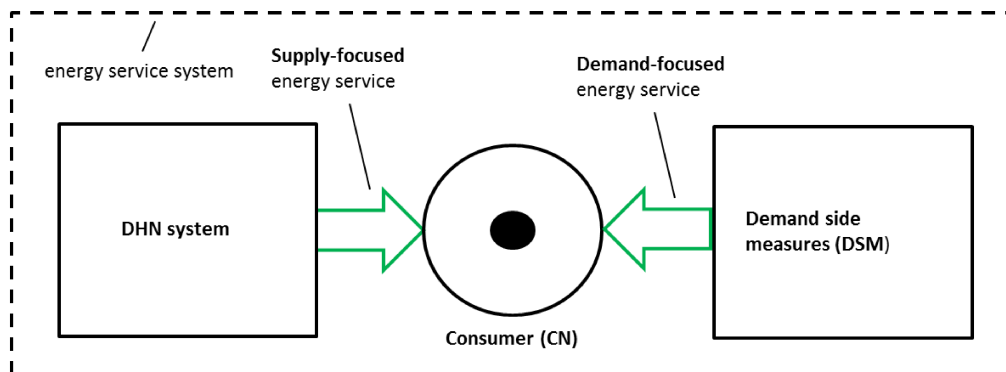
Figure 6-1: Service-oriented DHN system

The DHN system generalizes the concept of Figure 3-1 which possibly includes several producers and consumers. The objective of the DHN system is providing thermal heat as a service to the consumers. This service can be characterized as supply-focused, since it aims to fulfill the thermal request of the consumers through the production of thermal energy.

On the other hand side, demand-focused services can be imagined. Those can be summarized through the term demand side measures (DSM), which also aim in providing a service to the consumer. But in contrast to the DHN system, DSM are aiming to manipulate the demand characteristics of the consumers. An example is thermal insulation measures which provide a demand-focused service in the sense as they reduce the heat loss of a given building and consequently reduce its thermal demand. Another example is the characteristics of the building structures connected. Commercial buildings have different characteristics then residential consumers, which leads to a different demand profile. Thus adding or subtracting such consumer from the network unavoidably changes the demand profile which the DHN system must supply.

Thus, given a certain initial heat demand of a set of consumers connected to a DHN system, the idea of providing both supply- and demand focused service leads to a system description which is used as a basis to define an energy service system for small-to-medium scale DHN design. This limitation to small-to-medium scale systems lies in the fact that large DHN system are assumed to develop towards smart thermal networks. Since those have highly different behavior then small stand-alone systems,

certain assumption made in this work would be not valid. First, small-to-medium scale system are smaller in size with often only one production plant attached. The effects of transient behavior and thermal losses can be determined using the methodology described in Part A. During design, operational profiles might not be available and a detailed simulation of the system is therefore not possible. In industrial practice, constant losses are often used to consider those effects. In using this assumption, the system proposed in Figure 6-2 is used for single production plants only.
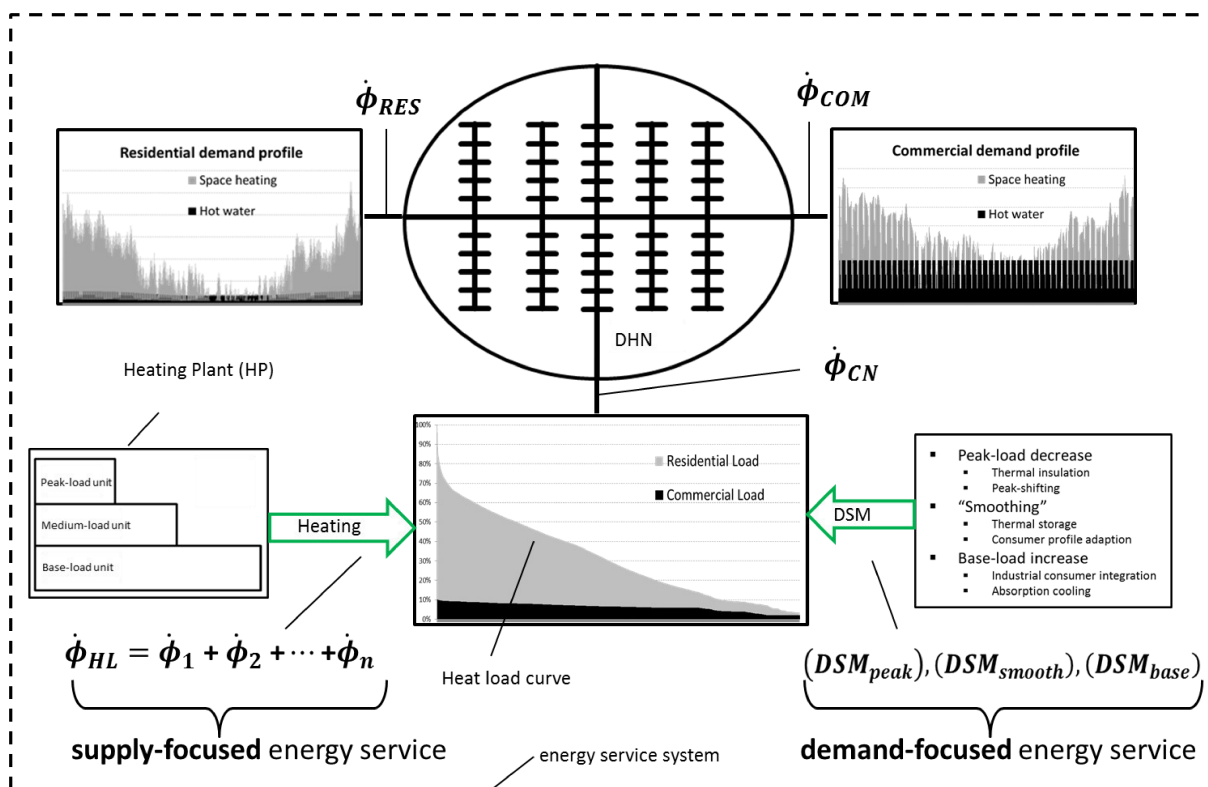
Figure 6-2: Generic energy service system for DHN systems

It was already mentioned, that the focus lies in the development of a design methodology which can be used in industrial practice. This also limits the detail a system designer is able to take into account. Given that during system design, e.g. heating loads can only be forecasted based on individual practice, the level of detail must be carefully defined. The following approach is used.

The basic idea is that DSM affects the initial thermal demand of the consumers and lead to different heat load curves. This heat load curve must be supplied by the production plant, which might consist of several production units. Those production units might use different fuel (e.g. biomass, natural gas etc.) and provide thermal energy depending on the current heat load.

When imagining the influence of DSM, e.g. thermal insulation does not only decrease the amount of total thermal demand, but also changes to the profile of the load curve. Considering that the production plant has a defined amount of units with certain nominal loads, the production of each unit is influenced by the heat load curve itself. Once the plant units are designed according to a certain nominal power, the production of each unit depends on the heat load profile. Taken into account that production units also suffer from partial-load losses the influence of the load curve is even higher. This offers the possibility to assess different DSM in the design of a single heating plant.

Assuming a green field project, a system designer's main decision lies on the sizing of the heating units. Depending on a forecasted heat load, base-, medium- and peak-load units must be installed. They are installed to maximize the duration of nominal operation in order to avoid losses associated with partial-load operation.

Hence, the proposed system in Figure 6-2 offers the possibility to assess the impact of DSM on the design of multi-unit heating plants given a certain initial heat demand by the consumers in the system. It contains the following system components:

- Consumer demand model
- Model for heating plant design
- Characterization of demand side measures

In the next sections, those models are detailed with the aim of providing a methodology which can be used e.g. for green field projects in industrial practice.

6.1.1 Consumer demand model

The consumer's heating request depends on a variety of factors, such as the geographical position, the climatic- and weather conditions and the personal-, social- or cultural behavior of the people (Gadd & Werner 2013). Prediction and forecasting of load profiles is done through measurements (Gadd 2012) or statistical methods such as fuzzy-methods or neural network approaches (Shamshirband et.al. 2015; Wojdyga 2014).

Those methods are suitable for improving DHN operation, but the forecasted, minute-based heat loads are not decisive for system design. In fact, global indicators based

on yearly heat load in hourly resolution are more useful for design purposes as shown e.g. for storage design (Gadd & Werner 2013).

A similar approach is followed in this work, using yearly load profiles of different German DHN systems as a database. The available data is based on results published by the German BMU (BMU 2012). This data consists of heat load profiles for different regions, all of them with a specific building structure, defined by the amount of residential- and commercial buildings connected. Occasionally, industrial consumers are also part of the DHN demand, but their contribution is mostly too small to affect the load curve significantly. In any case, those are excluded in this work. The original data was normalized and is based on the peak load in order to show how climate conditions and demand structure influence the heat demand.

At first, the normalized heat demand is affected by means of region, see Figure 6-3, representing the normalized demand of three real DHN in different regions of Germany.
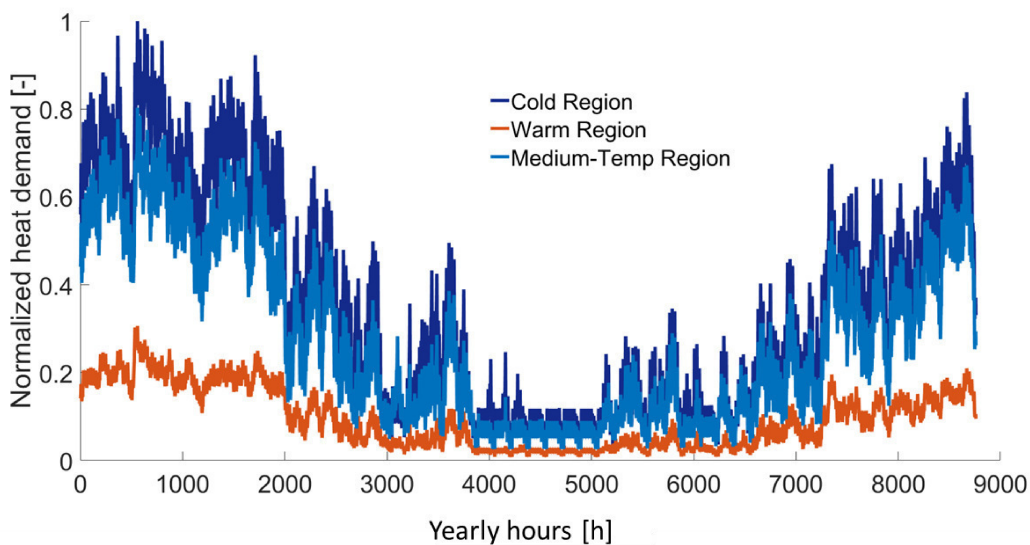
Figure 6-3: Normalized heat demand profiles of German regions

The normalized heat load curves represented are based on real consumption patterns by BMU (BMU 2012) who concluded representative load curves to model DHN demand of Germany. Here, only the load curve with the highest (cold region), lowest (warm region) and one in between (medium-temp region) are used to clearly show the differences both in magnitude and shape. The hourly distribution shows the normalized demand from 1st of January (h=0) to the 31st of December (h=8760). If the

total heat demand of a certain DHN is known, the normalized curves can be used to construct the yearly heat demand over time.

The cold region shows a high peak in winter with a significant drop during the warmer periods. The demand during summer is only about 10 % of the peak demand. On the contrary, the demand of the warm region shows a significantly lower peak with only about 30 % compared to that one in the cold region. Though the minimum demand in the warmer period is much lower, the peak-to-base ratio is also lower. This means that the difference between maximum- and minimum load of the warmer region is smaller compared to the cold region. This has an important influence on the resulting load curve. A DHN system located in the warm region has therefore a flatter heat load distribution compared to a system located in the cold region, given equal annual heat demand. This is an important finding since the design of the heating plant is affected by it.

Another influence on the demand profile is the structure of the buildings connected to the DHN, see Figure 6-4.
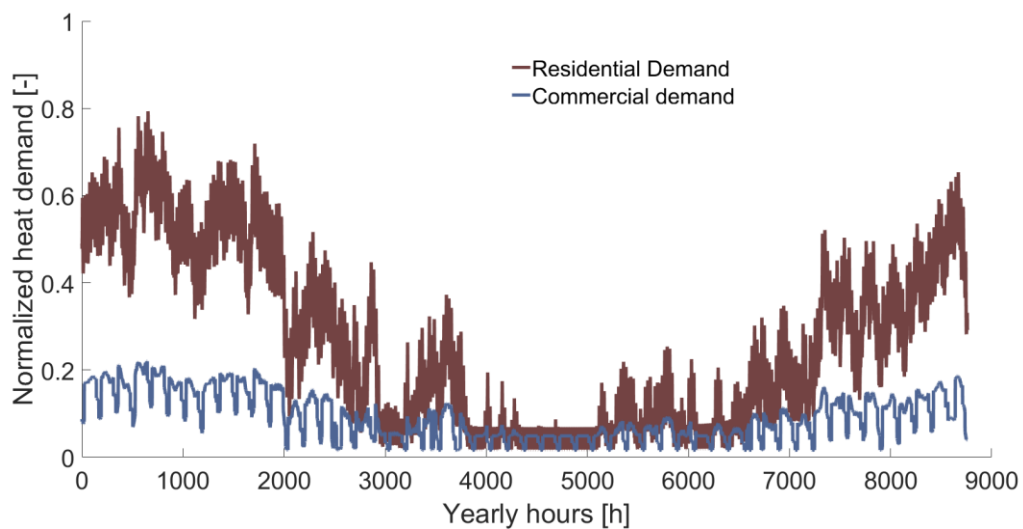
Figure 6-4: Normalized residential and commercial heat demand

The demand in the cold region is mainly composed by residential heat demand with about 80 % of its peak load, while demand from commercial buildings contribute to about 20 % at that time. Again, a significant higher peak-to-base ratio for residential buildings is seen, while commercial demand is nearly constant through large periods of time. Similarly to before, it can be concluded that the shape of the resulting heat load curve is highly influenced on the share of residential- and commercial buildings

connected to it. A DHN system with a high share of commercial buildings leads to a load curve which is much flatter than one with a high share of residential buildings.

As previously mentioned, heat load is a direct consequence of the consumer's personal- or social behavior, where the main demands are space heating and domestic/commercial hot water. Evidence for that is provided from the data by Figure 6-5 and Figure 6-6, respectively.
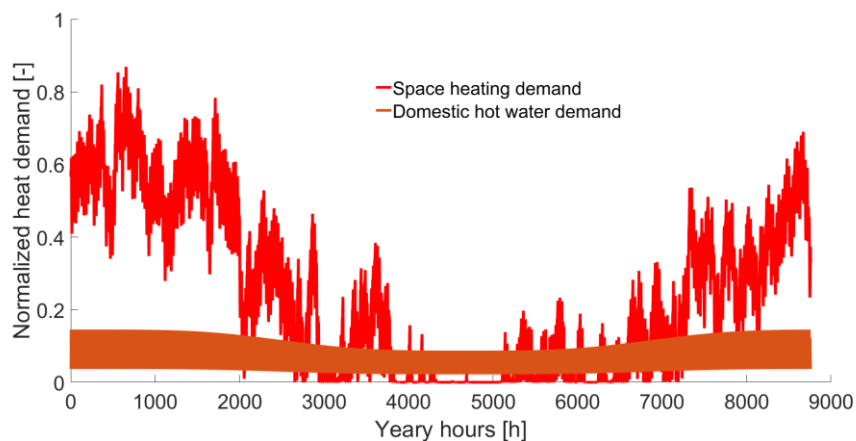
Figure 6-5: Space heating and domestic hot water demand for residential buildings in cold region
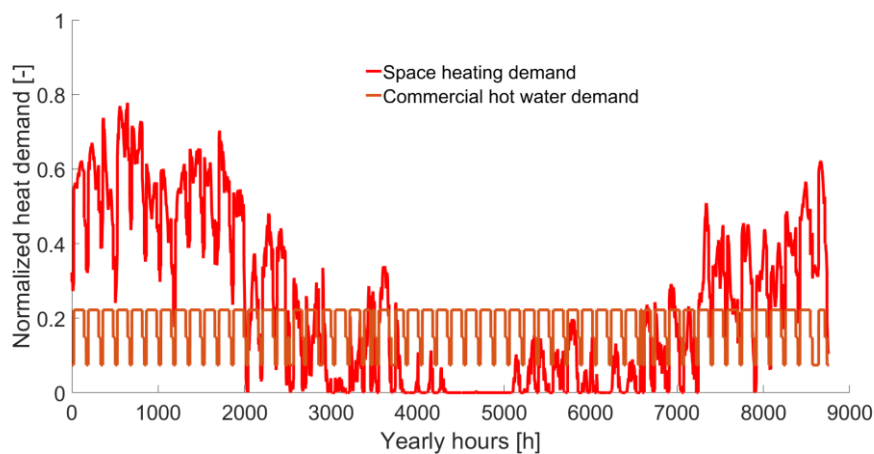
Figure 6-6: Space heating and commercial hot water demand for commercial buildings in cold region

For residential buildings, space heating demand is dominant showing its typical profile, while hot water demand is, though showing a high frequency throughout the day, quite constant on a yearly resolution. For commercial buildings a similar behavior is expected, but in this case, the hot water demand is much higher in terms of magnitude. Comparing the share of hot water demand of both building structures, the one of commercial buildings shows a significant higher one.

It is worth mentioning that demand in DHN systems generally decreases till 2050, due to a set of reasons which includes the reduction of general heating demand (building improvements), increased thermal insulation of existing buildings and a decrease of heat demand due to climate change, assessed by (Andric et.al. 2016; Dirks et.al. 2015). Those influences affect the load curve profiles and must be taken into account for DHN with long lifetimes.

Based on the analysis of normalized demand profiles, the following influences on the initial consumer heat demand can be summarized:

- Location and climate conditions
- Ratio of residential and commercial buildings
- Ratio of heating demand to hot water demand

Considering system design, annual heating demand can be estimated based on the amount of buildings connected to the DHN system. This might not be possible for the load curve itself, since operational behavior is unknown. The normalized load curves therefore provide important information on distribution of the annual heating demand and can be used to create a load profile which is based on general information such as amount of commercial and residential consumer, the location of the project and the total annual heat demand. This can be further used to construct an initial heat load curve based on an annual heating demand. In order to show the differences when different buildings structures are connected, Figure 6-7 provides a comparison between a system with 20 % and 50 % of commercial buildings connected.
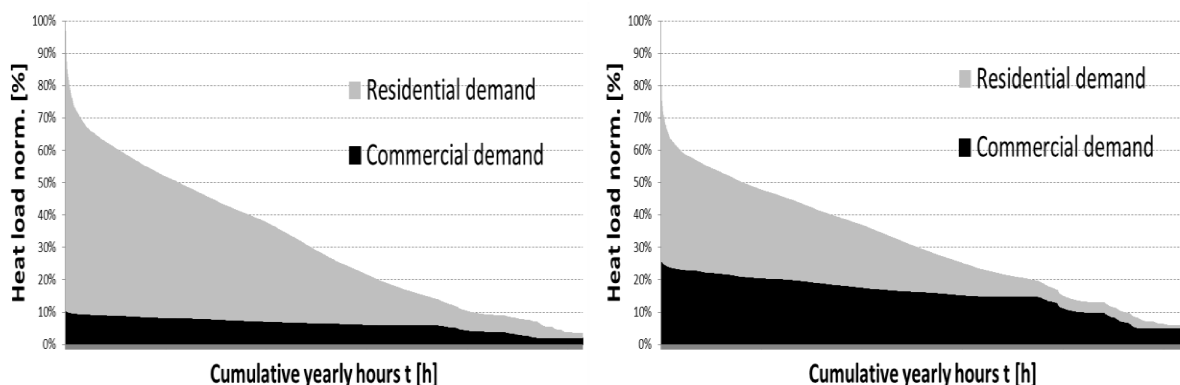
Figure 6-7: Load curves for different buildings structures, 20% commercial buildings (left) and 50% commercial buildings (right)

The load curves are the cumulative loads over time, where t indicates the cumulative hour of the year. This notation is further used.

A building structure with 50 % commercial buildings (in terms of total yearly heat demand) shows a peak load which is only about 80 % of the one with 20 % commercial buildings. Thus, the higher the amount of commercial buildings, the lower the peak demand and therefore the flatter the load curve with equal total annual heat demand. The peak demand refers to the maximum power of the load curve which must be supplied by the heating plant. This means that DSM can also be done through adaption of the consumer structure in the network. Since DSM was defined as manipulation of the load curve, the e.g. extension of a system towards commercial buildings might be useful to reduce the difference between maximum- and minimum load.

In order to study system behavior of different load curves, a mathematical modelling approach is developed, which is based on the fact that load curves can be represented using an exponential approach, see Figure 6-8.
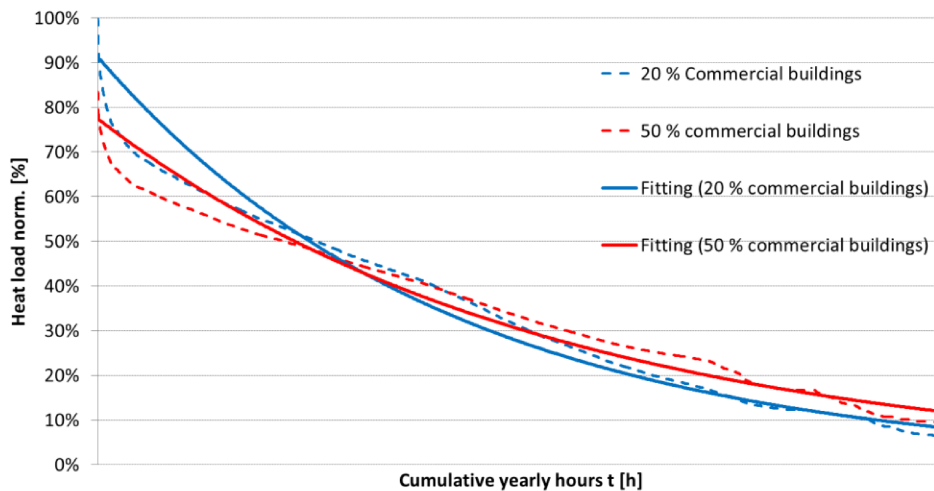
Figure 6-8: Exponential approach for load curve representation

Figure 6-8 shows the resulting load curves of both building structures of Figure 6-7, and their corresponding exponential fittings. Different fitting approaches can be applied; here a least-square approach is used. It can be observed, that the initial load curves as well as their exponential fittings show a decrease in maximum load and an increase of minimum load with 50 % commercial buildings compared to the one with only 20 %. Thus, the exponential fitting does represent this behavior and will therefore be used to represent load curves which takes the minimum- and maximum loads P_{min} and P_{max}, as well as the total yearly heat demand ϕ into account. The following

set of equations (6.1) – (6.4) are used for the exponential approach to model thermal power demand (P).

$$P(t) = a \cdot e^{b*t} \tag{6.1}$$

$$P(0) = P_{max} \tag{6.2}$$

$$P(T) = P_{min} \tag{6.3}$$

$$\phi = \int_0^T P(t) \, dt \tag{6.4}$$

The peak demand (P_{max}) refers to the maximum heating power, while the base-load demand is based on the minimum heating power (P_{min}) during the operational period (T). This allows to model any given load curve after (6.5).

$$P(t) = P_{max} \cdot e^{[P_{min} - P_{max}]\frac{t}{\phi}} \tag{6.5}$$

It must be noted that t is the cumulative time of the load curve and therefore different to the time at a specific hour of the year and that $P_{min} > 0$. In using (6.5) together with the information on normalized heat loads and the characteristics of the DHN building structure, the heat load profile can be modelled and used to for system design according to the model presented in Figure 6-2. It must be noted that this approach also takes into account losses which occur in the DHN. Since this approach focus on small-to-medium sized DHN, losses are taken into account on a constant basis without consideration of transient conditions.

6.1.2 Model for heating plant design

In this section, the model for the design of the heating plant is provided. This includes the definition of design variables for a heating plant consisting of various heating units in combination with a partial-load model.

6.1.2.1 Multi-unit design model

Depending on the heat load of the DHN system, the heating plant provides an energy service through supply of thermal heat requested. A multi-unit plant model is used to model the design of that heating plant. This is based on the fact, that a heating plant is usually composed of several units which are operated depending on the current load. Heating plants are usually composed by several units covering peak-, medium-

and base loads. Base loads are covered by units which are designed to supply constant loads at nominal power, whereas peak-loads are covered by units which are able to respond to fluctuating demand conditions. Since the objective is to provide a design methodology for the industrial context, the sizing of the heating units is defined as a major criterion. According to the author's knowledge, sizing is often done based on practical values. E.g. the base-load unit is sized to a nominal power of 60 % of peak load demand, because this value allows operating a maximum amount at nominal power. This design selection is useful in the case the heat load is well known but it does not allow to respond to load curves which are changed due to DSM. In the latter case, there is no guarantee that the optimum design of the base-load unit is at 60 % of the peak-load. This restriction is therefore overcome through the definition of the unit size as a design variable which must be carefully chosen in order to achieve optimum design. This concept is represented in Figure 6-9.
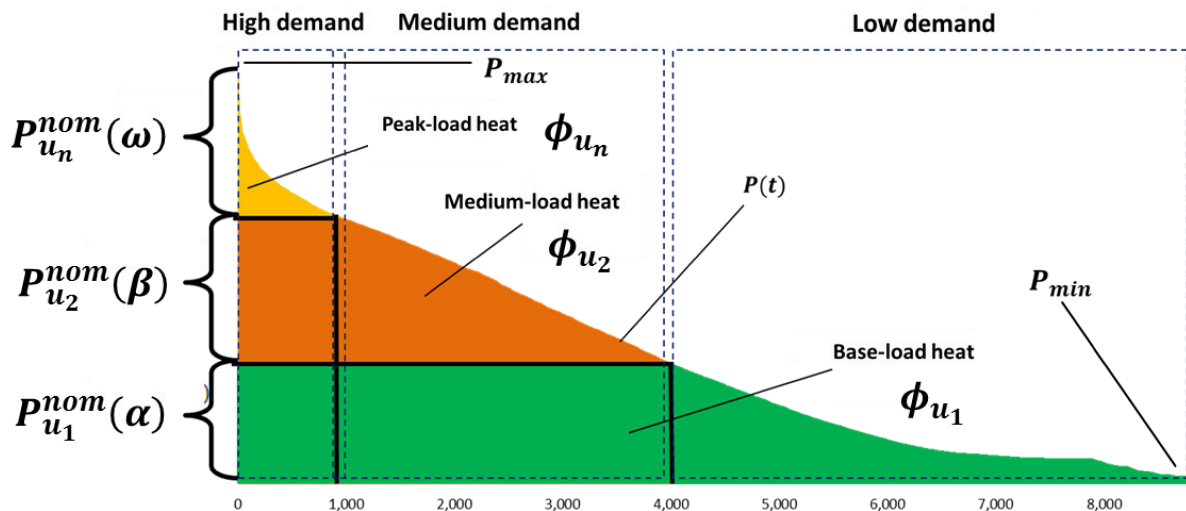
Figure 6-9: Multi-unit plant design model

Generally, the heating plant might be composed of n different units u depending on the size of DHN system and its corresponding production plant. In Figure 6-9, the heating plant design is exemplarily shown for common design approaches using three heating units for base, medium, and peak load but is not restricted to it. In fact the methodology permits the use of any amount of units, but it must be noted that computational effort highly increases due to the amount of design variables equal to n-1.

Considering that heat load curves may vary substantially in their profiles, setting the nominal powers of the production units to 60 % is not useful if optimum design wants to be achieved; simply because it is unknown if the heating system will operate in its best condition. The question of how to optimally size the heating units must therefore involve an optimization routine which is able to quantify the optimum sizes for a given load curve. For that, design variables α, β,..., ω are introduced to define the share of nominal installed power of each unit according to (6.6) - (6.7),

$$\alpha = \frac{P_{u_1}^{nom}}{P_{max}} \tag{6.6}$$

$$\omega = \frac{P_{u_n}^{nom}}{P_{max} - \sum_n P_{u_{n-1}}^{nom}} \tag{6.7}$$

The design variables are used to define the size of every unit, thus the ratio of the nominal power of the corresponding units $\left(P_{u_n}^{nom}\right)$ to the total maximum load P_{max}. The heat production from each unit is determined by the design conditions. The higher the nominal power of a unit, the higher its production as indicated by the areas under the load curve in Figure 6-9. This is not always of advantage, because operational efficiency is influenced by many factors such as the boiler characteristics, maintenance efforts or the unit's partial load operation. In any case, nominal efficiencies only are not sufficient for system design, because they neglect variations of efficiency during operation.

Depending on the design of the nominal powers, each unit operates in a certain condition defined by the heat load curve, assuming the heating units are powered according to the actual heat load. It can be seen, that e.g. the higher the nominal efficiency of a certain unit, the longer this unit operates under partial-load conditions. This duration of partial-load is not only influenced by the size of the unit but furthermore also depend on shape of the load curve. It can now be seen how the shape of the load curve and the sizing of the heating units are connected. A very flat load curve will permit the base-load unit to be sized much higher because it then operates longer time at nominal load. A very steep load profile would have the counter-effect leading to a lower sizing of the base-load unit.

Besides those considerations, the effect of the load curve is even higher when partial-load efficiencies are introduced. It was seen that the sizing of the units have influ-

ence on the duration of partial-load operation. In order to account for that, a system designer must be able to consider different partial-load behaviors of the units. This is taken into account through the use of a general partial-load model in the next section.

6.1.2.2 Partial-load model

The partial- load model is used to include the partial-load behavior of the units installed in the heating plant. The performance of heat production, usually measured in thermal efficiency, depends on current operation and load conditions. Even though nominal efficiencies are equal to about 65 % for biomass boilers and 90 % for gas-fired boilers, those values decrease in partial load operation due to inflexibility (RHC 2012) and thermal losses of different kinds (Torchio et.al. 2009), fluid temperature and excess air conditions. Biomass boilers are especially affected by partial-load behavior since the thermal inertia of the system does not allow operating at low partial-loads. Gas boiler systems are, in contrast to that, smaller and more flexible. This is an important factor which must be taken into account when optimum design is to be achieved.

To account for that, a partial-load model is developed which includes the decrease of thermal efficiency of a heating unit on system level. The partial-load behavior might depend on various factors, such as thermal losses and inflexibility, but also the fuel can have an influence, as has been shown for a biomass unit, which efficiency depends upon the actual wood humidity. Generally, the operation efficiency of a certain unit (η_u) is therefore a function of the partial load, thus the ratio of the actual thermal power of the unit (P_u) relative to its nominal design value P_u^{nom}, see (6.8).

$$\eta_u = f\left(\frac{P_u}{P_u^{nom}}\right) \tag{6.8}$$

Different kinds of functions can be considered, which e.g. resembles a logarithmic behavior, where the operation efficiency drops slightly with increasing partial-load or a linear behavior which represents a constant efficiency loss throughout partial-load. Considering the characteristics of biomass- and gas boilers, partial-load behavior can be integrated as shown in Figure 6-10.
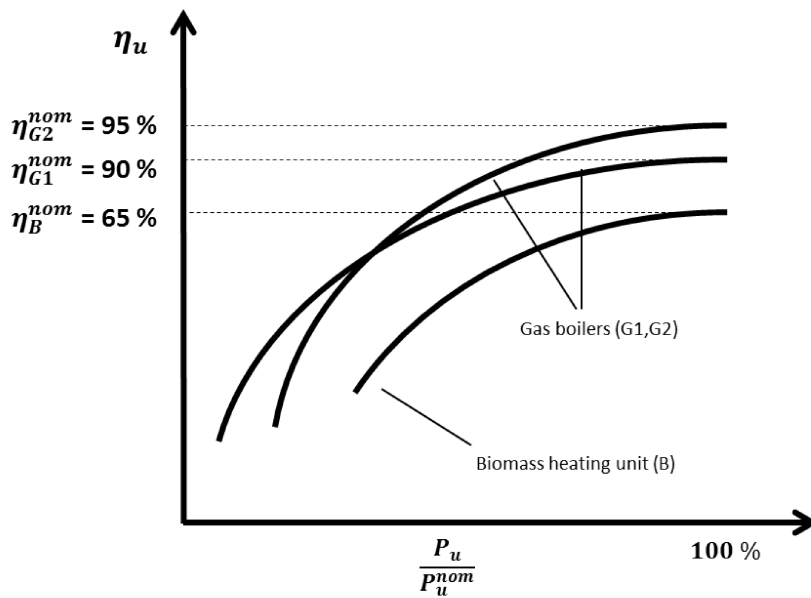
Figure 6-10: Generic partial-load model of biomass and gas boilers

For each unit, the behavior of the partial-load efficiency is introduced which shows typical values for nominal efficiency of heating units. The thermal efficiency of heat generated by a specific unit η_u is a function of the actual unit load P_u. The drop of thermal efficiency in partial load operation leads to a higher decrease in system performance directly related with the amount of time, a unit operates in partial load.

Gas boilers show a higher nominal efficiency $P_{G1}^{nom}, P_{G2}^{nom}$ but might have different characteristics during partial-load. In this example operating efficiency drops higher for gas boiler 2 η_{G2} compared to gas boiler 1 η_{G1}, even though its nominal efficiency is higher. The biomass unit has a lower nominal efficiency and also shows a sharp drop in operating efficiency during partial-load η_B.

This is a very important issue which must be considered for optimum plant design, because oversizing of the biomass unit will in this case reduce the operating efficiency drastically. This eventually results in a poor performance on a total yearly basis. Assuming that the biomass unit shows such a behavior, its size is very restricted. Since the shape of the load curve is the dominating factor for the duration of partial-load given a certain unit size, it can be expected that for flatter load profiles, a larger size of the biomass unit is possible despite the large drop in partial-load efficiency. Similarly an oil boiler could be considered in the analysis, but is not widely used for design due to environmental issues.

Furthermore, limitations are expected on the ability to operate in partial-load. A biomass unit might face a higher minimum load compared to a gas boiler due to the thermal inertia or other operating restrictions. This is also visualized in Figure 6-10 showing that the gas boilers have a wider range of operation compared to the biomass unit.

It must be noted, that the partial load model presented here is exemplary shown and must be very well known for system design.

6.1.3 Characteristics of demand side measures (DSM)

The load demand can be modelled with the exponential approach in (6.5), while its profile is a combination of geographical position, building structure and characteristic heat demand highly affecting its resulting shape.

Demand side measures (DSM) are measures to manipulate the load curve in a certain way through either decreasing total demand or shaping its profile in order to achieve a more suitable profile for supply. If a load curve is more suitable depends on the objective function considered. If only annual efficiency is considered, a load curve with a more steady profile is of advantage since an existing heating plant operates less time in partial-load. If other objective functions such as costs are considered, this is not necessarily true since the implementation of DSM is associated with capital expenses. It was described that the heating plant design is largely affected by the load curve. Especially when e.g. a biomass unit is considered as a unit for base-load production, the shape of the load curve will determine the duration of partial-load operation.

In order to study the effect of DSM and its associated energy service for the DHN systems under consideration, the impact of DSM on the load curve must be investigated. This approach must be able to provide information on the advantages potential applications of DSM have on the improvement of system design.

Based on the behavior of DSM approaches described in the state of the art, three categories of DSM can be differentiated covering (a) measures to decrease peak-load like thermal insulation of buildings or peak shifting, (DSM_{peak}), (b) "smoothing" measures which decrease peak-load while simultaneously increasing base and/or medium load through time-shifting as in storage integration, (DSM_{smooth}) and (c) the

increase of base-load through e.g. an increase of the amount of commercial buildings in the building structure, (DSM_{base}). This behavior can therefore be summarized into three different DSM techniques:

- DSM_{peak}:   DSM reducing peak-load, with base-load constant
- DSM_{smooth}:   Combination of peak-load reduction and base-load increase
- DSM_{base}:   DSM increasing base-load demand, with peak-load constant

Based on the given DSM technique, the heat load curve is manipulated in a certain way. This is made clear through the example of thermal insulation.

The objective of thermal insulation is to reduce heat transfer losses which effects room heating demand only. Since this demand is represented in the middle- and top parts of the heat load duration curve (Pardo et.al. 2012) only this amount of energy demand is reduced by thermal insulation. The base-load parts due to hot-tap water demand and distribution losses are not affected by a reduction of heat transfer losses; thus thermal insulation has no effect on them.

Thermal insulation measures therefore reduce the amount of heat demand mainly in peak-load areas, resulting in a decrease of the peak heat loads. This is in accordance with results found by (Danestig 2009) which implies that heat load reduction through thermal insulation leads to a flatter profile of the heat load curve. Based on those empirical facts, it can be concluded that thermal insulation has the following impacts on the heat load curve.

- Thermal insulation measures reduce the yearly heat demand
- The base-load demand is not influenced by thermal insulation
- The peak-load demand is reduced with increasing thermal insulation

Based on those findings, one can also image DSM approaches for smoothing and base load increase which have similar characteristics. Smoothing could be implemented through a combination of thermal insulation with the extension of commercial consumers or through the implementation of seasonal thermal storages. Especially the integration of storage is very interesting because it enables a higher load during the summer periods, which is of advantage for base-load units. This could be e.g. implemented through a storage solution which offers to run the storage during the base-load hours in charging mode, while discharging takes place during the medium

and/and or peak-loads. Thus a storage charging during base load and discharging during peak-load is a typical implementation of DSM_{smooth}.

Based on those considerations the following approach is used to consider DSM applied to a given load profile:

- DSM_{peak}:   Set P_{max} and solve (6.4) – (6.5)   with $P_{min} = const.$
- DSM_{smooth}:   Set P_{max} or P_{min} and solve (6.4) – (6.5)   with $\phi = const.$
- DSM_{base}:   Set P_{min} and solve (6.4) – (6.5)   with $P_{max} = const.$

For a better understanding, this is applied for an arbitrary normalized reference load curve in Figure 6-11.
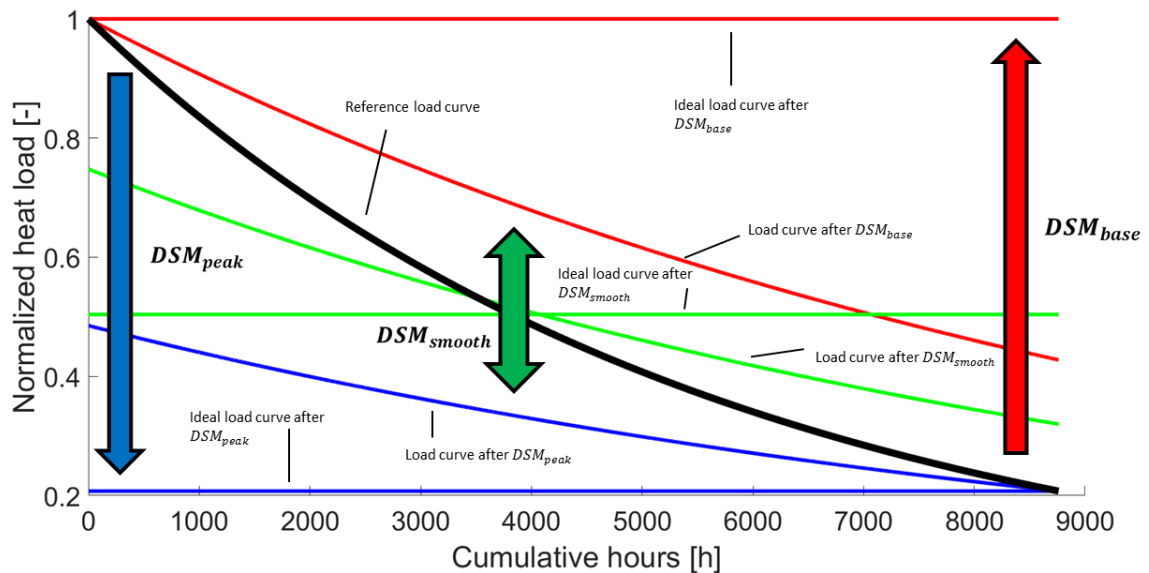
Figure 6-11: Behavior of DSM for normalized load curves

All three DSM techniques and their effects on the heat load curve are presented. For DSM_{peak}, peak-load decreases while maintaining a constant minimum load. This approach also reduces the amount of annual thermal heat demand ϕ. For DSM_{base}, the opposite is true maintaining a constant peak load, while increasing the base-load. In this scenario, the total annual heat demand increases. The hybrid approach DSM_{smooth} decreases peak- and increases base-load while maintaining a constant annual heat demand.

Through this definition, any type of DSM can be characterized in terms of its variation of the heat load curve. For every DSM technique two examples of DSM are shown in the previous figure. One which applies a certain magnitude of DSM leading to a flat-

ter shape while the second one is the most extreme case, where DSM is applied till the load curve is constant. It can be seen that independent of the DSM technique applied, the load curve gets flatter. This manipulation of the shape was already mentioned to be of advantage for design because it enables the use of larger base-load units.

Besides the manipulated heat load curves, constant load curves are defined as so called "ideal" load curves. The ideal load curve is defined at a constant average thermal power providing a given amount of ϕ. Ideal in this sense means that a constant thermal power is the most ideal distribution a certain annual heat demand can have. This concept has been led to the development of a methodology to characterize heat load curves according to their shape, which is carried out in the following section.

6.2 Linking DSM and DHN design: The load deviation index (LDI)

In the previous paragraph, the concept of an ideal load curve was introduced. This idea is further developed to a concept which aims to characterize heat load curves. This characterization should help identifying possible advantages through DSM and might provide a general benchmark of improvement. For each DSM technique two DSM scenarios are shown in Figure 6-11, which manipulate the shape of the load curve in a certain way; depending on the magnitude of the DSM.

The heating plant model considers a multi-unit design model at different, design dependent, operating efficiencies. It can be easily seen, that a constant heat load curve would make the introduction of the model unnecessary, since in such a case, one heating unit at highest nominal efficiency is deployed. Assuming, that the nominal efficiency is the highest a heating unit can provide, the total annual efficiency and thus the performance of heat supply are maximum. Therefore, according to similar findings from (Danestig 2009), the ideal thermal power (P_{ideal}) of a given annual heat request ϕ can be defined as in (6.9),

$$P_{ideal} = \frac{\phi}{T} \tag{6.9}$$

Based on the assumption, that partial load behavior reduces thermal efficiency, according to a distinct partial-load model, the ideal load curve for a given amount of

yearly energy demand can be expressed as a steady state profile with an ideal nominal power P_{ideal} and T equal to the yearly resolution. This value equals 8760 hours provided that the plants operate the whole year.

The constant lines in Figure 6-11 represent the extreme DSM scenarios, where the reference load curve is manipulated so that P_{ideal} is reached. In the case of thermal insulation for example, this would be the case, when thermal insulation reduces the heating demand to the point where only the base-load demand, e.g. the hot water demand, is left. Since hot water demand shows a low fluctuation on a yearly resolution, the resulting ideal load curve would represent a constant demand of hot-water. As described before, in this case, a simple heating unit can be installed operating at highest performance. This is therefore the ideal case of supplying the annual heat demand ϕ after DSM. The same concept can be applied to the other DSM techniques.

Apparently, the load curves for real applications are far from being steady state, but show an exponential behavior with a distinct maximum and minimum load demand. It is therefore interesting to investigate, if a method exists which allows the assessment of "how far" a real existing load curve is away from its ideal one. This would allow a characterization of load curves and provide a benchmark between load curves of different characteristics. One approach for characterization is to relate either the maximum P_{max} or the minimum P_{min} load to P_{ideal} and use its relation to quantify the difference between the actual load curve and its ideal one. This is yet not possible, since a high ratio of P_{max}/P_{ideal} would not consider a high P_{min} into account. This would lead to the situation where a load curve with high P_{max} and high (but slightly smaller) P_{min} would be very close to its ideal profile, which in fact is not the case. This approach does not seem to be useful, because it does not take the amplitudes of minimum and maximum load into account. A more promising way as to measure of how "far" a given load curve is away from its ideal profile is to relate the arithmetic mean (P_{mean}) according to (6.10) to P_{ideal}.

$$P_{mean} = \frac{P_{max} + P_{min}}{2} \qquad (6.10)$$

This allows establishing a general relation between the average load and the ideal load for any general heat load curve regardless of the specific distribution. This rela-

tion is expressed by the load deviation index (LDI) which is defined as the ratio between the ideal load and the arithmetic load average of maximum and minimum load according to (6.11),

$$LDI = \frac{P_{ideal}}{P_{mean}} = \frac{2}{P_{max}+P_{min}} \frac{\phi}{T} \tag{6.11}$$

where LDI is close to 1 if P_{max} and P_{min} are close to each other, and LDI increases with higher distances of the arithmetic mean from the ideal nominal value. Through that, LDI can vary theoretically between 0 and 1 and thus offers a normalized indicator of the relation between arithmetic load average and ideal load. This offers the possibility to quantify how a certain heat load is distributed throughout the year and can be used either to characterize and compare a given heat load curve through evaluating (6.11) or to quantify a certain DSM activity. Especially the latter issue of quantifying DSM is an integrated part of the load deviation index. The objective here is to define magnitudes of DSM through the definition of LDI relative to a reference scenario. Thus, using the initial characteristics of DSM, the approach including LDI can be written as follows:

- DSM_{peak}:   Set LDI and solve (6.4), (6.5), (6.11)   with $P_{min} = const.$
- DSM_{smooth}:   Set LDI and solve (6.4), (6.5), (6.11)   with $\phi = const.$
- DSM_{base}:   Set LDI and solve (6.4), (6.5), (6.11)   with $P_{max} = const.$

It must be noted that due to the nature of the LDI definition, it can neither be measured nor observed but only calculated from the load parameters. For setting LDI, this implies the knowledge of the reference load curve and its corresponding LDI value. Simply saying, LDI can be changed between 0 and 1 relative to its reference value according to the desired magnitude of DSM.

The load deviation index is a relative measure of average power to ideal power with the capability of assigning one single value to a given heat load curve. Since LDI is composed of the three characteristic values of P_{min}, P_{max} and ϕ any given load curve which follows an exponential approach can be described. Thus, when applying DSM to a given heat load curve, specific changes in the characteristic variables occur, which were already described in Figure 6-11. This will lead, depending on the magnitude of the imposed measure, to a value of LDI closer to 1 and will therefore decrease the relative difference of the load curve after DSM to its ideal load curve.

The behavior of the load curve parameters and the LDI can be investigated through the definition of different DSM scenarios, in which the load curve is manipulated in different magnitudes. In solving the load curve variables for different values of LDI, the behavior shown in Figure 6-11 can be transferred into a *load deviation plot*, given in Figure 6-12.
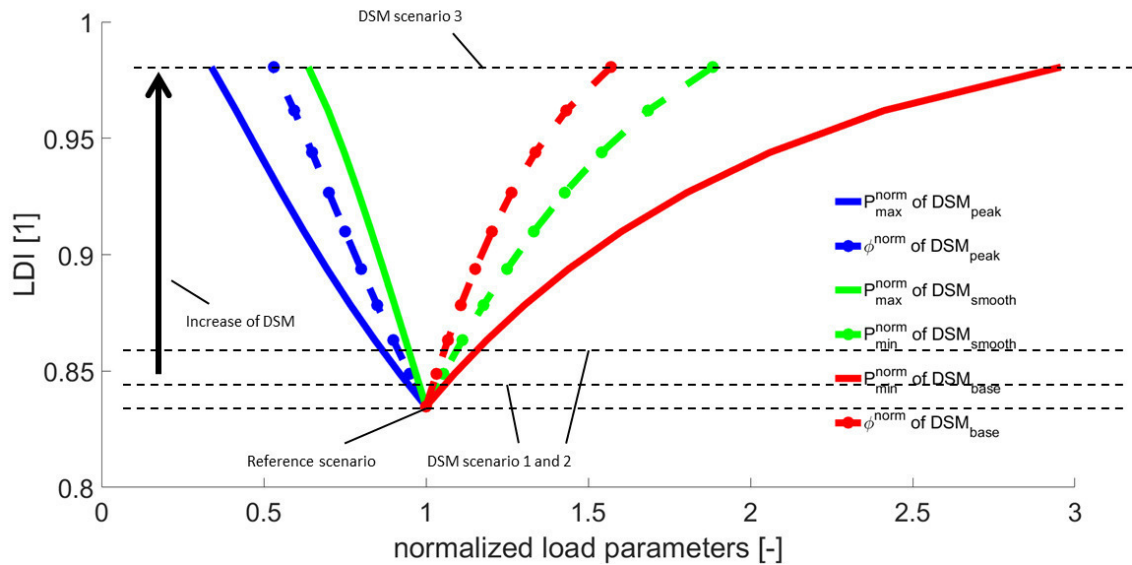
Figure 6-12: Load deviation plot

Each color corresponds to a certain DSM technique with DSM applied to a reference load curve. The example has the same load curves as shown in Figure 6-11.

The x-axis shows the normalization of the load parameters relative to their values in the reference condition according to (6.12).

$$P_{min}^{norm} = \frac{P_{min}}{P_{min}^{ref}} \qquad \phi^{norm} = \frac{\phi}{\phi^{ref}} \qquad P_{max}^{norm} = \frac{P_{max}}{P_{max}^{ref}} \qquad (6.12)$$

The reference condition includes the characteristic variables for the reference load curve. Thus the values of the reference load curve are marked at 1 with LDI of 0.83 for the reference load curve given in Figure 6-11. Three scenarios are shown as an example, implementing DSM at equal magnitudes for every DSM technique. Thus the load curves are constructed through the definition of a certain LDI:

- Scenario 1: LDI = 0.83
- Scenario 2: LDI = 0.86
- Scenario 3: LDI = 0.98

The red curves correspond to the behavior of the load parameters after the implementation of DSM_{peak}. Here, both maximum load and heat demand decrease nearly linearly compared to their reference value. Both parameters are a consequence of the LDI value which is set to quantify the DSM of the load curve. The load parameters can be directly deduced from the chart given a certain DSM scenario.

For each DSM technique only those two parameters which actually change are shown, while the third one, which is kept constant, corresponds to the reference point. This is achieved through the normalization in (6.12). Taking DSM scenario 3 as an example, LDI shows the highest value representing the flattest load curve. This load profile shows a high difference in its load parameters compared to the reference case. While in the case of DSM_{peak}, maximum load decreases by more than 50 %, this value is only about 30 % in DSM_{smooth}. A similar phenomenon can be seen comparing minimum load in DSM_{smooth} and DSM_{base}, where the change of the parameters is also significantly different. For a given reference load curve, this chart can be directly created using the given methodology and is useful for the quantification of DSM through the LDI.

Furthermore it can be used to deduce requirements for the load parameters in case system optimization should be done through DSM. This must be understood behind the context of the design of the DHN system. In cases LDI is higher, it can be expected that improved optimum design is possible, because a flatter load profile will enable a design with lower partial-load duration. This means that the load deviation plot can be used as a link between the optimum design of the system for various different DSM implementations and the resulting necessary change of the characteristic parameters of load curve. The LDI indicator and its related methodology is proposed as a benchmark and link between DSM and improved sustainable DHN design. In order to investigate the usefulness of the indicator for estimation of the possibilities of sustainable DHN system design, a case study is conducted in section 7.2.

Chapter 7: Applications of the design framework

In this chapter, tow case studies are developed which apply the framework of chapter 6. This is done to show the usefulness of DHN system design for industrial designers when considering service-oriented DHN system proposed in this thesis.

In the first case study in section 7.1 feasibility of substituting a decentralized gas boiler system through a biomass-based DHN system is investigated. For that, the new framework applies thermal insulation as a DSM technique while multi-criteria analysis is used to assess the sustainability of different design selection. A benchmark is provided with which different design selections are compared.

In the second case study in section 7.2, DSM is applied in a more general way in order to study the behavior of the load deviation index. The case study provides a thorough understanding of the usefulness and shows how the framework can be applied in the industrial context.

7.1 Multi-criteria sustainability analysis of a small-scale DHN system

In this section, a multi-criteria analysis is carried out for sustainable design of a small-scale DHN system. This DHN system is substituting a reference system, while the aim of the case study is to provide detailed insights into the conditions under which a substitution is sustainable. This decision is based on a multi-criteria analysis which addresses three dimensions of suitability: technological, environmental and economic sustainability. Apart from sustainable design, the impact of thermal insulation as a DSM is studied for this specific case study. This enables a first investigation on behavior of the methodology provided by DSM characterization in the theoretical framework.

The objective of the case study is threefold:

- Assessing the feasibility of substitution based on a multi-dimensional sustainability metric
- Assessment of thermal insulation as a DSM to the DHN system
- Benchmark and assessment of sustainable design selections

7.1.1 Introduction to the case study

The case study consists of a real existing DHN system in Nantes/France. The under-lying project substituted 25 decentralized gas boilers, supplying a total space area of 120.000 m² through a centralized heating plant. The heating plant uses biomass as base-load and a gas boiler system for peak-load supply. Data needed for the case study was available from the project documentation and was carefully examined and selected.

The aim of the case study is to apply multi-criteria sustainability analysis in order to investigate the benefits related with centralized supply and DSM compared to the decentralized gas boiler system. This decentralized gas-boiler system is defined to be the reference system and the small-scale DHN system is taken to be the alternative system. The performance in terms of sustainability is measured using a defined sustainability metric which is mainly based on energy efficiency, carbon footprint and emergy.

For the reference system, each individual natural gas consumption and the associated heat supply have been collected and averaged over the last 5 years. This allows estimating an average efficiency of the decentralized boilers. The decentralized gas boiler system showed an average energy efficiency of 82% while supplying an initial yearly heat demand ϕ_{init} of 4.28 E7 MJ to the consumers. Further data is based on literature or on the project data itself and is given in Appendix B.

The alternative system is composed of a heating plant, using biomass and natural gas as fuels including a transportation model which is used to consider efforts related with transport of wood, ash and employees. This transportation model has been developed in a previous work by (Jamali-Zghal et.al. 2013). The infrastructure for the gas transport is assumed to exist, thus no further expenditures are accounted for that. This approach allows comparing the performance of the two systems and enables to investigate the benefits and drawbacks related to centralized heat supply.

7.1.2 Definition of the energy service system

The centralized heating system is a small-scale DHN system providing heat supply to the consumers. In order to compare this system to the decentralized reference scenario, not only the performance of the heating plant but also the efforts related with

transport and investments due to thermal insulation must be taken into account. In addition to the heat supply, a demand-based model is needed to account for DSM applied. Given those constraints, the DHN system is modeled according to the theoretical framework of chapter 6 as an energy service system according to Figure 6-2. This results in a service-oriented energy system in Figure 7-1.
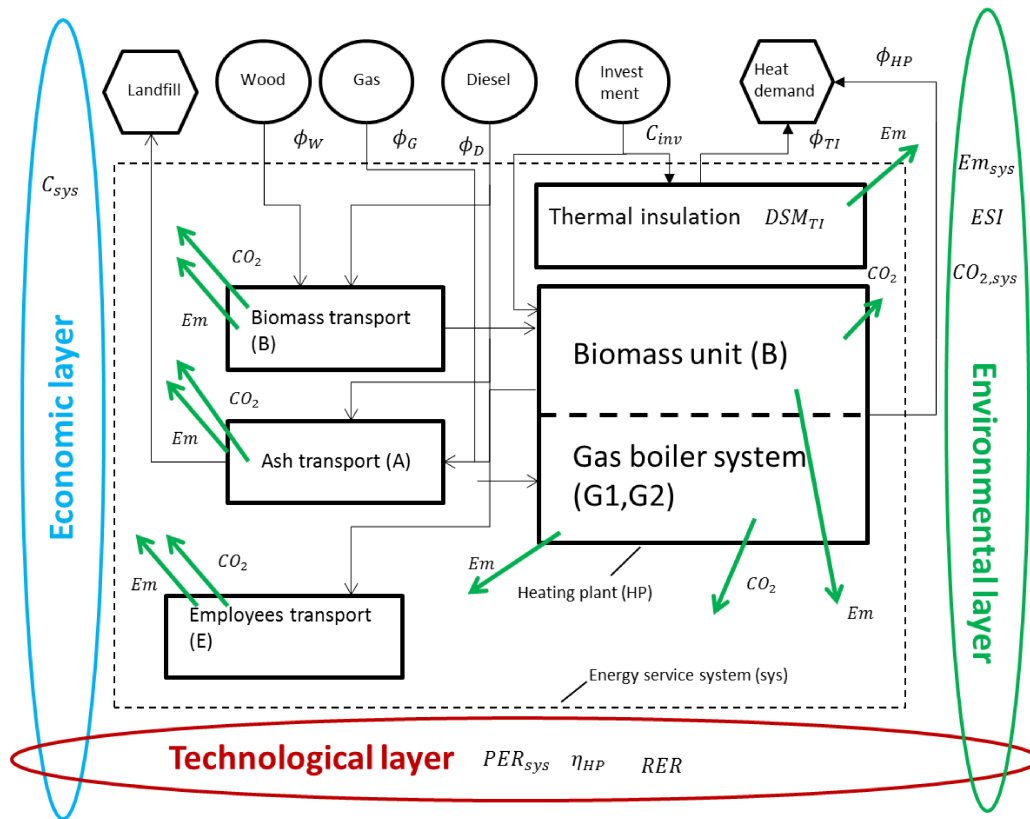
Figure 7-1: Energy service system for centralized heating system

The supply-focused energy service is provided by a heating plant, which supplies thermal heat to the consumers. This is represented by a certain load profile. It must be noted, that in this case study, the effects of the network itself are excluded, and thus thermal losses and transient conditions are not considered, because there was no detailed information on the load profile available in the project.

The underlying load curve is based on the consumption pattern of the medium-temp normalized load curve data, presented in section 6.1.1. Furthermore, a demand-focused energy service is provided in the form of thermal insulation as a DSM: DSM_{TI}. This DSM is a peak reduction measure DSM_{peak}. Furthermore, the transport of wood, to and from the heating plant as well as the transport of ash and employees needed to run the plant are taken into account.

The performance analysis is based on a multi-dimensional sustainability metric which includes a technological, environmental and an economic layer. For the multi-criteria analysis, certain performance indicators are defined for each layer which consists of various different indicators such as energy efficiency, carbon footprint or the environmental sustainability index.

Each system component consumes a certain fuel. The heating plant consumes natural gas and biomass, while it is assumed that the transport is fueled by diesel. Furthermore, there is a flow of capital needed to construct the heating plant and to apply DSM in the form of thermal insulation. Furthermore, operational costs must be considered which are associated with the cost of fuel. The main criteria for performance analysis in the environmental layer are carbon footprint and emergy flow. Those are explicitly represented in Figure 7-1 in order to emphasize their generation. Those two are furthermore used for a detailed assessment of sustainable design selections, while the remaining indicators are used for multi-criteria analysis. It is important to notice, that for thermal insulation, only the expenditures for implementation are taken into account.

Considering that the initial annual heat demand of the consumers (ϕ_{CN}) is reduced by an amount of thermal insulation (ϕ_{TI}), the resulting heat request for the heating plant (ϕ_{HL}) can be written as in (7.1).

$$\phi_{HL} = \phi_{CN} - \phi_{TI} \tag{7.1}$$

This states that heat load for the heating plant ϕ_{HL} is equal to the initial heat demand of the consumers ϕ_{CN} reduced by the amount of heat saved through thermal insulation ϕ_{TI}. Thermal insulation is applied to reduce the total yearly heat demand, while the remaining heat demand is met by a three-unit boiler system which contains a biomass-fired base-load unit and a gas boiler system for medium- and peak-load supply.

7.1.2.1 Initial heat load model

In order to model the initial heat load of the consumers, a specific load curve based on the ones provided in section 6.1.1 is used. The consumer characteristics and their respective normalized demand profiles where unknown in the project, so it was decided to use a typical load curve for a medium-temp region with a standard amount of

residential and commercial buildings and their characteristic demand of hot-water and heating.

The result of this selection is shown in Figure 7-2.
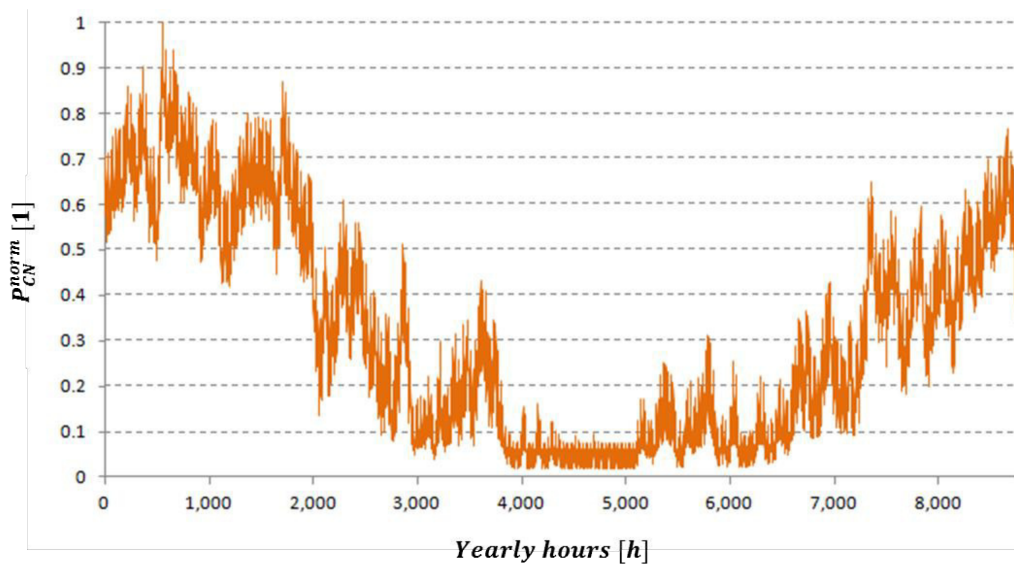
Figure 7-2: Normalized load curve for initial head demand

The normalized load curve is then upscaled so that the total amount of heat load equals ϕ_{CN} during the given timeframe of one year. The resulting initial peak power P_{max} is 5.55 MW with a minimum load P_{min} of 0.1 MW during the summer period. Based on this reference load curve, several DSM scenarios are defined which are used to study the effect of thermal insulation on the system. This is carried out in the following section.

7.1.2.2 DSM scenario definition for demand-based energy service

To integrate DSM as an energy service, the impact of thermal insulation must be quantified. This is done through the results obtained by the analysis of demand side measures in chapter 6. Thermal insulation is a measure reducing the peak load of the heat load curve represented by the characteristics of DSM_{peak}. Three scenario are defined which are based on different magnitudes of thermal insulation on the building structure.

- Scenario 1: $\phi_{TI} = 10\ \%\ \phi_{CN}$

- Scenario 2: $\phi_{TI} = 20\ \%\ \phi_{CN}$

- Scenario 3: $\phi_{TI} = 50\ \%\ \phi_{CN}$

In scenario 1, 10 % of the initial heat demand is reduced. In scenario 2 this is increased to 20 %, while in scenario 3, 50 % of the initial heat demand is reduced through thermal insulation. Those scenarios are chosen in order to show the impacts of various DSM magnitudes. A reduction of 20 % is furthermore representing the Horizon targets which foster a reduction of energy consumption of 20 %. It must be noted that those scenarios are not defined according to practical considerations but to show the impact of DSM for various magnitudes. The reference scenario is the one considering the initial heat demand without DSM.

Based on those definitions, the resulting heat load curves can be constructed using the methodology provided in section chapter 6, see Figure 7-3.
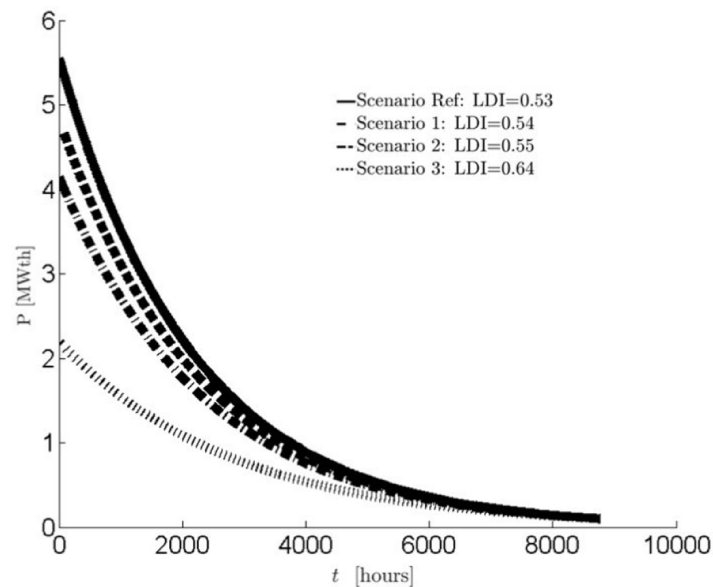
Figure 7-3: Heat load curves of the design scenarios

The heat load curve of the reference scenario is the result of the normalized load curve in Figure 7-2 upscaled by ϕ_{CN}. According to the scenario definitions, DSM_{peak} is applied to the initial load curve resulting in load curves, which have lower peaks and lower annual heat demand.

In addition, the methodology of the load deviation index is applied to the model. This consists of the calculation of LDI for every load curve, resulting in one single indicator. In the reference scenario a LDI of 0.53 is obtained while this value increases with increasing thermal insulation. For a 10 % reduction of ϕ_{CN}, an LDI of 0.54 is obtained, while for scenario 3, in which 50 % of the total annual heat demand is re-

duced, LDI equals 0.64. The more thermal insulation is applied, the closer LDI tends towards 1. This suggests that the resulting load curves tend towards their ideal load curve, which would be a constant heat load.

The numerical results of the different scenarios are summarized in Table 7-1.

Table 7-1: Numerical result of the application of DSM_{TI} to the DHN system

	ϕ_{CN} [E7 J]	ϕ_{TI} [E7 J]	ϕ_{HL} [E7 J]	P_{max} [MW]	P_{min} [MW]	LDI [1]
Scenario Ref	4.28	0.00	4.28	5.55	0.1	0.53
Scenario 1	4.28	0.43	3.85	4.84	0.1	0.54
Scenario 2	4.28	0.86	3.42	4.14	0.1	0.55
Scenario 3	4.28	2.14	2.14	2.20	0.1	0.64

The equation of (7.1) is fulfilled for every scenario, while the maximum load P_{max} decreases from initially 5.5 MW to 4.84 MW through a reduction of 10 % of ϕ_{CN} and up to 2.2 MW for a reduction of 50 % of ϕ_{CN} . The decrease follows a non-linear behavior, while the reduction of 10 % has a higher effect on the decrease of P_{max} than a decrease of 50 %. Furthermore LDI was calculated for the given scenarios showing an increase towards 1. Thus an increase of DSM_{TI} also leads to an increase of LDI.

7.1.2.3 Heating plant model for supply-based energy service

The resulting heat loads in every scenario must be met through the generation of heat by the heating system. The heating system consists of a biomass and a gas-boiler system, which supply the given amount of load. The main design variable for the heating plant is defined as the biomass unit size which can be expressed through the power ratio, generally defined in (6.6) – (6.7). This leads to the following design variable which will be further used in this case study, see (7.2).

$$\alpha = \frac{P_B^{nom}}{P_{max}} \tag{7.2}$$

This design variable has high influence on the heat generation since it defines the average efficiency of the system, which is furthermore determined through the partial-load model in Figure 6-10. For this case study, a certain partial-load behavior was assumed based on the project data. Since the data of the project was limited, the partial-load behavior in Figure 6-10 was not available for every operational point. To overcome that, a linear behavior for the drop of partial load efficiency was assumed.

The biomass unit has a nominal efficiency of 65 % which linearly decreases to 50 % efficiency during partial-load operation up to a nominative load of 75 %, while the gas boilers have a higher nominal efficiency of 85 % and drop to a partial-load efficiency of 10 % up to a partial-load of 50 %. Below the given partial load limitations, the partial-load efficiency was assumed to drop to 0 without taking into account minimum loads. This is done in order to assess the effects of load curves without the restriction of minimum loads.

It was already discussed that the partial load model effects the annual average efficiency given a certain design condition of α. In order to calculate the fuel associated with the operation of the heating plant, the annual average efficiency must be determined for every plant unit according to (7.3).

$$\eta_u^{av} = \int_1^T f\left(\frac{P_u}{P_u^{nom}}\right) dt \tag{7.3}$$

For every plant unit, an average efficiency can be calculated and used to determine the amount of fuel needed to generate the necessary heat demand, see (7.4) – (7.5),

$$M_W \cdot LHV_W = \frac{\phi_B}{\eta_B^{av}} \tag{7.4}$$

$$M_{NG} \cdot LHV_{NG} = \frac{\phi_{G1}}{\eta_{G1}^{av}} + \frac{\phi_{G2}}{\eta_{G2}^{av}} \tag{7.5}$$

where the amount of mass for wood (M_W) and natural gas (M_{NG}) are determined based on the amount of heat supplied by the biomass unit (ϕ_B) and the gas units (ϕ_{G1}, ϕ_{G2}), divided by their respective average annual efficiencies ($\eta_B^{av}, \eta_{G1}^{av}, \eta_{G2}^{av}$). This approach assumes the specific energy of each fuel equal to its lower heating value (LHV).

Besides the use of fuel for the heating plant, the expenditures related to transport must be taken into account. This is done through a transportation model which has been developed by (Jamali-Zghal et.al. 2013) and is adopted in this work. Basically, diesel fuel is considered for transport of wood, ash and labor. While transport of wood and ash depends on the amount of wood used, labor is considered constant for a yearly timeframe, see (7.6).

$$M_{Di} = \frac{e_{T,W}(1+lf_W)d_W \cdot M_W}{Cap_W \cdot LHV_{Di}} + \frac{e_{T,A}(1+lf_A)d_A \cdot f_A \cdot M_W}{Cap_A \cdot LHV_{Di}} + \frac{e_{T,Emp} \cdot d_{Emp}}{LHV_{Di}} \tag{7.6}$$

The transportation of wood and ash is carried out by trucks which have a certain maximum carrying capacity for wood (Cap_W) and ash (Cap_A), a certain specific energy consumption (e_T), which is extended by a load factor (lf). The load factor accounts for the unloaded back transportation of the vehicles. Diesel is assumed to be the energy carrier used for the trucks as well as for the passenger cars. Depending on the transportation distance (d) and the amount of wood and ash to be transported, the overall energy carrier consumption can be derived using the lower heating value to determine the amount of diesel needed. Furthermore, (f_A) is the "ash factor" considering the amount of ash per unit of wood that has to be transported to the landfill. The mass balance for the employees transport involves a constant yearly distance (d_{Emp}). This transport model allows including the additional expenditures related with a centralized heating plant, given the proposed system definition.

Based on the equations given, the total amount of fuel can be calculated for every design scenario. This is necessary for the performance assessment on which the multi-criteria sustainability analysis is based on.

7.1.3 Multi-criteria performance metric

In this section, the multi-criteria performance metric is defined. It was already mentioned that sustainability assessment must involve different dimensions to be addressed. This is done through the definition of indicators for all three system layers including:

- Technological system layer
- Environmental system layer
- Economic system layer

Each layer addresses a different perspective of sustainability and includes indicators which must be selected and defined. The next sections provide the selection and definition of the respective indicators for the given case study.

7.1.3.1 Technological system layer

In the technological system layer, the energy service system is assessed using a 1st-law approach, thus it is based on the energy efficiency of the system. The total energy consumption of the system (ϕ_{sys}) is given in (7.7),

$$\phi_{sys} = \phi_W + \phi_{NG} + \phi_{Di} \tag{7.7}$$

where $(\phi_W, \phi_{NG}, \phi_{Di})$ are the energy consumptions related with the fuels wood, natural gas and diesel, respectively. Those are derived through multiplying the amount of mass with its corresponding heating value, according to the example for wood consumption in (7.8).

$$\phi_W = M_W \cdot LHV_W \tag{7.8}$$

The total energy provided by the heating plant (ϕ_{HP}) is given in (7.9).

$$\phi_{HP} = \phi_W + \phi_{NG} \tag{7.9}$$

The first indicator used for evaluation is the energy efficiency of the heating plant (η_{HP}) according to (7.10).

$$\eta_{HP} = \frac{\phi_{HL}}{\phi_{HP}} \tag{7.10}$$

Transport is omitted in the definition of the energy efficiency of the heating plant to focus only on the efficiency behavior of the heating plant at the given design scenarios. Furthermore, energy reduction through thermal insulation is not included in η_{HP}. In order to provide an overall technological indicator for the whole system, primary energy ratio (PER_{sys}) is used according to (7.11),

$$PER_{sys} = \frac{\phi_{sys}}{\phi_{CN}} \tag{7.11}$$

which provides a total estimation of how much primary energy is needed to supply a given consumer demand. This is an important indicator to assess the impact of thermal insulation on the efficiency of the whole system. In order to compare the centralized heating system with the decentralized gas boiler system, a relative primary energy ratio is defined, see (7.12).

$$PER^{rel} = \frac{PER_{sys}}{PER_{ref}} \tag{7.12}$$

As a third indicator, the renewable energy ratio (RER_{sys}) is introduced in order to measure the amount of renewable energy used in the system. This is an important indicator according to the Horizon targets. It was already stated, that biomass can be considered as 100 % renewable energy given certain conditions are fulfilled. Since

natural gas and diesel cannot be considered as renewable energy, (RER_{sys}) is calculated through (7.13).

$$RER_{sys} = \frac{\phi_W}{\phi_{sys}} \tag{7.13}$$

Those indicators are used to assess the technological suitability of the DHN system compared to the reference system.

7.1.3.2 Environmental system layer

The environmental assessment includes carbon footprint and emergy analysis. The carbon footprint assessment determines the CO2 emissions of the energy service system and uses that indicator to evaluate its environmental performance. CO2 emissions are directly related with the use and consumption of fossil fuels.

The overall CO2 balance for the energy service system $(CO_{2,sys})$ is the sum of the carbon emissions related to each energy carrier, see (7.14).

$$CO_{2,sys} = CO_{2,W} + CO_{2,NG} + CO_{2,Di} \tag{7.14}$$

The carbon emissions of the energy carriers are calculated by multiplying the mass of each energy carrier with its specific carbon emissions containing both the specific upstream (ce_{up}) and utilization (ce_{util}) emissions. This is exemplarily shown for the energy carrier wood in (7.15).

$$CO_{2,W} = M_W \left(ce_{W,up} + ce_{W,util} \right) \tag{7.15}$$

This allows integrating all carbon emissions related with upstream processes as well as its current utilization. The resulting $CO_{2,sys}$ is therefore the carbon footprint of the system. For comparison to the reference system, relative carbon footprint is defined in (7.16).

$$CO_2^{rel} = \frac{CO_{2,sys}}{CO_{2,ref}} \tag{7.16}$$

Furthermore, emergy flow is used as a second indicator for environmental performance analysis. This has two reasons. First, emergy flow provides a much broader assessment of environmental impact considering the whole energy needed to deploy a given energy source. Unlike carbon footprint, emergy analysis includes a more de-

tailed framework of sustainability analysis which is not available for carbon footprint. Second, one objective of this case study is to study the relation between carbon footprint and emergy for different design selections.

The total system emergy (Em_{sys}) is determined through (7.17),

$$Em_{sys} = Em_W + Em_{NG} + Em_{Di} + Em_{cap} \qquad (7.17)$$

where the sum of emergy flow related to consumption of fuels depend on the technological performance of the system, and (Em_{cap}) is the emergy associated with capital expenditures of the system. The emergy flow of wood is exemplarily calculated in (7.18) with the help of the associated upstream (sT_{up}) and utilization (sT_{util}) solar transformities.

$$Em_W = \phi_W\left(sT_{W,up} + sT_{W,util}\right) \qquad (7.18)$$

The emergy flows associated with natural gas, diesel and capital investment are calculated similarly. The relative measure to the reference scenario is given in (7.19).

$$Em^{rel} = \frac{Em_{sys}}{Em_{ref}} \qquad (7.19)$$

Apart from the emergy flow which is used for comparison to carbon footprint, emergy offers a more detailed framework for sustainability assessment. This includes a variety of indicator discussed in the state of the art. In this work, the emergy sustainability index (ESI) is used as a global indicator for environmental assessment of the system. The calculation of ESI depends upon the underlying emergy flow diagram, which has already been presented in Figure 5-1. Based on the emergy methodology, ESI is defined as in (7.20).

$$ESI = \frac{Em_{Sys}}{Em_{Di} + Em_{cap}} \frac{Em_W}{Em_{Di} + Em_G + Em_{cap}} \qquad (7.20)$$

7.1.3.3 Economic system layer

For the economic evaluation, the capital costs and the operating costs of the energy service system are needed to derive the corresponding system costs (C_{sys}) according to (7.21).

$$C_{sys} = C_{capex} + C_{opex} \qquad (7.21)$$

The capital expenses C_{capex} are the sum of all investments including the thermal insulation and the costs for the heating plant units, divided by their lifetime (taken to be 20 years) in order to account for their depreciation, see (7.22).

$$C_{capex} = \frac{C_{TI}}{20} + \sum_u \frac{C_u}{20} \qquad (7.22)$$

The capital expenses related with thermal insulation are derived through multiplying the total amount of heat reduction with the specific cost of thermal insulation, see (7.23).

$$C_{TI} = \phi_{TI} \cdot c_{TI} \qquad (7.23)$$

For the capital expenses of the units, a more complex model is used taking into account the nominal power of each heating unit. The economic model assumes that the installation of the heating plant induces capital costs which need to be invested. The costs of such heating units depend on their size and performance. Investigations of the specific investment costs for large cogeneration natural gas-fired power plants and small block-type plants revealed that specific investments costs drop exponentially with rising plant size (Coss 2013). Thus, a similar behavior can be assumed for biomass-fired and natural gas-fired heating plants, while the costs at nominal power of the units are available from project documentation. Furthermore it can be assumed that costs rise with increasing nominal equipment efficiency. Those assumptions are implemented through an exponential approach, which is used to model the specific capital costs for a plant unit including the nominal design power and nominal equipment efficiency as characteristic criteria. The general behavior is expressed through (7.24),

$$C_u = \phi_u \left[f_u \cdot e^{P_u^{nom}(1 - \eta_u^{nom})} \right] \qquad (7.24)$$

which assumes an exponential approach for the decrease of specific capital costs with increasing nominal power and increase with increasing system efficiency. This model is based on project data available to the author. The factor (f_u) describes the shape of the cost function for each unit. The data used for this model is given in the Appendix.

Moreover, the operating costs of the system must be defined. These are derived through the specific costs of each fuel used, see (7.25).

$$C_{opex} = M_W \cdot c_W + M_{NG} \cdot c_{NG} + M_{Di} \cdot c_{Di} \qquad (7.25)$$

The data of specific costs for fuels and thermal insulation for this case study are also given in the Appendix.

At last, the difference of the costs between the DHN system and the reference system is defined as in (7.26),

$$\Delta C_{sys} = C_{sys} - C_{ref} \qquad (7.26)$$

where C_{ref} considers only the operating costs of natural gas consumption of the decentralized gas boilers.

This indicator ΔC_{sys} is used to compare additional costs associated with the substitution of the reference system and is an important factor for the assessment of optimum design solutions in the industrial context.

7.1.4 Multi-criteria sustainability analysis

In this section the multi-criteria analysis is carried out using the sustainability metric defined previously. This is done through the evaluation of the performance of the DHN system considering the defined DSM scenarios. In order to compare the results relative to the reference system, the data necessary to calculate the relative indicators are summarized in Table 7-2.

Table 7-2: Data of the reference system

Description	Item	Value	Unit
Mass (only gas)	$m_{NG,ref}$	1.30 E6	[kg]
Primary energy ratio	PER_{ref}	1.22	[-]
CO2 emissions	$CO_{2,ref}$	3.13 E6	[kg]
Emergy flow	Em_{ref}	5.02 E18	[seJ]
System costs	C_{ref}	65.000	[Euro]

Based on the project data, the reference system shows a total primary energy consumption of 5.22 E7 J which is supplied 100 % by natural gas. Based on the data for natural gas, carbon footprint and emergy flow was determined to be 3.13 E6 kg CO2 and 5.02 E18 seJ of emergy. System costs have been evaluated to 65.000 Euro considering only the fuel costs of natural gas. These values are used to compare the two systems in the following multi-criteria assessment.

7.1.4.1 Technological performance assessment

The technological performance assessment is used to determine the technological sustainability of the system. For that, certain criteria must be selected which are able to represent performance from an energetic viewpoint. Those include the energy efficiency of the heating plant η_{HP}, the relative primary energy ratio PER^{rel} as well as the renewable energy ratio RER_{sys}. The first three have been introduced as technological indicators and it was seen that they are widely used in research, policy making and practice. The following results are expressed for the design variable α as well as for every scenario defined. This allows a detailed analysis of design selection and their impacts on sustainability. The following analysis is carried out for $10\,\% \leq \alpha \leq 90\,\%$.

Relative primary energy consumption PER^{rel} rises with rising biomass plant size, see Figure 7-4.
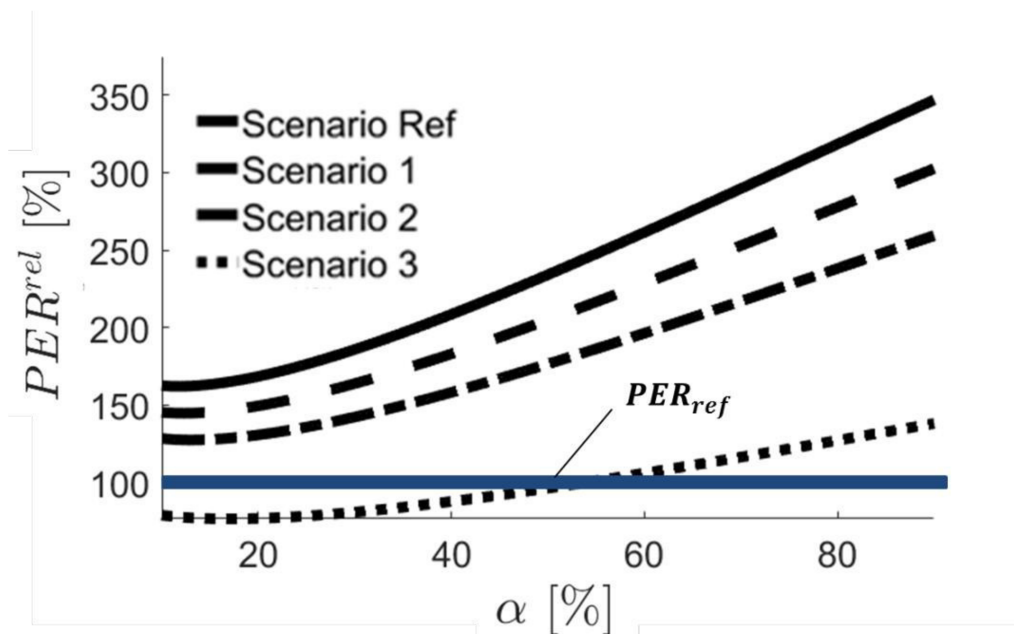
Figure 7-4: Primary energy ratio relative to the reference system

This increase is due to a decreasing overall efficiency on one side and due to a rising resource demand for diesel due to transportation effort on the other side. The optimum design point for a minimum primary energy consumption lies at a biomass unit size of about 15 %. For larger biomass unit sizes, primary energy consumption drastically increases. Thus the more biomass is used for heat generation the higher transportation increases the total primary energy consumption.

Thermal insulation, visible through the defined scenarios, clearly decreases primary energy consumption and is therefore a suitable measure if primary energy ratio should be reduced. This is mainly due to an improved operational performance which reduces losses through partial-load operation.

Relative to the reference system, only scenario 3 shows lower primary energy ratio below a biomass unit size lower than 50 %. This suggests that the centralized system consumes more energy compared to the reference system. Especially in the reference scenario, where no thermal insulation is applied, primary energy ratio is much higher compared to the reference system. The primary energy ratio is highly affected by the efficiency of the heating system.

The heating plant efficiency is decreasing with higher shares of biomass size since higher amounts of energy are produced under partial-load conditions, see Figure 7-5.
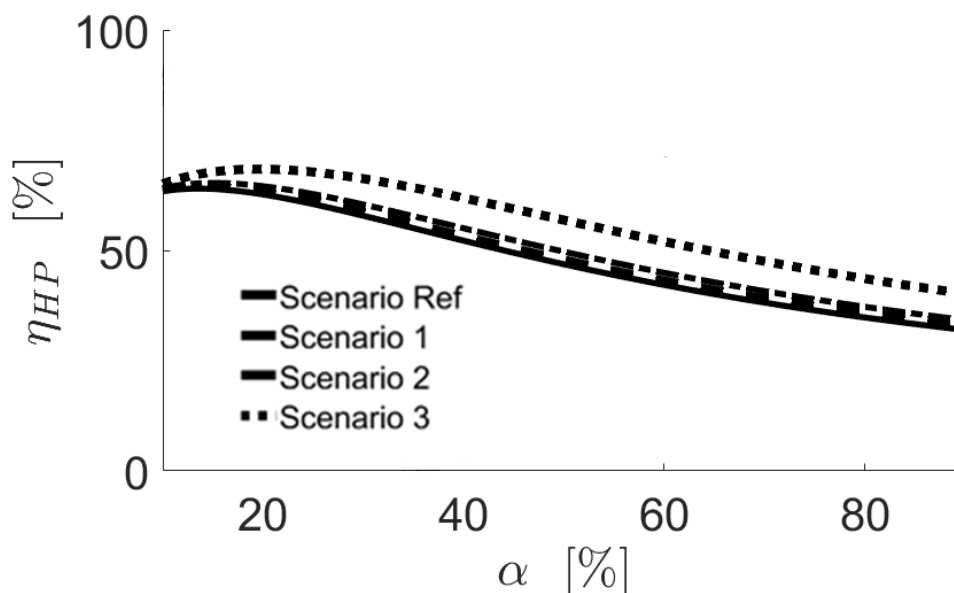
Figure 7-5: Energy efficiency of the heating plant for different design scenarios

Annual efficiency of the heating plant is optimum at the same biomass size as primary energy ratio. An interesting issue is the fact that plant efficiency slightly rises with an increase in thermal insulation. Since efficiency decrease is depends on the load curve and the partial-load operation, this efficiency gain can be traced back as the influence of the heat load curve and its characteristic profile. Thus, thermal insulation contributes to the heat load curve in a way which allows the plant units to operate more time at its nominal loads and therefore lead to a positive impact on the overall yearly efficiency.

Both PER^{rel} and the renewable energy ratio RER_{sys} correspond to the horizon targets, which aim is to reduce both by 20 %. Figure 7-6 show the results obtained for RER_{sys}.

Figure 7-6: Renewable energy ratio of the system

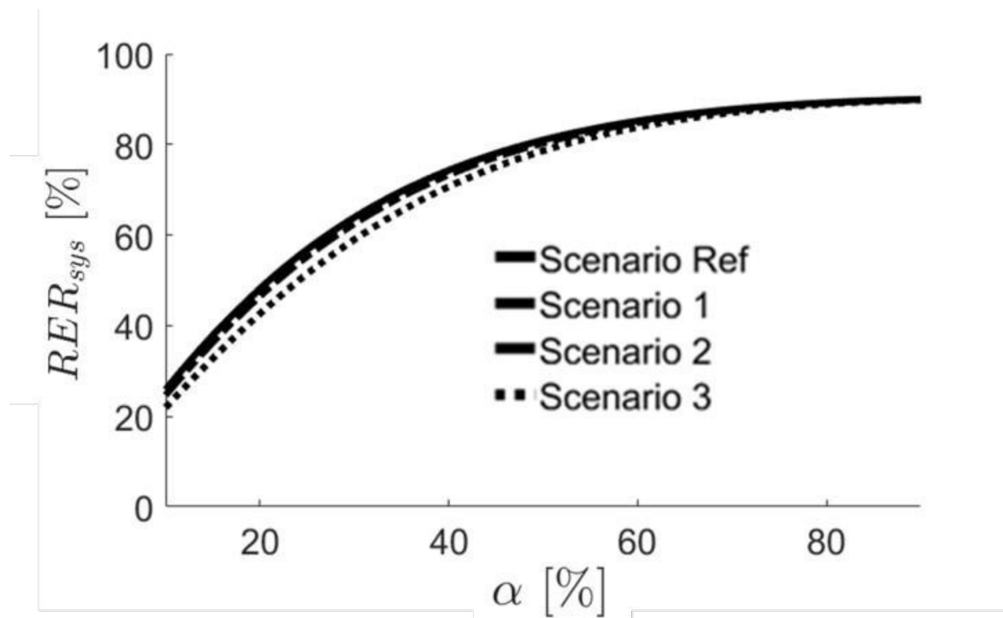Clearly, RER_{sys} increases with rising biomass share which is not surprising since the higher the biomass unit size, the more heat is produced from wood. It is worth mentioning that even for very high values of the biomass size, RER_{sys} does not reach 100 %. This is due to the transport of wood which causes a certain amount of diesel consumption.

Almost no effect of thermal insulation can be detected. This means that even in scenario 3, where 50 % of the initial heat demand is reduced, the share of biomass utilisation is almost equal. This suggests that the benefits of a flatter load curve do not occur for this indicator. Thus for this DHN system, thermal insulation has only a very low effect on the increase of renewable energy.

7.1.4.2 Environmental performance assessment

The environmental performance assessment investigates the environmental impact given the different design scenarios of the system. For that relative carbon footprint CO_2^{rel}, relative emergy flow Em^{rel} and the emergy sustainable index ESI are used.

The evaluation results of the carbon footprint analysis are given in Figure 7-7.
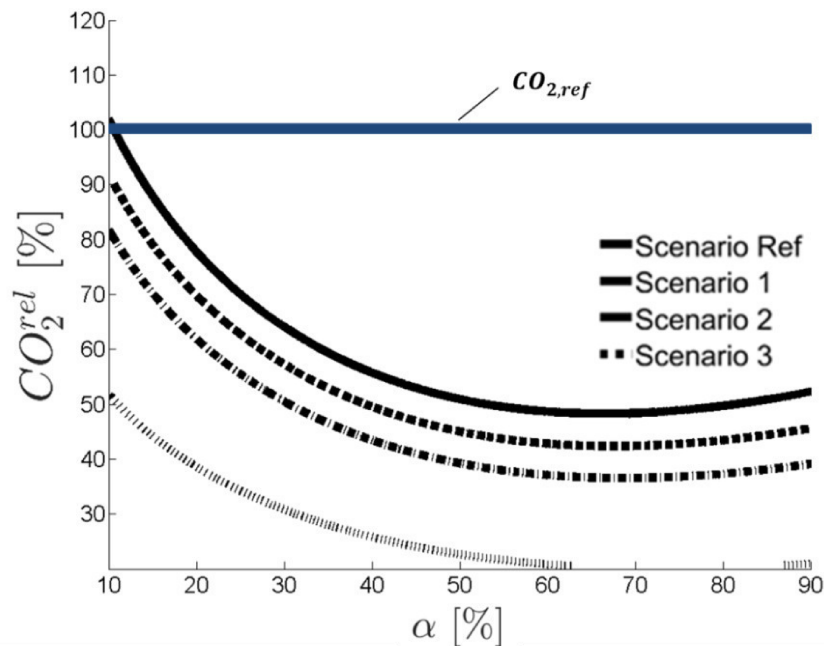
Figure 7-7: Results of carbon footprint analysis

The results of the carbon footprint analysis show that carbon emissions in the reference scenario decrease relative to the reference system to a certain minimum of 50 % at a biomass boiler size between 60 % and 70 %. With increase of thermal insulation, further reductions can be achieved, leading to a relative carbon footprint of about 45 % at a biomass size of 68% for scenario 2. In scenario 3, carbon footprint shows a 80 % reduction of carbon footprint given high values of the biomass size between 60 and 70 %.

It is interesting to see, that for higher value of α above the threshold between 60 and 70 %, carbon emission rise. This means that if the biomass unit is sized higher than 70 %, the carbon emission increase due to a reduction of operational efficiency. For all scenarios the lowest carbon footprint lies between 60 and 70 % of the biomass plant size, reducing the carbon emissions to a half or more compared to the decentralized reference system.

This huge drop in carbon emissions is influenced by the low specific emissions of the wood used in the biomass boiler and shows that the optimum design based on carbon footprint does not correspond to maximum biomass plant size (of e.g. 100 %) but to a certain value between 60 and 70 %. With increasing thermal insulation, carbon emissions are reduced linearly relative to the reference system. For any given biomass size, the performance of the DHN system in terms of carbon footprint analysis

shows better results than the reference system. Those results suggest that the optimum biomass size is between 60 and 70 % of the nominal load, regardless of the amount of thermal insulation applied.

The results of the emergy analysis in Figure 7-8 are the next part under investigation.
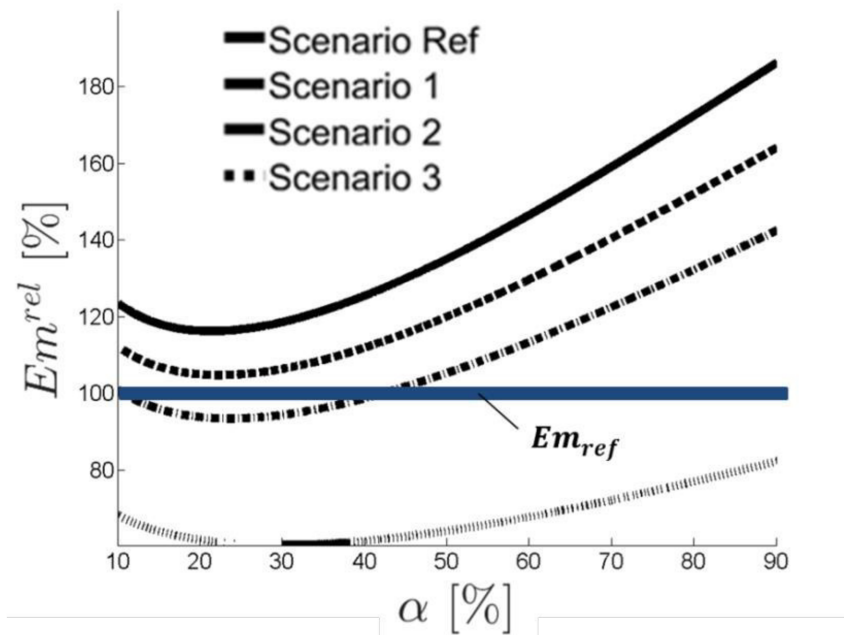
Figure 7-8: Relative emergy for the design scenarios

The results show that at a biomass unit size around 20 % leads to a minimum emergy flow in the reference scenario. Lower- and higher shares of the biomass unit are not favorable since overall emergy flow increases. Furthermore, compared to the reference system, emergy flow is generally higher.

Results show that Em^{rel} reaches a minimum of 119 % at plant size of 21 % for the reference scenario and 93 % at a size of 23 % in scenario 2. Further increase of the biomass plant leads to higher values of emergy flows, where at a plant size of 42 % the emergy flow of scenario 2 reaches again the same value as for the reference system. For a high share of biomass overall relative emergy is increasing rapidly and is larger than for the reference system for all scenarios except for scenario 2. The reason for that is, that emergy is (similar to the carbon-footprint method) based on the energy balance of the system but with the difference that biomass, even if it is carbon neutral, has a certain emergy production for its utilization. This leads to a higher impact at higher shares of biomass used. An interesting fact can be seen considering the minimum emergy flow, which would be the desired design optimum. It lies be-

tween 20 and 30 % of the biomass unit size. This is in contrast to the findings of the carbon footprint analyses, which suggested an optimum point between 60 and 70 %. It can be therefore concluded, that given a certain DHN system, design suggestions on the size of the biomass unit vary according to the assessment method used.

At last, the ESI is investigated which aims in providing a global sustainability indicator for the given system, see Figure 7-9.
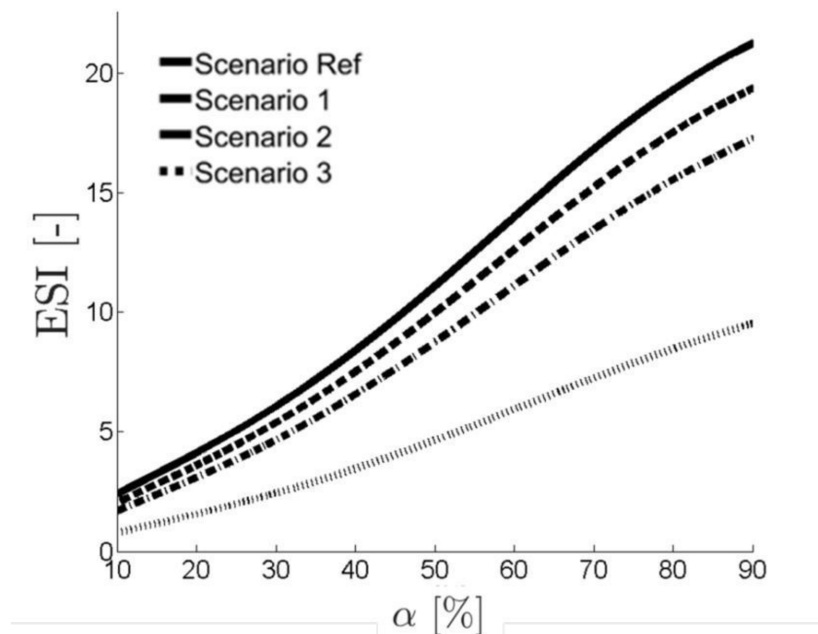
Figure 7-9: Emergy sustainability index

The ESI determines overall sustainability (including economic contribution) in the emergy framework, and clearly rises with increasing biomass size. On the other hand, thermal insulation decreases this indicator because investments costs for insulation are not considered as a positive contribution to the ESI. This results in higher ESI for higher shares of biomass but a huge drop in ESI for thermal insulation. This suggests, that sustainability according to the emergy framework is higher, the higher the amount of the biomass unit. This is in contrast to the previous findings which showed minima between 60 and 70 % for carbon footprint and 20 to 30 % for total emergy flow. Furthermore, thermal insulation is counterproductive to this index, because the capital expenditures of thermal insulation in the scenarios are not contributing to an increased renewability of the system.

7.1.4.3 Economic performance assessment

In the last section of the performance assessment, the economic indicator ΔC_{sys} is investigated in detail, see Figure 7-10.
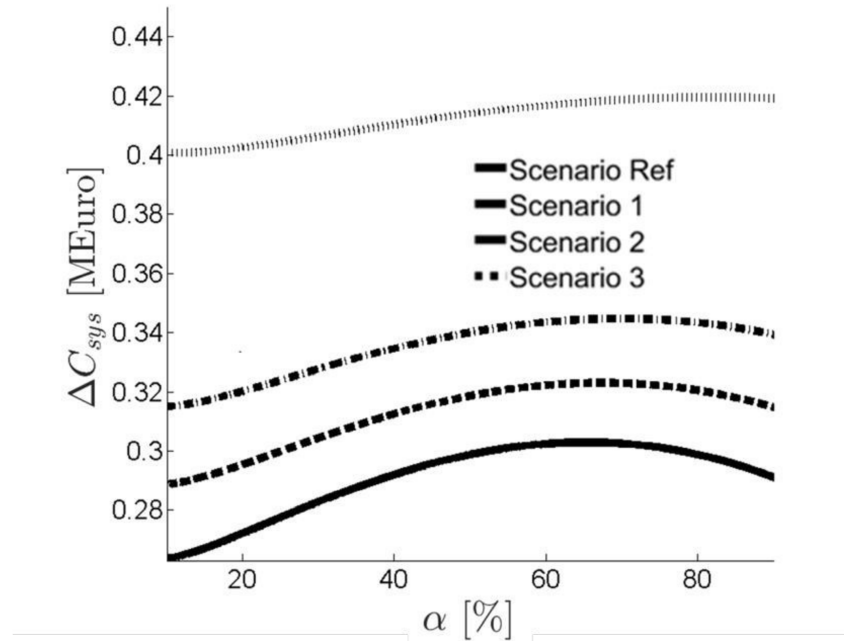
Figure 7-10: Economic performance assessment

Since in the reference scenario, only the operating costs, which are the fuel costs of natural gas, are used as C_{ref}, the DHN system shows higher relative costs for all design scenarios. The indicator shows that a very low or a very high biomass size would be the cheapest option. The highest cost can be seen between 60 and 70 % for scenario 1 and 2 as well as for the reference scenario. In scenario 3, the costs for thermal insulation are more dominant then the costs of the heating units which leads to relative system costs almost independent of the design of the biomass unit size.

This is an interesting result, since the relative system costs show their maximum in the same range as carbon footprint shows its minimum. This means, that maximizing environmental performance with carbon footprint, also maximizes the system costs. This clearly shows the contradictory objectives system designer face in real practice. Hence a multi-criteria analysis helps to identify the impacts of design decisions regarding costs and environmental performance. Those decisions can be benchmarked using the multi-criteria assessment metric.

7.1.4.4 Sustainability benchmark of selected designs

The previous chapter analyzed in detail the results of the performance assessment under different design conditions. The results showed the various indicators on a two-dimensional basis which are based on two design variables representing the biomass unit size and the amount of thermal insulation.

Those results can be used to benchmark different system configurations according to the sustainability metric proposed. This is an important tool for system designers to respond to external targets such as policy targets on certain criteria and help assessing the effect of certain design decisions on the sustainability of the underlying system.

For the sustainability benchmark two specific scenarios are chosen. First, the reference scenario is chosen, which represents the current state of the DHN system relative to its reference system. Second, scenario 2 is selected, which represents the Horizon target of a reduction of energy consumption on demand side as well as the increase of efforts towards thermal insulation.

For every selected scenario, different design selections of the biomass plant size are defined. Those include the two extreme design sections where the biomass unit is either seized at 10 % or at 90 % of the nominal heating load as well as a common design selection with a biomass unit size of 60 %. This value has already been discussed as a prominent value for base-load sizing. The corresponding nominal powers for the heating plant P_B^{nom} can be derived using (7.2). Furthermore, an optimum design selection for every criteria is given, which represent the best design selection associated with each indicator (Cr^{opt}) and its associated design variable (α^{opt}). With the help of the results obtained from the sustainability assessment, the design selection according to scenario and biomass unit size can be evaluated. The numerical results are summarized in Table 7-3. All units in [%] except ΔC_{sys} in [MEuro].

The minimum relative system costs ΔC_{sys} are reached at the lowest biomass plant size of 0.6 MW in the reference scenario and 0.4 MW in scenario 2. Those are 0.26 and 0.31 MEuro, respectively.

Table 7-3: Numerical results of the sustainability benchmark

		ΔC_{sys}	PER^{rel}	η_{HP}	RER_{sys}	Em^{rel}	CO_2^{rel}	ESI
Scenario Ref	$P_B^{nom} = 0.6\ MW$	0.26	162	63.03	26	124	102	2.39
	$P_B^{nom} = 3.3\ MW$	0.30	261	42.15	85	146	49	13.98
	$P_B^{nom} = 5.0\ MW$	0.29	347	32.17	90	186	52	21.26
	Cr^{opt}	0.26	160	64.65	90	118	48	21.26
	α^{opt}	10.00	11.72	13.69	90.00	21.28	66.50	90.00
Scenario 2	$P_B^{nom} = 0.4\ MW$	0.31	128	64.00	25	101	82	1.67
	$P_B^{nom} = 2.8\ MW$	0.34	196	45.75	85	115	37	11.11
	$P_B^{nom} = 3.7\ MW$	0.34	259	34.20	89	142	39	17.24
	Cr^{opt}	0.31	127	65.73	89	93	37	17.24
	α^{opt}	10.00	12.96	14.79	90	23.50	68.73	90.00

At higher biomass unit design, ΔC_{sys} increases for both scenarios relative to the optimum design. Relative primary energy ratio PER^{rel} results in 162 % and 128 % given a low biomass unit size of 0.6 and 0.4 MW.

With increasing size, PER^{rel} also increases, while the typical design selection of 3.3 MW for the reference and 2.8 MW for scenario 2 shows values of 261 % and 196 %. The optimum design according to PER^{rel} would be reached at 160 % and 127 % for biomass unit sizes of 11.72 and 12.96 %, respectively. Those values correspond to a biomass size of 0.65 MW and 0.53 MW. Heating plant efficiency shows optimum values of 64.65 and 65.73 % at biomass unit sizes of 13.69 and 14.79 % of total the peak load.

In contrast to that, the environmental assessment shows optimum values at 21.28 and 23.50 % biomass size for emergy and 66.5 and 68.73% for carbon footprint given the two scenarios. That means that the optimum based on emergy lies around 20-25 %, while a system minimizing CO2 emissions is given at higher biomass boiler shares between 65 and 70 %. Clearly, both RER and ESI show that maximizing renewability is only achieved by maximizing biomass plant size up to 90% at plant sizes of 5 and 3.7 MW.

Those numerical results are very helpful for design selection in the industrial context because the impact of design decisions can be investigating in detail. Furthermore it can be assessed if a typical sizing of 60% peak load is useful regarding different objectives. In order to provide a benchmark which can be used to compare different design decisions, a spider graph can be used. This spider graph offers the possibility to see the impact of different design selection relative to the reference system. Those representations are given in Figure 7-11 and Figure 7-12.
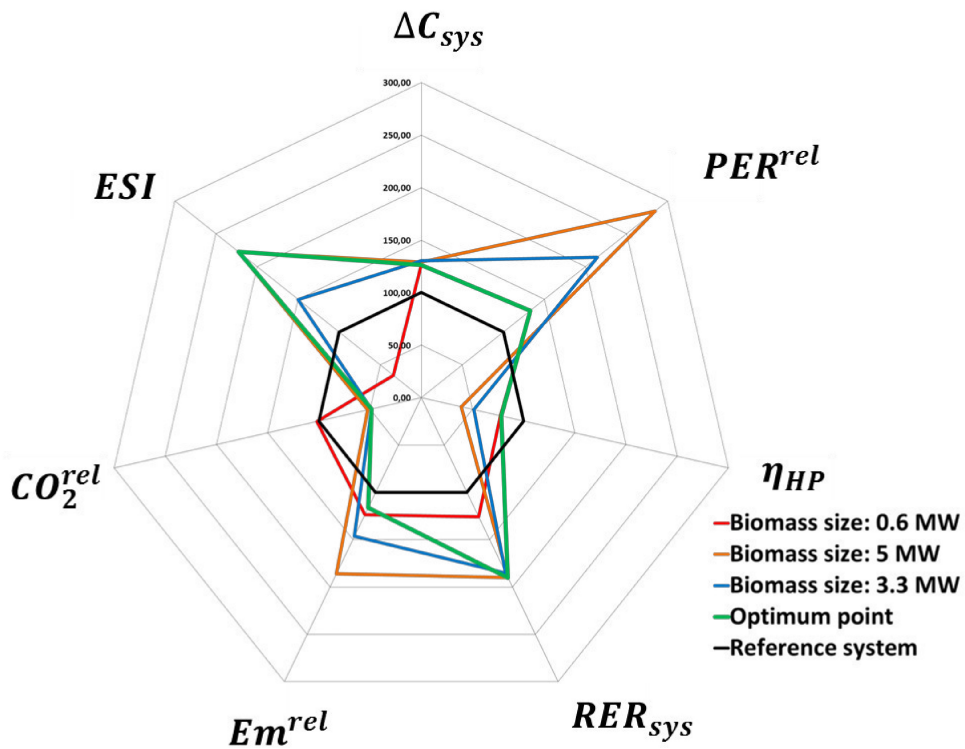
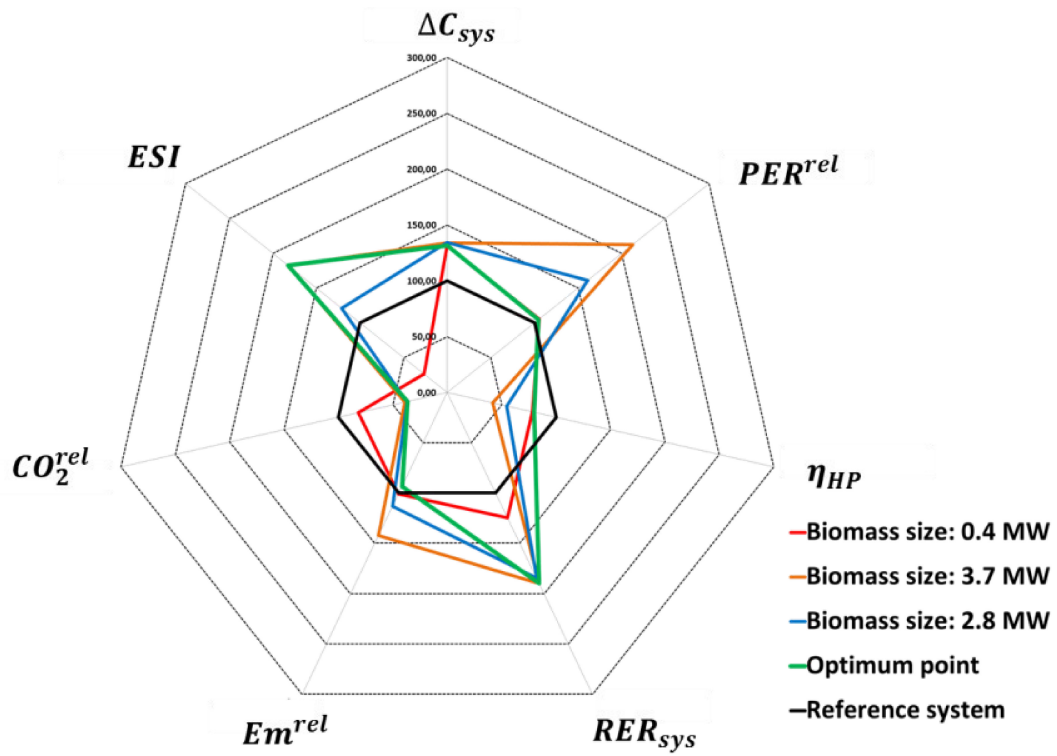Figure 7-11: Sustainability benchmark of the reference scenario

Figure 7-12: Sustainability benchmark of scenario 2

The total heat load of the reference scenario is 5.55 MW (see Table 7-3), which leads to design selections of the biomass unit of 0.6, 5.0 and 3.3 MW. Those correspond to the design selection of 10, 90 and 60 % biomass unit size. The reference system is marked at 100 % for every criterion in order to show the relative difference. It must be noted that e.g. for the emergy sustainability index, no reference value could be calculated. For scenario 2, a total load of 4.14 MW was estimated leading to nominal powers of 0.4, 3.7 and 2.8 MW.

It can be seen that system costs are higher for design selection relative to the reference system, because the reference system does not bear any investment costs and the operating costs are small compared to the capital expenditures. Primary energy consumption is also always higher but is close to the reference system in scenario 2 assuming that the biomass size was taken at its optimum value. Overall plant efficiency behaves mainly vice-versa to PER^{rel} while the renewable energy ratio is higher for every design selection.

The environmental sustainability indicators show that emergy flow is higher compared to the reference system; but carbon emissions are reduced to a high amount in scenario 2. Thus without thermal insulation, any configuration will lead to higher emergy flow than in the reference system, except for scenario 2 when the optimum point of emergy flow is selected. The ESI indicator is not possible to derive for the reference case, thus the base line is set to 0. It can be seen that optimized designs maximize the ESI, while thermal insulation in scenario 2 reduces it.

Those results clearly show the impacts of certain design decisions on the sustainability of the given metric. It shows that through this framework proposed, benchmarking of complex system models can be carried out using a holistic, multi-dimensional sustainability metric. Apart from sustainability analysis and benchmark, a Pareto study is carried out to determine the interdependency of carbon footprint and emergy flow in the design selection.

7.1.5 Inter-dependency of carbon footprint and emergy flow

This assessment is numerically carried out through evaluating the objective function for every given design criteria. It must be noted, that this is only possible for systems which can be solved in reasonable computational time. Otherwise, an optimization technique must be used to determine the Pareto curve. As objective functions, rela-

tive emergy Em^{rel} and relative carbon footprint CO_2^{rel} are used. The result of the assessment is provided in Figure 7-13.
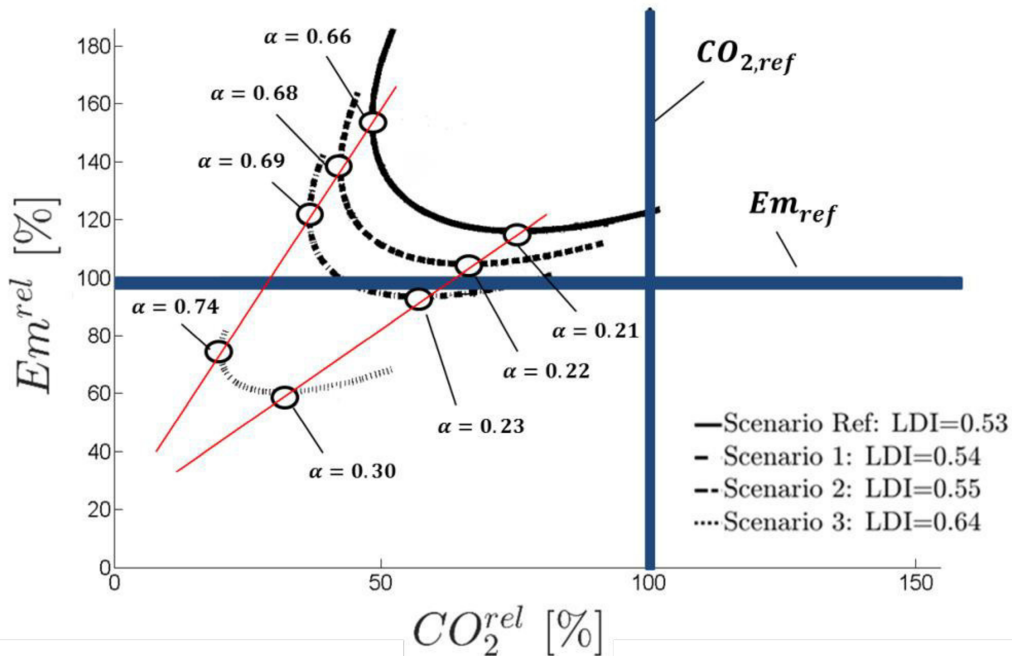

Figure 7-13: MRA of emergy and carbon footprint analysis

The objectives Em^{rel} and CO_2^{rel}, show contradictory behaviour. This means that both criteria cannot be fully optimized at the same time. For each DSM scenario, the optimized biomass plant size according to both objectives function is provided. First of all, the emergy optimum lies at smaller sizes of the biomass plant between 20 and 30 % depending on the scenario, while the optimum of carbon emissions tend to be between 66 and 76 %. Depending on the selection of α, the outcome of the objective function differ, while the general trend is clear

With increasing thermal insulation in the various scenarios, the optimum size of the biomass unit increases for both objectives. This means that the implementation of higher shares of biomass plant power is preferably in terms of those objectives. This is a very important finding, because it proves that with increase of thermal insulation, the optimum design for both emergy and carbon footprint lies at higher biomass unit sizes, given the data setting of the case study. This allows producing more amount of energy based on the renewable source of wood then with natural gas. It must be noted that this is not caused by the reduction of the heat load through thermal insulation, but through a higher average annual efficiency.

The chart can be further analyzed considering the different areas defined by the reference system. The upper right corner is the area, where the DHN system has a both lower performance in emergy and carbon footprint compared to the reference system. In contrast to that, the lower left corner shows DHN system designs relatively improved for both objectives. The upper left and lower right areas are the ones where either one of the objectives is better compared to the reference system.

Compared to the reference system, the reference scenario and scenario 1 show only a better performance for carbon footprint but not for emergy, while for scenario 2, this is only true for low biomass sizes. Nevertheless all of the scenarios show a lower carbon footprint compared with the reference system. Scenario 3 is exceptional in the sense that regardless of the biomass size, the system configuration shows always improvements. This suggests that a high implementation of thermal insulation is recommended given the specific design condition. It must be noted, that those results are highly dependent on the design condition and the data used for the models..

Furthermore, the results are analyzed under the viewpoint of the proposed load deviation index. For every scenario, LDI is provided which was initially calculated based on the underlying load curves, see Table 7-1. It can be seen that the optimum designs for the both objective functions tend to follow a linear trend line. This trend line represents the behavior of the optimum design of every objective function. It can be seen that with increasing LDI, the optimum design points of the objective function lead to higher values of α. This means that when LDI is increasing, due to a load curve which is closer to its ideal profile, the size of the biomass unit will also increase given that the design selection was based upon the optimum points. Hence, this suggests, that LDI, which describes the shape of the heat load curve, has a distinct relation with optimum design points which can be achieved.

At last, the relational factor is calculated which can be used to determine the change of emergy relative to carbon footprint (or vice-versa), see Figure 7-14.

The relational factor shows two areas. Below a biomass size of about 42 %, emergy increases relative to carbon footprint while above the relative change of emergy decreases. For this representation, not the normalized but the absolute values have been used.
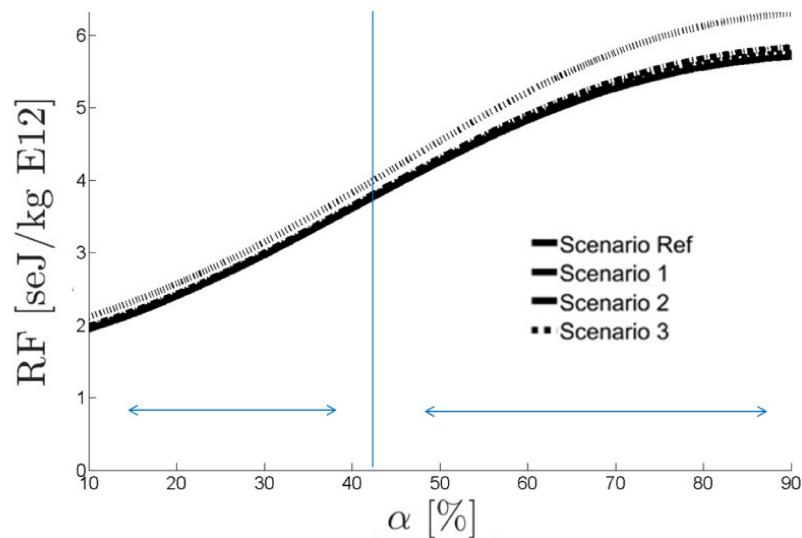
Figure 7-14: Relational factor for emergy and carbon footprint

Considering a design selection of 42 %, emergy flow is about 3.6 E12 seJ per kg of CO2. For that chart, the absolute values of emergy can be directly deduced from the CO2 emission given a certain selected design.

While for a low value of α at 10 % emergy is about 2 E12 seJ/kg, this value is 5.1 for a design selection of 90 % for the reference scenario. This suggests that the relative increase of emergy at lower biomass sizes is less than for higher ones. Besides those findings, the impact of thermal insulation can be evaluated. In general, thermal insulation has very little impact on the relation between emergy and CO2 emission. This can be seen through the relational factor which is almost equal for the design scenarios except as for scenario 3. Here, the relative increase of emergy flow is considerably higher at higher biomass sizes.

This case study provides a framework for sustainable design of a small-scale DHN system which can be used for industrial applications. In the next section, a more theoretical investigation of the behavior of the load deviation index is presented.

7.2 Investigation of DSM through multi-objective optimization

In this case study, a simplified version of the previous DHN system is used to study the DSM approach in a more general way. For that, a multi-objective optimization (MOO) is applied using a distinct sustainability metric. In order to analyze possible DSM scenarios, a parametric study of heat load curves is carried out using the MOO approach.

The aim of the case study is to investigate the effect of demand side measures on the possible design improvements which can be achieved. Furthermore, the behavior of the load deviation index is studied in a more general way, which can be used as a tool to link DSM and design improvement.

7.2.1 Introduction to the case study

In the previous case study, a real-existing small-scale DHN system was studied using only thermal insulation as a DSM. It was shown that, thermal insulation has positive impact on the performance of both emergy flow and carbon footprint of the given system. Furthermore it showed a distinct relation between the optimum design points of the system with the LDI. Only DSM_{peak} was applied, while the other techniques have been omitted. They are now taken into account to study the behavior of DSM for all three DSM techniques.

This is done using the previously discussed case study with slight modifications for the sake of simplicity. The transportation model is excluded from the analysis in order to focus purely on the effect of DSM on heating plant design. Furthermore, a three-unit design approach is used which includes two design variables α and β. Those represent the design of the nominal load of base-load and medium-load units according to equations (6.6) – (6.7). Different to the previous case study, a peak-load boiler is introduced which is independent of the medium-load boiler. This refers to practical consideration where heating plants might be composed of a biomass unit as base-load, a gas boiler as medium-load and an oil boiler for peak-load supply. In this case study, both medium- and peak-load boilers are fueled by natural gas.

Several adjustments to the data have been done based on updated information. The lower heating values, specific emissions and transformities have been used equally. Furthermore, it was assumed that the biomass unit has typically higher cost then a gas boiler, with the difference that with higher sizes, the costs drop relatively higher for the biomass unit then for the gas unit. For that, an exponential cost curve has been deployed after (7.27),

$$C_{cap} = (a \cdot e^b) \cdot P^{nom} \tag{7.27}$$

which defines the capital cost associated with investments for heating units. For the biomass unit the following values have been used: a=550 Euro/kW; b= -2E-4 and for

the gas unit: a=95 Euro/kW; b= -1E-4, which are based on previous works (Coss 2013).

Furthermore, the partial-load model has been adapted according to industrial practice. The biomass unit efficiency drops to 50 % efficiency at a partial-load of 50 %, while the gas boilers drop to 80 % efficiency at 20 % partial load. This is a meaningful assumption, since the biomass unit is used for base-load supply and might suffer high losses at partial-load. Apart from that, the nominal efficiency is 65 % and therefore much lower than for the gas boilers (90 %). This partial-load model represents the operational behavior of the units in industrial practice and allows investigating under which condition the size of the biomass unit can be increased without high drawbacks form partial-load losses.

In order to account for the losses in the DHN network, a constant thermal loss of 10 % of the peak load has been assumed. This value was found as an average value in part A of this thesis and is also in accordance with industrial practice. The remaining data has been used similarly as for the previous case study and can be looked up in the Appendix.

7.2.2 Parametric study of demand side measures

In order to analyze the impact of DSM in a general way, a parametric study of a given reference load curve is carried out. This study defines a set of load curves which are created through applying the DSM approach for every DSM technique with equal LDI values. This corresponds to potential DSM scenarios in which DSM is applied at different magnitudes. For that, a reference load curve is defined which is based on the same nominal load distribution which has been used in the previous case study. The total yearly heat demand has been set equally to 4.27 E7 J with a peak load of 3.41 MW and a minimum load of 0.35 MW. For this case study, a slightly higher amount of commercial buildings have been used. This was done to create a load curve with a higher base-load demand for integrating an additional heat loss term for the network

The DSM approach has been applied to the reference curve for every DSM technique given 10 distinct values of LDI. The LDI values have been calculated through a logarithmic approach between the value of the reference curve and 1. A higher resolution can also be used, but computational time increases rapidly because the MOO

is applied to every load curve. For a resolution of x, 3*x+1 load curves must be solved.

The results of the DSM modelling and the corresponding load curves is given exemplarily for DSM_{smooth} in Figure 7-15.
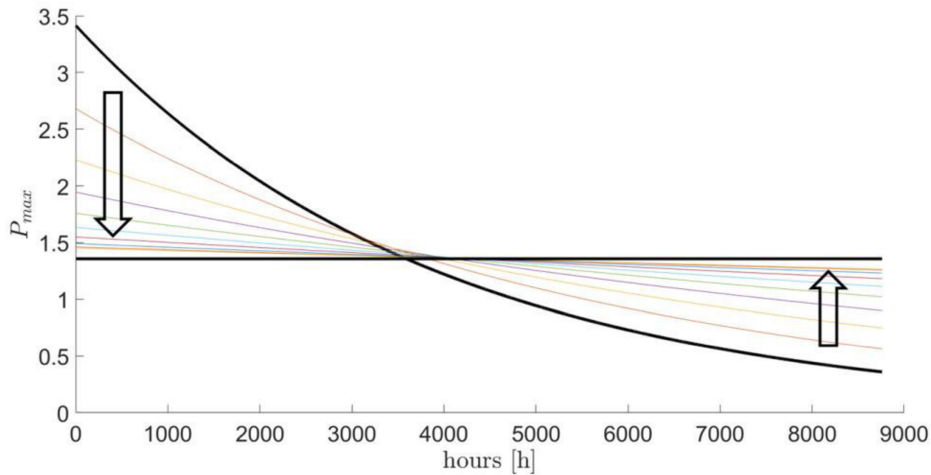

Figure 7-15: Load curves of DSM_{smooth}

The figures for the remaining DSM techniques are given in the Appendix in Figure B1 – Figure B-2. Through applying this DSM, the peak-load is reduced while the minimum load is increases. It can be seen that the load curve gets flatter, the higher this reduction/increase is applied. The total heat supply is not affected by this measure.

For a better overview of the results the numerical results are shown from which the load curves can be constructed, see Table 7-4.

Table 7-4: Numerical results of the load curves

	LDI [-]	P_{max} [MW]			P_{min} [MW]			ϕ [E7 J]		
		DSM_{peak}	DSM_{smooth}	DSM_{base}	DSM_{peak}	DSM_{smooth}	DSM_{base}	DSM_{peak}	DSM_{smooth}	DSM_{base}
Reference scenario	0.719	3.41	3.41	3.41	0.35	0.35	0.35	4.27	4.27	4.27
Scenario 1	0.836	1.71	2.68	3.41	0.35	0.56	0.71	2.73	4.27	5.44
Scenario 2	0.911	1.07	2.23	3.41	0.35	0.74	1.14	2.05	4.27	6.54
Scenario 3	0.953	0.77	1.94	3.41	0.35	0.90	1.58	1.70	4.27	7.51
Scenario 4	0.976	0.61	1.75	3.41	0.35	1.02	1.98	1.50	4.27	8.31
Scenario 5	0.987	0.52	1.63	3.41	0.35	1.11	2.32	1.38	4.27	8.94
Scenario 6	0.993	0.47	1.54	3.41	0.35	1.18	2.60	1.30	4.27	9.43
Scenario 7	0.997	0.43	1.49	3.41	0.35	1.23	2.82	1.24	4.27	9.80
Scenario 8	0.998	0.41	1.46	3.41	0.35	1.25	2.98	1.21	4.27	10.07
Scenario 9	0.999	0.39	1.45	3.41	0.35	1.26	3.10	1.18	4.27	10.27
Scenario 10	1.000	0.35	1.35	3.41	0.35	1.35	3.41	1.13	4.27	10.77

The reference load curve has a LDI of 0.719, while the 10 scenarios correspond to certain magnitudes of DSM. It must be noted, that the calculation of LDI is not reflecting constant increases as for the previous case study. Here, the focus lies on the investigation of the behavior for load curves approaching their ideal stead-state profile. Hence, the LDI was defined for analyzing a broad spectrum of load curves between the reference and the ideal load curve. Scenario 10 corresponds to the load curve in ideal-state, therefor where its profile is steady state.

The definition of equal value of LDI for every DSM technique is crucial for the analysis, since the aim is to provide evidence that load curves with similar LDI also have similar impacts of DHN system design. Therefore, every DSM scenario corresponds to the same LDI for every DSM technique.

Apart from the load curves provided in the Appendix and their corresponding numerical results, the load deviation plot is deployed providing more information upon the behavior of the load parameters with different magnitude of DSM, see Figure 7-16. Hence, the plot provides information of the resulting characteristic load parameters which are obtained through a certain DSM scenario.

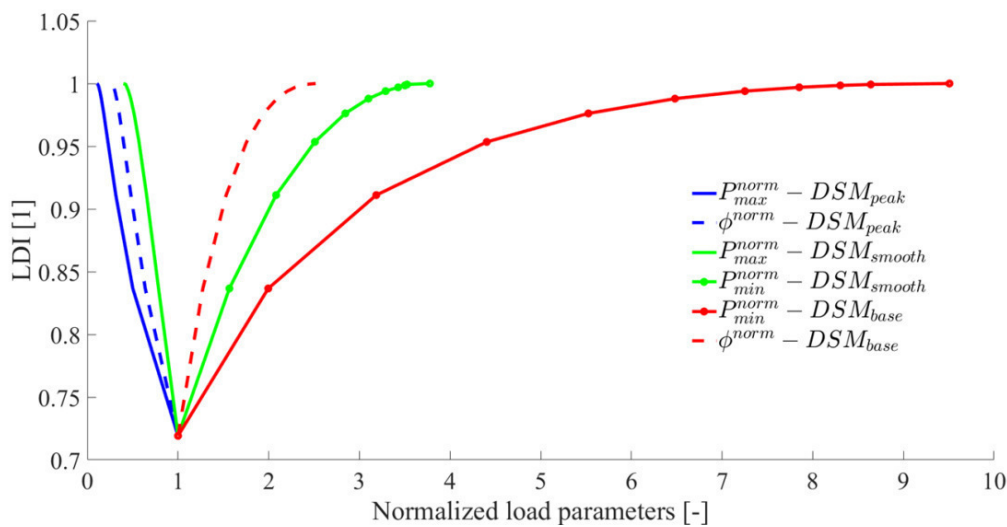

Figure 7-16: Load deviation plot for the given system

This plot is of vital use in combination with the results obtained from the MOO, which will be further detailed in the coming sections. In any case, the load deviation plot offers a compact overview of the behavior of the characteristic load parameters with the implementation of DSM. It furthermore allows deriving the necessary changes of

parameters, when a certain load curve with distinct LDI is to be achieved according to system design.

7.2.3 Performance metric for sustainable assessment

The performance metric is used to evaluate the sustainable design of the given system. Since different DSM techniques are applied to the system, the performance metric must be independent of the actual total annual heat supply. Only then, the results of the DSM scenarios can be compared between the DSM techniques.

To assess technological sustainability, system efficiency η_{sys} is defined according to (7.10), which covers the efficiency of the heat supplied by the heating plant. Unlike in the previous case study, η_{sys} represents the same effects as PER_{sys}, because the transport system is not taken into account. The respective calculation is equal to the previous case study using the heating plant design and partial load model to calculate the heat supplied by the respective heating units.

For the analysis of environmental sustainability, the emergy methodology is used. It was shown in the previous case study, that emergy is a more conservative measure of sustainability than carbon footprint, since it extends its system boundaries to upstream processes and also includes capital investments to sustainability considerations. In order to compare the emergy flow of different DSM scenarios, a specific emery flow is defined as in (7.28),

$$em_{sys} = \frac{Em_{sys}}{\phi} \tag{7.28}$$

where Em_{sys} can be derived from (7.17). This allows calculating a specific emergy flow per unit of heat supplied and can therefore be used to benchmark load curves with different annual heat supply ϕ.

At last, economic sustainability is measured using levelized costs. Levelized costs are the total system costs (capital and operating costs) needed to generate one unit of heat according to (7.29),

$$c_{lev} = \frac{C_{sys}}{\phi} \tag{7.29}$$

where C_{sys} is calculated from the equations previously given in (7.21).

In using this performance metric for sustainability analysis, a three-objective cost function is defined for the multi-objective optimization. This is implemented using the Matlab solver for MOO. A genetic algorithm has been used as the solving technique using the following setup,

Optimize: $f(x)$

Subject to: $x^{low} \leq x \leq x^{up}$

$$g(x) \leq 0$$

$$h(x) = 0$$

where $f(x)$ is the vector containing the objective functions depending on the design vector x, which contains the design variables. Those are constrained between an upper x^{up} and lower x^{low} bound. Using the indicators defined for system optimization, the problem gets:

maximize: $f_{\eta_{sys}}(x) = \eta_{sys}(\alpha, \beta)$

minimize: $f_{em_{sys}}(x) = em_{sys}(\alpha, \beta)$

minimize: $f_{c_{lev}}(x) = c_{lev}(\alpha, \beta)$

Subject to: $\alpha + \beta \leq 2$ and $\begin{bmatrix} \frac{P_{min}}{P_{max}} \\ 0 \end{bmatrix} \leq \begin{bmatrix} \alpha \\ \beta \end{bmatrix} \leq \begin{bmatrix} 1 \\ 1 \end{bmatrix}$

The objective functions depend on the design variables α and β which represent the nominal power design of the biomass unit and the medium-load gas boiler, respectively. For the design variable α a lower bound is set to $\frac{P_{min}}{P_{max}}$ for two reasons. First of all, the biomass unit must at least supply the minimum load P_{min} of the given heat load, due to practical considerations. A design where a gas boiler supplies a certain amount of base-load is unrealistic. Second, the general aim is to increase biomass utilization for heating purposes. Thus, in the case the heat load curve is time-constant, this lower-bound ensures that the biomass unit is deployed as 100 % of the heating load. In this case, no natural gas boilers are used and $\beta = 0$.

The MOO is furthermore applied to all load curves, while the results are presented in the next section.

7.2.4   Results of the MOO for DSM_{smooth}

In this section, the results of the MOO is exemplarily given for the load curves obtained by applying DSM_{smooth}. The numerical values are given in Table 7-4, while the profiles of the load curves are presented in the Appendix. The MOO is applied to all 10 scenarios leading to a set of Pareto solutions for each scenario. In Figure 7-17, the resulting Pareto solutions are presented.
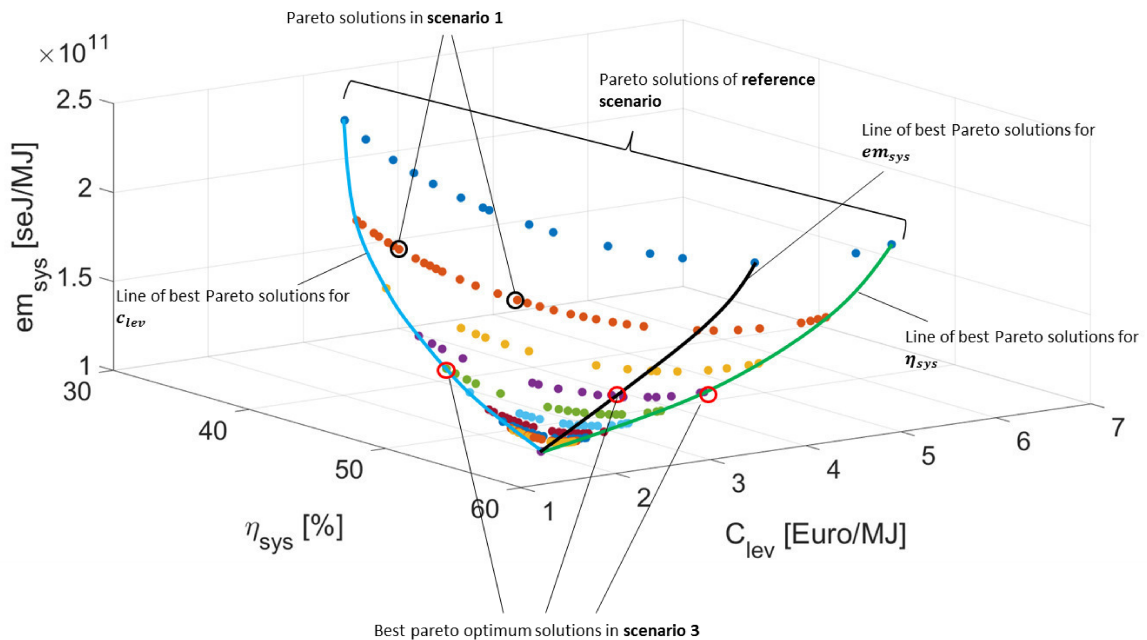
Figure 7-17: Results of the MOO for DSM_{smooth}

The figure shows the results in three-dimensional space for the objective functions, system efficiency η_{sys}, specific emergy flow em_{sys} and levelized costs c_{lev}. For every DSM scenario in DSM_{smooth} and its corresponding load curves, the Pareto frontier is shown through the set of points with equal colours. Those Pareto frontiers indicate the dominating solutions of the system design and are therefore the favorable design states according to the designer's preference.

The a-posteriori application of the MOO allows the system designer to investigate all possible design states without the need of a pre-defined weighting factor. For a certain system design, one Pareto solution must be selected.

This selection can be done using four different strategies:

- Efficiency-focus: Selection of Pareto solution maximizing η_{sys}
- Environmental-focus: Selection of Pareto solution minimizing em_{sys}
- Cost-focus: Selection of Pareto solution minimizing c_{lev}
- Hybrid-strategy using a weighting factor

In the first strategy, a designer might focus only on maximizing efficiency. Thus the Pareto solution with the highest system efficiency would be selected. This is indicated through the red circle on the green line in Figure 7-17. When focusing on environmental sustainability, the solution at minimum specific emergy flow is selected, highlighted by the red circle of the black line. Similarly, this is true for the cost-focus. A hybrid strategy might define a certain weighting factor to select the desired solution. In doing that, certain drawbacks for every objective function are unavoidable.

The green, black and blue lines correspond to the Pareto solutions of every DSM scenario corresponding to the mentioned strategies. The Hybrid strategy is not presented. Those lines follow a certain path and meet in one single point. This point is the Pareto solution for scenario 10 given a steady-state load profile. There, only the biomass unit is operating. Thus the result of the objective functions correspond to a design value of $\alpha = 1$.

Only one solution is possible, which is the biomass unit size of 100 %. At this point, the difference to the nominal efficiency of the boiler is only governed by the heat losses, because the unit is not operating in partial-load. Furthermore, it can be observed, that all objective functions improve towards this ideal point. System efficiency, specific emergy flow and levelized costs are minimum for scenario 10 compared to the others. It must be noted, that a higher efficiency could be achieved if the restriction of the lower boundary of the biomass unit is omitted.

Therefore the flatter the load curve, the higher the optimum Pareto results for system efficiency, specific emergy flow and levelized costs. This is a very important result, since it reflects the improvement of the whole sustainability metric. With an increase of DSM, every objective function improves. It must be noted, that those results are based on the given data set and are only valid for the case study considered. For every system design, the technological and economic data must be carefully examined before the optimization.

7.2.5 The effect of DSM on optimum design

In this section, the possible design improvements associated with the implementation of DSM are investigated in detail. For that the results of the objective functions in Figure 7-17 are normalized to the values of the reference scenario. This allows seeing the improvements of the DSM relative to the reference scenario.

It was shown in Figure 7-17, that, depending on the design strategy applied, the selection of the design state focusing on one objective only, will unavoidably decrease the performance of the others. In Figure 7-18, the normalized results are shown when the efficiency-focus design strategy is applied.
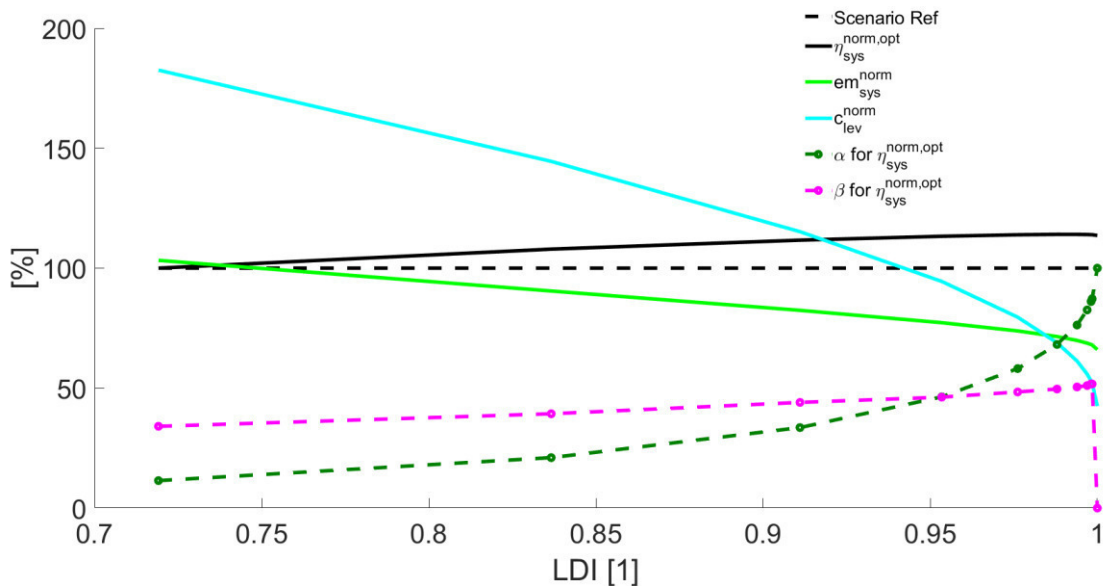

Figure 7-18: Design strategy: Efficiency focus

In this figure, the objective functions and the associated design variables of the optimum solution for system efficiency are drawn with respect to the LDI. In the reference scenario, system efficiency is 100% and is increasing with increasing LDI. This means, given that when the system designer applies an efficiency focus, the optimum solution for system efficiency improves with flatter load curves. This is due to the fact, that flatter load curves allow a higher share of the biomass unit which is reflected in α increasing.

Even though the biomass unit principally suffers from a high partial-load loss of efficiency, this loss is over-compensated by a flatter load curve, which in return allows the unit to operate longer time at nominal load. The profiles for specific emergy and

levelized costs show the associated values of the Pareto solution of those objective functions.

Both specific emergy and levelized costs have higher values in the reference case. This means, the values do not correspond to their best possible solution. It is remarkable, that levelized costs are much higher than the optimum value which can be achieved. With increasing LDI, both specific emergy flow and levelized costs decrease. This has already been seen in Figure 7-17, and is also clearly visible on a normalized basis. This is important information for the system designer. All three objective functions improve with increasing LDI. At high value of LDI > 0.94 the levelized costs are also lower than the optimum value which can be achieved in the reference scenario. This however, demands a high magnitude of DSM.

The corresponding design variables show that the biomass unit size increases with increasing LDI and reaches 100 % for scenario 10. There the peak load is equal to the nominal power of the biomass unit, while the gas boilers are not deployed. This is the reason for $\beta = 0$ at that point. This is a discontinuity and refers to the fact that no lower bound was set for gas boilers, which leads the gas boiler associated with β to slightly increase with higher values of LDI while being equal to 0 in the case $\alpha = 1$.

Similarly, the design selections can be investigated from a pure focus on environmental performance. Since the results are very similar to the efficiency-focus, the figure is provided in the Appendix. There, considering the reference scenario, a focus on the best solutions for specific emergy flow causes a higher levelized cost and slightly lower system efficiency. Similar behavior as for the system efficiency can be seen, with the difference that levelized costs hit the value of the reference scenario at a lower value of LDI < 0.9. At last the results are given for a pure cost-focus in design in Figure 7-19.

In this case, the optimum solution minimizing levelized costs is chosen for every DSM scenario. Specific emergy flow and system efficiency suffer from substantial lower values compared to their optimum values in the reference case. Nevertheless, the objectives improve with increasing LDI. It must be noted that β is always equal to 50 %. This means both gas boilers have the same nominal power, because the economic data is equal for both heating units. In scenario 10, $\beta = 0$.
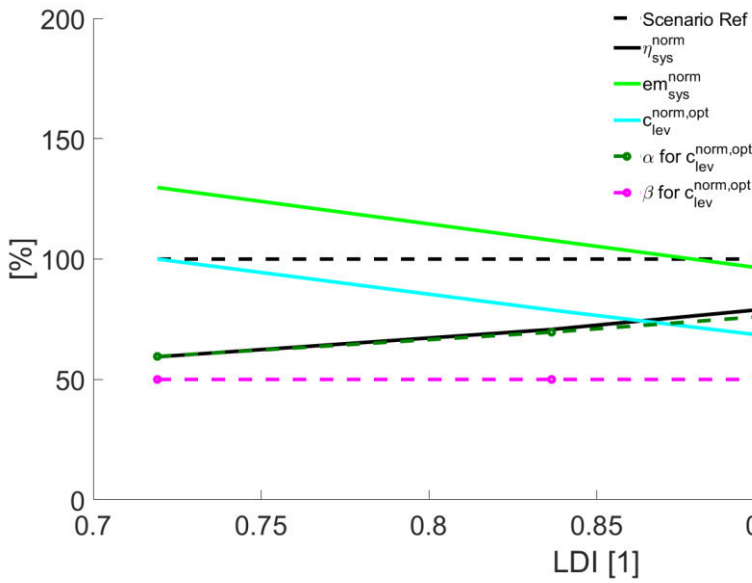
Figure 7-19: Design strategy: Cost focus

At last, Figure 7-20 provides an overview of the optimums designs comparing all three design strategies relative to their reference values.
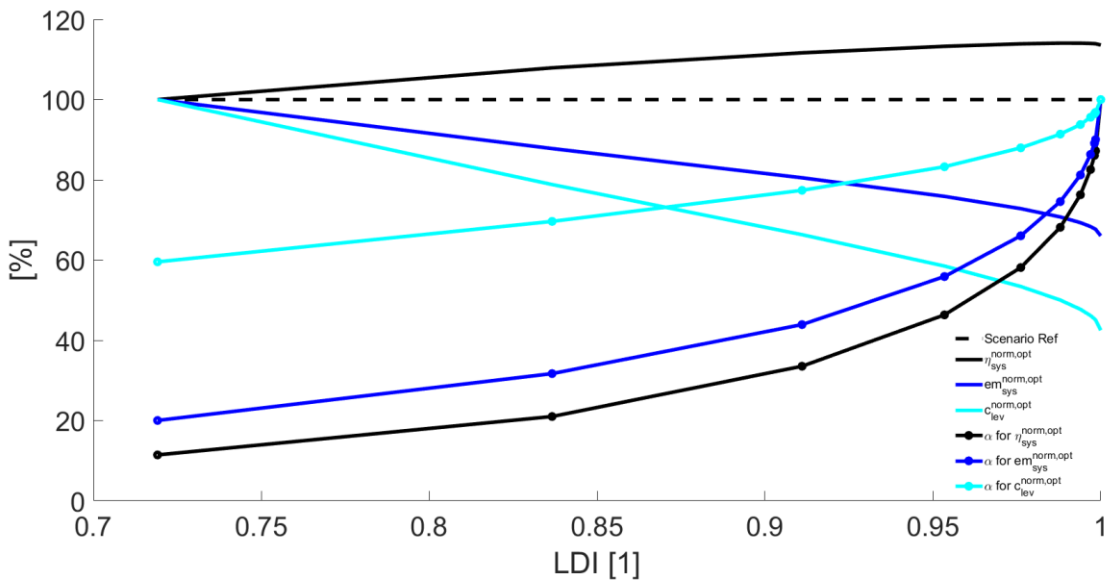
Figure 7-20: Comparison of design strategies for DSM_{smooth}

All three objective functions have normalized value at 100 % at the reference load curve. A focus on system efficiency will allow increasing values with increasing LDI. This implies that the implementation of DSM through decrease of peak-load and increase of base-load offers higher system efficiencies, the higher the magnitude of the measure. Similarly, specific emergy flow decreases with increasing LDI, which allows

a higher environmental performance of the heat produced by the system. The same is true for levelized energy cost. They decrease with higher LDI, because of an increase of the biomass unit which has substantially lower operating costs due to relatively lower price compared to natural gas.

Remarkably, the system design at optimum levelized costs corresponds to a higher value of α compared to the other objectives. One might assume that minimum specific emergy flow shows optimum values with higher values of α. In that assumption, it is neglected that investments costs have high impact on that objective function, and that they are substantially higher for the biomass unit then for the gas units. For the reference scenario, this results in an optimum biomass size of about 20 % for environmental focus and 60 % for the cost focus. The lower value for efficiency focus can be explained through the much lower nominal efficiency and partial-load performance of the biomass unit. Furthermore, it is remarkable that the optimum design point for minimum levelized costs is at about 60 % and corresponds to the same value which is used by common system design in practice. Hence, traditional system design seems to be oriented to minimize costs while the drawbacks in system efficiency or environmental burden are neglected.

Apart from those considerations, Figure 7-20 provides a very important result. All objective functions improve with increasing LDI. Thus, the flatter the load curve, the better the optimum results of the objectives considered. This implies that DSM is a very important measure for sustainability increase and can lead to substantial gains according to the magnitude considered.

This analysis has been carried out for DSM_{smooth} only. In the next step, the MOO results are compared between all three DSM techniques which will allow investigating the possible improvements between different DSM techniques.

7.2.6 Comparison of DSM techniques

In this last section, the results of the optimum Pareto solutions obtained from the MOO are compared for the three different DSM techniques. Figure 7-21 shows the results obtained from the analysis.

The blue curves show the result for levelized costs, the black ones for system efficiency and the green curves correspond to specific emergy.
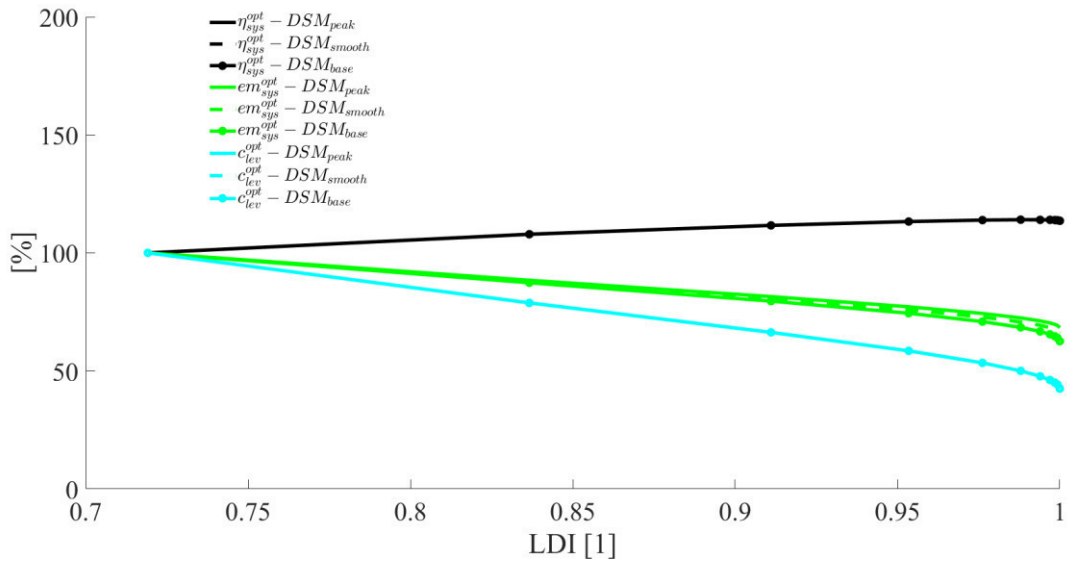
Figure 7-21: Comparison of DSM techniques

All curves have been evaluated for the given design scenarios of Table 7-4 and normalized to the reference scenario. Similar to what was explained before, system efficiency, specific emergy and costs are improving with increasing LDI. This representation highlights the fact that the improvement is almost independent of the DSM technique applied. Given system efficiency, the optimum solution for the load curve in each scenario is equal for every DSM technique.

This means, that the load curves with equal LDI have equal optimum solutions regardless if the load curve has been subject to a certain DSM technique. Similarly this is true for the other objectives with the difference, that at values of LDI close to 1, a certain difference exists. Especially for the specific emergy this difference is clearly visible and it derives from the fact that the value of specific emergy is not equal for the ideal load curves of different DSM techniques. The ideal load curve for DSM_{base} is at a much higher peak-load then DSM_{peak}. Since specific emergy is effected by both system efficiency and the investment costs for the heating plant, the specific emergy is lower for an ideal load curve in DSM_{base} compared to DSM_{peak}, because in the latter case much more heat is produced which lowers the specific emergy to a higher magnitude relative to the increase of the equipment costs.

It must be noted that those results are highly dependent on the actual data set used for the models. This implies a careful examination of data in order to draw correct conclusions. The focus of this study lies in the analysis of the behavior of DSM on the

optimum design of the heating system and clearly shows that, given the data used, the integration of DSM can improve the sustainability of the system given the proposed performance metric.

Furthermore, Figure 7-21 can be used in combination with the load deviation plot in Figure 7-16, to draw conclusions upon the usefulness and the magnitude of DSM implementation. Given the LDI of the reference scenario, a certain improvement of an objective function can directly converted into LDI which can be used to determine the necessary change of minimum and/or maximum load from Figure 7-16. This allows to properly estimating the necessary measures for DSM and their impacts on sustainable system design.

7.3   Closing remarks

The framework for the design of DHN systems using a service-oriented approach provides a thorough methodology for industrial designers, which combines demand side measures and optimum design of heat supply based on the principles of sustainability. This enables system designers to include especially demand side measures into the design phase and enables to assess the feasibility of certain measures according to their impact on sustainable design. Referring to the case study in section 7.1, the framework provides essential improvements for the design selection of small-scale DHN systems. There, the proposed approach for modeling thermal insulation in combination with the multi-criteria analysis offers a more detailed view on the feasibility of substitution of decentralized systems based on fossil fuels, to a centralized solution using renewable energy (biomass) as a fuel. Multi-criteria analysis helps analyzing the impacts of certain sustainability objectives and leaves the system designer with the freedom of choice of a proper selection. The impact of thermal insulation, as a mean of decreasing peak-load, shows essential improvements especially in terms of system efficiency and environmental targets such as emergy and carbon footprint.

Furthermore, detailed insights into the relation between carbon footprint and emergy analysis are provided for different design selections. The definition of the design variable of using nominal power of the heating units enables the analysis of possible improvements from demand side measures, which has not been possible by the previous approach using resource distance as main design criteria. This analysis is car-

ried out for a very specific example of a real-exiting project. Hence, in section 7.2, the framework is applied in a more general way to a generic DHN system.

There, the load deviation index, which is proposed for a characterization of heat load curves, is studied in more detail, especially for their usefulness in DHN design. In using multi-objective optimization, the drawbacks of multi-criteria analysis are overcome and show that the load deviation index is able to characterize load curves in DHN systems according to their contributions of sustainable design. It is found that the flatter the load curve, the better optimum design is possible, which is expressed through a numerical value of the LDI. It can therefore be used to benchmark given load curves as well as scenarios of different magnitudes of demand side measures. In combination with the load deviation plot, which connects the LDI with the characteristic values of the load curve, possible design improvements of DSM can directly be converted into necessary change in the characteristic values according to the DSM technique. This offers to include policy targets as well as environmental targets in a quantitative way and provides the system designer with an a-priori estimation of the impact of DSM onto the objectives under consideration.

Conclusions

In this thesis, advanced methods for improved operation and design of DHN systems under the perspective of sustainability are developed. Several different key research questions are tackled which are associated to different applications of DHN system.

In part A, the focus of investigation is laid upon DHN systems and their future operation as smart thermal networks in integrated energy systems. The key issue addressed is providing a methodology for estimating the value of thermal energy in such networks with regards to the usefulness from a thermodynamic viewpoint. This issue is closely related with the developments of smart thermal networks and 4th-generation DHN as presented. In order to provide such a methodology, thermoeconomics is identified to be most suitable for assessing the thermodynamic value expressed in economic terms. Apart of the current research activities of DHN system, which cover a vast amount of issue related with optimization of supply and generation as well as thermoeconomic analysis on DHN system level, a lack of knowledge is identified for applying thermoeconomics to operation of DHN using modeling- and simulation techniques. Hence, the main contribution of this work lies in the development of a thermoeconomic model which can be applied to a specific modeling approach of DHN systems: graph-based or looped-network models. The benefits of using graph-based approaches where thoroughly described and show that this approach is especially suitable for large networks with any amount of heat production and consumption units and are therefore a suitable model technique for the application of smart thermal networks. Based on a previously deployed graph-based simulation tool, a thermoeconomic model is developed which can be directly integrated and complies with the theory of thermoeconomics.

The usefulness of the thermoeconomic model is studied in two case studies, which are based on a real-exiting large DHN system. Those case studies tackled two main issues related with large DHN systems: The problem of black-box costing and the influence of decentralized thermal generation with an example from waste heat integration. Regarding the first application, it is found that black-box costing, as applied in today's industrial system, has massive drawbacks when applied to such systems.

This derives mainly from the lack of information on dynamic conditions of the network and leads to a wrong allocation of costs. The individual contributions of the consumer (substations) losses cannot be correctly evaluated and make it impossible to determine the true reasons of inefficiencies. The results of the thermoeconomic model do not only provide information on those individual contributions and offer the possibility for a benchmark of different heat consumers but also allow identifying the magnitude of error through black-box allocation of costs. In the industrial context, the results of the thermoeconomic model are useful information for a set of measures:

- The development of new business models in cases where DHN systems operate as thermal markets with third-party access (especially of renewables) and distributed generation
- The assessment of feasibility of waste heat integration depending on the characteristics profiles of excess heat of industrial plants
- Identification of "critical" consumer, which have high influence on network inefficiencies, such as thermal losses and cause peak loads
- Suitability of temperature reduction in the network depending on the specific need of consumers
- A-priori estimation of the impact of new consumer (or new districts) on the cost generation of the network
- Possibility for dynamic pricing or semi-dynamic pricing using common heat profiles

Apart from developments towards improvement of DHN operation in large application, a need for an improved methodology to include cross-cutting approaches such as demand side measures and sustainability improvements into DHN design is identified. This is especially true for small-scale DHN systems, which are not suitable for operation as smart thermal networks due to several reasons. Key research questions are extracted which include a more business-focused design of DHN systems which is able to include policy- and environmental targets. The use of biomass as a renewable energy source and the application of demand side measures are identified to help achieving these goals.

Based on that, a framework for sustainable design of small-scale DHN systems, especially suitable for industrial designers aiming for new business models, is devel-

oped. There, both a formulation of a service-oriented DHN system design as well as advanced methods which provide additional information during the design method are developed. A new indicator called load deviation index is proposed to link possible improvements from demand side measures to system design.

The framework is applied to two case studies. Those case studies use different elements of the design approach for different research questions. In the first, a real-existing DHN system is analyzed using the service-oriented system model to answer questions on optimum sizing of the heating plant with various scenarios of thermal insulation. The outcomes clearly indicate the necessity of multi-criteria analysis and the definition of proper design variables and show that sustainable design might lead to different design selection according to the designer's strategy. Furthermore the multi-criteria methodology is used to give additional information on the behavior of different design choices including different environmental assessment methods. Through that, the relation between different sustainability objectives can be interrelated and compared.

The second case study is used to apply the framework to a generic DHN system in order to study the newly proposed load deviation index. Throughout the application using a multi-objective optimization for a given sustainability metric, improvements of DHN system design correlate with the load deviation index. Since the latter is a quantitative measure of the deviation of a certain load curve to its ideal profile, it can therefore be used to characterize load curves a-priori according to the impact of different DSM scenarios. Furthermore, the LDI is used in combination with the load deviation plot to directly relate the improvements related with increasing DSM measures and provides the system designer with a quantitative tool to assess its feasibility. As a summary the following advancements can be deduced:

- Service oriented DHN system offers the possibility to include both supply-based and demand-based measures in design
- Interrelation of carbon footprint and emergy analysis was studied using a realistic design model for a biomass-based small-scale DHN system
- Load deviation index characterizes DSM measures on the load profile of DHN consumers and enable the deduction of possible sustainability improvements or policy targets
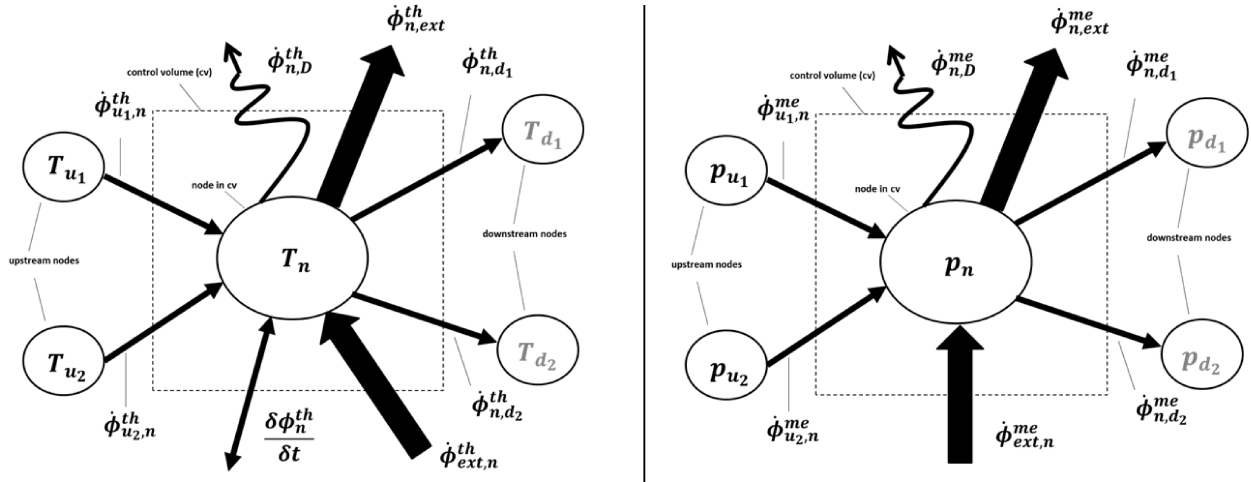
Appendix A

Figure A-1: Cv for thermal (left) and mechanical (right) energy

$$\sum_i \dot{\phi}_{u_i,n}^{th} + \dot{\phi}_{ext,n}^{th} - \sum_j \dot{\phi}_{n,d_j}^{th} - \dot{\phi}_{n,ext}^{th} - \frac{\delta\phi_n^{th}}{\delta t} - \dot{\phi}_{n,D}^{th} = 0 \qquad (A.1)$$

$$\dot{\phi}_{u,n}^{th} = \dot{m}_{u,n} \cdot cp(T_u - T_{ref}) \qquad (A.2)$$

$$\frac{\Delta\phi_n^{th}}{\Delta t} = M_n \cdot cp\left(\frac{T_n^t - T_n^{t-1}}{t}\right) \qquad (A.3)$$

$$\sum_i \dot{\phi}_{u_i,n}^{me} + \dot{\phi}_{ext,n}^{me} - \sum_j \dot{\phi}_{n,d_j}^{me} - \dot{\phi}_{n,ext}^{me} - \dot{\phi}_{n,D}^{me} = 0 \qquad (A.4)$$

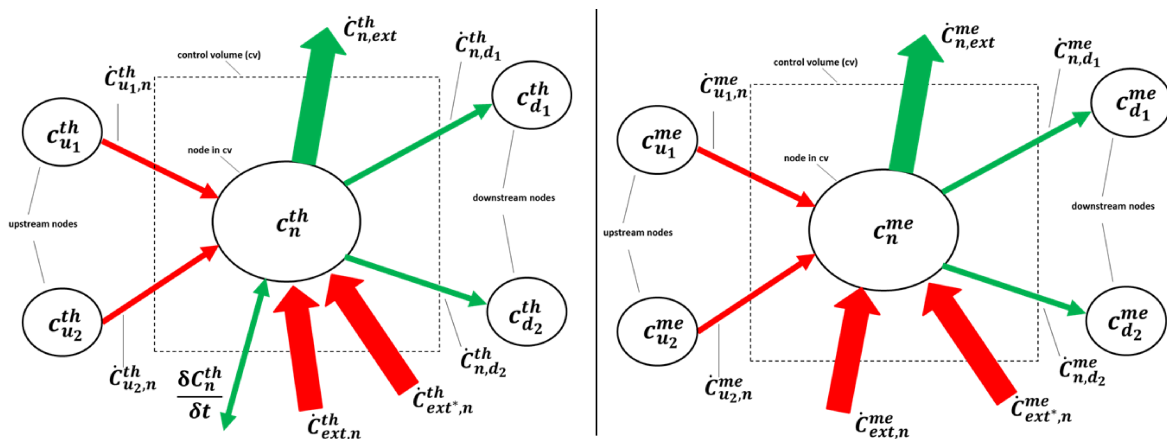$$\dot{\phi}_{u,n}^{me} = \dot{m}_{u,n}\left[\frac{p_u - p_{ref}}{\rho}\right] \qquad (A.5)$$

Figure A-2: Cv for thermal (left) and mechanical (right) energy costing

$$\sum_i \dot{\phi}_{u_i,n}^{th} \cdot c_{u_i}^{th} + \dot{C}_{ext,n}^{th} + \dot{C}_{ext^*,n}^{th} - c_n^{th}\left(\sum_j \dot{\phi}_{n,d_j}^{th} + \dot{\phi}_{n,ext}^{th} + \frac{\delta\phi_n^{th}}{\delta t}\right) = 0 \quad \text{(A.6)}$$

$$\sum_i \dot{\phi}_{u_i,n}^{me} \cdot c_{u_i}^{me} + \dot{C}_{ext,n}^{me} + \dot{C}_{ext^*,n}^{me} - c_n^{me}\left(\sum_j \dot{\phi}_{n,d_j}^{me} + \dot{\phi}_{n,ext}^{me}\right) = 0 \quad \text{(A.7)}$$
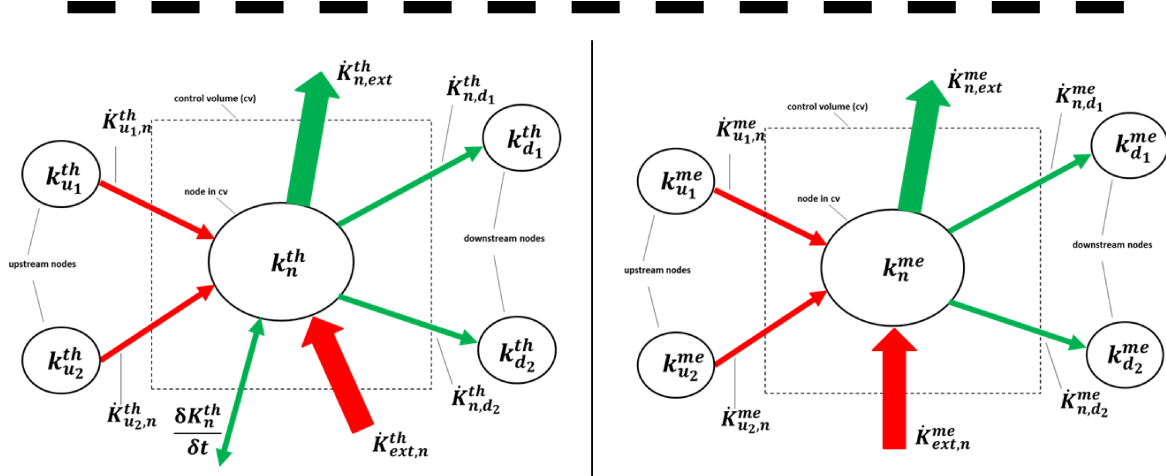

Figure A-3: Cv for thermal (left) and mechanical (right) exergy costing

$$\sum_i \dot{\psi}_{u_i,n}^{th} \cdot k_{u_i}^{th} + \dot{K}_{ext,n}^{th} - k_n^{th}\left(\sum_j \dot{\psi}_{n,d_j}^{th} + \dot{\psi}_{n,ext}^{th} + \frac{\delta\psi_n^{th}}{\delta t}\right) = 0 \quad \text{(A.8)}$$

$$\sum_i \dot{\psi}_{u_i,n}^{me} \cdot k_{u_i}^{me} + \dot{K}_{ext,n}^{me} - k_n^{me}\left(\sum_j \dot{\psi}_{n,d_j}^{me} + \dot{\psi}_{n,ext}^{me}\right) = 0 \quad \text{(A.9)}$$

$$\dot{\boldsymbol{\phi}}^{th,me} = \begin{bmatrix} \left|\dot{\phi}_{b_1}^{th,me}\right| \\ \left|\dot{\phi}_{b_2}^{th,me}\right| \\ ... \\ \left|\dot{\phi}_{b}^{th,me}\right| \end{bmatrix} \quad \text{(A.10)} \qquad \frac{\delta\boldsymbol{\phi}^{th}}{\delta t} = \frac{\delta}{\delta t}\begin{bmatrix} \left|\phi_{n_1}^{th}\right| \\ \left|\phi_{n_2}^{th}\right| \\ ... \\ \left|\phi_n^{th}\right| \end{bmatrix} \quad \text{(A.11)}$$

$$\dot{\boldsymbol{\phi}}_{extOut}^{th,me} = \begin{bmatrix} \left|\dot{\phi}_{n_1,ext}^{th,me}\right| \\ \left|\dot{\phi}_{n_2,ext}^{th,me}\right| \\ ... \\ \left|\dot{\phi}_{n,ext}^{th,me}\right| \end{bmatrix} \quad \text{(A.12)} \qquad \dot{\boldsymbol{C}}_{extIn}^{th,me} = \begin{bmatrix} \left|\dot{C}_{ext,n_1}^{th,me}\right| \\ \left|\dot{C}_{ext,n_2}^{th,me}\right| \\ ... \\ \left|\dot{C}_{ext,n}^{th,me}\right| \end{bmatrix} \quad \text{(A.13)}$$

$$\boldsymbol{c}^{th,me} = \begin{bmatrix} \left|c_{n_1}^{th,me}\right| \\ \left|c_{n_2}^{th,me}\right| \\ ... \\ \left|c_n^{th,me}\right| \end{bmatrix} \quad \text{(A.14)}$$

$$\left\{ \left[A \times I\dot{\phi}^{th} \times [A^+]^T \right] + I \left[\dot{\phi}^{th}_{extOut} - \frac{\delta\phi^{th}}{\delta t} \right] \right\} c^{th} = \dot{C}^{th}_{extIn} \tag{A.15}$$

$$\left\{ \left[A \times I\dot{\phi}^{me} \times [A^+]^T \right] + I\dot{\phi}^{me}_{extOut} \right\} c^{me} = \dot{C}^{me}_{extIn} \tag{A.16}$$

$$\dot{\psi}^{th,me} = \begin{bmatrix} |\dot{\psi}^{th,me}_{b_1}| \\ |\dot{\psi}^{th,me}_{b_2}| \\ \dots \\ |\dot{\psi}^{th,me}_{b}| \end{bmatrix} \tag{A.17}$$

$$\frac{\delta\psi^{th}}{\delta t} = \frac{\delta}{\delta t} \begin{bmatrix} |\psi^{th}_{n_1}| \\ |\psi^{th}_{n_2}| \\ \dots \\ |\psi^{th}_{n}| \end{bmatrix} \tag{A.18}$$

$$\dot{\psi}^{th,me}_{extOut} = \begin{bmatrix} |\dot{\psi}^{th,me}_{n_1,ext}| \\ |\dot{\psi}^{th,me}_{n_2,ext}| \\ \dots \\ |\dot{\psi}^{th,me}_{n,ext}| \end{bmatrix} \tag{A.19}$$

$$\dot{K}^{th,me}_{extIn} = \begin{bmatrix} |\dot{K}^{th,me}_{ext,n_1}| \\ |\dot{K}^{th,me}_{ext,n_2}| \\ \dots \\ |\dot{K}^{th,me}_{ext,n}| \end{bmatrix} \tag{A.20}$$

$$k^{th,me} = \begin{bmatrix} |k^{th,me}_{n_1}| \\ |k^{th,me}_{n_2}| \\ \dots \\ |k^{th,me}_{n}| \end{bmatrix} \tag{A.21}$$

$$\left\{ \left[A \times I\dot{\psi}^{th} \times [A^+]^T \right] + I \left[\dot{\psi}^{th}_{extOut} - \frac{\delta\psi^{th}}{\delta t} \right] \right\} k^{th} = \dot{K}^{th}_{extIn} \tag{A.22}$$

$$\left\{ \left[A \times I\dot{\psi}^{me} \times [A^+]^T \right] + I\dot{\psi}^{me}_{extOut} \right\} k^{me} = \dot{K}^{me}_{extIn} \tag{A.23}$$

Appendix B

Table B-1: Data of the case studies in part B

Definition	Item	Unit	Amount	Ref.
Lower heating value bio-mass	LHV_W	[MJ/kg]	12.34	(Saidur et.al. 2011)
Lower heating value natu-ral gas	LHV_{NG}	[MJ/kg]	43.98	Based on project data
Lower heating value diesel	LHV_{Di}	[MJ/kg]	38.00	(Yao et al., 2010)
Ash content of wood	f_A	[%]	20.00	(Jamali-Zghal et.al. 2013)
Fuel consumption bio-mass-truck	$e_{T,W}$	[MJ/km]	11.61	(Shunping et.al. 2010)
Fuel consumption ash-truck	$e_{T,A}$	[MJ/km]	8.83	(Shunping et.al. 2010)
Fuel consumption car	$e_{T,Emp}$	[MJ/km]	3.36	(Shunping et.al. 2010)
Maximum capacity wood-truck	Cap_W	[kg]	15,000	(Shunping et.al. 2010)
Maximum capacity ash-truck	Cap_A	[kg]	7000	(Shunping et.al. 2010)
Loading factor wood-truck	lf_W	[−]	0.75	(Jamali-Zghal et.al. 2013)
Loading factor ash-truck	lf_A	[−]	0.75	(Jamali-Zghal et.al. 2013)
Transport distance wood	d_W	[km]	990	(Jamali-Zghal et.al. 2013)
Transport distance ash	d_A	[km]	50	(Jamali-Zghal et.al. 2013)
Transport distance em-ployees	d_{Emp}	[km]	13,200	(Jamali-Zghal et.al. 2013)
Investment costs of bio-mass plant at nominal power	C_B	[M€]	3.5	Based on project data
Investment costs of gas plant 1 at nominal power	C_{G1}	[M€]	3.0	Based on project data
Investment costs of gas plant 2 at nominal power	C_{G2}	[M€]	3.0	Based on project data
Fuel price wood	c_W	[€/kg]	0.01	Based on project data
Fuel price natural gas	c_{NG}	[€/kg]	0.05	Based on project data
Fuel price diesel	c_{Di}	[€/kg]	0.14	Based on project data
Specific thermal insulation cost	c_{TI}	[€/MJ]	0.23	Based on project data
Specific upstream carbon emissions wood	$ce_{W,up}$	[kgCO2/unit]	0.04	(Jamali-Zghal et.al. 2013)

Specific upstream carbon emissions natural gas	$ce_{NG,up}$	[kgCO2/ unit]	0.38	(Jamali-Zghal et.al. 2013)
Specific upstream carbon emissions diesel	$ce_{Di,up}$	[kgCO2/unit]	0.35	(Jamali-Zghal et.al. 2013)
Specific utilization carbon emissions wood	$ce_{W,util}$	[kgCO2/ unit]	0	(Jamali-Zghal et.al. 2013)
Specific utilization carbon emissions natural gas	$ce_{NG,util}$	[kgCO2/ unit]	1.9	(Jamali-Zghal et.al. 2013)
Specific utilization carbon emissions diesel	$ce_{Di,util}$	[kgCO2/ unit]	3.22	(Jamali-Zghal et.al. 2013)
Upstream solar transformity wood	$sT_{W,up}$	[seJ/unit]	5.62 E4	(Odum 1996)
Upstream solar transformity natural gas	$sT_{NG,up}$	[seJ/unit]	7.73 E4	(Odum 1996)
Upstream solar transformity diesel	$sT_{Di,up}$	[seJ/unit]	1.07 E5	(Odum et.al. 2000)
Utilization solar transformity wood	$sT_{W,util}$	[seJ/unit]	0.00	Assumed
Utilization solar transformity natural gas	$sT_{NG,util}$	[seJ/unit]	1.74 E4	(Romitelli 1999)
Utilization solar transformity diesel	$sT_{Di,util}$	[seJ/unit]	0.00	(Odum 1996)
Solar transformity capital	$sT_{cap,up+util}$	[seJ/unit]	1.2 E12	(Jamali-Zghal et.al. 2013)
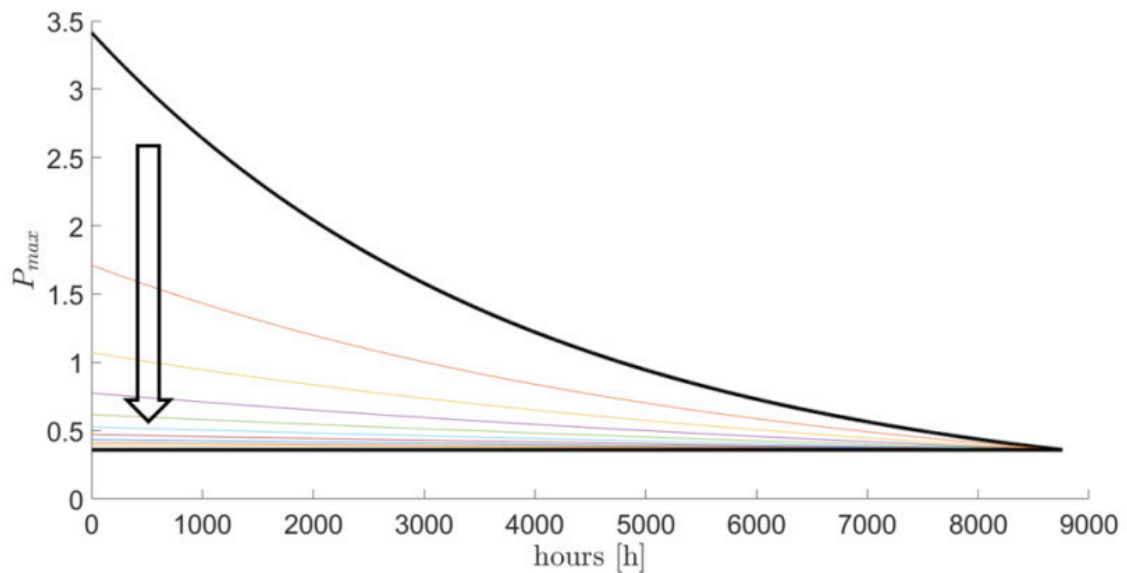
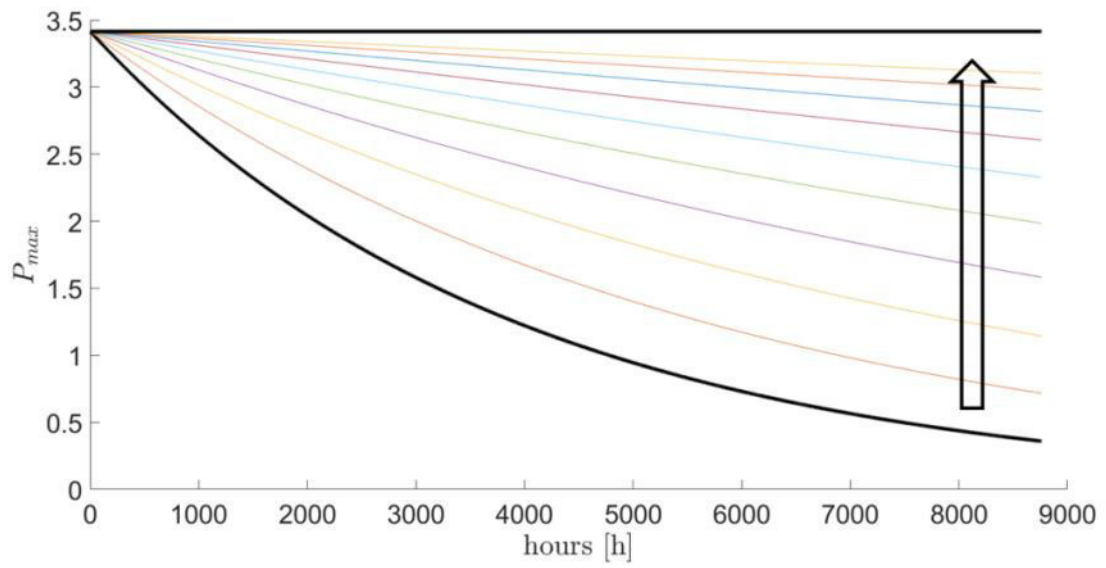Figure B-1: Load curves of DSM_{peak}
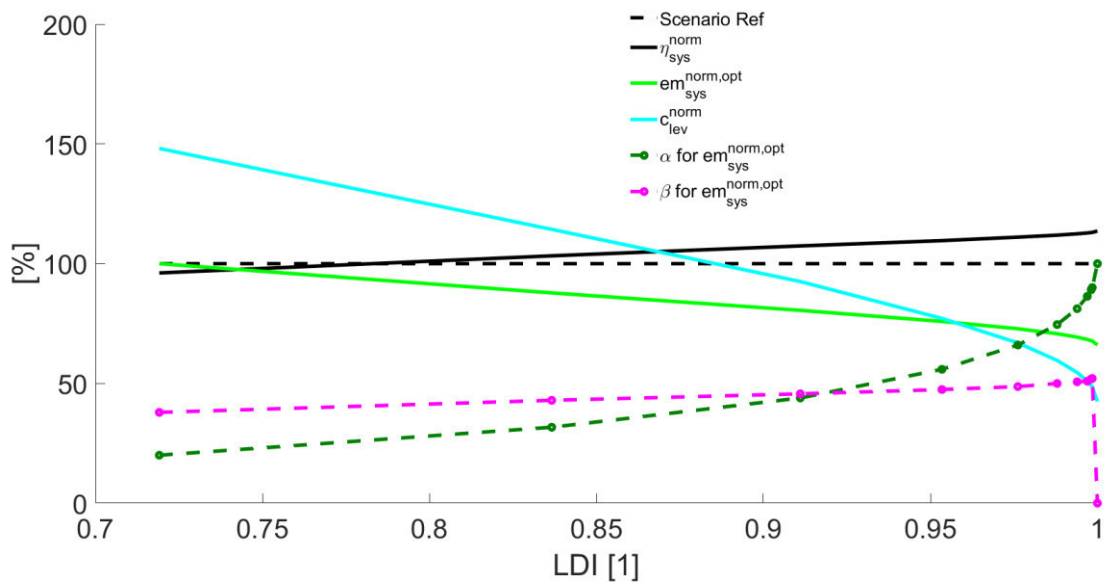
Figure B-2: Load curves of DSM_{base}

Figure B-3: Design strategy: Environmental focus

Bibliography

Afgan N.H., Carvalho M.G. (2002): Multi-criteria assessment of new and renewable energy power plants. Journal of Energy, 27, 739-755

Al-Mansour F., Zuwala J., (2010): An evaluation of biomass co-firing in Europe. Biomass Bioenergy 34 (5), 620-629

Andric I., Jamali-Zghal N., Santarelli M., Lacarriere B., Le-Corre O. (2014): Environmental performance assessment of retrofitting existing coal fired power plants to co-firing with biomass: carbon footprint and emergy approach. Journal of Cleaner Production 1-15

Andric I., Gomes N., Pina A., Ferrao P., Fournier J., Lacarriere B., Le Corre O. (2016): Modeling the long-term effect of climate change on building heat demand: Case study on a district level. Energy and Buildings, 126, 77-93

Apajalahti E.L., Lovio R., Heiskanen E. (2015): From demand side management (DSM) to energy efficiency services: a Finnish case study. Journal of Energy Policy 81, 76-85

Ayres R.U., Warr B. (2009): The Economic Growth Engine. How Energy and Work Drive Material Prosperity. Edward Elgar Publishing Limited, ISBN 978-1-84844-182-8

Baehr H.D. & Kabelac S. (2009): Thermodynamik: Grundlagen und technische Anwendungen. 13th edition Springer. ISBN-13 978-3-540-32513-0

Baldvinsson I., Nakata T. (2014): A comparative exergy and exergoeconomic analysis of a residential heat supply system paradigm of Japan and local source based district heating system using SPECO (specific exergy cost) method. Journal of Energy, 74, 537-554

Baldvinsson I., Nakata T. (2016). A feasibility and performance assessment of a low temperature district heating system – A North Japanese case study. Journal of Energy, 95, 155-174

Beccali M., Cellura M., Mistretta M. (2003): Decision-making in energy planning. Application of the Electre method at regional level for the diffusion of renewable energy technology. Journal of Renewable Energy, 28, 2063-2087

Begic F., Afgan N.H. (2007): Sustainability assessment tool for the decision making in selection of energy system-Bosnian case. Journal of Energy, 32, 1979-1985

Bejan A., Kraus A.D. (2003): Heat Transfer Handbook. Wiley ISBN 0-471-39015-1

Bendig M., Marechal F., Favrat D. (2013): Defining waste heat for industrial processes. Journal of Applied Thermal Engineering, 61(1), 134-142

Bithas K., Kalimeris P. (2013): Re-estimating the decoupling effect: is there an actual transition towards a less energy-intensive economy? Journal of Energy 51, 78-84

BMU (2012) Langfristszenarien und Strategien für den Ausbau der erneuerbaren Energien in Deutschland bei Berücksichtigung der Entwicklung in Europa und Global. Schlussbericht BMU, FKZ 03MAP146.

Brown L., (2003): Plan B: Rescuing a Planet under Stress and a Civilization in Trouble.W. W. Norton and Company, New York. ISBN 978-0393325232

Brown M.T., Ulgiati S. (1997): Emergy-based indices and ratios to evaluate sustainability: monitoring economies and technology toward environmentally sound innovation. Journal of Ecological Engineering, 9, 51-69

Brown M.T., Ulgiati S. (2004): Energy quality, emergy, and transformity: H.T. Odum's contributions to quantifying and understanding systems. Journal of Ecological Modeling, 178, 201-213

Buehler F., Petrovic S., Karlsson K., Elmegaard B. (2017): Industrial excess heat for district heating in Denmark. Journal of Applied Energy, 205, 991-1001

Capon-Garcia E., Papadokonstantakis S., Hungerbuehler K. (2014): Multi-objective optimization of industrial waste management in chemical sites coupled with heat integration issues. Computational Chemical Engineering, 62, 21-36

Chapagain K., Hoekstra Y. (2004): Water footprint of nations. Volume 1: main report. Value Water. Unesco-IHE

Carpaneto E., Lazzeroni P., Repetto M. (2015): Optimal integration of solar energy in a district heating network. Journal of Renewable Energy, 75, 714-721

Comakli K., Yueksel B., Comakli OE. (2004): Evaluation of energy and exergy losses in district heating network. Journal of Applied Thermal Engineering, 24(7), 1009-1017

Coss S. (2013): Bewertung der Flexibilitaet netzgebundener Kraft-Waerme-Kopplung. Akademikerverlag, Saarbrücken, ISBN 978-3-639-47594-4

Cowie A.L., Gardner D.W. (2007): Competition for the biomass resource greenhouse impacts and implications for renewable energy incentive schemes. Biomass Bioenergy 31, 601-607

Cui L.B., Peng P., Zhu L. (2015): Embodied energy, export policy adjustment and China's sustainable development: a multi-regional input-output analysis. Journal of Energy, 82, 457-467

Danestig M. (2009): Efficient Heat Supply and Use from an Energy-system and Climate Perspective. Dissertation Linkoping Institute of Technology Sweden, ISBN 978-91-7393-694-1

Di Somma M., Yan B., Bianco N., Graditi G., Luh P.B., Mongibello, L. Naso V. (2015): Operation optimization of a distributed energy system considering energy costs and exergy efficiency. Energy Conversion and Management, 103, 739-751

Dinca C., Badea A., Rousseaux P., Apostol T., (2007) : A multi-criteria approach to evaluate the natural gas energy systems. Journal of Energy Policy, 35, 5754-5765

Dirks J.A., Gorrissen W.J., Hathaway J.H., Skorski D.C., Scott M.J., Pulsipher T.C., Rice J.S. (2015): Impacts of climate change on energy consumption and peak demand in buildings: A detailed regional approach. Journal of Energy, 79, 20-32

Diwekar U. (2005): Green process design, industrial ecology, and sustainability: a systems analysis perspective. Resource Conservation Recycling 44 (3 SPEC. ISS.), 215-235

Edrisi S.A., Abhilash P.C. (2015): Sustainable bioenergy production from woody biomass: prospects and promises. Journal of Cleaner Production 102, 558-559

EIA - Energy Information Agency (2013): International Energy Outlook 2013. Available at: http://www.eia.gov/forecasts/ieo/pdf/0484(2013).pdf.

El Sayed Y.M. (2003): The Thermoeconomics of Energy Conversions. Elsevier.

Esen H., Inalli M., Esen M. (2007): A techno-economic comparison of ground-coupled and air-coupled heat pump system for space cooling. Building and Environment, 42, 1955-1965

European Parliament (2009): Directive 2009/28/EC of the European Parliament and of the council of 23 April 2009 on renewable energy. Office Journal of the European Union directive

European Parliament (2012): Directive 2012/27/EU of the European Parliament and of the Council of 25 October 2012 on Energy Efficiency, pp. 1-56. Official Journal of the European Union Directive

Frangopoulos C., Keramioti D.E. (2010): Multi-Criteria evaluation of energy systems with sustainability considerations. Journal of Entropy, 12 (5), 1006-1020

Gabillet P. (2015): Energy supply and urban planning projects: Analyzing tensions around district heating provision in a French eco-district. Journal of Energy Policy, 78, 189-197

Gadd H. (2012). To Measure Is To Know. Lund University ISSN 0282-1990

Gadd H., Werner S. (2013): Daily heat load variations in Swedish district heating systems. Journal of Applied Energy, 106, 47-55

Gallopin G., Herrero L.M.J., Rocuts A. (2014): Conceptual frameworks and visual interpretations of sustainability. Journal of Sustainable Development, 17 (3), 298-326

Gerber L., Fazlollahi S., Marechal F. (2013): A systematic methodology for the environomic design and synthesis of energy systems combining process integration, Life Cycle Assessment and Industrial Ecology. Journal of Computational Chemical Engineering 59, 2-16

Gładys P., Ziebik A. (2013): Complex analysis of the optimal coefficient of the share of cogeneration in district heating systems. Journal of Energy, 62, 12-22

Graedel T.E., Allenby B.R. (2002): Hierarchical metrics for sustainability. Environmental and Quality Management, 12, 21-30

Guelpa E. (2016): Modeling strategies for multiple scenarios and fast simulations in large systems: applications to fire safety and energy engineering. Politecnico di Torino. PhD thesis

Guelpa E., Sciacovelli A., Verda V. (2017a): Thermo-fluid dynamic model of large district heating networks for the analysis of primary energy savings. Journal of Energy, 1-11

Guelpa E., Barbero G., Sciacovelli A., Verda, V. (2017b): Peak-shaving in district heating systems through optimal management of the thermal request of buildings. Journal of Energy, 137, 706-714

Hau J.L., Bakshi B.R. (2004): Expanding exergy analysis to account for ecosystem products and services. Environment Science and Technology, 38 (13), 3768-3777

Hendricks A.M., Wagner J.E., Volk T.A., Newman D.H., Brown T.R. (2016): A cost-effective evaluation of biomass district heating in rural communities. Journal of Applied Energy, 162, 561-569

Herendeen R. (2004): Energy analysis and Emergy analysis - a comparison. Journal of Ecological Modeling, 178, 227-237

Horizon 2020 Available at http://ec.europa.eu/europe2020/europe-2020-in-anutshell/targets/index_en.htm (Accessed: 27 July 2015).

Hoyt E. (2003): The challenge of sustainability. Grassroots Dev. 24, 46-51

Iddrisu I., Bhattacharyya S.C. (2015): Sustainable Energy Development Index: a multi-dimensional indicator for measuring sustainable energy development. Renewable Sustainable Energy Reviews 50, 513-530

Jamali-Zghal N., Amponsah N.Y., Lacarriere B., Le-Corre O., Feidt M. (2013) : Carbon footprint and emergy combination for eco-environmental assessment of cleaner heat production. Journal of Cleaner Production 47, 446-456

Jiang X.Z., Zheng D., Mi Y. (2015): Carbon footprint analysis of a combined cooling heating and power system. Energy Conversion and Management, 103, 36-42

Johansson C., Wernstedt F., Box P.O. (2010): Heat load reductions and their effect on energy consumption. The 12th International Symposium on District Heating and Cooling

Kaerkkainen S., Sipilae K., Pirvola L., Esterinen J., Eriksson E., Soikkeli S., Nuutinen M., Aarnio H., Schmitt F., Eisgruber C. (2004): Demand side management of the district heating systems. VTT Research Notes 2247 ISBN 951–38–6472–3

Kauko H., Kvalsvik K.H., Rohde D., Hafner A., Nord N. (2017): Dynamic modelling of local low-temperature heating grids: A case study for Norway. Journal of Energy, 139, 289-297

Kecebas A. (2011): Performance and thermo-economic assessments of geothermal district heating system: A case study in Afyon, Turkey. Journal of Renewable Energy, 36(1), 77-83

Keebas A., Alkan A.M., Bayhan M. (2011): Thermo-economic analysis of pipe insulation for district heating piping systems. Journal of Applied Thermal Engineering, 31(17-18), 3929-3937

Kharrazi A., Kraines S., Hoang L., Yarime M. (2014): Advancing quantification methods of sustainability: a critical examination emergy, exergy, ecological footprint, and ecological information-based approaches. Journal of Ecological Indicators 37, 81-89

Koroneos C.J., Nanaki E.A., Xydis G.A. (2012): Sustainability indicators for the use of resources-the exergy approach. Journal of Sustainability 4 (8), 1867-1878

Kotas T.J. (1995): The exergy method of thermal plant analysis. Reprinted edition. Krieger Publishing Company ISBN 0-89464-941-8

Laajalehto, T., Kuosa, M., Mäkilä, T., Lampinen, M., & Lahdelma, R. (2014). Energy efficiency improvements utilising mass flow control and a ring topology in a district heating network. Journal of Applied Thermal Engineering, 69, 86-95

Lazzaretto A., Toffolo A. (2004): Energy, economy and environment as objectives in multi-criterion optimization of thermal systems design. Journal of Energy, 29, 1139-1157

Leduc S., Wetterlund E., Dotzauer E., Kindermann G. (2012): CHP or biofuel production in Europe? Energy Procedia. 20, 40-49

Li H., Sun Q., Zhang Q., Wallin F. (2015): A review of the pricing mechanisms for district heating systems. Renewable and Sustainable Energy Reviews, 42, 56-65

Li H. Wang S.J. (2015): Load Management in District Heating Operation. Energy Procedia, 75, 1202-1207

Li Y., Rezgui Y., Zhu H. (2017): District heating and cooling optimization and enhancement – Towards integration of renewables, storage and smart grid. Renewable and Sustainable Energy Reviews, 72, 281-294

Loken E., Botterud A., Holen A.T. (2009): Use of the equivalent attribute technique in multi-criteria planning of local energy systems. Journal of Operations Research, 197, 1075-1083

Lozano M.A., Valero A. (1993): Theory of exergetic cost. Journal of Energy, 18(9), 939-960

Lundstroem L., Wallin F. (2016): Heat demand profiles of energy conservation measures in buildings and their impact on a district heating system. Journal of Applied Energy 161, 290-299

Lund H., Moeller B., Mathiesen B.V., Dyrelund A. (2010): The role of district heating in future renewable energy systems. Journal of Energy, 35(3), 1381-1390

Lund H., Werner S., Wiltshire R., Svendsen S., Thorsen J.E., Hvelplund F., Mathiesen B.V. (2014): 4th Generation District Heating (4GDH). Integrating smart thermal grids into future sustainable energy systems. Journal of Energy, 68, 1-11

Lund R., Ostergaard D.S., Yang X., Mathiesen B.V. (2017): Comparison of Low-temperature District Heating Concepts in a Long-Term Energy System Perspective. Journal of Sustainable Energy Planning and Management, 12(0), 5-18

Lund P.D. (2009): Effects of energy policies on industry expansion in renewable energy. Journal of Renewable Energy 34 (1), 53-64

Mallikarjun S., Lewis H.F. (2014): Energy technology allocation for distributed energy resources: A strategic technology-policy framework. Journal of Energy, 72, 783-799

Mathiesen B.V., Lund H., Connolly D., Wenzel H., Ostergaard P.A., Moeller B., Nielsen S., Ridjan I., Karnoe P., Sperling K., Hvelplund F.K. (2015): Smart Energy Systems for coherent 100% renewable energy and transport solutions. Journal of Applied Energy, 145, 139-154

Morvaj B., Evins R., Carmeliet J. (2016): Optimizing urban energy systems: Simultaneous system sizing, operation and district heating network layout. Journal of Energy, 116, 619-636

Noussan M., Cerino Abdin G., Poggio A., Roberto R. (2014): Biomass-fired CHP and heat storage system simulations in existing district heating systems. Journal of Applied Thermal Engineering, 71(2), 729-735

Odum H.T. (1996): Environmental Accounting, Emergy and Environmental Decision Making, vol. 194. John Wiley, New York, USA ISBN

Odum H.T., Peterson N. (1996): Simulation and evaluation with energy systems blocks. Journal of Ecological Modeling, 93, 155-173

Odum H.T., Brown M.T., Brandt-Williams S. (2000): Introduction and global budget. In: Handbook of Emergy Evaluation. The Center for Environmental Policy, Environmental Engineering Sciences, Gainesville, Florida, USA

Papadopoulos A., Karagiannidis A. (2008): Application of the multi-criteria analysis method Electre III for the optimization of decentralized energy systems. Omega 36 (5), 766-776

Pardo N., Vatopoulos K., Krook-Riekkola A., Moya J.A., Perez A. (2012): Heat and Cooling Demand and Market Perspective. JRC Scientific and Policy Reporting. ISBN 978-92-79-25310-2

Patankar S.V. (1980): Numerical heat transfer and fluid flow. Series in Computational Methods in Mechanics and Thermal Sciences. ISBN 0-07-048740-5

Qier A., Haizhong A., Wei F., Lang W. (2014): Embodied energy flow network of Chinese industries: a complex network theory based analysis. Energy Procedia, 61, 369-372

REN 21 (2014): Renewables 2014-Global Status Report. Renewable Energy Policy Network for the 21st Century. ISBN 978-3-9815934-2-6

REN 21 (2016): Renewables 2016-Global Status Report. Renewable Energy Policy Network for the 21st Century. ISBN 978-3-9818107-0-7

RHC (2011): Common Vision for the Renewable Heating & Cooling Sector in Europe. European Technology Platform on Renewable Heating and Cooling. ISBN 978- 92-79-19056-8

RHC (2012): Strategic Research Priorities for Biomass Technology. Retrieved from www.rhc-platform.org on 09.07.2015.

Robert K.H., Schmidt-Bleek B., de Larderel A., Basile G., Jansen J.L., Kuehr R., Thomas P.P., Suzuki M., Hawken P., Wackernagel M. (2002): Strategic sustainable development - selection, design and synergies of applied tools. Journal of Cleaner Production 10, 197-214

Rosen M.A, Dincer I. (2003): Thermoeconomic analysis of power plants: an application to a coal fired electrical generating station. Energy Conversion and Management, 44, 2743-2761

Saidur R., Abdelaziz E.A., Demirbas A., Hossain M.S., Mekhilef S. (2011): A review on biomass as a fuel for boilers. Renewable and Sustainable Energy Reviews 15 (5), 2262-2289

Sameti M., Haghighat F. (2017): Optimization approaches in district heating and cooling thermal network. Journal of Energy and Buildings, 140, 121-130

Sartor K., Quoilin S., Dewallef P. (2014): Simulation and optimization of a CHP biomass plant and district heating network. Journal of Applied Energy 130, 474-483

Schwarz J., Beloff B., Beaver E. (2002): Use sustainability metrics to guide decision making. Chemical Engineering Processes, 8, 58-63

Sciubba E. (2001): Beyond thermoeconomics? The concept of Extended Exergy Accounting and its application to the analysis and design of thermal systems. Journal of Exergy, 1 (2), 68-84

Sciubba E., Ulgiati S. (2005): Emergy and exergy analyses: complementary methods or irreducible ideological options? Journal of Energy, 30, 1953-1988

Sciubba E., Wall G. (2007): A brief commented history of exergy from the beginnings to 2004. Journal of Thermodynamics, 10 (1), 1-26

Shamshirband S., Petkovic D., Enayatifar R., Hanan Abdullah A., Markovic D., Lee M., Ahmad R. (2015): Heat load prediction in district heating systems with adaptive neuro-fuzzy method. Renewable and Sustainable Energy Reviews, 48, 760-767

Shen Y.C., Lin G.T.R., Li K.P., Yuan B.J.C. (2010): An assessment of exploiting renewable energy sources with concerns of policy and technology. Journal of Energy Policy 38 (8), 4604-4616

Steinberger J.K., van Niel J., Bourg D. (2009): Profiting from negawatts: Reducing absolute consumption and emissions through a performance-based energy economy. Journal of Energy Policy, 37(1), 361-370

Stratego (2015): Enhanced Heating and Cooling Plans to Quantify the Impact of Increased Energy Efficiency in EU Member States. Main Report Executive Summary. Available at: http://heatroadmap.eu/publications.php

Sun F., Fu L., Sun J., Zhang S. (2014): A new waste heat district heating system with combined heat and power (CHP) based on ejector heat exchangers and absorption heat pumps. Journal of Energy, 69, 516-524

Szargut J., Morris D.R., Steward F.R. (1988): Exergy Analysis of Thermal, Chemical and Metallurgical Processes. Hemisphere, New York, NY. ISBN-13: 978-0891165743

Torchio M.F., Genon G., Poggio A., Poggio M. (2009): Merging of energy and environmental analyses for district heating systems. Journal of Energy 34 (3), 220-227

Torres C., Valero A., Serra L., Royo J. (2002) : Structural theory and thermoeconomic diagnosis: Part I. On malfunction and dysfunction analysis. Energy Conversion & Management, 43, 1503-1518

Tribus M., Evans R.B. (1962): A contribution to the theory of thermoeconomics. UCLA Report no. 62 36, August, University of California, Department of Engineering, Los Angeles

Tsatsaronis G., Pisa J. (1994): Exergoeconomic Evaluation and Optimization of Energy Systems – The CGAM Problem. Journal of Energy, 19, 287-321

United Nations (1998): Kyoto Protocol to the United Nations Framework. Retrieved from https://unfccc.int/resource/docs/convkp/kpeng.pdf on 22.03.2015

United Nations (2015): Adoption of the Paris agreement. In: Conference of the Parties on its Twenty-first Session, 21932 (December), 32

Valero A., (2015): Thanatia. The Destiny of the Earths Mineral Resources. World Scientific Publishing Co. ISBN 978-9814273930

Verda V., Colella F. (2011): Primary energy savings through thermal storage in district heating networks. Journal of Energy, 36(7), 4278-4286

Verda V., Baccino G. (2012): Thermoeconomic approach for the analysis of control system of energy plants. Journal of Energy, 41(1), 38-47

Verda V., Kona A. (2012). Thermoeconomics as a tool for the design and analysis of energy savings initiatives in buildings connected to district heating networks. Journal of Thermodynamics, 15(4), 221-229

Verda V, Caccin M, Kona A (2016): Thermoeconomic cost assessment in future district heating networks. Journal of Energy, 117, 485-491

Vesterlund M., Toffolo A., Dahl J. (2017): Optimization of multi-source complex district heating network, a case study. Journal of Energy, 126, 53-63

Wackernagel M., Rees W. (1996): Our Ecological Footprint: Reducing Human Impact on the Earth. New Society Publication Gabriola Island, BC. ISBN 978-0865713123

Wackernagel M., Lewan L., Hansson C.B. (1999): Evaluating the use of natural capital with the ecological footprint. Ambio 28, 604-612

Wall G. (1986): Exergy - a Useful Concept. Physical Resource Theory Group. 3rd edition. ISBN 91-7032-269-4

Wang J.J., Jing Y.Y., Zhang C.F., Zhao J.H. (2009): Review on multi-criteria decision analysis aid in sustainable energy decision-making. Renewable and Sustainable Energy Reviews, 13, 2263-2278

Wang H., Yin W., Abdollahi E., Lahdelma R., Jiao W. (2015): Modelling and optimization of CHP based district heating system with renewable energy production and energy storage. Journal of Applied Energy, 159, 401–421

Wang H., Wang H., Haijian Z., Zhu T. (2017): Optimization modeling for smart operation of multi-source district heating with distributed variable-speed pumps. Journal of Energy, 138, 1247-1262

Weidema B.P., Thrane M., Christensen P., Schmidt J.H., Lokke S. (2008): Carbon footprint: a catalyst for life cycle assessment? Journal of Industrial Ecology, 12 (1), 3-6

Wilson R.J. (1996): Introduction to Graph Theory. 4th edition. Addison Wesley Longman Limited. ISBN 0-582-24993-7

Wojdyga K. (2014). Predicting Heat Demand for a District Heating Systems. International Journal of Energy and Power Engineering, 3(5), 237

Yao M., Wang H., Zhang Z., Yue Y. (2010): Experimental study of n-butanol additive and multi-injection on HD diesel engine performance and emissions. Fuel, 89, 2191-2201.

Yi H.S., Hau J.L., Ukldwe N.U., Bakshi B.R. (2004): Hierarchical thermodynamic metrics for evaluating the environmental sustainability of industrial processes. Environnemental Progress 23 (4), 302-314